METALLIFEROUS MINERALIZATION IN THE WESTERN ANTARCTIC PENINSULA.

A thesis submitted for the degree of Doctor of Philosophy in the Department of Geological Sciences, University of Aston in Birmingham.

Michael John Littlefair

December, 1978.

Front-piece Galindez Island Base Huts (in fore-ground) on the Argentine Islands, with the Lemaire Channel in the far distance. January, 1977. 135 mm, f8. Kodachrome.

THE METALLIFEROUS MINERALIZATION IN THE WESTERN ANTARCTIC PENINSULA

MICHAEL JOHN LITTLEFAIR PhD; 1978

SUMMARY

This work involved the study of various types of mineralisation at a number of localities, during two season's field-work in the Antarctic Peninsula. A number of additional localities of minor mineralisation have also been described. Mineralisation described in previous literature is listed.

The "Quartz-Pyrite" rocks of the South Shetland Islands have been investigated and field-work and laboratory studies have shown them to consist of three types of hydrothermally altered lavas; advanced argillic, intermediate argillic and phyllic alteration. These deposits appear to have formed by solfataric-epithermal alteration.

A porphyry copper-molybdenum deposit has been discovered north of Charity Glacier, Livingstone Island, that shows metallogenetic zonation from a bornite-chalcopyrite-molybdenite core to an outer zone of galena-sphalerite-chalcopyrite. Breccia dykes and propylitic alteration of the host tonalites are associated with the mineralisation.

A porphyry molybdenum deposit has also been discovered on Argentine Islands, north west Graham Land. Molybdenite occurs along sheet joints in granodiorite and is surrounded by thin quartz-pyrite and thick quartz-magnetite veins. Quartz-monzonite dykes are associated with the molybdenite. The deposit shows zonation from a core of phyllic alteration (associated with molybdenite) to an outer propylitic zone.

A porphyry copper deposit also occurs on Horseshoe Island, Marguerite Bay.

Chemical data using atomic absorption spectrometery and electron microprobe methods has shown the igneous rocks associated with these deposits to be calc-alkaline and the sulphides to be similar to those in other calc-alkaline deposits.

A model is proposed for the mineralisation in the Antarctic Peninsula. Tectonically, it shows some similarity to the Andean Cordillera of South America. It is proposed that a porphyry copper belt is present along the western side of the Antarctic Peninsula, which is followed eastwards by a polymetallic belt, both of which run parallel to the trend of the Antarctic Peninsula.

KEY WORDS ;

ANTARCTIC PENINSULA, QUARTZ-PYRITE, SOLFATARIC,

PORPHYRY COPPER, HYDROTHERMAL ALTERATION.

ACKNOWLEDGEMENTS

I am grateful to Professor D. D. Hawkes and Dr. R.A. Ixer for the advice, patience and supervision of this work and to other members of staff for their help and advice.

I would also like to express my gratitude to the technicians of the departments of Geological Sciences and Metallurgy for their technical assistance. Mr. J. H. Williams is thanked for his help throughout and Mr. R. G. Howell of the department of Metallurgy for his help during the electron probe work. I am also grateful to the Natural Environment Research Council for the finance to carry out the work, and especially the British Antarctic Survey for their help with field-work and logistical problems. I would like especially to thank Dr. R. Adie and Dr. Swithenbank for their help and for the provision to study a suite of rocks from Smith Island in the South Shetland Islands. Captains' Laurence and Elliot are also thanked for their assistance. I would also like to thank Mrs. P. Swingler for typing the thesis.

M. J. LITTLEFAIR
DECEMBER, 1978.

LIST OF CONTENTS

List of Figures.

List of Tables

List of Plates

CHAPTER I

INTRODUCTION

The Antarctic Continent is one of the most remote and inaccessible areas of the world and has a landmass larger than Europe, Australia and the United States. Although the Antarctic was discovered over 150 years ago by Captain Cook, it was not until 1930 that knowledge of this continent began to expand by the work of various national expeditions. It should be noted that the nations signing the Antarctic Treaty of 1959 defined Antarctica as the ice covered continent and "The Antarctic" as that part of the earth that lies south of 60° S latitude. The conflicting claims of various nations having interests in the Antarctic was resolved in 1959 by the signing of the Antarctic Treaty, which reserved the Antarctic for scientific work alone, but endorsed no national claims. Since 1959 scientific work has been steadily increasing, although to date no detailed description of occurrences of the mineralisation has been undertaken in the Antarctic Peninsula, or Antarctica as a whole. Since the Antarctic Peninsula is geologically similar to the Andes (Adie, 1954; Dalziel, 1971 and 1972; Elliot, 1975) and since the Andes contain a number of rich mineral deposits, it can be reasoned that similar occurrences should be present in the Antarctic Peninsula. Statistically it is unlikely that a large number of mineral occurrences will be found in the Antarctic Peninsula, or for that matter in the Antarctic in general, since 95 to 98% of the land surface is covered by ice, which in places can reach thicknesses of 14,000 feet (4,600 m), which limits exposure of bare rock over the entire continent to about 100,000 square miles.

This work represents the first attempt to make a detailed study of the mineralisation in the Western Antarctic Peninsula. Although economic mineral occurrences may be found in the Antarctic Peninsula in future, the severe climate, short summer and distance from centres of industry may mean that only high grade ores of the precious metals can be extracted economically. The logistical problems of acquiring

a work force would also be a formidable obstacle (Swan, 1962) although some authors do not appear to consider this factor (Law, 1965).

1.1 Present Study

The present study attempts to describe several metallic mineral deposits visited during the investigations and to present a metallogenetic zoning scheme for the Antarctic Peninsula (north of 69° South). Correlation of previously recorded mineral occurrences has also been carried out, but no attempt has been made to subdivide these into economic or sub-economic. The recorded mineralisation may vary from small localised occurrences to large scale deposits, but only detailed geological field-work will reveal their true potential. A brief review of alteration assemblages has also been attempted, mainly from the present field-work and laboratory studies, but some from the previous literature (which appear to be rather vaguely described).

The field-work was carried out during two Antarctic summers in 1975/1976 and 1976/1977 from December to March of each year. The South Shetland Islands were visited in the first season and landings were made from the RRS John Biscoe and RRS Bransfield by gemini inflatable boats. H.M.S. Endurance also moved the field parties by helicopter on two occasions. The first eight days (28th November to 6th December, 1975) were spent making landings on Livingstone Island and MacFarlaine and English Straits. Various landings were later made on King George Island (7th December to 13th January, 1976 - Fildes Peninsula; 14th to 18th January, 1976 - Admiralty Bay; 19th and 20th January, 1976 - O'Caine Point, Nelson Island; 21st January to 14th February, 1976 - Barton and Keller Peninsulas). From the 14th to 17th February, 1976 the field party visited Half-Moon Island and Livingstone Island (north of Charity Glacier) from the 18th to 28th February, 1976. The field party camped on the various islands whilst away from the ship. During the 1977 field season a month was spent on the Argentine Islands, north west Graham Land (4th January to 2nd February, 1977) at the Galindez

Island base. Small boats were used to move between the various islands of the group. Brief landings were made by gemini from the RRS Bransfield on Anvers Island, Prospect Point, Rothera Point, Horseshoe Island, Stonington Island and Red Rock Ridge in Neny Fjord during February, 1977.

1.2 Recorded Occurrences of Mineralisation in the Antarctic Peninsula

A number of workers have made a specific study of particular sites of mineralisation in the Western Antarctic Peninsula; Ferguson (1921) made a study of the "Quartz-Pyrite" rocks of the South Shetland Islands and concluded they were "lodes" of massive quartz and pyrite. Barton (1964) and Hawkes (1961) (based on field work by Jardine) also came to the same conclusion. In fact, these rocks have been shown to be hydrothermally altered lavas (present study). Kossack (1955) has made a study of chromite mineralisation in the Elephant Island Group, Mueller (1963) the mineralisation on Greenwich Island and Valle et al (1975) has recorded Pb-Zn-Cu mineralisation in fault controlled breccias on Miers Bluff, Livingstone Island. The breccias have been intruded into a folded Palaeozoic greywacke - shale sequence (Miers Bluff Series). The authors concluded that the mineralisation which includes chalcopyrite, sphalerite, galena, bornite and covellite was deposited from hypothermal to mesothermal solutions, these being genetically related to the tonalite pluton located in False Bay. Pb-Zn-Cu-Ag mineralisation has also been recorded from the Gerlache Strait region (Vieira et al, 1978), where veins of chalcopyrite, galena and sphalerite have been found in Upper Palaeozoic sediments, which also contain some disseminated sulphides. Vein type copper (chalcopyrite and pyrite) has been reported in the Spring Point Area, with porphyry copper deposits on Eastern Anvers Island and magmatic iron deposits present on Brabant Island. Vieira et al, (1978) concludes that Tertiary plutonic rocks are the source of the metals and that they were deposited from hypothermal to mesothermal solutions. A porphyry copper deposit has also been described from the Lassiter Coast of Palmer Land by Rowley et al (1975) and Rowley et al (1977).

Here the porphyry copper mineralisation is associated with a porphyritic quartz-monzonite stock dated at 95 my. This concentrically zoned body was followed by the intrusion of granodiorite porphyry dykes, followed in turn by shearing, hydrothermal alteration and copper mineralisation. The host plutons show argillic and propylitic alteration. The above authors concluded from this that the Antarctic Peninsula forms part of the Circum-Pacific copper province. The majority of recorded mineral occurrences however are to be found in general geological reports dealing mainly with stratigraphy and petrology. The metallic mineral occurrences both previously recorded and those found in the present study are briefly described under the various elements, and are shown on an accompanying map (Fig. 1:1). A number of reviews of the mineralisation have been attempted in the recent past. Notable amongst these are reports by Potter (1969) who concluded the vast ice cover over the continent and isolated location make it unlikely that economic deposits of minerals will be found in the Antarctic in the foreseeable future, although in all probability the Antarctic will have as many mineral deposits as any other continent. Wright and Williams (1974) also conclude from a statistical study that economic mineral deposits are unlikely to be found in the Antarctic, but if they are to be found, the Western Antarctic Peninsula is the most favourable part of the continent. A brief review of recorded mineral occurrences has also been attempted. Ericksen (1976) in a brief review of metallogenic provinces in the South East Pacific region concluded that the mineral deposits in the Antarctic Peninsula are probably similar to the Andean province of South America. A number of broad, scanty discussions of the mineral potential of the Antarctic have also appeared (Chalmers, 1957; Runnels, 1970; Smith, 1972). A report by Elliot (1977) discusses the possible environmental effects of mineral development on the Antarctic environment. A number of recent reviews of the mineralisation in the Antarctic Peninsula have appeared.

Hawkes (1978) has attempted a review of significant occurrences of mineralisation recorded in the literature. Rowley and Pride (1978), however, have selected a number of recorded occurrences and attempted highly speculative interpretations of their genesis. They conclude that most known mineral occurrences on the Antarctic Peninsula are associated with Mesozoic and Tertiary plutonic rocks.

IRON

Iron mineralisation recorded on the Antarctic Peninsula can be divided into two major types; sulphides and oxides.

Sulphides

The pyrite can be subdivided on the basis of genesis into sedimentary, volcanic and pyrite associated with mineralisation.

Sedimentary

Pyrite as a diagenetic sulphide occurs in greywackes of Carboniferous age on Powell Island in the South Orkney Islands (Thompson, 1973; Pirie, 1925) and in Septarian nodules in sandstones on Miers Bluff on Livingstone Island (Hobbs, 1963). Pyrite of sedimentary origin occurs in Jurassic sedimentary rocks on the Bowman and Wilkins Coast (Fraser and Grimley, 1972), on Adelaide Island (Dewer, 1970) and in Carboniferous sediments on Alexander Island (Bell, 1974).

Volcanogenic

Pyrite occurs as a normal accessory mineral in Jurassic volcanic rocks on the Graham Coast (Adie, 1955; Curtis, 1966), the Oscar II Coast (Fleet, 1968) and the Batterbee Mountains in North West Palmer Land (Davies, 1977). Pyrite in association with pyrrhotite occurs in altered Jurassic andesites on the Outcast and Jobin Islands (Hooper, 1962) and in association with marcasite in lavas at Paradise Harbour and Wilhemine Bay areas of the Grandier Channel (Vieira et al, 1978) and Danco Coast (West, 1974). Pyrite also occurs as an accessory mineral in gabbros, diorites, tonalites and granodiorites of Andean age at Hope Bay (Adie, 1955) and the Graham Coast (Curtis, 1966). Magnetite,

ilmenite and pyrite occur in gabbros on the Anagram Islands (Fraser, 1964) and Horseshoe Island. Magnetite, pyrrhotite, pyrite and chalcopyrite occur in tonalites of Palaeozoic age on the Loubet Coast (Goldring, 1962). Pyrite is also present in dolerite dykes on Coronation Island in the South Orkneys (Thompson, 1974), in aplite veins cutting tonalites on the beach below Copper Peaks on Anvers Island, and in lamprophyres cutting granites at Cape Roquemaurel on the Trinity Peninsula (Tyrrell, 1945). Pyrite is also present in hornblende-porphyry dykes of Andean age in the Elgar Uplands of Alexander Island (Bell, 1974).

Pyrite Associated With Mineralisation

Pyrite is present in calcite - siderite veins of Tertiary age on Powell Island in the South Orkneys (Thompson, 1973) and in veins of quartz and calcite on Joinville Island, Trinity Peninsula and James Ross Island, which are post-Andean in age (Elliot, 1967; Bibby, 1960 ; Bibby, 1966). Hydrothermally introduced pyrite occurs on Mushroom Island in Marguerite Bay (Knowles, 1945). Pyrite, pyrrhotite and chalcopyrite occur in Jurassic lavas on the Argentine Islands (Elliot, 1964). On Adelaide Island (at Rothera Point) a gabbro has intruded Jurassic sediments (Dewer, 1970). The sediments show phyllic alteration caused by hydrothermal solutions derived from the gabbro. The altered rocks consist of anhedral quartz, $2M_1$ muscovite, pyrite and hematite (showing ilmenite exsolution lamelli). Ferrian dravite is also present in small veinlets cutting these rocks, with late stage fractures infilled with quartz and hematite. These rocks probably represent low temperature hydrothermal alteration zones. In the South Shetland Islands pyrite has been recorded in "Quartz-Pyrite" rocks (Ferguson, 1921; Hawkes, 1961 and Barton, 1964). A field and laboratory study of these rocks (present study) has shown that they represent low temperature hydrothermal alteration zones associated with the peripheral zones of porphyry copper deposits. Pyrite in association with epidote has been found in a volcanic breccia on Nelson Island.

Oxides

Magnetite has been found in large quartz veins cutting tonalites and granodiorites on the Argentine Islands, that appear to have formed in the basal parts of a porphyry molybdenum deposit (present study). Magnetite-hematite flows occur on Brabant Island which are assumed to be of Pleistocene age (Vieira et al, 1978) and are similar to the Lacur-Sur deposit in the Andes.

COPPER

Copper, mainly in the form of sulphides has been recorded from several localities on the Antarctic Peninsula and a number of new discoveries have been made during the present investigations. Copper staining is widespread over the Peninsula and has been recorded on Elephant Island (Wordie, 1921) and in the GerlacheStrait area (Thomas, 1921) where chalcopyrite, bornite, native copper and para-atacamite have recently been found (Vieira et al, 1978) in volcanic rocks and metasediments that have been intruded by Tertiary plutonic rocks. A conspicuous malachite stain occurs on Copper Peaks on the western side of the Lemaire Channel (Hooper, 1962) and mineralisation at the base of the exposure is confined to infrequent aplite veins containing sparse chalcopyrite, pyrite and pyrrhotite. Malachite stains have been found near the old British base at Adelaide Island, and on two islands ten miles to the south west (Nichols, 1955). Blocks of cupriferous vein material have been found in screes south of Starbuck Glacier, on the Oscar II Coast which probably originated in veins on the glacier walls (Fleet, 1968). Chalcopyrite showing alteration to bornite and malachite along with fluorite, quartz and epidote are present. Chalcopyrite occurs disseminated in, and along joint planes in Tertiary plutonic rocks, notably diorites on Casabianca Island (Ferguson, 1921), Adelaide Island (Dewer, 1970) and Southern Arrowsmith Peninsula in sheared tonalites (Hudson, 1964). Chalcopyrite also

occurs in epidote rich nodules in altered gabbros on the Anagram Islands (Fraser, 1963) and in minor amounts in quartz-magnetite veins on the Argentine Islands. Chalcopyrite, cuprite and chalcocite have been found in an olivine gabbro on Horseshoe Island, which contains abundant malachite stains similar to those found on the Skua Gull and Tierra Firma Islands in a layered gabbro (Adie, 1955). Chalcopyrite, magnetite and pyrrhotite occur in aplite veins cutting tonalites on the Jobin Islands, with the same minerals recorded in inclusions within the tonalites (Hooper, 1962). Copper sulphides also occur in augite andesites on Coughtrey Island (Ferguson, 1921; Bayly, 1957) and in banded rhyolites on Little Thumb (Fraser, 1963). Chalcopyrite has also been recorded in "Basement Complex" rocks on Brian Island, Postillion Rock, Roman Four Promontary (Hoskins, 1961) and Stonington Island (Grimley, 1963 ; Grimley, 1966). A vent agglomerate of (?) Jurassic age has been recorded in North Western Palmer Land in the Mount Pitman area which contain copper, iron and sulphur mineralisation (Skinner, 1973). A vein of chalcopyrite has been recorded on Anvers Island (Potter, 1969) and chalcopyrite is also present in a quartz-tourmaline breccia on Doumer Island. Chalcopyrite has also been recorded in veins on Greenwich Island (Mueller, 1963) in association with pyrite from a granodiorite at Atlantis Nunatak in north east Palmer Land (Ayling, 1977), on an island north of the Fleming Glacier and at Cape Bloggs (Knowles, 1945). Pyrrhotite, pyrite, chalcopyrite and chalcocite have also been recorded in feldspathic greywackes on the Robert English Coast, Palmer Land (Laudon et al, 1964.) Native copper has been found on Dee Island and Keller Peninsula, King George Island in the South Shetland Islands (present study). Tennatite - tetrahedrite, tenorite, chalcocite, bornite, chalcopyrite, malachite and azurite have been recorded at Miers Bluff, Livingstone Island (Valle et al, 1975). Here the mineralisation occurs as small veins and disseminated in a fault controlled breccia. This

mineralisation is peripheral to a porphyry copper - molybdenum deposit discovered by the author in south east False Bay. Here chalcopyrite, bornite, molybdenite and pyrite occur in veinlets in a tonalite intrusion north of Charity Glacier. Small amounts of disseminated chalcopyrite and pyrite are present in the host intrusion (present study). This deposit shows a metallogenetic zonation typical of porphyry copper deposits. A porphyry copper deposit has also been found in the Rare Range at Copper Nunataks on the Lassiter Coast (Rowley, 1975; Rowley et al, 1975; Rowley et al, 1977). The copper mineralisation is associated with a porphyritic monzonite pluton that has been invaded by granodioritic dykes, and occurs along shear planes in the pluton. The major ore minerals are chalcopyrite, pyrite, magnetite, malachite, molybdenite, hematite and chalcocite.

MOLYBDENUM

Molybdenite has been recorded in association with epidote and quartz in shear fractures cutting lapillistones and tuffaceous granulestones on Eastern Mount Barré, Adelaide Island (Dewer, 1970), in vugs, with pyrite, siderite, fluorite, limonite and orthoclase in the Red Rock Ridge granite (Nichols, 1955) and in a biotite granite at the head of North East Glacier, Neny Fjord (Hoskins, 1961). Molybdenite has also been recorded in a brecciated quartz zone cutting Basement Complex rocks on Stonington Island (Knowles, 1945) and in small veinlets nine miles east of Stonington Island. Molybdenite has also been found in veinlets cutting tonalites and aplites north of Charity Glacier, Livingstone Island in a porphyry copper - molybdenum deposit (present study), at Palmer Station on Anvers Island with associated chalcopyrite and pyrite (in veinlets cutting a tonalite) and on joint planes in granodiorites on the Argentine Islands with chalcopyrite in a porphyry molybdenum deposit.

CHROMIUM, NICKEL AND COBALT

Chromite, cobalt and nickel (as unnamed minerals) have been recorded in an ultrabasic segregation deposit on Gibbs and Aspland Islands in the Elephant Island Group (Kossack, 1955) and could also occur in association with ultrabasic intrusives in the Paradise Harbour area on the Danco Coast (Vieira et al, 1978). Chromite also occurs as an accessory mineral in a basalt pipe on Southern Square Peninsula, Adelaide Island (Dewer, 1970) in olivine phenocrysts in palagonite tuffs near Mimas Peaks on the Beethoven Peninsula, Alexander Island (Bell, 1973) and in an amphibolite dyke near Mount Pitman on the Robert English Coast (Laudon et al, 1964). Chromite has also been recorded in rhythmically layered Andean gabbros on the Central Black Coast, Palmer Land (Singleton, 1976) but from the petrographic description it is probably a misidentification of hematite or ilmenite.

GOLD AND SILVER

Silver has been recorded in association with lead-zinc mineralisation from the Wilhemine Bay area on the Danco Coast (Vieira et al, 1978). Low grade gold-silver ore (in pyrite) is present in red and grey granitic dykes and irregular and elongate areas in Basement gneiss in Neny Fjord, in pegmatites on Neny Island, and at locations nine, twelve and eighteen miles east of Stonington (Nichols, 1955; Knowles, 1945). Gold-silver ore also occurs in the Eternity Range on Palmer Land in pegmatites and in massive pyrite in hornblendites near Cape Bloggs (Knowles, 1945) with the grade of ore generally 0.03 oz/ton Au and 0.02 oz/ton of Ag. Analyses of pyrite in the South Shetland Islands indicates it is not very auriferous (approximately 50 ppb).

LEAD AND ZINC

Galena and sphalerite have been recorded in veinlets and disseminated in breccias on north western Hurd Peninsula (Valle et al, 1975) and is present as a halo around the porphyry copper-molybdenum deposit in eastern False Bay. Veins of galena, sphalerite and chalcopyrite have also been recorded in the Wilhemine Bay area of the Danco Coast (Vieira et al, 1978). Sphalerite and pyrite has been recorded in the groundmass of banded gneiss at Postillion Rock in Neny Fjord (Hoskins, 1963) and in lavas on Eastern Alexander Island at Ablation Point (Bell, 1973).

MANGANESE

Manganese stains (pyrolusite) are fairly common over the Antarctic Peninsula, and are present on dyke rocks on Horseshoe Island, Jurassic lavas at Little Thumb in Neny Fjord (Hoskins, 1961), on Miocene lavas on Fildes Peninsula, King George Island, and on Stonington Island where Basement gneiss has been invaded by chalcopyrite (Fraser, 1963). Pyrolusite has also been recorded nine miles east of Stonington (Knowles, 1945) and on gabbros on the Tierra Firma Islands (Nichols, 1955). Manganese nodules have been found on the sea bed south of 60° south latitude (Wright and Williams, 1974; Potter, 1969).

TIN

(?)Cassiterite of unusual occurrence has been reported from Southern Alexander Island in veins with penninite, quartz, albite and zoned schorlite. These veins emanate from plutonic intrusions of Cretaceous age that intrude Carboniferous subgreywackes and arkoses and have metamorphosed them to albite-epidote homfels (Bell, 1973).

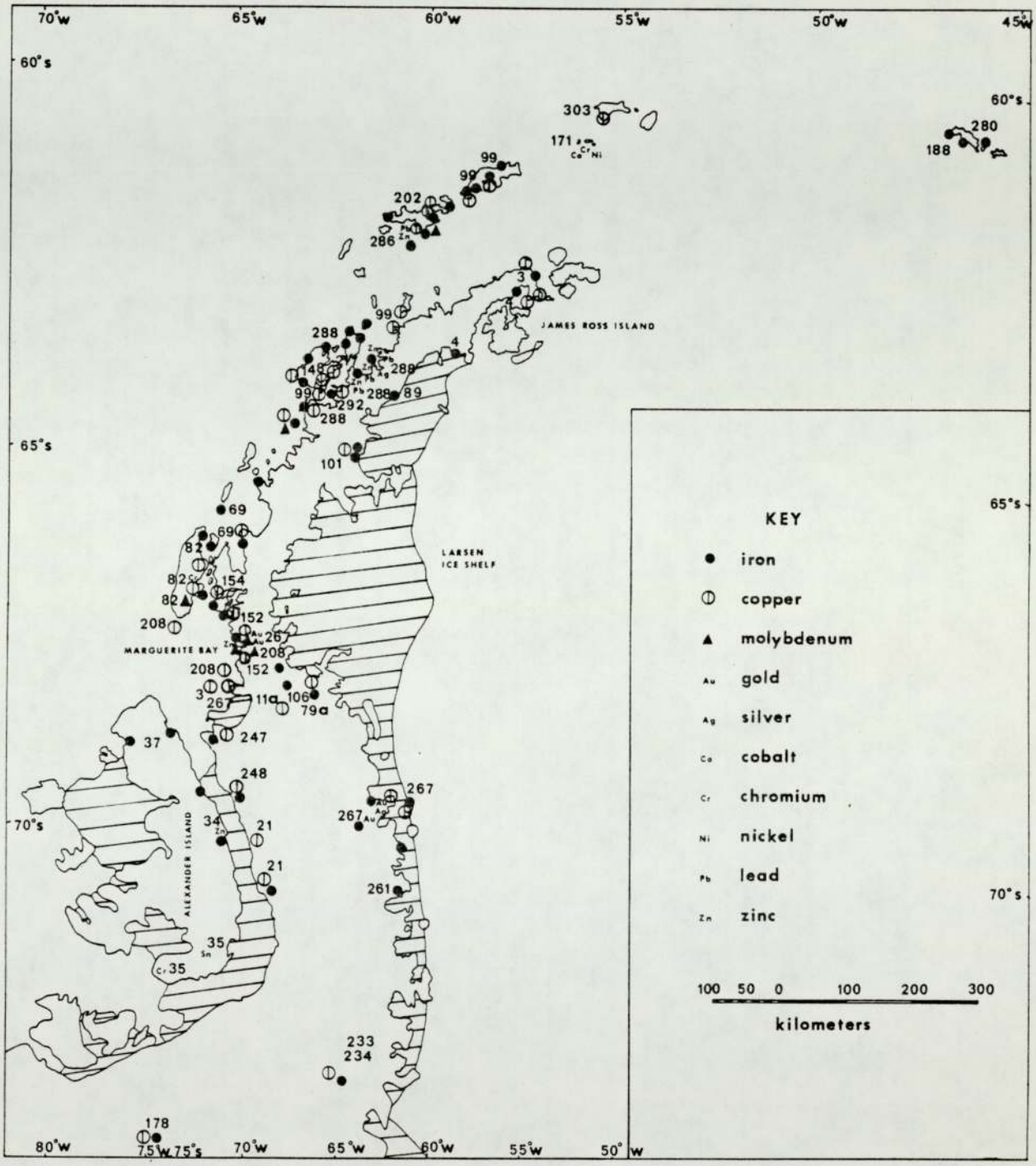

FIG.1:1 MAP OF KNOWN METALLIC MINERAL OCCURENCES IN THE WESTERN ANTARCTIC PENINSULA. NUMBERS IN BRACKETS REFER TO REFERENCES IN APPENDIX. UNNUMBERED LOCATIONS WERE VISITED BY THE AUTHOR.

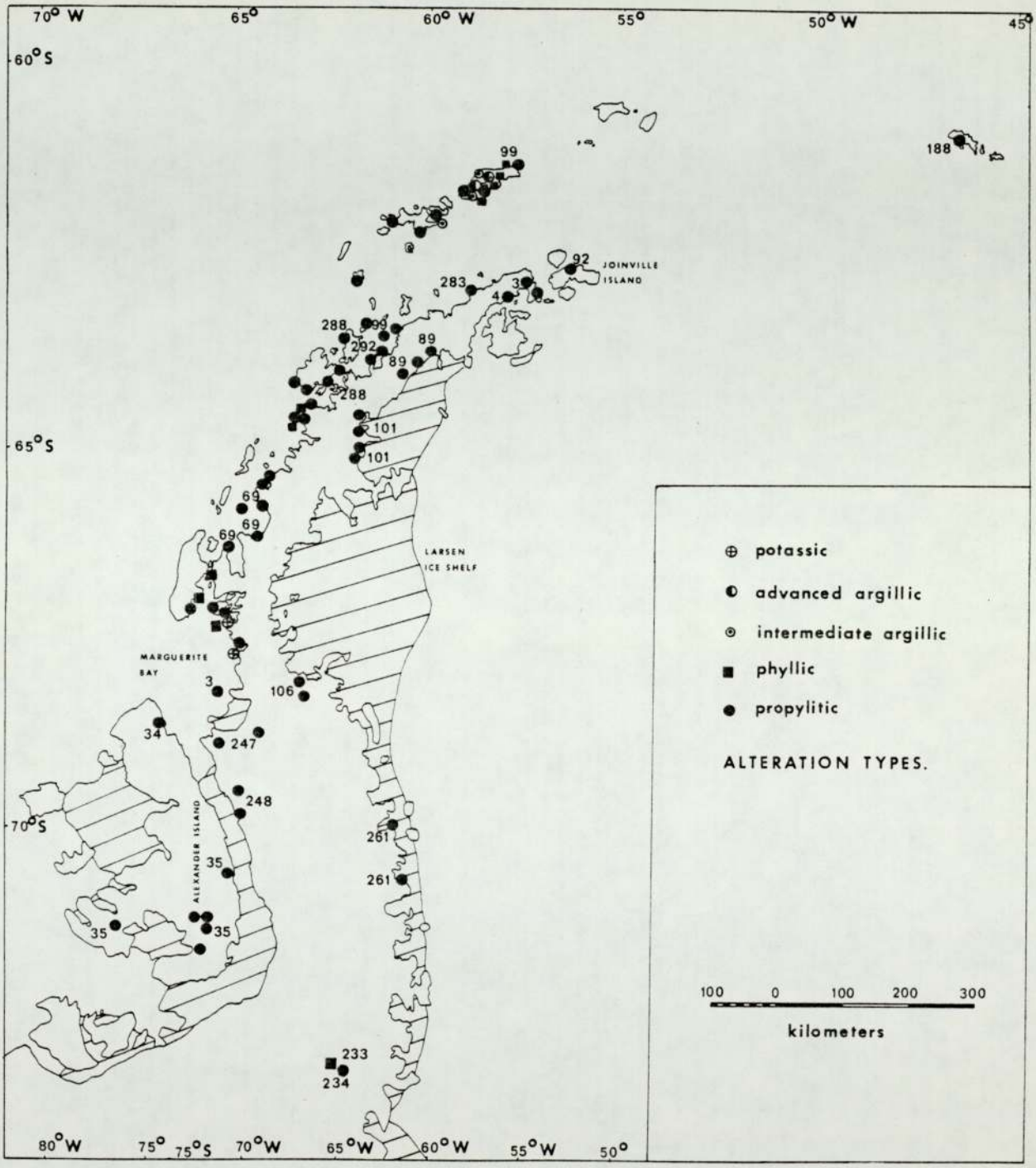

FIG.1:2 MAP OF ALTERATION TYPES IN THE WESTERN ANTARCTIC PENINSULA. NUMBERS REFER TO REFERENCES IN APPENDIX, UNNUMBERED TO LOCALITIES VISITED BY THE AUTHOR.

FLUORITE

Fluorite has been recorded in volcanic conglomerates near Mount Argus on the Bowman and Wilkins Coast (Fraser and Grimley, 1972) and north of Starbuck and Punchbowl Glaciers on the Oscar II Coast (Fleet, 1968). The fluorite occurs in association with pegmatites which have developed on joint planes in lavas and rarely as veins in granites. Fluorite has also been recorded in Basement Complex pyroxene skarn and granite gneiss in Neny Fjord, in Palaeozoic granites on Millerand Island (Hoskins, 1963) and in vugs in the Red Rock Ridge granite.

1.3 Hydrothermal Alteration

Hydrothermally altered rocks often form extensive halos around mineral deposits and can help pin-point the position of otherwise concealed deposits. Areas of propylitic alteration often surround porphyry copper deposits in the Andes and North America (Lowell and Guilbert, 1970), whilst low temperature advanced argillic and phyllic alteration formed by solfataric-epithermal activity can be guides to concealed porphyry copper, and base and precious metal deposits (Branch, 1976; Sillite, 1977). These alteration halos are typical of epigenetic deposits, but are not as well defined in syngenetic (sedimentary or volcanogenic) deposits.

Most of the descriptions listed below were described in the present investigations and are listed under the alteration assemblages defined by Meyer and Hemley (1967) and Lowell and Guilbert (1970). Some have been recorded in previously published literature, but in most cases it was found difficult from these descriptions, to differentiate between propylitic alteration and low grade albite-epidote-hornfels metamorphism. However, where veinlets of quartz, chlorite, epidote or carbonate have been recorded with similar alteration in the host rocks it has been classed as propylitic alteration. This alteration type is

the most widespread on the Antarctic Peninsula. A map (Fig. 1:2) shows the locations of the various alteration types recorded on the Antarctic Peninsula.

Advanced Argillic Alteration

Rocks showing alteration to a mineral assemblage consisting of quartz, alunite, sericite, tourmaline, kaolinite, pyrophyllite and pyrite are considered to represent advanced argillic alteration (Meyer and Hemley, 1967). Areas of (?) Jurassic lavas showing advanced argillic alteration have been found on Northern Barton and Keller Peninsulas, King George Island in the South Shetland Islands. These deposits consist of alunite, natroalunite, quartz, pyrophyllite, kaolinite, native sulphur, gypsum, fluorite and pyrite (present study).

Intermediate Argillic Alteration

Rocks showing this alteration consist of a mineral assemblage of quartz, carbonate, kaolinite, sericite, pyrite and chlorite, (Meyer and Hemley, 1967). Tuffs and lavas showing intermediate argillic alteration have been discovered on Fildes Peninsula, Keller Peninsula and Headland Opposite Dufayel Island on King George Island, and Half-Moon Island, in the South Shetland Islands (present study). These deposits consist of a mineral assemblage of quartz, ferroandolomite, ferroancalcite, kaolinite, pyrite and minor rutile. Argillic alteration has also been recorded at Copper Nunataks on the Lassiter Coast, which is associated with porphyry copper mineralisation in Cretaceous plutons (Rowley et al, 1975).

Phyllic Alteration

Phyllic alteration consists of an assemblage of quartz, muscovite (sericite) and pyrite (Meyer and Hemley, 1967; Lowell and Guilbert, (1970). Phyllic alteration is widespread on the Antarctic Peninsula,

and has been recorded in the present investigations at Precious Peaks, Ullman Spur, Stenhouse Bluff, Crépin Point, Dufayel Island, Headland Opposite Dufayel Island, Southern Barton Peninsula and Ester Harbour (Ferguson, 1921) on King George Island. On the Antarctic Peninsula, this alteration type has been recorded in the Gerlache Strait area (Vieira et al, 1978) and at Copper Nunataks on the Lassiter Coast (Rowley et al, 1975). The present investigations have shown that phyllic alteration is also present in the Lemaire Channel, Argentine Island, Adelaide Island (at Rothera Point), the Arrowsmith Peninsula (Jones Ice Shelf area) and Horseshoe Island in Marguerite Bay. This alteration seems to affect pre-Andean lavas and some Tertiary plutonic rocks.

Potassium Silicate Alteration

Potassium silicate alteration consists of an assemblage of potassium feldspar, biotite, chlorite, sericite and pyrite. It has not been widely reported on the Antarctic Peninsula, but has been recorded on the Thompson Peninsula in the Gerlache Strait (Vieira et al, 1978), the Red Rock Ridge granite in Neny Fjord, Horseshoe Island in Marguerite Bay and the Argentine Islands.

Propylitic Alteration

Propylitic alteration consists of an alteration mineral assemblage of quartz, chlorite, sericite, pyrite, carbonate and tourmaline (Meyer and Hemley, 1967). The present investigations have shown that areas of propylitic alteration are present on King George Island, Nelson Island, Greenwich Island (Mueller, 1963) Robert Island, Half-Moon Island and Livingstone Island in the South Shetland Islands, mainly affecting the pre-Andean lavas and pyroclastics. On the Antarctic Peninsula propylitic alteration of (?) Jurassic lavas, pyroclastics and some Tertiary plutons have been recorded on the sides of the Neumayer Channel (Vieira et al, 1978), Anagram Islands (Fraser, 1964),

Prospect Point, Adelaide base on Adelaide Island and at Copper Nunataks on the Lassiter Coast (Rowley et al, 1975). Petrographic descriptions of pre-Andean lavas and some Tertiary plutonic rocks indicated that areas of propylitic alteration are present on the Trinity Peninsula (Elliot, 1967), Nordenskjold Coast, Joinville Island (Elliot, 1967), Oscar II Coast (Fleet, 1968), Bowman and Wilkins Coast (Fraser and Grimley, 1972), Graham Coast (Curtis, 1960), Loubet Coast (Goldring, 1962), Danco Coast (West, 1974), Adelaide Island (Dewer, 1970), Alexander Island (Bell, 1973 and 1974) and northern Palmer Land (Skinner, 1973).

1.4 Conclusions

These areas of pre-Andean rocks showing hydrothermal alteration are indications of the presence of concealed mineral deposits on the Antarctic Peninsula. Detailed investigations in these areas will reveal whether or not economic mineral prospects are present. This literature survey and the field studies suggest that the areas most favourable for mineralisation in the Western Antarctic Peninsula based on alteration assemblages and recorded occurrences of sulphide minerals are the South Shetland Islands, Anvers Island and surrounding area and Palmer Land.

CHAPTER 2

GENERAL GEOLOGY OF THE WESTERN ANTARCTIC PENINSULA AND SOUTH SHETLAND ISLANDS

2.1 Stratigraphy

Pre-Cambrian to Late Palaeozoic

The oldest known rocks in the Antarctic Peninsula are orthogneisses and paragneisses (Adie, 1954) comprising the metamorphic Basement Complex rocks. Although the rocks are widespread in this region (northern Palmer Land, Marguerite Bay etc.) their correlation, significance and tectonic relationships are not well understood, although recently De Wit (1977) suggested these rocks represent the trench-arc gap environment of an east-dipping Gondwanide subduction zone, whilst Elliot (1975) suggested they formed in the Borchgrevink Orogen. Whole rock K/Ar age dating of these rocks give ages ranging from 177 my to 235 my (Miller, 1960; Rex, 1967; Grikurow et al, 1967; Grikurov et al, 1966; Halpern, 1972). These ages have been ascribed to the effects of early Mesozoic folding of the late Palaeozoic sedimentary sequences (Miller, 1960) or partial loss of radiogenic argon during a thermal event associated with the Andean Orogeny (Dalziel, 1972).

These rocks are generally dioritic, granitic and biotite-garnet gneisses, quartzofeldspathic, semimicaceous or micaceous schists and phyllites (Thompson, 1974; Hoskins, 1963; Fraser and Grimley, 1972). Hornblende schists occur in some areas (Hoskins, 1963; Thompson, 1974) which probably represent metamorphosed basic volcanics and associated dykes (Adie, 1954). Greenstones have been recorded in northern Palmer Land (Skinner, 1976 .) and by comparison with Southern Africa may represent an ancient marginal basin (Groves et al, 1978). Impure marbles have been recorded from the South Orkney Islands (Thompson, 1974) with pyroxene and epidote-garnet skarn rocks present in the Neny Fjord area (Hoskins, 1963). Elephant Island in the South Shetland

Islands is composed of high grade garnet-hornblende-albite-mica and quartz-calcite-amphibole schists dated by K/Ar methods at 80 my (Dalziel, 1972). Inclusions of metamorphic rocks have been found widely scattered in most of the later volcanic and plutonic rocks (Goldring, 1962) with Basement Complex fragments recorded in the Lions Rump and Penguin Island lavas in the South Shetland Islands (Hawkes, 1961).

Non-gneissic plutonic rocks occur in the Marguerite Bay, Loubet Coast and Danco Coast areas which are cataclastically deformed and are presumed to be of Palaeozoic age (Adie, 1954; Goldring, 1962; West, 1974), although Rb/Sr dating of these rocks on the Debenham Islands gave ages of 98-117 my (Halpern, 1972). Some metamorphic rocks in north western Palmer Land have been ascribed a Palaeozoic age (Skinner, 1973).

The greywacke-shale sequence of the Trinity Peninsula Series which is invariably several kilometres thick and intensely deformed is late Palaeozoic in age (Adie, 1954). Sparse palaeontological and age dating data (197 my, Dalziel, 1972) indicate these rocks are Carboniferous to Triassic in age. Deposition of these rocks took place along the Pacific margin of Gondwanaland (Dalziel and Elliot, 1973) and they probably form part of an early Mesozoic Gondwanide fold belt (Du Toit, 1973). These rocks occur over a large part of the Antarctic Peninsula (Trinity Peninsula, Palmer Land etc.) and on central Alexander Island, where interbedded lavas and abundant volcanic clasts have been interpreted as suggesting eugeosynclinal deposition (Adie, 1957; Grikurov et al, 1968; Bell, 1973). The presence of pillow lavas in the sequence (Bell, 1973) suggests these rocks may represent a closed marginal basin.

Generally the Trinity Peninsula Series consists of a uniform shale-sandstone-greywacke facies, although limestones are occasionally present (Fleet, 1968). Deposition seems to have occurred by turbidity currents, and in places the sediments are associated with basic to intermediate

volcanics (Elliot, 1966) with keratophyres and volcanics in north east Palmer Land, and Oscar II Coast forming isolated arcs (Fleet, 1968; Fraser and Grimley, 1972). Occasionally, the sediments contain glacial pebbles with some tilloids also present (Aitkenhead, 1965). The rocks tend to show cataclastic deformation, with the fold axes generally parallel to the regional trend of the Antarctic Peninsula (Katz, 1973). On Miers Bluff, Livingstone Island the rocks represent the inverted limb of a recumbent fold of nappé proportions (Caminos et al, 1968). The rocks have also suffered low grade regional metamorphism to greenschist facies (Elliot, 1966) and local thermal metamorphism where they have been intruded by Andean plutons (Adie, 1954; West, 1974).

Mesozoic to Tertiary

In most areas an angular unconformity separates the folded Trinity Peninsula Series from the slightly deformed Jurassic volcanics and sediments, the classic locality being Hope Bay (Bibby, 1966) (Table 2:1). The Upper Jurassic Volcanic Group which is present over the entire length of the Antarctic Peninsula has an overall thickness ranging from 300 to 3,000 metres. The volcanics also form a large part of the South Shetland Islands where some have been suggested to be comagmatic with Tertiary plutonic rocks (Grikurov and Polyakov, 1968).

Conglomerates and sandstones of Upper Jurassic age occur in the South Orkney Islands (Adie, 1964) with shallow marine mudstones and sandstones present on southern Alexander Island, Graham Land and north western Palmer Land (Bell, 1973; Skinner, 1973), which appear to predate the volcanism (Table 2:1). The Upper Jurassic volcanics consist mainly of subaerially erupted lavas, agglomerates and tuffs which range in composition from basaltic andesite, andesite and dacite to rhyodacite and occasionally rhyolite, representing a normal calc-alkaline suite, with the sequence being repeated several times in the volcanic cycle (Adie, 1964). The Upper Jurassic volcanics show no penetrative deformation,

except in the southernmost Antarctic Peninsula (De Wit, 1977), but the entire Mesozoic sequence is highly cleaved, as in southernmost South America (Williams et al, 1972).

The petrology of the (?) Jurassic volcanics has been described in the South Shetland Islands by Hawkes (1961), Hobbs (1963) and Barton (1964). They have been shown to consist of phenocrysts of plagioclase and pyroxene in a holocrystalline groundmass of andesine microlites and small grains of pyroxene and magnetite. Interstitial devitrified glass is occasionally present, especially in the acid varieties. Xenocrysts of quartz and feldspar are present, often embayed and corroded. The plagioclase is often replaced by chlorite, epidote, albite and clinozoizite, whilst the mafic minerals are replaced by chlorite, calcite, quartz, epidote and leucoxene. Although the original ferromagnesian minerals in these rocks have been completely altered, Hawkes (1961) determined the original rocks were olivine basalts, hypersthene - augite andesites and augite andesites.

On Byers Peninsula, Livingstone Island, in the South Shetland Islands a gently folded sequence of Mesozoic sediments of late Tithonian - late Barremian age (Araya and Herve, 1966; Gonzalez-Ferran et al, 1970; Valenuela and Herve, 1972) occur which are interbedded with basaltic andesites and augite andesites, (Hobbs, 1963).

Intruded into the Upper Jurassic Volcanic Rocks, and forming a major part of the backbone of the Antarctic Peninsula are late Mesozoic to early Tertiary plutonic rocks. K/Ar age dating of these plutonic rocks indicates a wide range of ages from 105 to 40 my (Fleet, 1968; Halpern, 1965; Scott, 1965; Grikurov et al, 1972; Dalziel et al, 1973 and Angelelli et al, 1970). Adie (1972) has suggested the intrusive activity falls into four distinct episodes; early to middle Jurassic, late Jurassic, middle Cretaceous and late Cretaceous to early Tertiary. These plutonic rocks underlie much of the South Shetland Islands with the Mount Friesland Ridge on Livingstone Island, and the central axis of King George Island

(both trend WSW - ENE) probably underlain by these plutonic rocks (Hawkes, 1961; Hobbs, 1963).

The intrusive contacts are generally sharp and crosscutting with the metamorphic grade in the thermal aureoles rarely exceeding the hornblende hornfels facies. In places, large scale metasomatism derived from the intrusive rocks has reconstituted both the late Jurassic volcanics and earlier plutonic rocks (Hooper, 1962). The composition of these intrusions varies from gabbro to alkali granite (Goldring, 1962), although tonalite is the most common rock type (Adie, 1955). Many are hybrid rocks formed by mixing of gabbroic and granodioritic magmas (Curtis, 1966; Goldring, 1962; Hooper, 1962). The petrology of the tonalites and granodiorites from the South Shetland Islands has been described by Hawkes (1961), Hobbs, (1963) and Barton (1964). Their descriptions show they are medium-grained rocks with an hypidiomorphic texture consisting predominantly of plagioclase laths, augite, hornblende, quartz and orthoclase with rare hypersthene. Minor biotite, chlorite, epidote, calcite, apatite and magnetite are also present. These rocks belong to a normal calc-alkaline suite (Adie, 1955) that probably formed due to partial melting of oceanic crust subducted beneath the Antarctic Peninsula.

In the South Shetland Islands sodic amphibole schists have been found on Smith and nearby Barlow Islands (Rivano and Cortes, 1976) that have been dated at 90 my (Davies, per comm.), although Smellie and Clarkson, (1975) proposed (without supporting evidence) that they are pre-Upper Jurassic. Quartz, lawsonite, albite, epidote, chlorite, garnet, stilpnomelane and calcite are present in these rocks. Smellie and Clarkson (1975) state glaucophane is present in all these rocks, but a study of their specimens (P220.3) indicates some of the sodic amphibole is clearly crossite. X-Ray diffraction indicates omphacite is also present. This assemblage indicates the presence of a high pressure - low temperature mineral association, suggesting a metamorphic belt along the Pacific margin of the Antarctic Peninsula (Rivano and Cortes, 1976). Emplacement of dunite-sepentinite sheets has occurred

on Gibbs, Elephant and Aspland Islands, during the Tertiary (Dalziel, 1972) and is probably associated tectonically with the sodic amphibole schists (Rivano and Cortes, 1976).

Sediments of Cretaceous age occur on north east Graham Land (Trinity Peninsula) and James Ross Island and surrounding islands. Lower Cretaceous beds were deposited, but have been removed by erosion as indicated by the presence of Aucellina Andina in pebbles in the Cretaceous beds and abundant glauconitic clasts in Cretaceous conglomerates. Cretaceous sediments outcrop on James Ross, Vega, Snow Hill, Seymour, Cockburn and Hump Islands (Biddy, 1966). They comprise loosely cemented sandstones which contain distinctive ammonites, coarse well cemented sandstones, sandy shales and shales known as the Snow Hill Island Series.

Tertiary to Recent

On Seymour Island the Cretaceous beds are overlain with angular unconformity by the lower Miocene Seymour and Cockburn Island beds, which have a similar lithology to the underlying strata (Bibby, 1966). These beds are overlain unconformably by the James Ross Island Volcanic Group. These volcanic rocks are mainly alkali olivine basalt lavas and palagonite tuffs and breccias, although where they have been extruded into water, pillow lavas, bedded tuffs and agglomerates are present and occur as deltaic structures around James Ross Island (Nelson, 1975). Palagonite breccias were probably produced by subaqueous eruptions (Nelson, 1975). Dykes, sills, volcanic plugs and laccoliths are the intrusive rocks associated with these volcanics, with analcite occurring in the basaltic plugs and laccoliths.

In the South Shetland Islands a series of stratified andesitic and basaltic lavas, tuffs and agglomerates with occasional interbedded sandstones and conglomerates of Miocene age occur (Hobbs, 1963). They outcrop mainly on southern and western Livingstone Island, King George Island, Robert Island (where the volcanics are Miocene to Oligiocene),

(Caballero and Fourcade, 1958) and Greenwich Island (where basaltic lavas are Miocene to Eocene), (Gonzalez-Ferran and Katsui, 1970). Volcanic plugs of the same age probably representing the vents from which these lavas were extruded occur at a number of localities including Edinburgh Hill (Ferguson, 1921), Inott Point, Vietor Rock and South Beaches on Livingstone Island (Hobbs, 1963) and on Flat Top, Fildes Peninsula, Buddington Peaks, Three Brothers Hill, Point Thomas and Ternych Needle on King George Island (Hawkes, 1961). Andesitic and basaltic dykes are commonly associated with these Tertiary volcanics (Hawkes, 1961; Caballero and Fourcade, 1958).

Overlying these Miocene to Eocene volcanics in both the South Shetland Islands and the Trinity Peninsula is a conglomerate containing numerous Pecten shells, known as the Pecten Conglomerate. It rests on a marine platform cut across the volcanics and is probably Pleistocene in age (Hennig, 1911). Overlying this conglomerate on the Trinity Peninsula are a series of volcanics of Pleistocene to Recent age known as the Seal Nunatak Volcanics which are similar in petrology to the James Ross Island Volcanic Group (Dalziel and Elliot, 1973). In the South Shetland Islands (King George Island) a series of olivine basalts overlie the Pecten Conglomerate which are known as the Penguin Island Group (Hawkes, 1961). Although the Penguin Island volcano is a recent volcanic vent, the first lavas were erupted in Pliocene times (Hawkes, 1961).

The most recent volcanic activity is represented by the Deception Island lavas, the volcano erupting most recently in 1967, 1969 and 1970 (Baker, 1972). The lavas are soda rich (Baker, 1974) and are mildly undersaturated hawaiities (Baker, 1972). Hawkes (1961) suggested the lavas originated as a local alkaline derivative from the normal andesite-rhyolite association of the South Shetland Islands, but Baker (1972) proposed they originated from progressively lower levels within a differentiated magma situated at a high level in the crust. The composition of the lavas compares favourably with those found in association with

Table 2:1 General Geology of The Western Antarctic Peninsula and South Shetland Islands

(based on Elliot (1975); Dalziel (1974); Adie (1954); De Wit (1977); Hobbs (1963) and Barton (1964).

AGE	ANTARCTIC PENINSULA	SOUTH SHETLAND ISLANDS	TECTONICS
RECENT	GLACIAL DEPOSITS AND RAISED BEACHES	DECEPTION ISLAND LAVAS (soda rich hawaiites) GLACIAL DEPOSITS AND RAISED BEACHES	
PLIOCENE TO RECENT PLIOCENE TO PLEISTOCENE	SEAL NUNATAK VOLCANICS (olivine basalt) PECTEN CONGLOMERATE	PENGUIN ISLAND GROUP (olivine basalt) PECTEN CONGLOMERATE	
OLIGIOCENE TO MIOCENE	DYKE INTRUSION JAMES ROSS ISLAND VOLCANIC GROUP (olivine basalt and palagonite tuffs) SEYMOUR AND COCKBURN ISLAND SERIES (sandstones)	DYKE INTRUSION AND VOLCANIC VENTS MIOCENE LAVAS (basaltic andesites and andesites)	unconformity faulting unconformity
CRETACEOUS	SNOW HILL SERIES (sandstones and shales)		
CRETACEOUS TO LOWER TERTIARY (105-40 my)	ANDEAN INTRUSIVE SUITE (gabbro to granite, mainly tonalites)	ANDEAN INTRUSIVE SUITE tonalites and granodiorites	uplift, erosion and deformation (open folding)
LATE CRETACEOUS 90 - 80 my		SMITH ISLAND sodic amphibole schist, ELEPHANT ISLAND dunite sepentinite sheets	high pressure - low temperature metamorphism
TITHONIAN - BARREMIAN		BYERS PENINSULA SERIES (sandstones and andesites)	
UPPER JURASSIC	CALC ALKALINE VOLCANICS (andesite-rhyolite) JURASSIC SEDIMENTS (sandstone and conglomerates)	CALC-ALKALINE VOLCANICS (andesite-rhyolite)	uplift, erosion, polyphase deformation and low grade regional metamorphism (Gondwanian orogeny) UNCONFORMITY
CARBONIFEROUS TO TRIASSIC	TRINITY PENINSULA SERIES (Greywacke-Shale) EARLY PALAEOZOIC PLUTONICS (granodiorite)	MIERS BLUFF SERIES (Greywacke-Shale)	
PRE-CAMBRIAN TO EARLY PALAEOZOIC	METAMORPHIC BASEMENT COMPLEX (orthogneisses and para-gneisses)	METAMORPHIC BASEMENT COMPLEX (garnet-hornblende schists)	unconformity

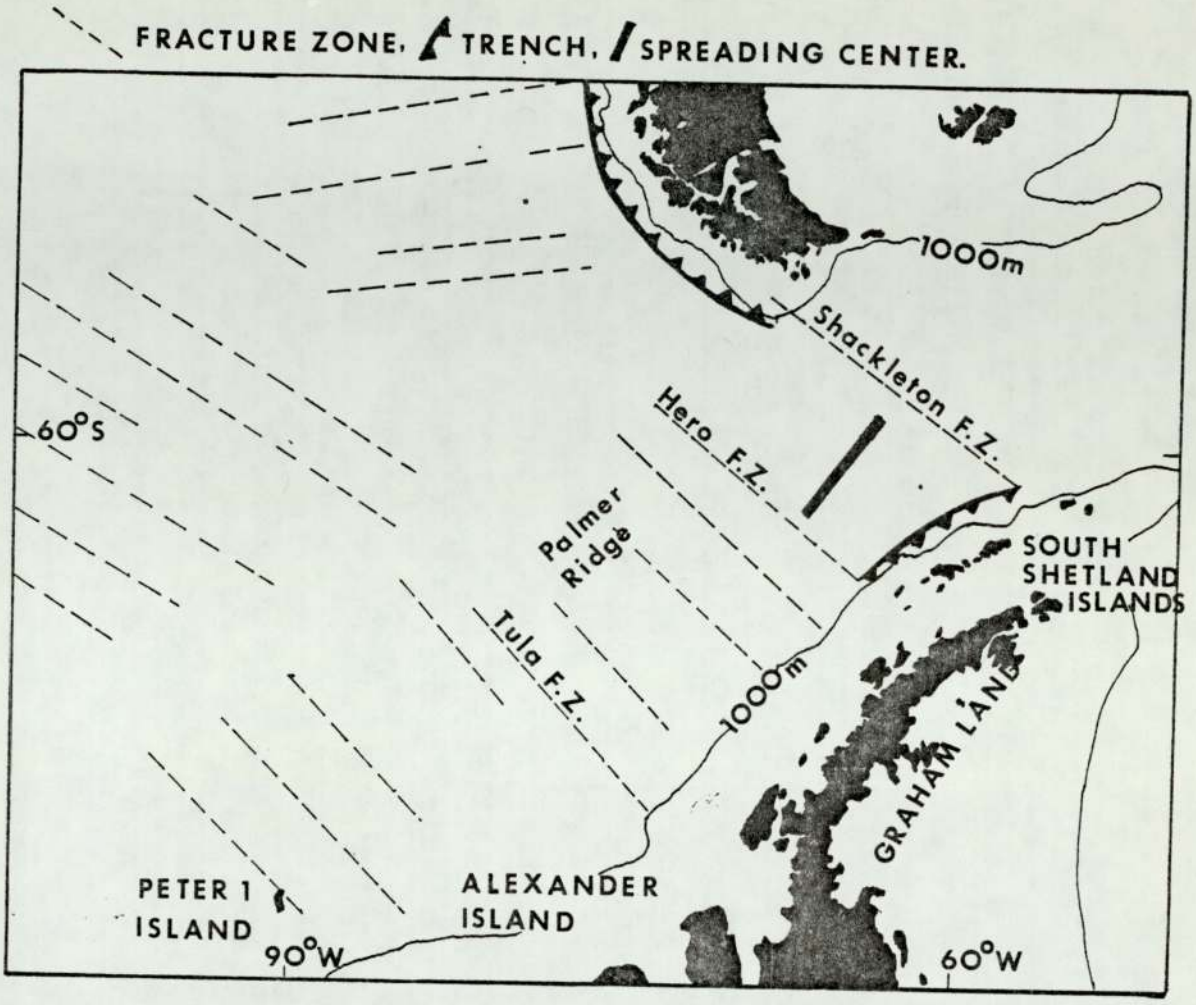

FIG 2:1 DIAGRAM SHOWING FRACTURE ZONES AND SPREADING CENTERS IN THE SOUTHEASTERN PACIFIC OCEAN, (after Herron and Tulcholke 1976).

rift valleys, faulted continental margins and islands on the crests of mid-ocean ridges (Baker, 1972).

2.2 Tectonics of the Western Antarctic Peninsula

Barrow (1831) was the first to suggest that the Andean and West Antarctic Cordilleras were once continuous, and early reconstructions of pre-Mesozoic Gondwanaland showed a straight land bridge between the two, that fragmented with the formation of the Scotia Arc (Matthews, 1959; Hawkes, 1962). The similarities in geology north and south of the Scotia Sea have been discussed by Halpern (1968) and Dott (1972), and this also indicates that a former connection between the two continents was once present or there was at least a similarity in tectonic environments. Katz (1972), however, concluded that the Antarctic Peninsula and Andean Cordillera evolved along different structural patterns and suggested the Scotia Sea developed as a composite feature by juxtaposition of tectonic elements of entirely different origin and character and has undergone only partial bending. However, as pointed out by Dalziel (1974) changes in tectonic style take place along the Andean Cordillera itself, consequently the differences either side of the Scotia Sea would not preclude the original continuity of the two cordilleras. Dalziel and Elliot (1971 and 1973) considered that the Andean Cordillera was a rectilinear feature continuing into the Antarctic Peninsula until at least the late Cretaceous. By proposing the closing up of the Cenozoic spreading centres in the Scotia Sea which have evolved in the last 40 my (Baker, 1970), Barker and Griffiths (1972) have suggested the original connection between the two continents was cusp-shaped, although Dalziel and Elliot (1973) indicated this configuration is open to doubt as it leaves the South Georgia platform on the Atlantic side of the Andean Cordillera. De Wit (1977) proposed, however, that the central part of the Scotia Sea is Cretaceous in age and that the Antarctic Peninsula - South America join was originally rectilinear.

The development of the marginal basin in southern South America, and the formation of the North and South Scotia ridges occurred due to relative motion between the Antarctic Peninsula Plate and the South American Plate.

At the time of the opening of the South Atlantic (late Jurassic to early Cretaceous) the Antarctic Peninsula was attached to the South American Plate. The clockwise rotation of East Antarctica resulted in the opening of the Weddell Sea (Barker and Griffiths, 1977). De Wit (1977), however, proposed the Weddell Sea is a back arc basin, a conclusion also suggested by the presence of pillow lavas on James Ross Island (Bibby, 1966).

Recent work proposed that Western Antarctica, until at least the Palaeogene, was composed of a number of small plates separated from East Antarctica (Herron and Tucholke, 1976). In the Cenozoic the Andean-West Antarctic Cordillera was disrupted to form the Scotia Arc, and the Antarctic Peninsula transferred from the South American to East Antarctic Plate, which continued rotating clockwise, thus opening the Scotia Sea (Baker, 1974).

The oroclinal bending of the Antarctic Peninsula appears to have taken place prior to the intrusion of the Tertiary plutonic rocks (Dalziel et al, 1973), although a plate linkage mechanism could also account for the bending as in the North American Cordillera (Heptonstall, 1977). Both before and after the break up of Gondwanaland (late Mesozoic) Pacific Oceanic crust was consumed along the western margin of the Cordillera, or at least since the Jurassic (Suarez, 1976). Indeed, bathymetric contours show the presence of a deep trench to the north west of the South Shetland Islands (Davey, 1972). Magnetic anomalies on the Pacific Sea floor indicate subduction has been occurring here for at least the last 20 my (Herron and Tucholke, 1976), with the accompanying calc-alkaline volcanism persisting well into the Tertiary (Barker and Griffiths, 1977). Seismic surveys indicated the northern and southern extremeties of the

South Shetland trench are bounded by transcurrent faults or fracture zones (Herron and Tucholke, 1976) (Fig. 2:1).

The generation of oceanic crust on the sea floor west of the Antarctic Peninsula began at the latest in the Late Cretaceous (76 my) and ceased during the Miocene when the spreading centre was subducted beneath the Antarctic Peninsula. However, the segment that generated the plate south of Alexander Island was subducted in the Paleocene (Herron and Tucholke, 1976). The age of the oceanic basement generated at the Aluk ridge is late Cretaceous, but younger ages obtained at other sites suggested a phase of Miocene intraplate volcanism (Herron and Tucholke, 1976). Subduction seems to have been more rapid south of the Tula fracture zone which passes under the Antarctic Peninsula approximately where it widens in area (Fig. 2:1). This rapid subduction relative to the segment of plate north of this fracture zone would have led to greater volumes of volcanic outpourings and magma, and could account for the greater width of the Antarctic Peninsula, south of the Wordie Ice Shelf. Sediments have now infilled the trench and there is little evidence of its former existence from either seismic or bathymetric data (Vanney and Johnson, 1976).

In more recent times the South Shetland Islands separated from the Antarctic Peninsula by a process of back-arc extension along the Bransfield Strait as a corollary to subduction at the South Shetland Trench in the Early Tertiary (Barker and Griffiths, 1972), although it has been suggested to be a fault graben (Gonzalez-Ferran, 1972). The West Antarctic Peninsula has been affected during the Mesozoic and Cenozoic by tectonic activity related to convergent plate boundaries, strike slip faulting and normal faulting. The major phase of faulting appears to be post-Jurassic and pre-Andean, although there seems to have been a widespread phase of post-Miocene faulting in the South Shetland Islands which upfaults the (?) Jurassic volcanics against the Miocene volcanics on King George Island (Barton, 1964).

There appear to have been at least three phases of deformation in the Antarctic Peninsula, a polyphase deformation affecting basement complex rocks (Pre-Cambrian), a period of polyphase deformation with dominant overfolding from the north west and low grade regional metamorphism that affected the Trinity Peninsula Series, probably associated with the break up of Gondwanaland in the late Mesozoic, and a phase of broad open folding and faulting associated with the intrusion of Andean plutons during the Cretaceous to Tertiary (Dalziel and Elliot, 1973).

It seems that the fragmentation of Gondwanaland was accompanied in the Antarctic Peninsula by the development of calc-alkaline volcanism and batholith emplacement associated with eastward dipping subduction of the Pacific Plate beneath the Antarctic Peninsula. The lack of late Mesozoic deformation along the Antarctic Peninsula was probably due to the absence of a marginal basin (De Wit, 1977).

CHAPTER 3

THE "QUARTZ-PYRITE" ROCKS OF THE SOUTH SHETLAND ISLANDS

3.1 Introduction

The "Quartz-Pyrite" rocks of the South Shetland Islands occur mainly on King George Island, but also on Half-Moon Island which lies at the south western end of McFarlane Strait (Fig. 3:1, 3:2). Broadly they can be divided into three alteration types on the basis of mineralogy and chemistry; advanced argillic (quartz-alunite-kaolinite-pyrite), intermediate argillic (quartz-carbonate-kaolinite-pyrite) and phyllic alteration (quartz-muscovite-pyrite). Areas of intense propylitic alteration (quartz-muscovite-chlorite-pyrite) are present in some areas, which are not true "Quartz-Pyrite" rocks, but appear to be related to them. All the deposits are related mineralogically, chemically and genetically to the Tertiary intrusive rocks, and seem to represent hydrothermally altered (?) Jurassic lavas, tuffs and Tertiary plutonic rocks. Often the lavas surrounding these deposits show weak propylitic alteration.

In the past the term "Quartz-Pyrite lode" has been used to describe these deposits (Ferguson, 1921). The present investigations have shown, however, that they are not lodes, but the two minerals common to all the alteration types are quartz and pyrite, consequently the term "Quartz-Pyrite" has been retained as it encompasses all the rock types. These deposits probably represent alteration zones associated with the peripheral areas of porphyry copper-molybdenum deposits.

3.2 Previous Work

The "Quartz-Pyrite" rocks of the South Shetland Islands were first studied by Ferguson (1921) who described them as "lodes", a view also held by later authors (Hawkes, 1961 (based on field work by Jardine); Barton, 1964). Barton (1963) suggested these deposits formed along shatter zones as mineralised breccia in pre-Tertiary faults. Deposits

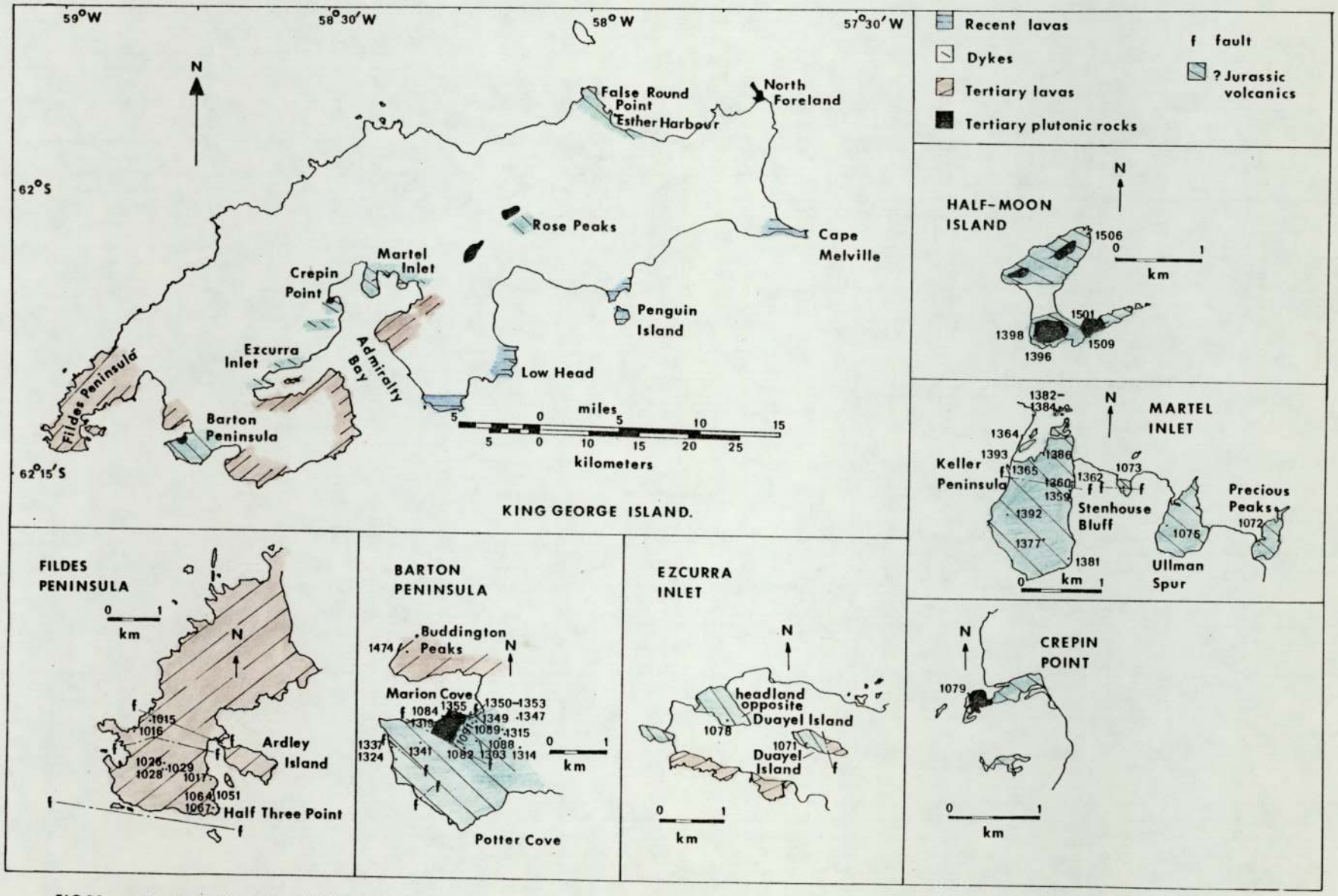

FIG.3:1 MAP SHOWING SPECIMEN LOCATIONS AND GENERAL GEOLOGY IN KING GEORGE ISLAND, SOUTH SHETLAND ISLANDS. (based on data by Hawkes (1961) and Barton (1964)). INSERTS SHOW DETAIL OF AREAS INDICATED ON THE CENTRAL MAP.

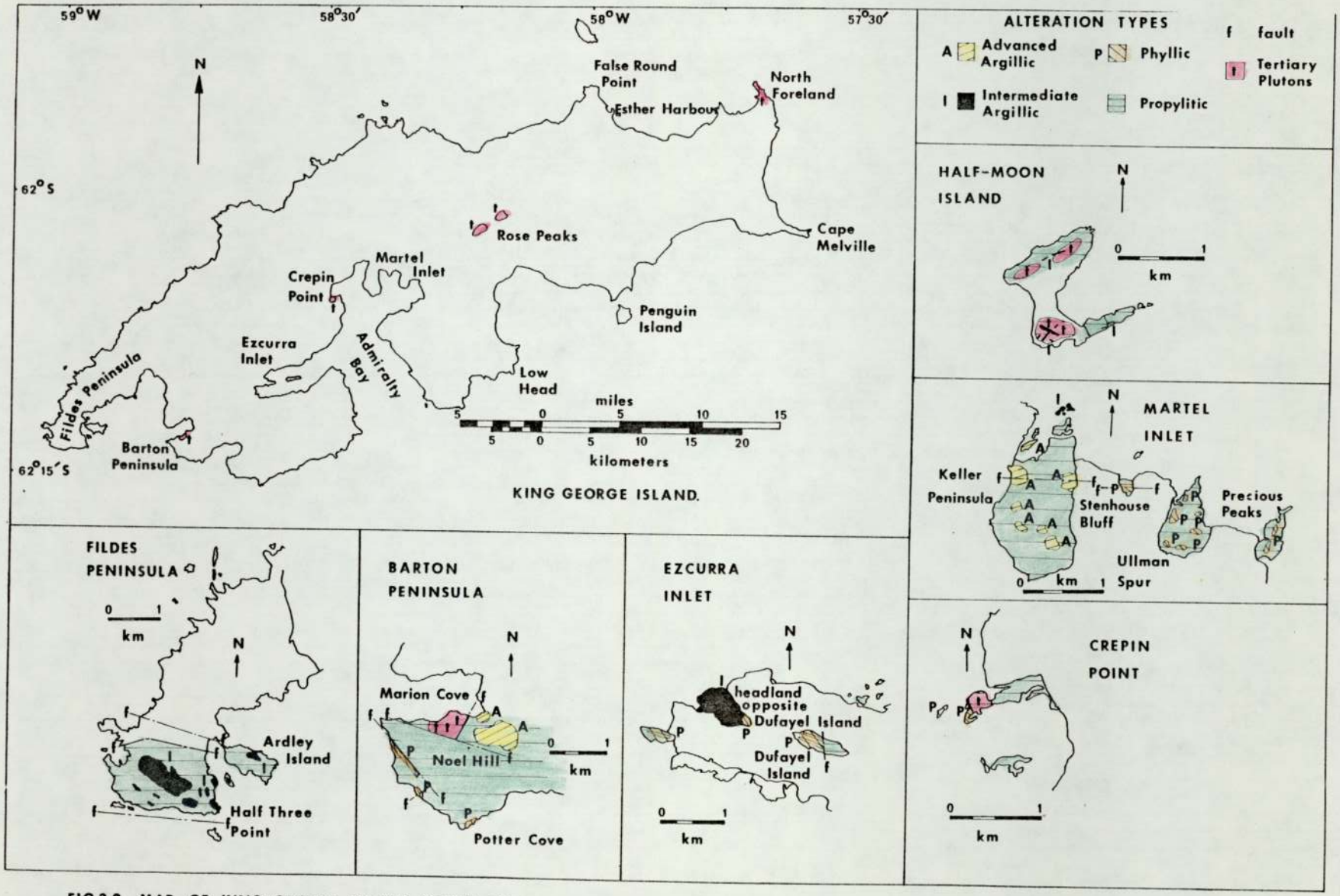

FIG.3:2 MAP OF KING GEORGE ISLAND, SOUTH SHETLAND ISLANDS. INSERTS SHOW DETAIL OF ALTERATION TYPES IN AREAS INDICATED ON CENTRAL MAP.

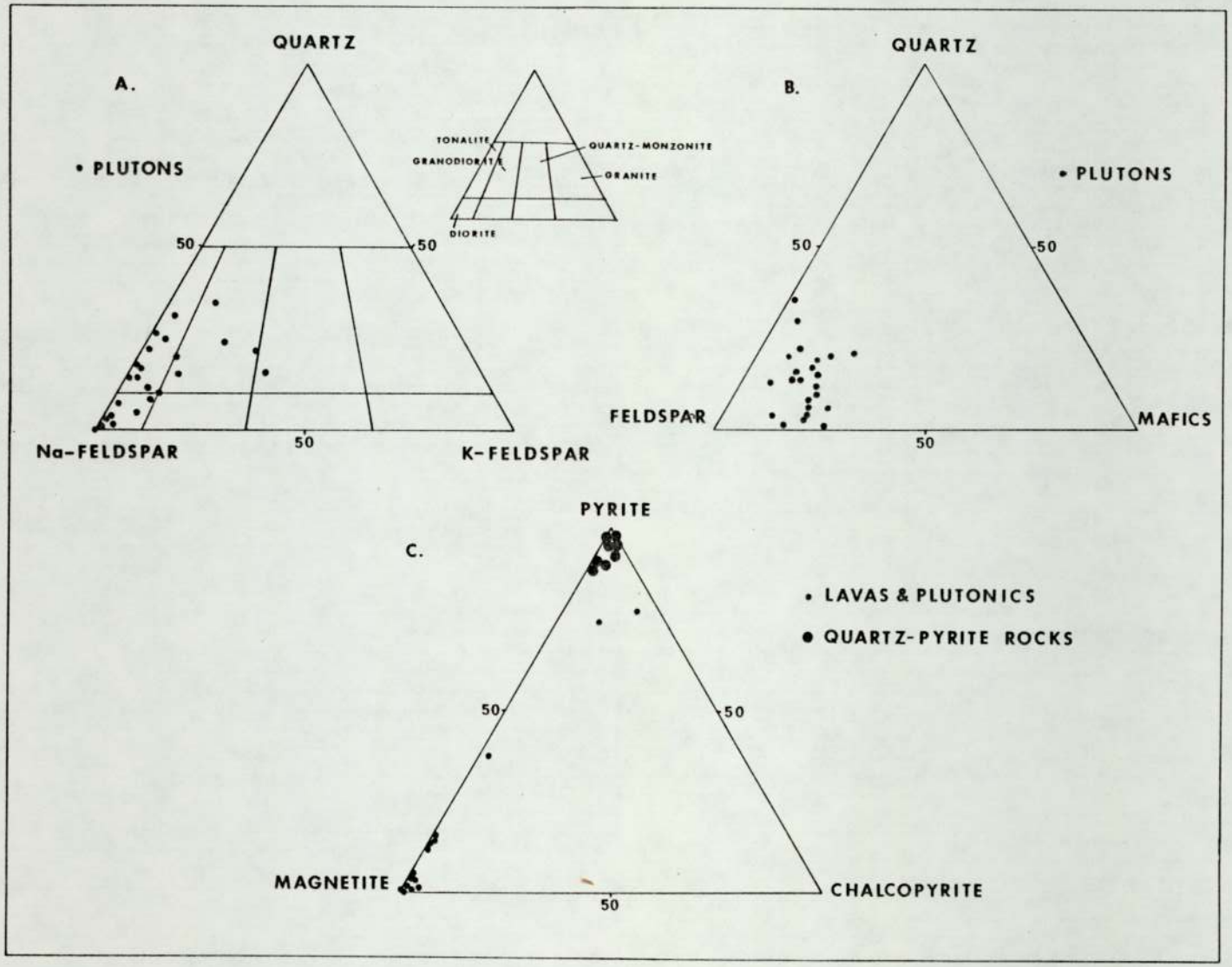

Fig 3:3 TERNARY DIAGRAMS OF MODAL DATA, KING GEORGE ISLAND. A, quartz-sodium feldspar-potassium feldspar; B, quartz-feldspar-mafics (FOR PLUTONIC ROCKS); C, RATIO OF OPAQUE MINERALS (pyrite-chalcopyrite-magnetite) IN PLUTONIC ROCKS AND ?JURASSIC LAVAS.

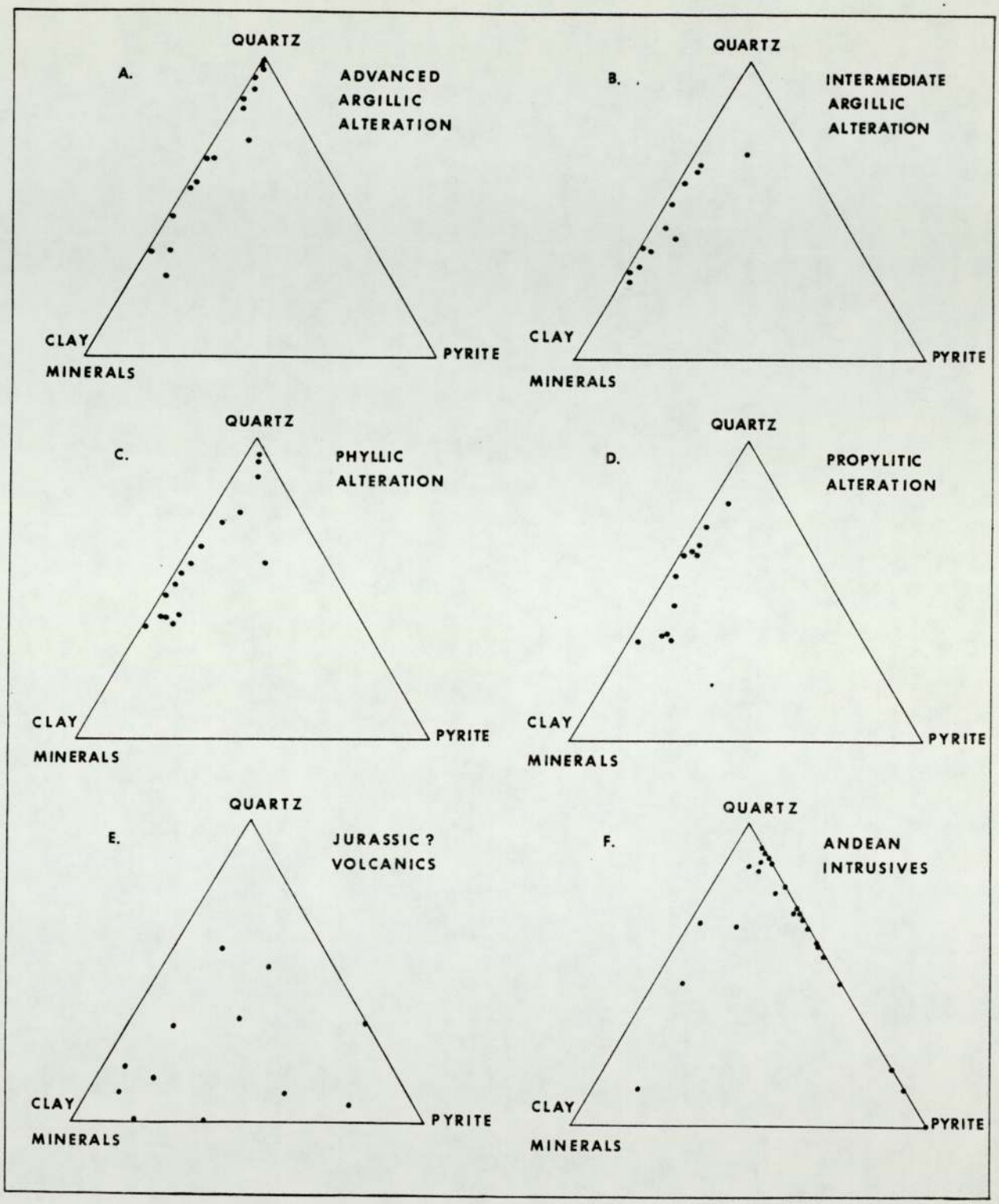

Fig 3:5 TERNARY PLOTS OF MODAL DATA FOR VARIOUS ROCK TYPES, KING GEORGE ISLAND. PLOTS OF QUARTZ–PYRITE–CLAY MINERALS FOR 1, ALTERATION ZONES ('QUARTZ–PYRITE' ROCKS) A, advanced argillic; B, intermediate argillic; C, phyllic; D, propylitic; 2, E, ?Jurassic lavas; F, Tertiary plutonic rocks.

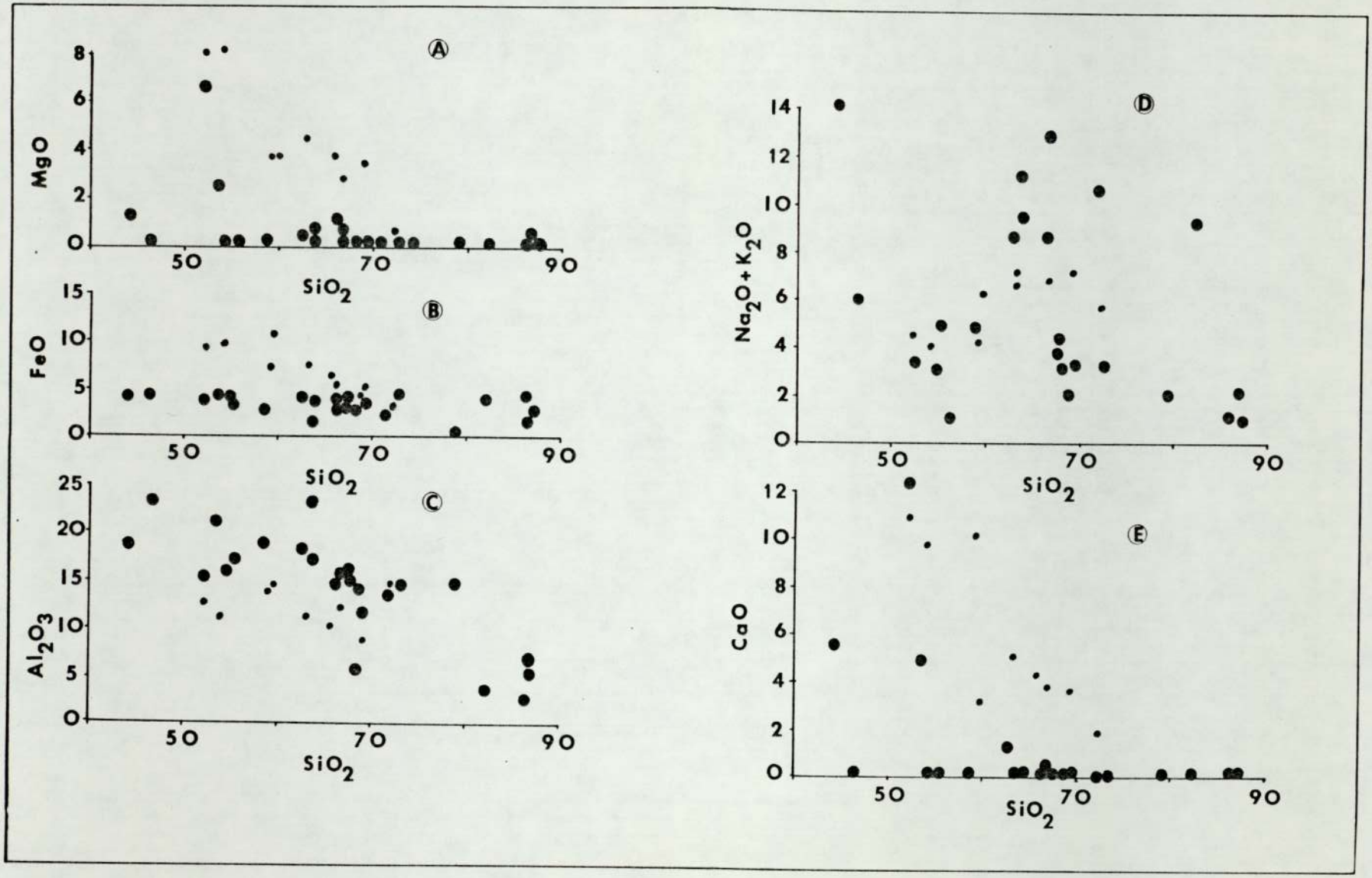

Fig3:6 CHEMICAL VARIATION DIAGRAMS FOR LAVAS (•) AND QUARTZ-PYRITE ROCKS (●); Ⓐ, MgO; Ⓑ, FeO; Ⓒ, Al_2O_3; Ⓓ, $Na_2O + K_2O$; Ⓔ, CaO; VERSUS SiO_2, KING GEORGE ISLAND.

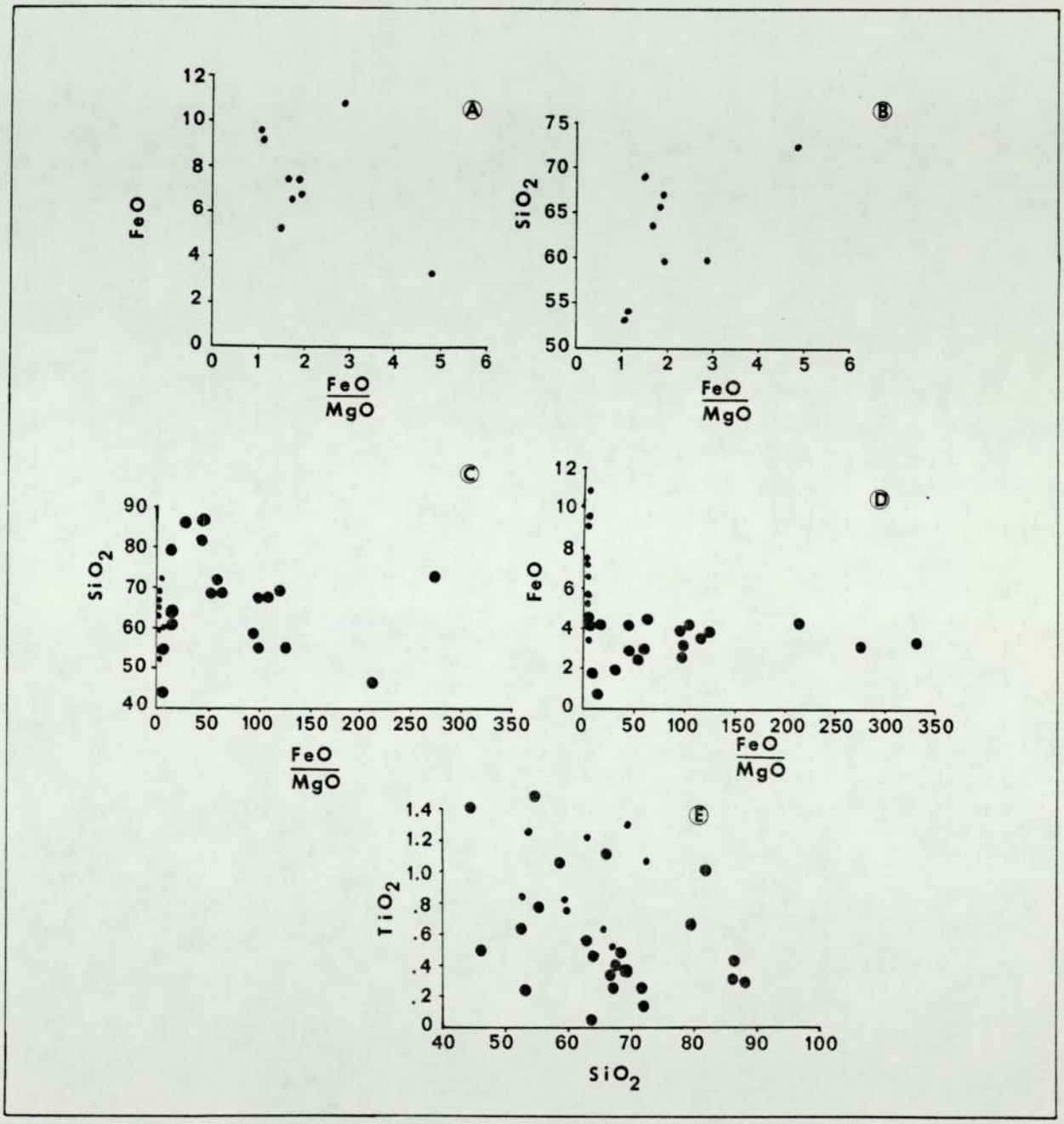

FIG.3:7 PLOTS OF MAJOR ELEMENT OXIDES (Ⓐ, FeO; Ⓑ, SiO_2 for ? Jurassic lavas (•), AND Ⓒ, SiO_2; Ⓓ, FeO for ? Jurassic lavas (•) and 'Quartz-Pyrite' rocks (●)), VERSES $\frac{FeO}{MgO}$ RATIO. Ⓔ, IS PLOT OF TiO_2 VERSUS SiO_2 FOR ? Jurassic lavas and 'Quartz-Pyrite' rocks. KING GEORGE ISLAND.

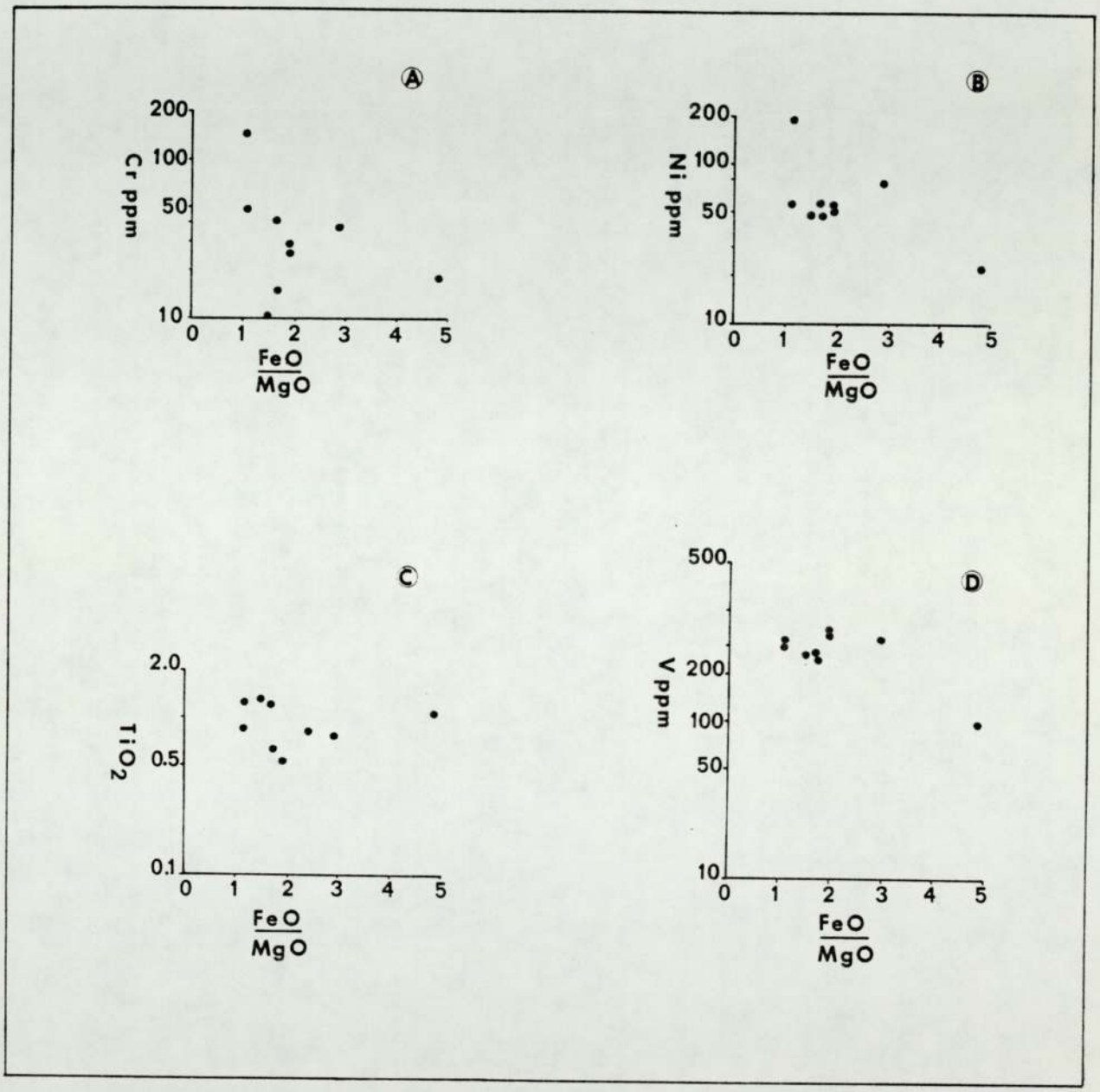

FIG.3:7 DIAGRAMS ILLUSTRATING VARIATION OF TRACE ELEMENTS WITH $\frac{FeO}{MgO}$ RATIO FOR ?JURASSIC LAVAS, KING GEORGE ISLAND. A, Cr; B, Ni; C, TiO_2 (major oxide); D, V.

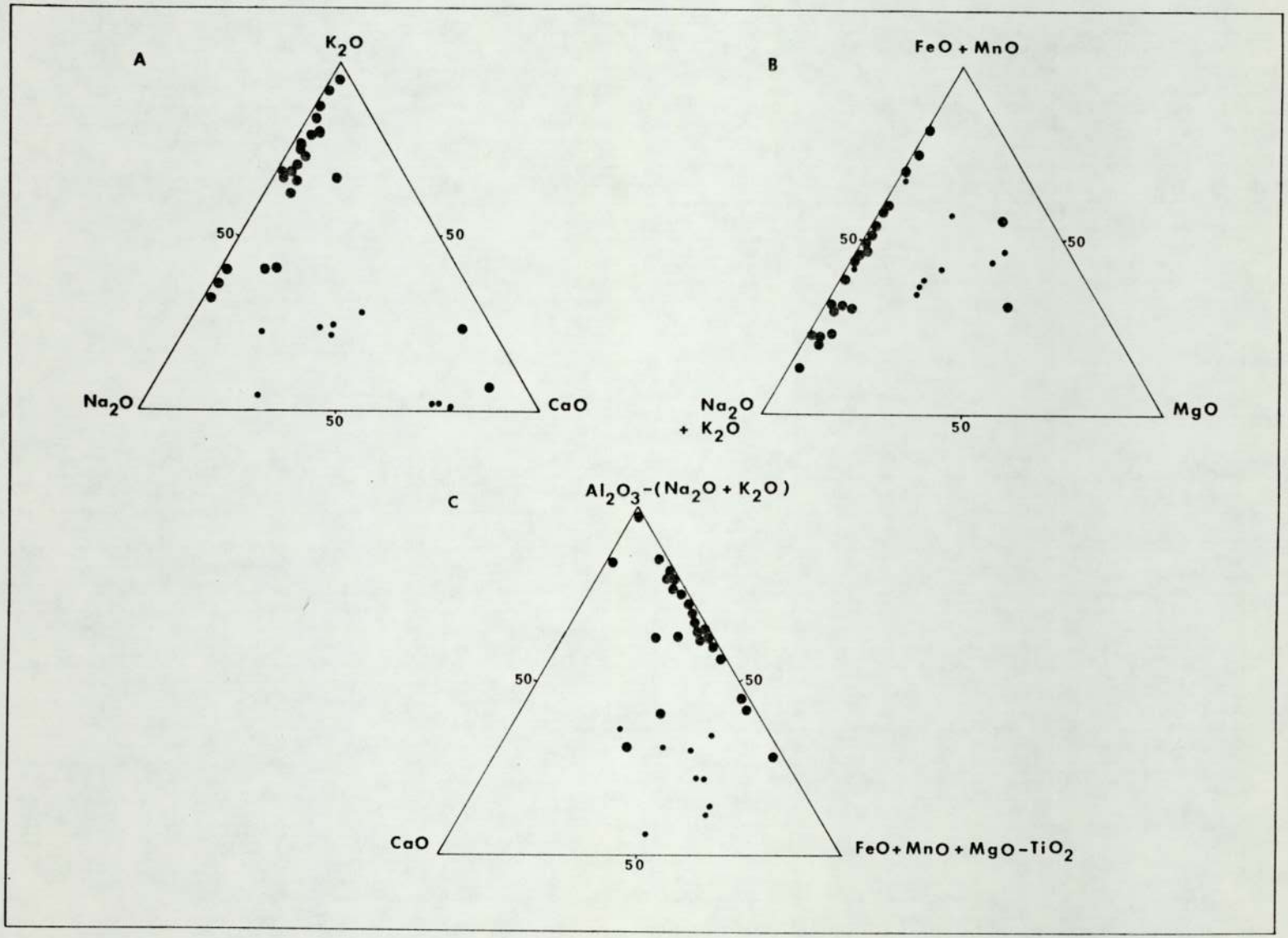

FIG.3:8 TERNARY PLOTS OF CHEMICAL DATA FOR ?JURASSIC LAVAS(•) AND 'QUARTZ-PYRITE' ROCKS(●).
A, K_2O-Na_2O-CaO; B, Na_2O+K_2O-FeO + MnO-MgO; C, CaO-$Al_2O_3-(Na_2O+K_2O)$-FeO + MnO + MgO-TiO_2.

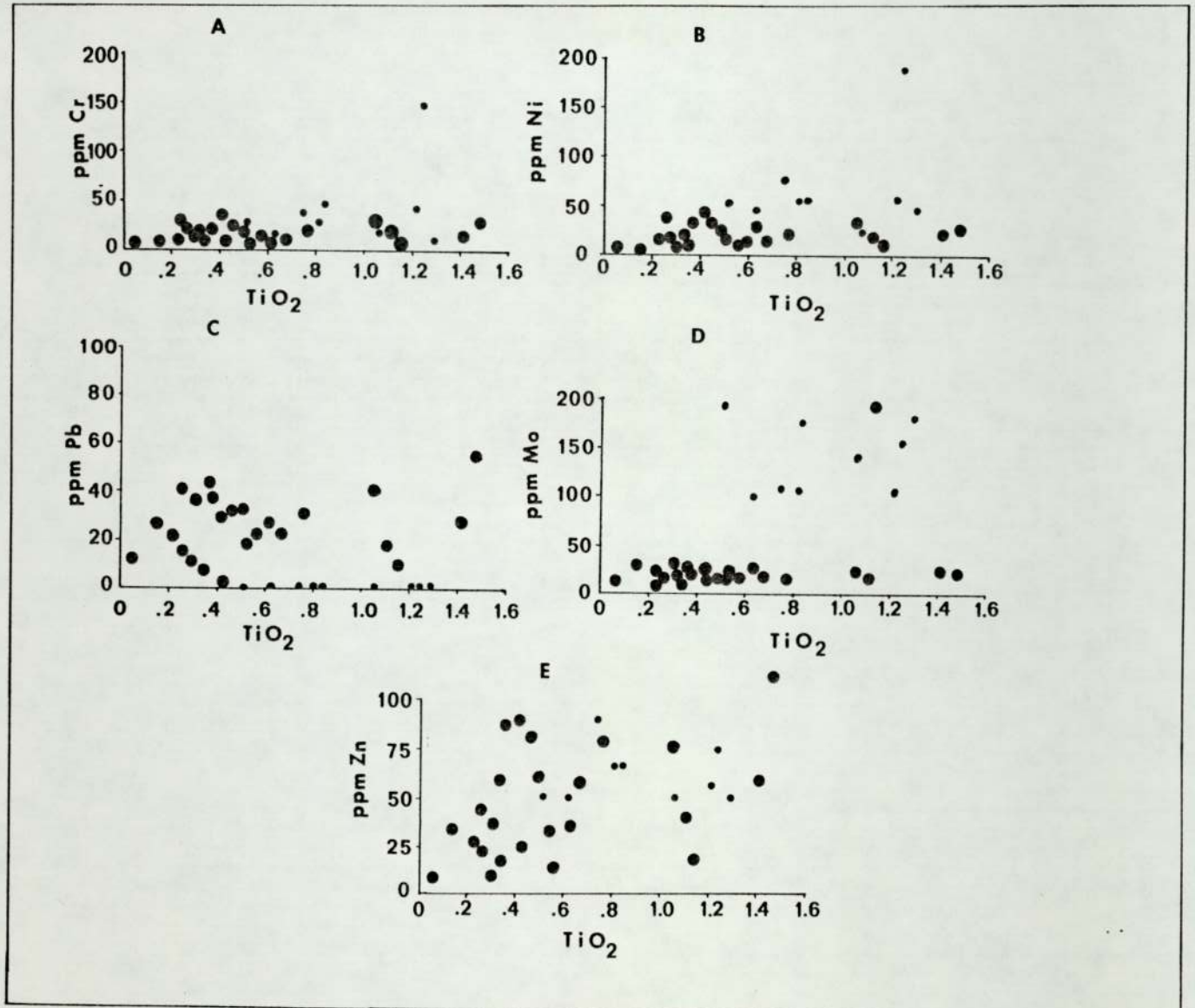

FIG.3:9 PLOTS OF TRACE ELEMENTS (A, Cr; B, Ni; C, Pb; D, Mo; E, Zn) VERSES % TiO_2 FOR ?JURASSIC LAVAS (•) AND 'QUARTZ-PYRITE' ROCKS (◉), KING GEORGE ISLAND.

on Keller Peninsula, King George Island containing pyrite, gypsum, (?) alum and (?) rock salt have been suggested to be "fumarolic vents" (Mueller, 1963). Altered tuffs on Fildes Peninsula, King George Island have been regarded as pyritised pyroclastics (Barton, 1964), volcanic conglomerates (Schauer and Fourcade, 1963) and carbonitized and mineralised pyroclastics (Grikurov, et al 1968). More recent work has postulated the "Quartz-Pyrite" rocks represent "volcanogenic massive sulphide" deposits effected by faulting and plutonism, or hydrothermal solutions in the faulted roof of a batholithic complex (Rowley and Pride, 1978).

3.3 Field Relationships of the "Quartz-Pyrite" Rocks

Generally, these rocks have a creamy-brown to greenish-yellow colour (plate 3:1) due to surface oxidation of pyrite to limonite and jarosite, although a few centimetres beneath this outer crust is fresh, greyish white "Quartz-Pyrite" rock. They are generally blocky, massive rocks, although in places brecciation of the lavas had occurred prior to the alteration process (1359.1, plate 3:2) with individual fragments between 5 to 50 millimetres. Where the deposits have formed by replacement of localised, minor fault breccias, they are often confined to the southern side of such faults.

Although generally fresh, in places frost shattering has created a creamy coloured gossan composed of coarse fragments of altered rock in a matrix of finer-grained material, with the exposed surfaces often stained with pyrolusite, calcite and chalcedony.

The alteration can be found adjacent to impermeable barriers such as the base of a sill, or a thick lava flow (Keller Peninsula, 1364) presumably caused by "ponding" of the solutions. In places a concentric banding can be found in these rocks (1089.3) identical to structures in the surrounding lavas (1314.1) a clear indication of their replacement origin (plate 3:4). These are similar to "onion" structures described from Japan (Iawaskai, 1963). Where the contact between these rocks and

the surrounding lavas is exposed, there is generally a gradation between the two over 0.2 - 10 metres. Tuffs surrounding these deposits often show more extensive alteration than the blocky lavas.

Many of the areas of phyllic alteration have a linear form due to alteration along well defined faults. In places these faults (about 3 metres wide) have been infilled by euhedral vein quartz containing euhedral pyrite (DufayelIsland, plate 3:16). Brecciated wall rock fragments also occur often cemented by ferroandolomite, calcite and ferroancalcite (1071.4). The adjacent wall rock has been sericitized and silicified up to 10 metres from the fracture, although in places epidotised lavas occur adjacent to the fault. This probably reflects the varying permeability of the wall rock to the circulating solutions. Amethystine quartz has also been found.

Miocene tuffs (Barton, 1964) on the Headland Opposite Dufayel Island have also been affected by the "Quartz-Pyrite" alteration. The presence of stringers of quartz and carbonate in these rocks suggest the process was contemporaneous with the deposition of the tuffs.

On Half-Moon Island andesitic dykes and sills intruded into late Cretaceous (105 my, Grikurov et al, 1968) plutons and surrounding lavas have been affected by hydrothermal solutions and show intermediate argillic alteration (plate 3:13). The surrounding plutonic rocks and lavas are unaffected, although fragments of the altered dykes occur enclosed by quartz and ferroandolomite in a central fracture zone running through many of these rocks. The alteration is most intense around these fractures and decreases towards the edges of the dykes.

Many of the areas showing hydrothermal alteration often contain late stage veinlets of quartz, ferroandolomite, ferroancalcite and calcite (1071.5). Stratigraphically beneath many of these areas are veins (less than 5 cm wide) composed of quartz, chalcopyrite and pyrite. Halos of secondary minerals occur around many of these deposits, generally as vesicle infillings in the relatively unaltered lavas. They are mainly white

fibrous stilbite, green apophyllite, natrolite, ferroandolomite, ferroancalcite, calcite, siderite, chlorite, chalcedony and agate (plate 3:14, 3:15). Veinlets of red and green jasper are common.

Intense propylitic alteration of the Palaeocene (57 my, Grikurov et al, 1972) granodiorite and surrounding lavas on Barton Peninsula is present around fracture zones on Eastern Marion Cove. The fresh white-grey granodiorite has been altered to a blue-grey coloured rock. About 200 metres above and 100 metres laterally from this alteration the granodiorite and lavas show phyllic alteration. This suggests the areas of intense propylitic alteration represent the lower extremities of the "Quartz-Pyrite" rocks, where the aqueous fluids had little oxidising power. Around many deposits the (?) Jurassic lavas and Tertiary plutons show weak propylitic alteration, and on Half-Moon Island veinlets of quartz, epidote and pyrite are present often surrounded by halos of chlorite, traversing the plutons and lavas. "Pods" (25 mm wide) of epidote and pyrite occur in the plutons often with a sericitised margin (1509). Minor disseminated pyrite and rare chalcopyrite (with overgrowths of pyrite) occur around these veinlets. On Keller Peninsula weakly propylitized tuffs contain cubes of pyrite (less than 10 mm) and euhedral calcite (less than 20 mm).

A study of Ferguson's (1921) specimens indicate the presence of "Quartz-Pyrite" rock at Ester Harbour, on the north coast of King George Island.

3.4 Petrology of the "Quartz-Pyrite" Rocks

On the basis of petrology, four types of alteration assemblages have been recognised, and are described below:

3.4.1 Advanced Argillic Alteration

This alteration type occurs on Northern Barton and Keller Peninsulas on King George Island (Fig. 3.1 and 3.2).

Petrographically, this rock type consists of a granular mosaic of microcrystalline quartz (less than 0.2 mm), often showing undulose extinction, which presumably represents a recrystallized silica gel (Iawo, 1970; Anderson, 1935). Crystal aggregates of alunite and natroalunite also occur (plate 3:5) which are pseudomorphing feldspar (3 mm, 1315.1; 1359.9) although some relict feldspars are present (less than 0.3 mm, 1315.2). X-Ray diffraction measurements of {102} reflections indicate the alunite to natroalunite ratio varies between 4:1 to 1:4 (using the data of Cunningham and Hall, 1976).

In places pyrophyllite is the main alteration phyllosilicate (1089.2, 0.4 - 0.2 mm) and is frequently associated with porphyroblasts of fluorite, containing inclusions of pyrite, rutile and quartz. Veinlets of quartz traverse these rocks (0.1 - 0.2 mm, 1091.4) although some contain abundant alunite (1315.1, plate 3:6), an indication that alunite can be deposited from solution as suggested by Anderson (1935). Areas of fine-grained kaolinite and minor dickite (less than 0.1 mm) occur and often seem to be replacing former ferromagnesian minerals (1393.1). Native sulphur is present in intergranular masses and lath shaped cavities left by leached feldspar phenocrysts (2 - 0.5 mm, 1089.3, plate 3:7).

Minor anhedral rutile, sometimes skeletal after ilmenite (less than 0.1 mm) is disseminated through these rocks, the pale brown flecks being clearly visible in the hand specimen. Rare subhedral gypsum, barite, diaspore and partially resorbed amphibole (plate 3:8) are present (1359.8, 1359.11 and 1362.1). Cavities present in these rocks probably represent leached gypsum. Euhedral to subhedral pyrite (less than 0.3 mm) is the main opaque phase, and sometimes contains inclusions of rutile (1359.7). It is also frequently surrounded by alunite laths (1359.7), and often occurs around grain boundaries of quartz (1362.5, plate 3:23). The proportion of pyrite and alunite increase towards the centre of these deposits. Some veinlets of quartz and pyrite cut the rocks (1359.9).

Modal analyses of the rocks (table 3.8A) indicate quartz (25.3-96.3%) and alunite (nil to 63%) are the major phases present.Pyrophyllite varies from nil to 62%,with rutile and pyrite less than 3.5 and 0.3-9.8% respectively. Fluorite,gypsum,native sulphur,diaspore,resorbed amphibole and plagioclase are generally less than 5%.Kaolinite,the major clay mineral present varies from nil to 38%.

3.4.2. Intermediate Argillic Alteration.

Andesitic rocks showing this type of alteration occur on Fildes Peninsula,Headland Opposite Dufayel Island and Northern Keller Peninsula, King George Island and Half-Moon Island (Fig 3.1 and3.2).

Petrographically,they consist of anhedral ferroandolomite porphyroblasts (1.5-0.2mm,plate 3.9) and granular aggregates of quartz showing undulose extinction.Quartz sometimes forms a granular ring around ferroandolomite or kaolinite crystals (plate 3.10),and may represent vesicle infillings.Vugs also occur in these rocks containing euhedral ferroancalcite (15- 5mm) and barite crystals (4mm,1384).Veinlets of ferroandolomite frequently traverse these rocks (5-0.1mm,1382.1B,1064).In some instances aggregates of quartz crystals occur surrounded by ferroandolomite (1024.5) probably representing altered clasts.Banding of lenticular quartz (2-0.5mm,1051.1) or ferroandolomite (1382.1) is present parallel to the bedding in some altered tuffs.In tuffs on the Headland Opposite Dufayel Island,stringers of $2M_1$ muscovite,quartz and ferroandolomite occur parallel to the bedding and contain subrounded pyrite, magnetite,goethite and rutile (1078.6C).Later quartz-ferroandolomite veinlets cut these,which contain only euhedral pyrite (plate 3.11 and 3.12).The groundmass of these rocks consists of microcrystalline quartz,carbonate and kaolinite with minor $2M_1$ muscovite,much of the kaolinite probably replacing former ferromagnesian minerals.Minor anhedral rutile (less than 0.06mm) and rare euhedral apatite (less than 0.03mm,1028) are also presemt.Relict plagioclases occur (2-0.5mm,1383.2) frequently replaced by quartz, ferroandolomite or $2M_1$ muscovite (1386.1).

The dykes showing intermediate argillic alteration on Half Moon Island are similar petrographically, to the above, but where the alteration is less intense, relict igneous textures from the dykes can be seen with subparallel aligned plagioclase laths (An_{35-45}) often partially replaced by quartz (1396.5) or carbonate. Subhedral pyrite is also associated with the carbonate (1396.6). The tonalite wall rock to these dykes shows few signs of alteration of the silicate minerals, but magnetite shows alteration to hematite.

The veins occurring stratigraphically beneath these alteration zones are composed of quartz, chalcopyrite and pyrite with ferroandolomite occurring as a late stage infilling to these fractures (1067.1). Where the minerals were presumably oxidised by oxygen rich fluids, veinlets of quartz, chlorite, ferroandolomite, tenorite, chalcocite and hematite are present (1017.2A; plate 3:27, 3:28). Around these are small veinlets of chalcopyrite and quartz, which are cut by quartz and ferroandolomite veinlets containing pyrite.

Modal analyses indicate quartz (12.7 - 50.2%) kaolinite (nil to 35.7%) and carbonate (9.3 - 56.2%) are the major phases present, although in some rocks muscovite is the main phyllosilicate (nil to 53.4%). Plagioclase varies from nil to 37.5% with rutile and pyrite present in small amounts, less than 2.8% and 0.5 - 4.7% respectively (table 3.8B).

3.4.3 Phyllic Alteration

This is the most widespread of the alteration types occurring in the andesitic lavas, and is present on Southern Barton Peninsula, Dufayel Island (plate 3:14), Crepin Point, Stenhouse Bluff, Ullman Spur and Precious Peaks.

Petrographically these deposits consist of partially resorbed plagioclase laths (An_{40-35}, <1mm) showing alteration to 2M, muscovite and anhedral quartz. The quartz occurs in two sizes; greater than 0.2 mm and less than 0.05 mm (plate 3:17, 1073.7) and often shows undulose extinction.

Acicular rutile is sometimes present in the quartz. $2M_1$ muscovite is present interstitially to the quartz and often seems to be replacing former ferromagnesian minerals (1337.7). Former vesicles have a rim of granular quartz and an infilling of $2M_1$ muscovite (plate 3:18, 1073.1A). Minor amounts of subhedral barite, granular zircon and epidote are present (1073.7) with some late stage anhedral carbonate. In places chlorite occurs replacing ferromagnesian minerals (1075.12). Laumontite (1.5 - 0.1 mm) is present in some rocks replacing feldspar and as veinlets in altered tuffs (1072.7A). Sparse interstitial jarosite and rare kaolinite and montmorillorite (1319.1) can also be found. Where this alteration has affected the granodiorites and tonalites partially resorbed biotite laths occur pseudomorphed by muscovite or chlorite (1303.1).

Modal analyses show this alteration type consists predominantly of quartz (26.3 - 58.3%) and muscovite (8.4 - 55.8%) with plagioclase (nil to 7.3%) and laumontite varying from nil to 62.5%. Rutile is less than 1.3% with pyrite 0.4 to 23.7%. (Table 3:8C)

3.4.4 Propylitic Alteration

Propylitic alteration is present on Barton Peninsula where it affects the granodiorite and surrounding lavas and (?) shales.

Petrographically, the altered rocks consist of a granular mass of anhedral quartz (some pseudomorphing feldspar) and plagioclase (An_{0-8}), in a groundmass of 2M, muscovite, chlorite (in places showing alteration to muscovite) and anhedral quartz (less than 0.1 mm, 1351.2). Corroded feldspars also occur showing alteration to 2M, muscovite and anhedral carbonate (1 - 0.3 mm, 1350.2). Carbonate porphyroblasts are also present and sometimes replace uralite (1353.1). Chlorite laths replace biotite, although this alteration decreases in intensity away from the fractures (1353.2) as does the alteration of magnetite to hematite, and hornblende to uralite. Granular epidote is also present.

Where the alteration has affected shaley horizons, the rock consists of granular quartz, chlorite laths and veinlets (X.R.D. indicates daphnite based on data by Hallimond, 1938) which often occur in clusters with muscovite, in a matrix of fine-grained $2M_1$ muscovite (1352.2, 1352.3, plate 3:19). Minor sphene, euhedral apatite, zircon and feldspar also occur (0.5 - 0.1 mm) as do microveinlets of muscovite (1319.1) and stringers of quartz. A blue subhedral, dichroic (pink to blue, plate 3:20), ferrian dravite tourmaline occurs in the rock up to 10 metres from the fracture zone and is often closely associated with pyrite and pyrrhotite. This tourmaline could be the "blue amphibole" described by Tyrrell (1921). Where the shale has suffered thermal metamorphism by the Tertiary granodiorite, subhedral andalusite is present (less than 0.2 mm), which seems unaffected by the alteration process.

Modal analyses indicate quartz (25.7 - 70.1%), muscovite (nil - 55.1 %), chlorite (0.3 - 19.5%) and plagioclase (nil to 53.2%), are the most abundant phases in these rocks. Kaolinite and carbonate are less than 11%, with epidote and tourmaline less than 3.4%. Rutile, uralite and amphibole are generally 3% or less. Pyrite and pyrrhotite vary from 0.1 - 12.9% (table 3:8D).

Summary of Modal Analyses of "Quartz-Pyrite" Rocks

The minerals that are common to all alteration types are quartz, clay minerals (kaolinite and muscovite) and pyrite. Ternary plots of the modal data for the "Quartz-Pyrite" rocks, (?) Jurassic lavas and Tertiary plutonic rocks, with these minerals as end members (Fig. 3:5) show that during the alteration process the proportion of quartz and clay minerals increase relative to pyrite. This suggests that the main effect of the alteration process is to convert silicate minerals to quartz and phyllosilicates, and simply to convert magnetite in the lava to pyrite (Fig. 3:3C) with little introduction of iron by the hydrothermal solutions.

plate 3:1 Area of advanced argillic alteration in andesitic lava, Western Keller Peninsula, King George Island (1365).
Note yellowish jarosite and red-brown limonite as surface oxidation coating upon greyish, fresh rock.

plate 3:2 Breccia at margin of advanced argillic alteration, in andesitic lava, Eastern Keller Peninsula, King George Island (1359.1).

plate 3:3 Area of intermediate argillic alteration (white) in andesitic tuff composed of quartz and ferroandolomite forming by alteration of lavas (grey), Fildes Peninsula, King George Island (1028).

plate 3:4 Concentric banding (or "onion") in area of advanced argillic alteration in Andesitic lava, Barton Peninsula, King George Island (1089.3).

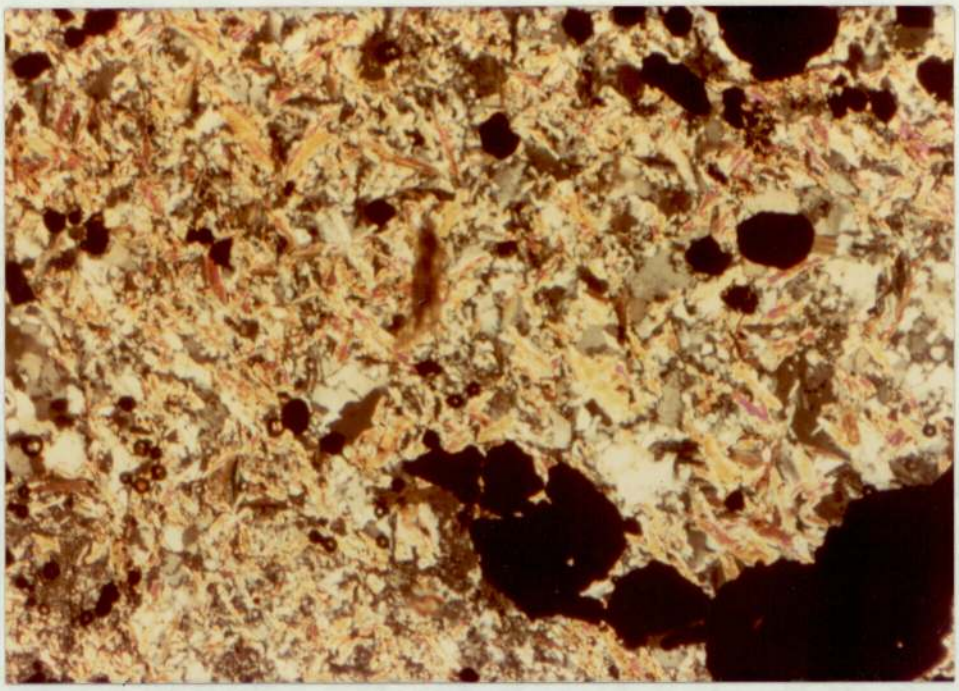

plate 3:5 Anhedral quartz (first order grey to white), alunite and natroalunite laths (second order yellows and reds) and pyrite (black), in rocks showing advanced argillic alteration in andesitic lavas. Keller Peninsula, King George Island (1359.8). Transmitted light, crossed polars, X60.

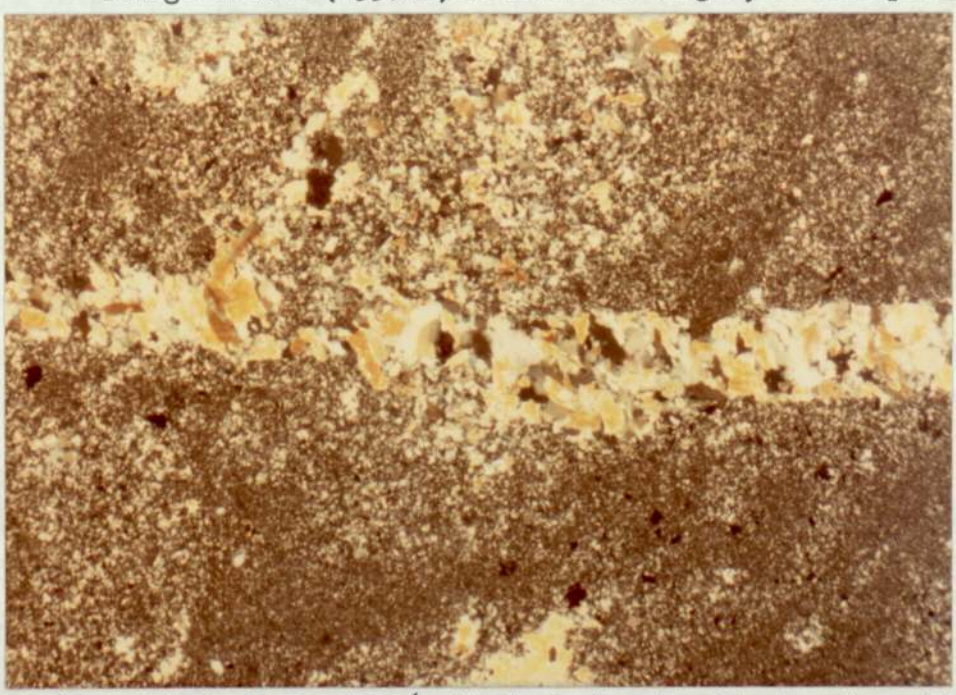

plate 3:6 Veinlet of alunite (subhedral, showing first order whites and yellows), in groundmass of microcrystalline quartz and alunite. Area of advanced argillic alteration in andesitic lava. Barton Peninsula, King George Island (1315.3). Transmitted light, crossed polars, X60.

plate 3:7 Native sulphur (yellow) in rock showing advanced argillic alteration in andesitic lavas.Barton Peninsula,King George Island.(1089.3).

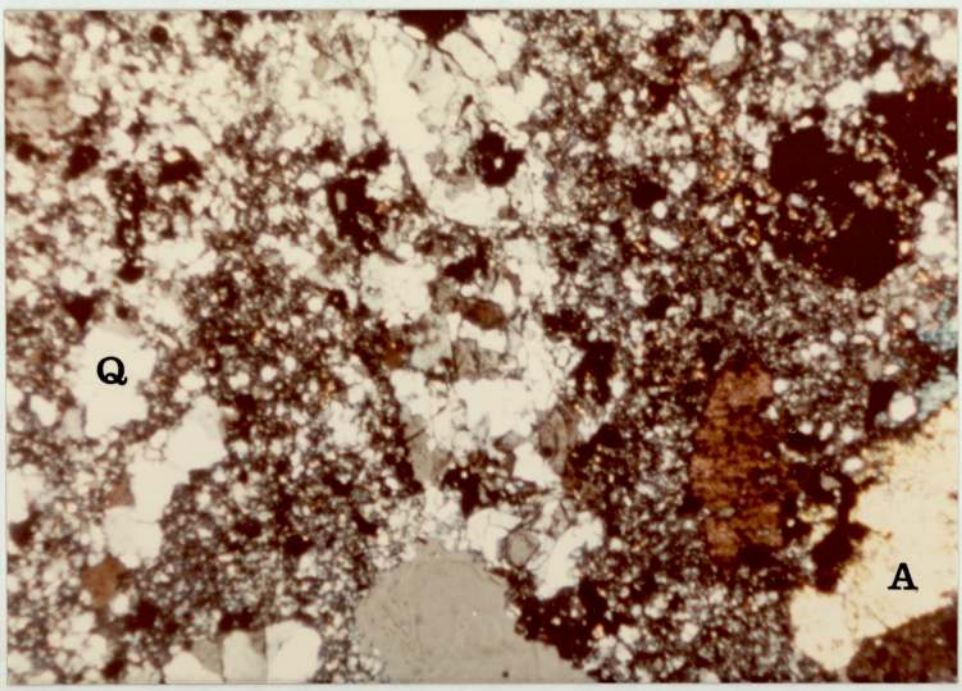

plate 3:8 Partially resorbed amphibole (bottom right of plate, showing second order blues and yellows,subhedral),in area of advanced argillic alteration in andesitic lavas. Keller Peninsula,King George Island,(1359.11).Transmitted light,crossed polars,X60.Amphibole (A),quartz (Q) and pyrite (black).

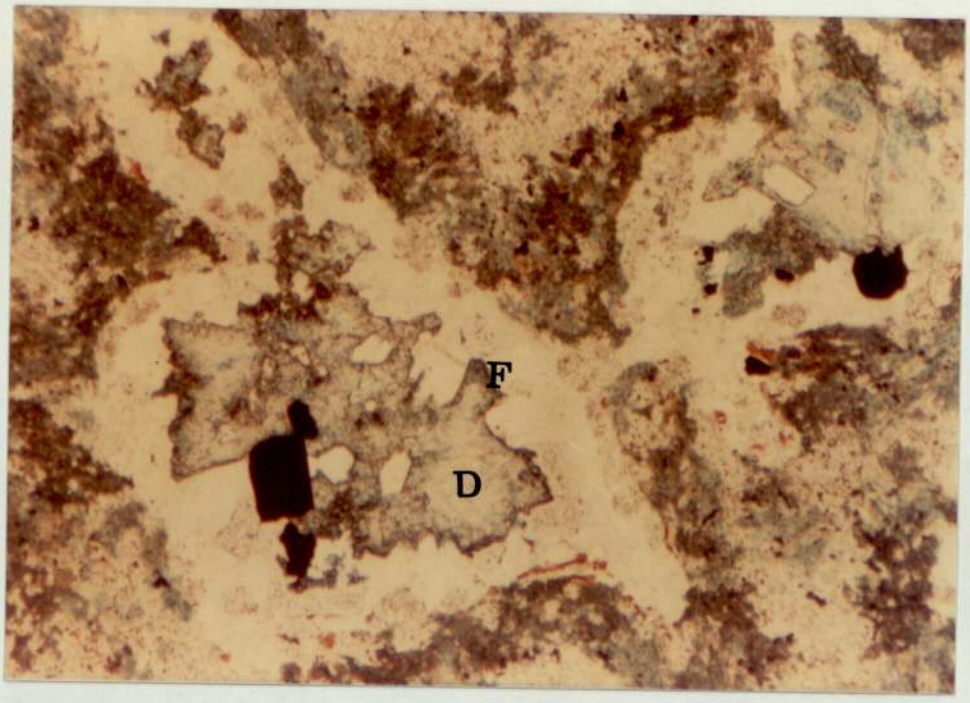

plate 3:9 Ferroandolomite crystals in andesitic tuff showing intermediate argillic alteration.Note the centres of the crystals are clear (dolomite) and the edges are blue (ferroandolomite).Rock has been stained with ferrocyanide. Fildes Peninsula,King George Island (1051.1).Transmitted light plane polarized light,X80.Dolomite (D),ferroandolomite (F).

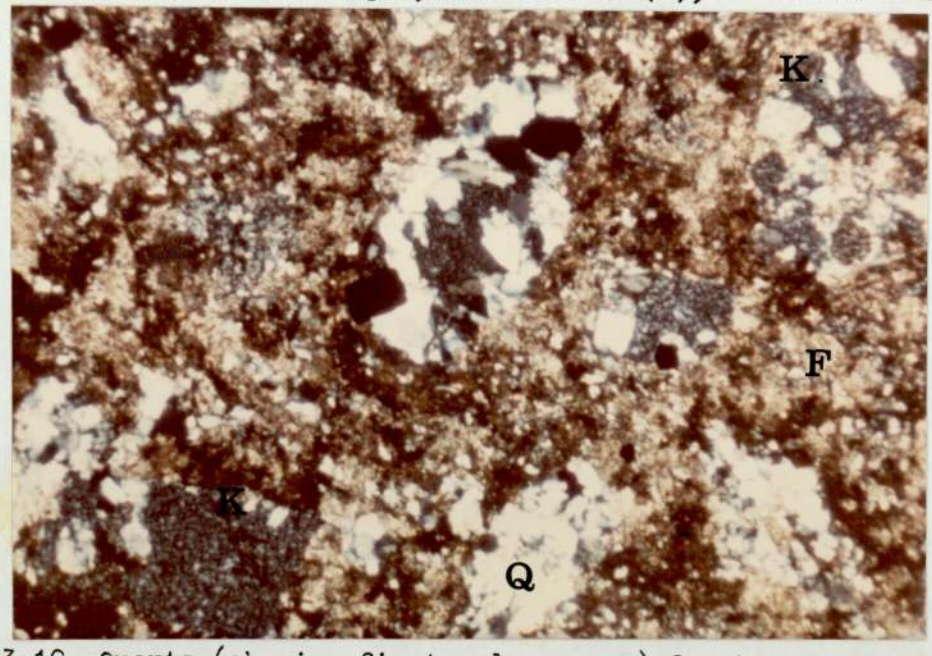

plate 3:10. Quartz (showing first order greys) forming a ring around amygdales which have been infilled by later ferroandolomite and kaolinite.Groundmass consists of ferroandolomite and quartz.Fildes Peninsula,King George Island (1051.1). Transmitted light,crossed polars,X60.Quartz (Q), ferroandolomite (F) and kaolinite (K).

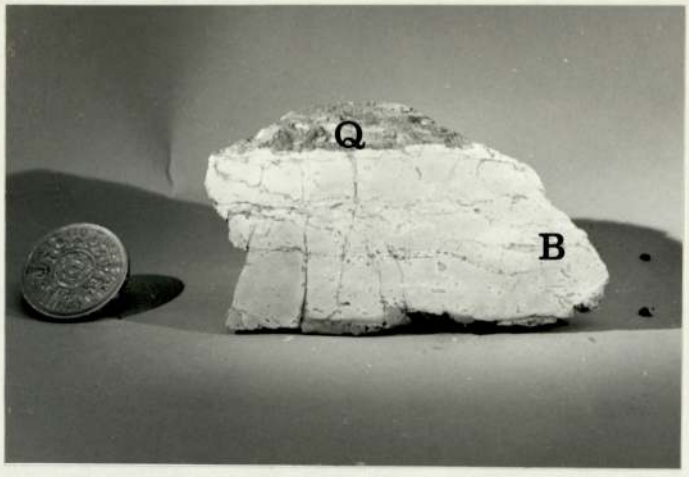

plate 3:11 Quartz and carbonate veinlets in altered tuff, Headland Opposite Dufayel. Note later quartz veins (Q) cutting earlier ones parallel to the bedding (B). King George Island (1078.20).

plate 3:12 Pyrite crystals parallel to the bedding in altered tuffs, Headland Opposite Dufayel Island, King George Island. (1078.20). Reflected light, in oil, X120.

plate 3:13 Dyke rock showing intermediate argillic alteration (D) cutting tonalite, Half Moon Island (1396). The dyke runs down the gully in the centre of the plate.

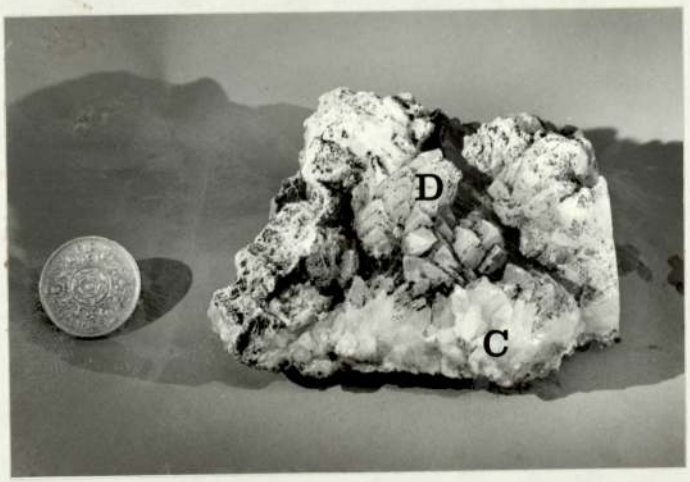

plate 3:14 Ferroandolomite (D) and ferroancalcite (C) which occur as infillings in amygdales in altered tuffs, Fildes Peninsula, King George Island (1015).

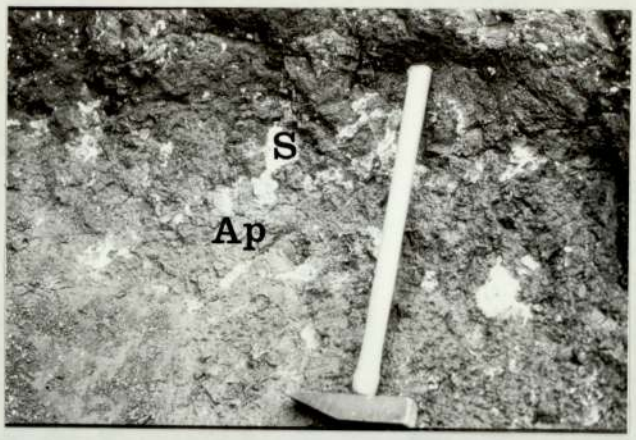

plate 3:15 Stilbite (S) (white) and apophyllite (Ap) (grey) filling amygdales in altered tuff, Fildes Peninsula, King George Island (1016).

plate 3:16 Subvertical vein (V) of quartz and pyrite (oxidation of which gives rise to brown limonite stains) cutting altered lavas, south east Dufayel Island, King George Island (1071).

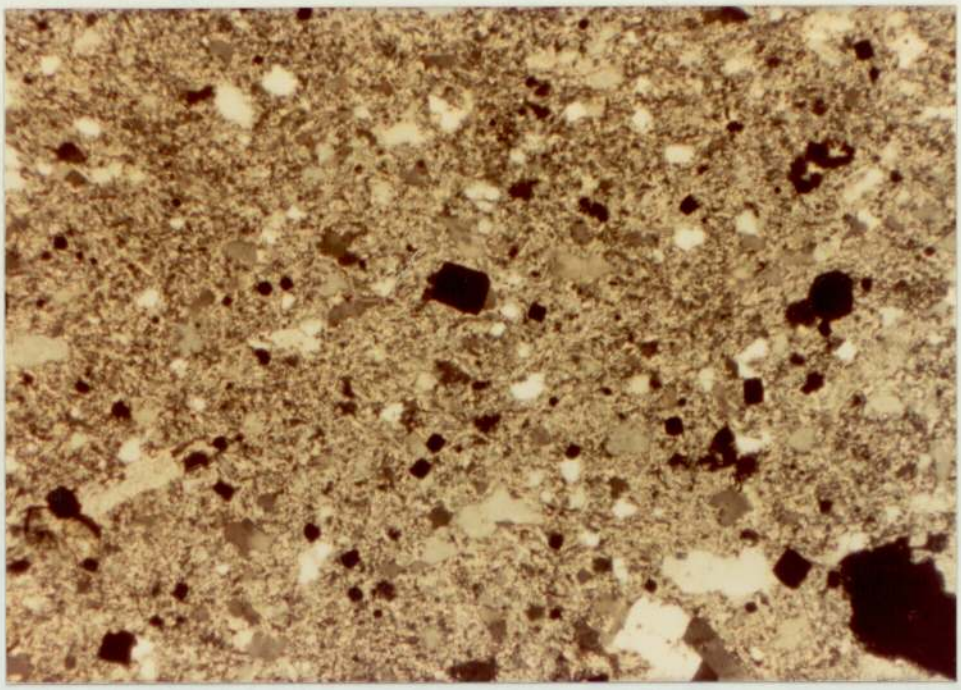

plate 3:17 Anhedral quartz (showing first order greys) and euhedral pyrite (black) in a groundmass of $2M_1$ muscovite (second order yellows) and microcrystalline quartz in andesitic lava showing phyllic alteration.Stenhouse Bluff,King George Island (1073.7). Transmitted light,crossed polars,X40.

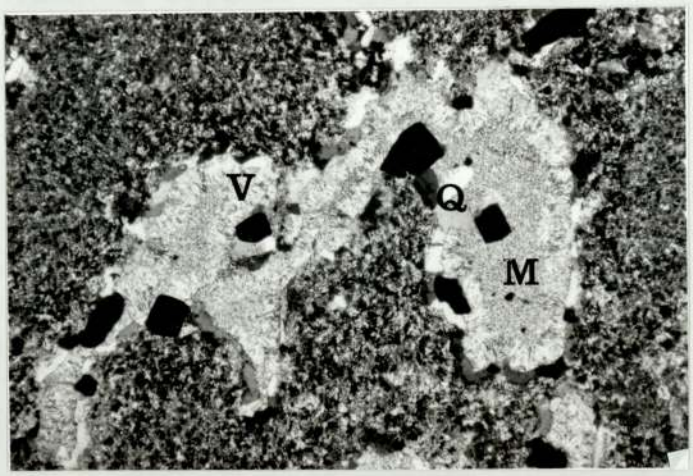

plate 3:18 Vesicles in altered lava infilled by $2M_1$ muscovite (grey to white fibrous crystals),euhedral pyrite (black) and quartz (grey to white,around edges of vesicles),in a groundmass of $2M_1$ muscovite and microcrystalline quartz.Zone of phyllic alteration in andesitic lava,Stenhouse Bluff,King George Island.Transmitted light,crossed polars,X40.(1073.1A). Quartz (Q),muscovite (M),vesicles (V).

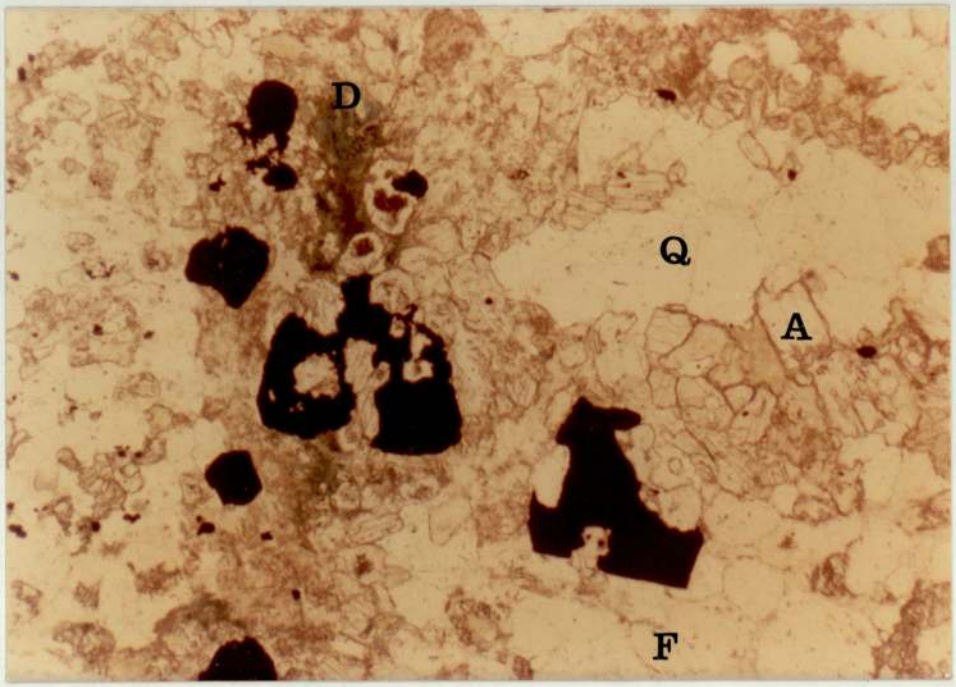

plate 3:19A. Quartz (colourless,low relief),feldspar (colourless,low relief), andalusite (colourless,high relief),and showing one distinct cleavage,pyrite and pyrrhotite (black) and ferrian dravite (blue) in zone of propylitic alteration.Barton Peninsula, King George Island (1352).Transmitted light,plane polarized light,X60.Quartz (Q),andalusite (A),sulphides (black), ferrian dravite (D) and feldspar (F).

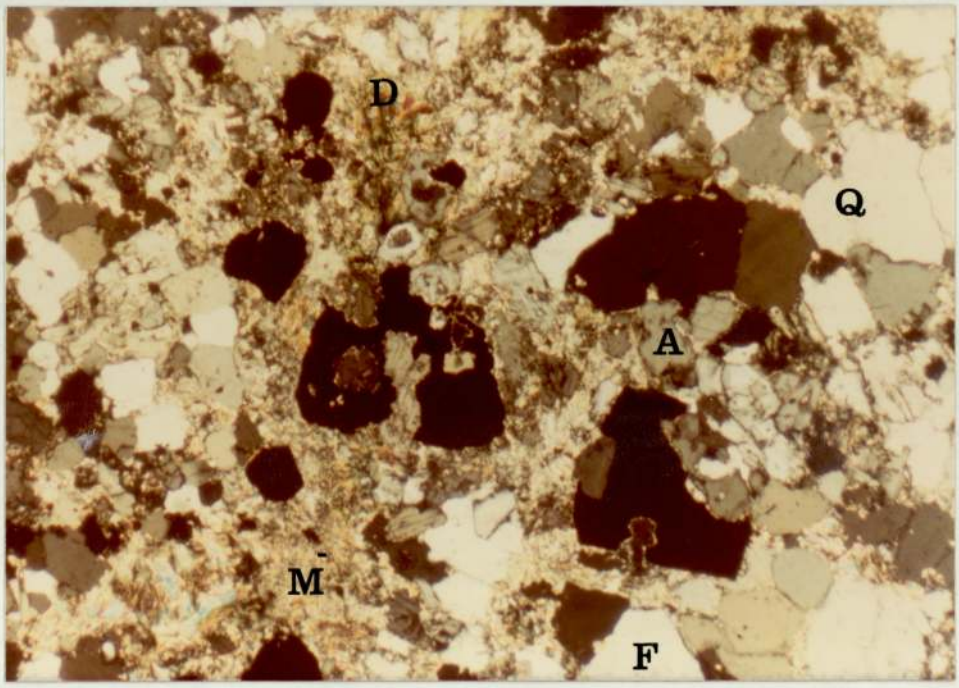

plate 3:19B Quartz (showing first order greys),feldspar (first order greys and albite twinning),andalusite (first order greys with one distinct cleavage),pyrite and pyrrhotite (black),ferrian dravite (second order reds and yellows) and muscovite (second order reds and yellows).Zone of propylitic alteration (1352).Barton Peninsula,King George Island.Transmitted light,crossed polars,X60.Quartz (Q),andalusite (A),ferrian dravite (D),feldspar (F) and muscovite (M).

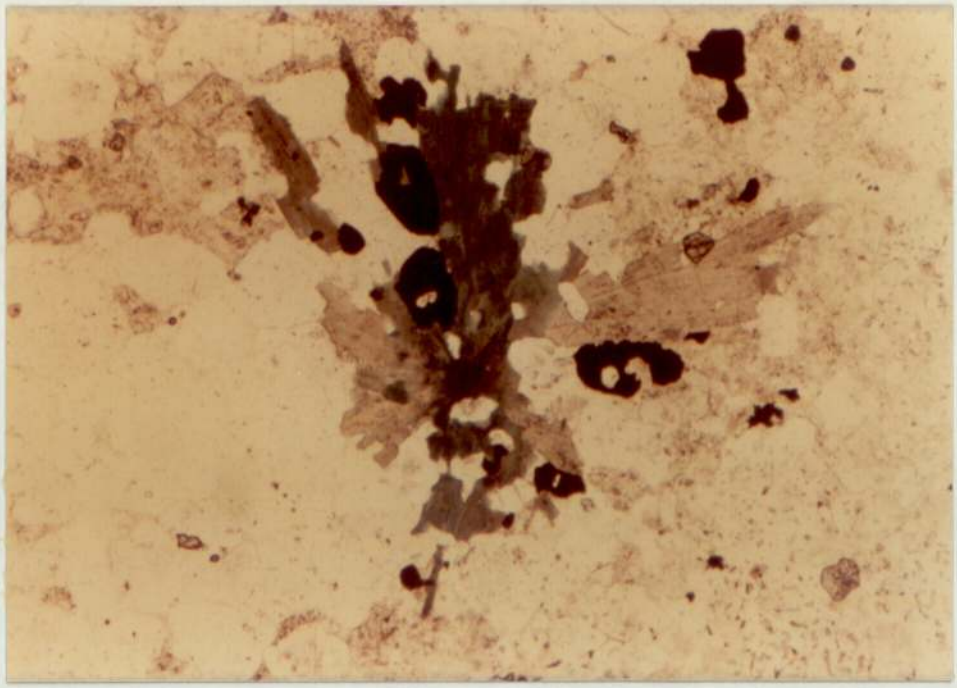

plate 3:20. Ferrian dravite showing dichroism (pink to blue), pyrite and pyrrhotite (black) and quartz and feldspar (colourless).Zone of propylitic alteration (1352),Barton Peninsula,King George Island. Transmitted light,plane polarized light,X120.

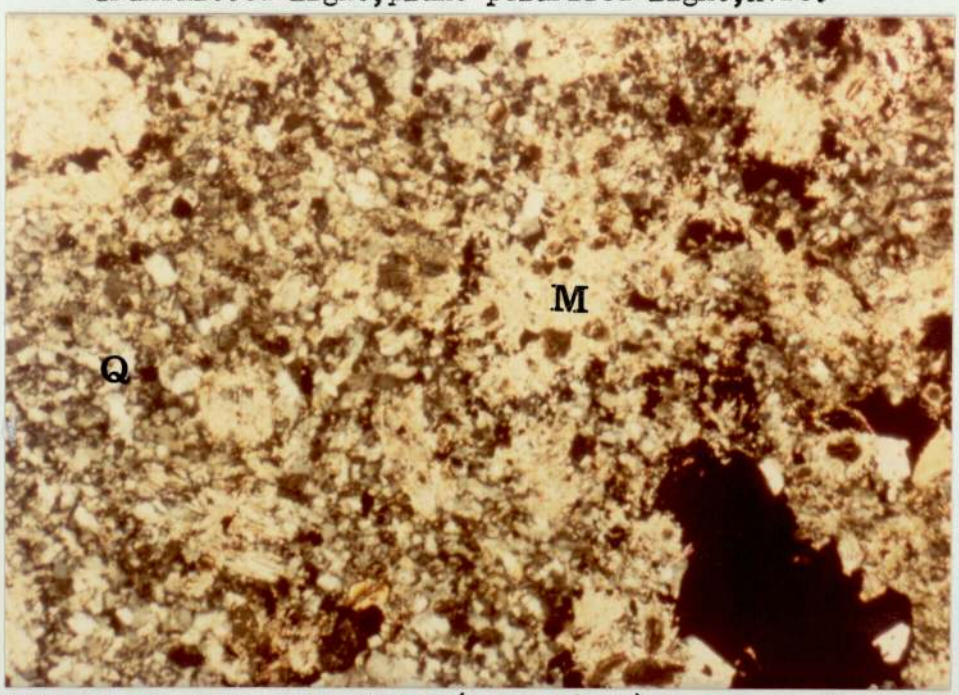

plate 3:21. Lavas vertically above (appx. 600m) the area of propylitic alteration,showing phyllic alteration.Pyrite (black), muscovite (second order yellows and reds,) and microcrystalline quartz (first order greys).Barton Peninsula,King George Island. (1082).Transmitted light,crossed polars,X60. Muscovite (M),quartz (Q).

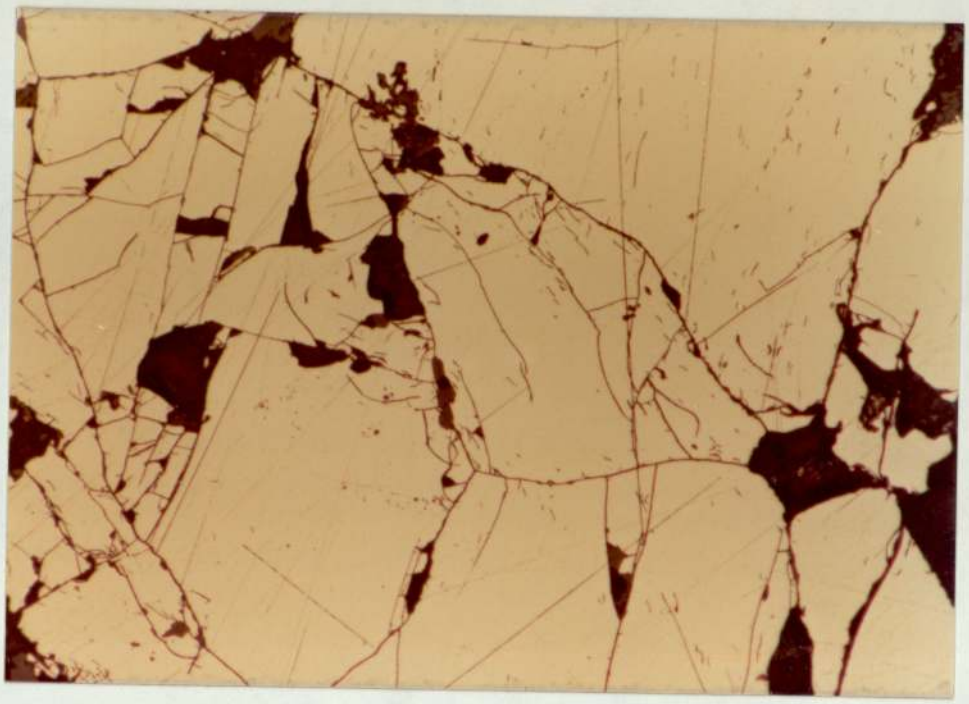

plate 3:22 Fractured pyrite in area of advanced argillic alteration, Keller Peninsula, King George Island (1059.8). Reflected light X100.

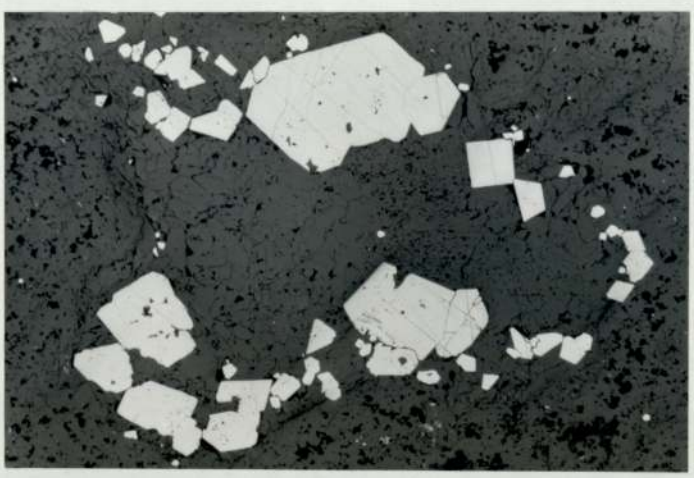

plate 3:23 Euhedral pyrite occurring around quartz crystals in rocks showing advanced argillic alteration, Keller Peninsula, King George Island (1059.7) Reflected light X60.

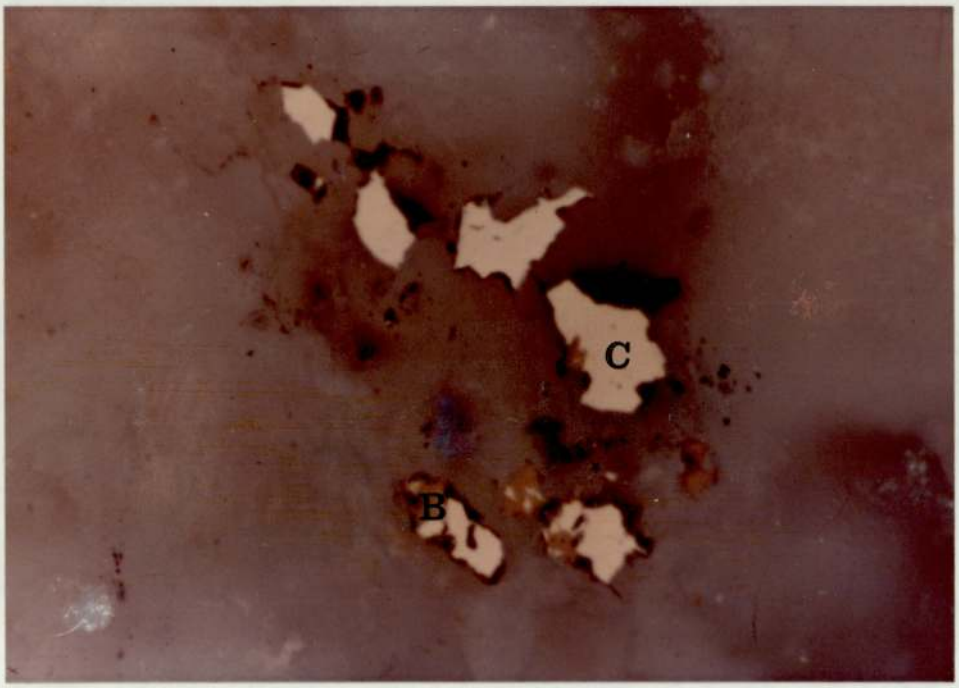

plate 3:24 Chalcopyrite (yellow) showing alteration to bornite (brown) in rocks showing intermediate argillic alteration, Fildes Peninsula, King George Island (1064.1). Reflected light X60. Chalcopyrite (C), Bornite (B).

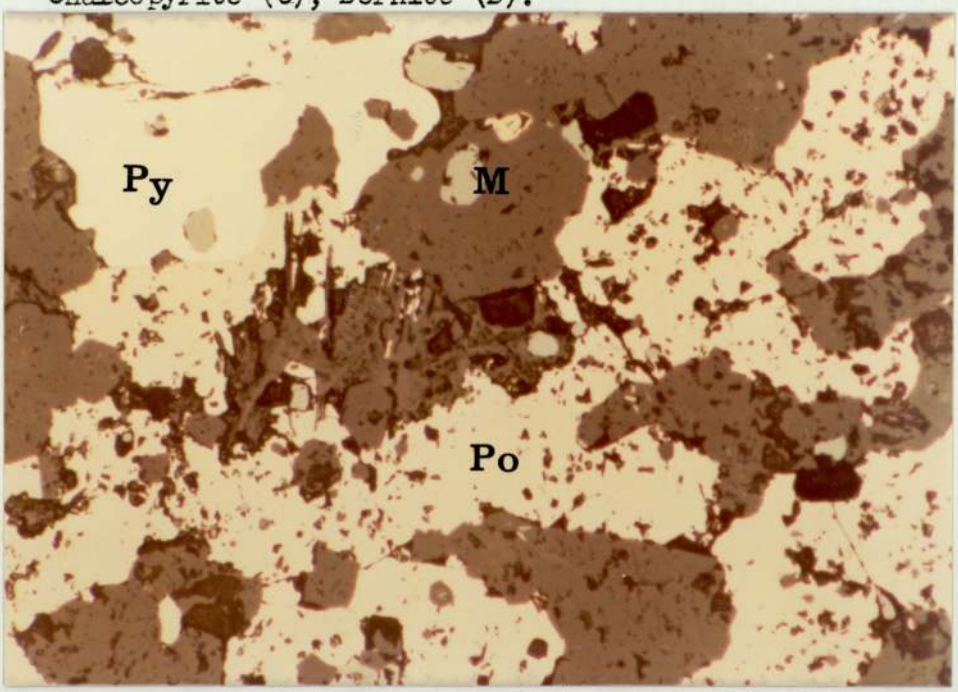

plate 3:25 Pyrite (yellow) and pyrrhotite (dark yellow) porphyroblast in zone of propylitic alteration, Barton Peninsula, King George Island (1352.1) Reflected light X60. Pyrrhotite (Po), Pyrite (Py), Magnetite (M).

plate 3:26 Clasts of "Quartz-Pyrite" Rock occurring in Tertiary volcanic breccia, near Buddington Peaks, King George Island (1474.1). Note the large amounts of iron staining due to oxidation of pyrite in these clasts to limonite.

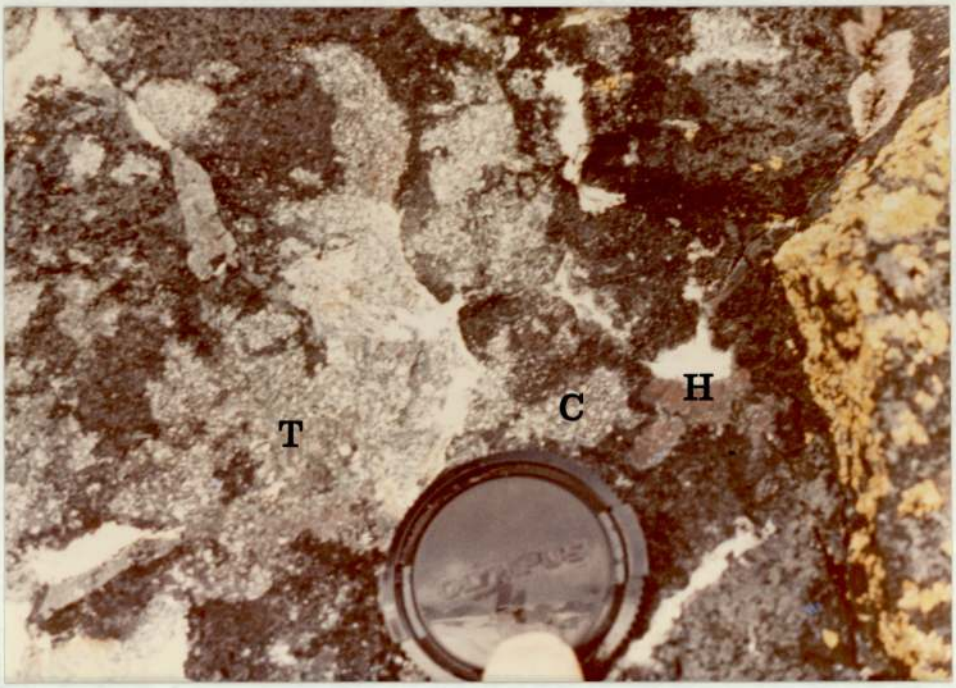

plate 3:27 Chalcocite (C), tenorite (T) and hematite (H) in quartz, ferroandolomite, chlorite vein cutting altered lavas, Fildes Peninsula, King George Island (1017.2A).

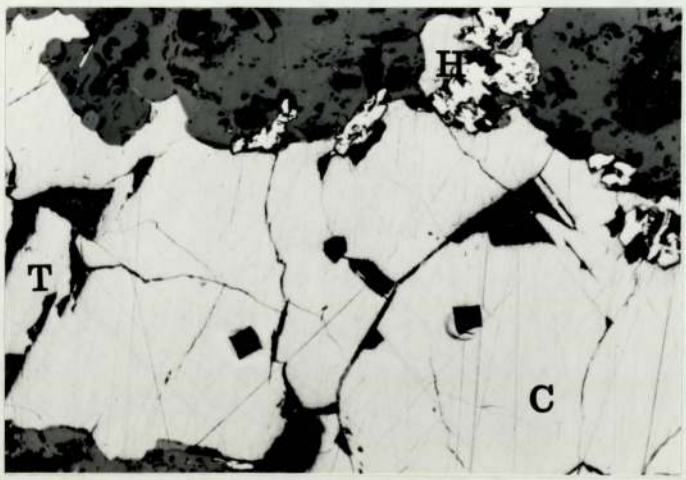

plate 3:28 Chalcocite (C), tenorite (T) and hematite (H) in quartz, carbonate, chlorite vein. Fildes Peninsula, King George Island (1017.2A) Reflected light, X100. Square holes in the minerals are microhardness indentations.

3.4.5 Weak Propylitic Alteration of Pre-Upper Tertiary Rocks

Both plutonic rocks and lavas show sericitization of plagioclase with biotite showing alteration to chlorite, and augite, hypersthene and hornblende altering to uralite (Hawkes, 1961). In proximity to the "Quartz-Pyrite" alteration the change becomes more intense with chlorite completely replacing biotite, hornblende, augite and hypersthene (1324.1). Feldspar shows sericitization (with the calcic cores more strongly altered than the sodic margins), and alteration to carbonate (1337.1) or more rarely epidote (1073.16). Veinlets of quartz, pyrite and epidote traverse the lavas, often with a halo of chlorite (1073.1). Occasionally veinlets of quartz and ferroandolomite occur with carbonate clearly the later phase (1079.6A). Some highly altered lavas consist predominantly of quartz and ferroandolomite and are clearly transitional to "Quartz-Pyrite" rock. Magnetite and ilmenite show alteration to hematite and hematite and rutile respectively, and with progressive alteration, to pyrite (Fig. 3:3, table 3.9). Magnetite veinlets traverse the lavas on Southern Barton Peninsula.

3.5 Paragenesis of the Opaque Minerals in the "Quartz-Pyrite" Rocks

The opaque minerals occurring in the "Quartz-Pyrite" rocks are described in their assumed paragenetic sequence (Fig. 3:4). This sequence was deduced by the study of approximately one hundred polished and one hundred and fifty thin sections.

Magnetite

Magnetite which is a relic from the original lava is present in small amounts in partially altered rocks, and is generally euhedral to subhedral, with a grain size of less than 0.2 mm. It is isotropic and brownish-grey in colour and is largely pseudomorphed by hematite.

Fig.3:4 Paragenesis of the "Quartz-Pyrite" Rocks.

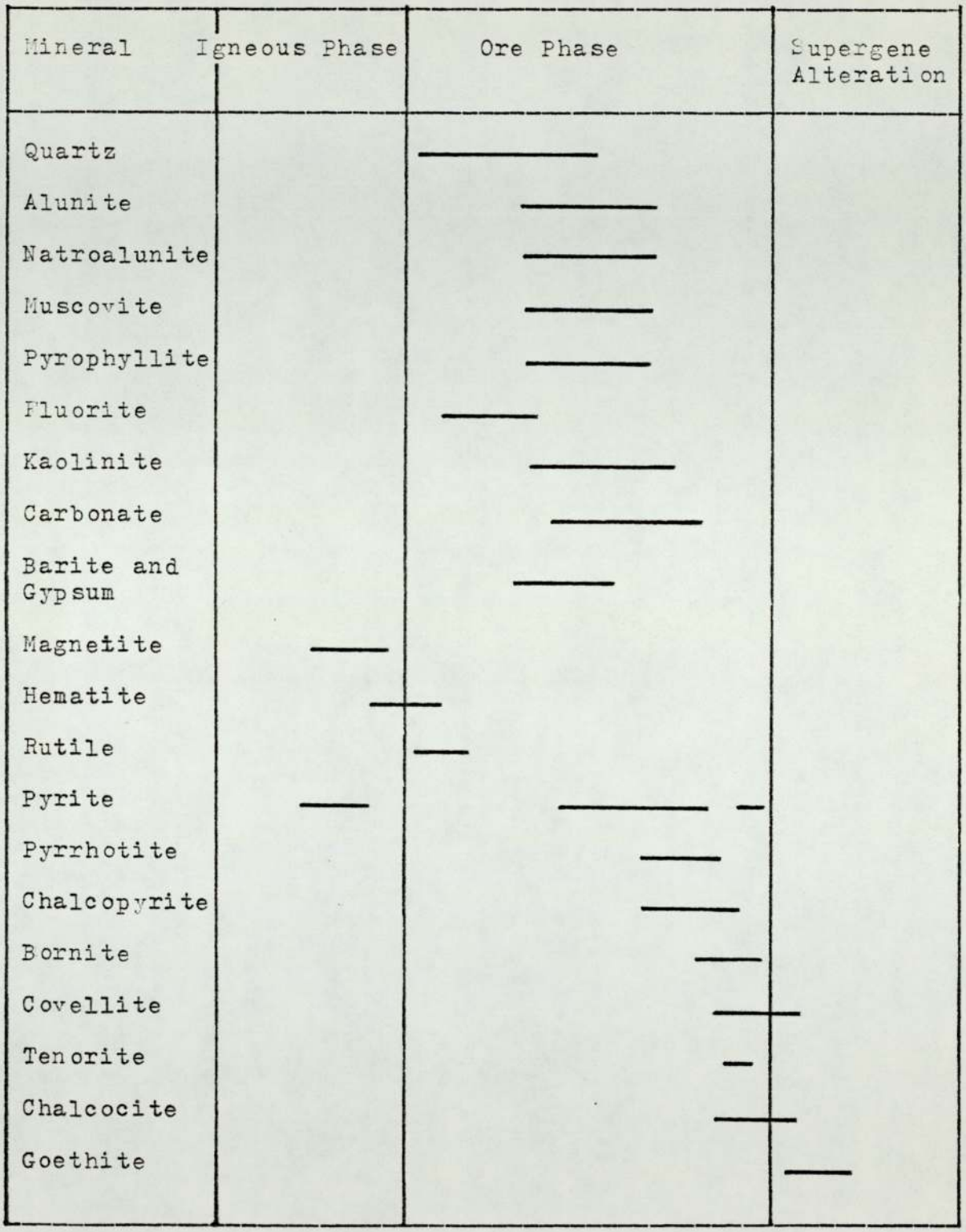

Hematite

Hematite is present in small quantities in the "Quartz-Pyrite" rocks and is invariably pseudomorphous after magnetite. It is anisotropic from light to dark grey, and under crossed polars in oil shows deep red internal reflections. Hematite has a grain size of less than 0.5 mm. Reflectivity values (at 589 nm) of 24% and Vickers Hardness Number (at 100 g load) of approximately 900 (table 3.6) are well within the range for pure hematite.

Titanium Dioxide

Titanium dioxide occurs disseminated throughout the "Quartz-Pyrite" rocks and is generally granular with a grain size of less than 0.4 mm, although it is occasionally skeletal after ilmenite. The mineral is anisotropic and in oil under crossed polars shows abundant, red internal reflections. It is light grey in plane polarised light, with a reflectivity of 16% at 589 nm.

It is difficult to differentiate between rutile and anatase, the two main polymorphs of titanium dioxide, although anatase tends to be faintly anisotropic with white or bluish internal reflections, whereas rutile is anisotropic with red internal reflections. This suggests the majority of the titanium dioxide in these rocks is rutile, although a small proportion may be anatase.

Pyrite

Pyrite is pale yellow in colour, isotropic to faintly anisotropic and euhedral to subhedral in shape. Pyrite has a grain size of less than 1 mm. Reflectivity values at 589 nm are between 49 and 53.2% with Vickers Hardness Values at 100 g load being between 1030 to 2205 (table 3.6) and are well within the range for pure pyrite as defined by Burke et al (1971). Cell dimensions for the pyrite a_o = 5.418 (table 3.7) are within the range for pure pyrite (a_o = 5.417, JCPDS) and seems to possess an undistorted lattice.

There seems to be evidence for at least three phases of pyrite formation:-

a) An early, partially resorbed phase which is probably pyrite from the original lava.

b) Main phase of pyrite formation. Pyrite is euhedral to subhedral (plate 3.22) and contains emulsion droplets of pyrrhotite (generally less than 0.01 mm, 1024.7, 1362.2) or more rarely chalcopyrite (1359.8, 1064.1.) Occasionally, chalcopyrite and bornite occur along fractures in the pyrite (1073.6). Pyrite can occur clustered around quartz crystals (plate 3.23) and the majority are pyritohedral (1362.2). The pyrite often contains inclusions of quartz, rutile (generally near the edges) and hematite (after magnetite), with rare alunite in the cores of the crystals (1089.2).

c) A later phase of pyrite formation (rare) often porphyroblastic and lacking emulsion droplets of pyrrhotite.

Pyrrhotite

Apart from minor occurrences of pyrrhotite as emulsion droplets in pyrite in areas of advanced argillic, intermediate argillic and phyllic alteration, the main occurrence of pyrrhotite is in rocks showing intense propylitic alteration. Here it is present as subhedral porphyroblasts with a grain size of less than 15 mm (1084.3, 1352.1, plate 3.25) with emulsion droplets of pyrite. Pyrrhotite shows reflection pleochroism from reddy brown to creamy brown, and is strongly anisotropic from brown to greeny blue. The pyrrhotite contains inclusions of quartz, muscovite, rutile, rare hematite and chalcopyrite, and often occurs in simple intergrowths with pyrite. It shows alteration to a "marcasite-pyrite" like substance (Ramdor, 1969) with typical "birds eye" texture, with goethite along fractures. Pyrrhotite also occurs along fractures in the pyrite.

Etching with HI and X-Ray diffraction data indicate the pyrrhotite consists of two phases in flame-like intergrowths. These are a magnetic monoclinic phase and an easily etched hexagonal phase, with the ratio of the two varying between specimens.. The pyrrhotite has a composition(table 3:1), $N_{FeS} = 0.93 - 0.95$ obtained from X-Ray diffraction measurements based on graphs of Yund and Hall (1969) and electron microprobe analysis gives a composition of Fe_7S_8 (table 3.2).. Reflectivity values at 589 nm 34 - 39% and Vickers Hardness Numbers at 100g load of 382 - 248 (table 3.6) are within the range for pure pyrrhotite.

Chalcopyrite

Chalcopyrite is generally anhedral, isotropic or faintly anisotropic and yellow in colour.. The grain size is usually less than 0.2 mm, with reflectivity values at 589 nm about 40% and Vickers Hardness Numbers of approximately 250 (at 100g load).. These figures are within the accepted values for chalcopyrite (Burke et al, 1971).

Chalcopyrite is most common in carbonate rich assemblages although it also occurs as inclusions and along fractures in pyrite. Where pyrite and pyrrhotite occur in simple intergrowths a zone of chalcopyrite often occurs between the two (1082.1, 1351.3).. This texture suggests the three sulphides were present initially as a single high temperature phase which exsolved on cooling into three phases (Sugaki et al, 1975).

Bornite

Bornite is anhedral, generally pinkish brown in colour and isotropic to faintly anisotropic with a grain size of less than 0.1 mm. Bornite seems to be the latest copper iron sulphide and is most common in carbonate rich rocks, frequently having formed by alteration of chalcopyrite (1064.1).

Covellite

Covellite characteristically shows reflection pleochroism from pale blue to dark blue and is strongly anisotropic from orange-red to copper brown. It is usually subhedral to anhedral in shape with a grain size

of less than 0.1 mm. Covellite occurs in carbonate rocks forming by alteration of chalcopyrite and bornite.

Tenorite

Tenorite is usually anhedral and white-grey in colour with reflection pleochroism to white which is more noticeable in oil. The grain size is less than 2 mm. One Vickers Hardness Number at 100g load gives a figure of 236. It shows anisotropy, especially in oil. The mineral occurs in association with hematite (plate 3:27, 3:28.).

Chalcocite

Chalcocite is anhedral, faint bluish white in colour and tends to be faintly anisotropic, with a grain size of less than 2mm. Chalcocite occurs in association with tenorite.

3.6 Geochemical Analyses of "Quartz-Pyrite" Rocks and Comparison with (?) Jurassic Volcanics

The major oxides SiO_2, Al_2O_3, CaO, MgO, FeO, Na_2O and K_2O and the minor oxides MnO, TiO_2 and SO_2 were determined for eight (?) Jurassic lavas (table 3.10) and nineteen "Quartz-Pyrite" rocks (table 3.3, 3.4). Twelve trace elements were also determined on these rocks.

For the (?) Jurassic lavas the contents of major oxides were as follows; silica varies between 52.29 - 72.3%, alumina 8.81 - 14.67%, ferrous oxide 3.28 - 10.86%, lime 1.83 - 10.89%, magnesia 0.68 - 4.49%, sodium oxide 3.27 - 4.77% and potassium oxide 0.97 - 2.71% (table 3.10). Comparison of these values for calc-alkaline lavas with those found in the Andes and Australia suggests the results obtained lie within that of other andesitic rocks (Siegers et al, 1969; Taylor et al, 1969).

Levels of trace elements in these rocks were Cr, 29 ppm; Ni, 60 ppm, both probably present mainly in pyroxenes and magnetite, (Taylor and White, 1966), Cu 60 ppm, Mo, 140 ppm and Zn 60 ppm, probably present as minute sulphide inclusions, and Sr 140 ppm which is substituting for Ca in plagioclase. Se at 100 ppm and Te 35 ppm are substituting for sulphur in sulphides, with V at

300 ppm associated with magnetite. All the trace elements are present in approximately the same order of magnitude as in other calc-alkaline lavas (Siegers et al, 1969; Taylor et al, 1966).

Ternary plots of selected chemical data show these lavas are part of a calc-alkaline suite as defined by Carmichael et al (1974), and this is confirmed by plots of FeO*, SiO_2 and TiO_2 against a differentiation index (FeO*/MgO, Fig. 3.7) and plots of trace elements (Cr, Ni, Ti and V) against the same index (Fig. 3.7) as defined by Miyashiro and Shido (1975).

For the "Quartz-Pyrite" rocks silica varies from 44.17 - 86.94%, alumina 2.38 - 21.07%, lime 0.03 - 12.52%, magnesia 0.01 - 6.59%, ferrous oxide 0.59 - 4.37%, sodium oxide 0.21 - 10.33% and potassium oxide 0.46 - 5.11%.

Silica seems to be present mainly as quartz, alumina in clay minerals and alunite along with sodium and potassium oxides. Lime and magnesia are present mainly in carbonates with ferrous oxide present in pyrite and jarosite. Titanium dioxide (0.26 - 1.48%) is occurring as rutile, with sulphur fairly high in rocks containing alunite (SO_3 1.52 - 16.22%), but considerably lower in other alteration types, where sulphur occurs primarily in pyrite.

Levels of trace elements in the "Quartz-Pyrite" rocks are Cr 5 - 30 ppm substituting for Al in alunite, with Ni 6 - 37 ppm present in pyrite. Cu (21 - 429 ppm), Mo (11 - 26 ppm), Pb (<55 ppm) and Zn (10 - 112 ppm) are present as sulphides, notably chalcopyrite, molybdenite, galena and sphalerite, which are probably submicroscopic. Se (14 - 466 ppm) and Te (<39 ppm) are substituting for sulphur in pyrite. Sr (less than 97 ppm) is substituting for Ca in carbonate and V at 23 ppm is present in pyrite.

Plots of the major oxides on silica variation diagrams (Fig. 3.6) clearly show the increase in alumina and decrease of magnesia, lime, manganese oxide and ferrous oxide during the alteration process. The

alkali metals seem relatively unaffected. Plots of major oxides against a differentiation index (FeO^*/MgO) for the (?) Jurassic lavas and "Quartz-Pyrite" rocks indicate a vast increase in the FeO^*/MgO ratio for a given SiO_2 or FeO^* content (Fig. 3.7). This suggests magnesia is being selectively leached from the lavas relative to FeO^* and SiO_2 during the alteration process.

Ternary diagrams of selected chemical data (Fig. 3.8) indicate a plot of $FeO^* + MnO$; $Na_2O + K_2O$; MgO shows MgO is depleted in the "Quartz-Pyrite" rocks relative to the (?) Jurassic lavas. A plot of Na_2O; K_2O; CaO indicates CaO is depleted in the "Quartz-Pyrite" rocks relative to the (?) Jurassic lavas, except in the carbonate rich deposits, where it has increased. Finally, a plot of CaO, $(FeO^* + MnO + MgO - TiO_2)$, $Al_2O_3 - (Na_2O + K_2O)$ shows again that CaO is depleted in the altered rocks, or the relative proportion of $Al_2O_3 - (Na_2O + K_2O)$ has increased.

Titania tends to be a relatively immobile phase during the alteration process (Winchester and Floyd, 1975) and this appears to be confirmed by the fact that the TiO_2 levels are about the same in the "Quartz-Pyrite" rocks as in the (?) Jurassic lavas (Fig. 3.9). The trace element data for the "Quartz-Pyrite" rocks and (?) Jurassic lavas plotted against TiO_2 suggests that Mo, Pb and Cu have increased and Au, Cr, Ni, Sr and V have decreased during the alteration process. Levels of Zn, Se and Te seem to have remained about the same.

3.7 Crystal and Minor Element Chemistry of the Pyrite From the "Quartz-Pyrite" Rocks

Chemical analysis of the pyrite from the "Quartz-Pyrite" rocks has been carried out using atomic absorption spectrometry. Separation of the pyrite from the silicate phases was achieved using heavy liquids (bromoform).

The pyrite contains relatively small amounts of metal ions other than iron in the lattice, manganese (< 2486 ppm), zinc ($< 22{,}080$ ppm)

and copper (<864 ppm) are the most abundant, although these high values are probably due to inclusions of pyrolusite, sphalerite and chalcopyrite (table 3.2, 3.5).

Ni (<104 ppm) and Co (50 - 230 ppm) are substituting for iron, with Co invariably greater than Ni ($Co/_{Ni} > 1$). Pb varies greatly, but is less than 240 ppm and probably present as submicroscopic inclusions of galena. Se (575 - 30 ppm) is substituting for sulphur, in the pyrite lattice. These values are within the range found in other pyrite specimens elsewhere (Ryall, 1977, Fleischer, 1955). The high Co/Ni ratio (greater than 1) and $S/_{Se}$ ratio, (less than 20,000) suggests the pyrite probably had a hydrothermal volcanogenic origin (Loftus-Hills and Solomon, 1969).

A few rare inclusions of sphalerite were found in pyrite but no inclusions of pyrolusite were found. Thus, manganese is probably present as undetected inclusions of pyrolusite.

3.8 Tectonics and Age of the "Quartz-Pyrite" Rocks.

A study of the structural data from these deposits (Fig. 3.2) indicates they occur mainly along linear zones trending E - W and N - S on King George Island. Some faulting is clearly later than these rocks on King George Island, as many deposits have been faulted against pyritised volcanics, for example on Northern Keller Peninsula. These deposits occur on the northern side of a major fault zone that crosses the length of King George Island (Barton, 1964), and are clearly on the upthrow side.

The "Quartz-Pyrite" alteration affects the (?) Jurassic lavas and some Tertiary plutons (Barton Peninsula Granodiorite at 57 my - (Grikurov et al, 1972)). The apparently contemporaneous alteration of the Miocene tuffs (Barton, 1964) on the Headland Opposite Dufayel Island, and the unaltered nature of Tertiary dykes that cut the "Quartz-Pyrite" rock on Keller Peninsula and Precious Peaks suggests the alteration took place in Miocene times or slightly later. Clasts of "Quartz-Pyrite" rock have been found in Tertiary volcanic breccias (1474, plate 3:26) near Buddington Peaks, and in association with rounded inclusions of granite in the Fildes

Peninsula and Point Hennequin lavas (Barton, 1964) and also suggest the deposits are of early to middle Tertiary age. These lavas have been dated at 57 my and 89 my (Grikurov et al, 1968; Davies per comm.) The deposits also show a close spatial relationship to the Tertiary plutons in this region.

It seems unlikely that the "Quartz-Pyrite" alteration in the various areas occurred at precisely the same time, but seems to have been an intimate part of the thermal processes associated with the intrusion of the various plutons in the South Shetland Islands.

TABLE 3:1 X-RAY DIFFRACTION DATA FOR PYRRHOTITES, BARTON PENINSULA.

Specimen Number	d(102) in Å	N_{FeS}
1082.1	2.060	0.93
1084.3	2.066	0.94
1084.3	2.066	0.94
1084.3	2.074	0.95

(Values of N_{FeS} based on Data by Yund and Hall, 1969).

TABLE 3: 2 ELECTRON MICROPROBE ANALYSIS OF PYRITE AND PYRRHOTITE, FROM ZONE OF PROPYLITIC ALTERATION, BARTON PENINSULA.

SPECIMEN NO.	SULPHIDE	LOCATION	Fe	S	Co	Cu	Ni	Totals
1084.3	Pyrite	Barton Peninsula,	46.55	53.45	0.285	0.071	0.045	100.41
1084.3	Pyrite	Zone of propylitic	46.55	53.45	0.125	0.059	0.056	100.25
1084.3	Pyrrhotite	alteration	59.40	40.46	0.133	0.104	0.077	100.17
1084.3	Pyrrhotite	" "	59.32	40.41	0.200	0.001	0.077	100.01
1082.1	Pyrrhotite	" "	60.02	40.27	0.133	0.001	0.022	100.44

TABLE 3:3 CHEMICAL ANALYSES OF ?JURASSIC LAVAS IN THE SOUTH SHETLAND ISLANDS.

Specimen Number	Location	Rock Type	SiO_2	Al_2O_3	TiO_2	FeO*	MnO	CaO	MgO	Na_2O	K_2O	S	Au	Cr	Cu	Mo	Ni	Pb	Se	Sr	Te	V	Zn	Total
1072.1	Precious Peaks	Andesite	59.30	13.78	0.82	7.30	0.14	10.15	3.76	3.27	0.97	0.23	59	29	60	114	56	nd	nd	234	35	340	65	99.72
1072.2	Precious Peaks	Dacite	63.27	11.07	1.22	7.45	0.12	5.01	4.49	3.93	2.68	0.14	56	43	80	110	58	nd	95	162	23	265	55	99.38
1073.5	Stenhouse Bluff	Rhyodacite	69.20	8.81	1.30	5.22	0.21	3.63	3.47	4.77	2.48	0.05	53	10	30	180	47	nd	161	50	16	257	50	99.14
1079.7	Crepin Point	Andesite	59.60	14.51	0.75	10.86	0.24	3.15	3.75	4.74	1.58	0.30	71	39	70	119	79	nd	146	124	74	320	90	99.44
1347.1	Barton Peninsula	Andesite	52.29	12.61	0.84	9.14	0.19	10.89	8.04	4.27	0.25	0.37	49	49	80	178	56	nd	556	219	36	300	65	98.89
1314.1	Barton Peninsula	Rhyolite	72.30	14.67	1.07	3.28	0.12	1.83	0.68	4.51	1.24	0.21	47	19	76	140	23	nd	66	60	53	96	50	99.91
1383.5	Keller Peninsula	Dacite	65.80	10.05	0.63	6.52	0.08	4.33	3.78	4.75	2.49	0.16	54	15	40	100	47	nd	106	118	37	260	50	98.59
1392.1	Keller Peninsula	Dacite	66.90	12.37	0.52	5.57	0.17	3.81	2.88	4.15	2.71	0.26	50	27	40	195	53	nd	83	55	16	346	50	99.34
Characteristic Andesite (Taylor and White,1966).			60.1	17.2	0.7	8.1	0.1	7.1	3.5	3.3	1.3			80	45		31	9		235		175		

Major oxides are in weight percent,trace elements in parts per million (ppm).

(Except Au which is in parts per billion,ppb).

TABLE 3:4A CHEMICAL ANALYSES OF "QUARTZ-PYRITE" ROCKS.(A) MAJOR OXIDES.

Specimen Number	Location	Alteration Type	SiO_2	Al_2O_3	TiO_2	FeO	MnO	CaO	MgO	Na_2O	K_2O	CO_2	S^{2-}	SO_3	Native Sulphur	H_2O-	Total
1051.1A	Fildes Peninsula	Intermediate Argillic	38.9	15.08	0.63	3.80	0.11	12.52	6.59	0.76	2.52	18.85	0.14	-	-	0.10	100.0
1064.1	Fildes Peninsula	Intermediate Argillic	44.17	18.71	1.41	4.10	0.22	5.57	1.23	10.33	3.78	8.83	1.07	-	-	0.46	99.88
1073.7	Stenhouse Bluff	Phyllic	62.68	18.44	0.54	3.96	0.03	1.33	0.52	4.56	4.17	-	2.33	-	-	0.24	98.80
1089.3	Barton Peninsula	Advanced Argillic	86.40	2.83	0.43	4.32	0.04	0.19	0.01	0.21	0.82	-	1.10	-	2.29	0.08	98.72
1337.6	Barton Peninsula	Phyllic	66.90	15.31	0.34	3.14	0.05	0.03	0.56	7.56	5.38	-	0.12	-	-	0.10	99.49
1352.1	Barton Peninsula	Propylitic	72.60	18.69	0.26	4.15	0.03	0.05	0.02	0.74	2.47	-	-	-	-	0.10	99.11
1359.1	Keller Peninsula	Advanced Argillic	86.94	6.74	0.30	2.83	0.01	0.12	0.06	0.53	0.46	-	1.08	-	-	0.04	99.11
1359.2	Keller Peninsula	Advanced Argillic	79.20	14.66	0.67	0.59	0.01	0.15	0.04	0.69	1.38	-	0.30	1.52	-	0.08	99.28
1359.3	Keller Peninsula	Advanced Argillic	86.60	5.62	0.31	1.92	0.01	0.12	0.06	0.35	1.85	-	0.20	1.67	-	0.09	98.79
1359.4	Keller Peninsula	Advanced Argillic	68.20	14.66	0.47	2.76	0.01	0.09	0.05	0.98	2.24	-	0.40	10.42	-	0.10	100.37
1359.5	Keller Peninsula	Advanced Argillic	68.70	5.62	0.37	4.37	0.01	0.07	0.07	0.56	1.49	-	2.54	14.99	-	0.39	99.17
1359.6	Keller Peninsula	Advanced Argillic	67.50	15.10	0.26	3.21	0.01	0.25	0.03	1.10	2.58	-	1.54	7.18	-	0.04	98.79
1359.7	Keller Peninsula	Advanced Argillic	69.17	11.45	0.34	3.54	0.01	0.17	0.03	0.78	2.55	-	1.76	8.93	-	0.06	98.78
1359.8	Keller Peninsula	Advanced Argillic	46.40	23.64	0.50	4.28	0.01	0.08	0.02	0.85	5.11	-	2.60	15.22	-	0.04	98.74
1359.9	Keller Peninsula	Advanced Argillic	55.27	16.92	0.77	3.76	0.01	0.14	0.03	0.90	3.91	-	2.10	14.18	-	0.03	98.01
1359.10	Keller Peninsula	Advanced Argillic	58.58	18.73	1.06	2.84	0.01	0.17	0.03	1.08	3.75	-	2.28	11.18	-	0.04	99.74
1359.11	Keller Peninsula	Advanced Argillic	54.91	15.94	1.48	3.97	0.01	0.14	0.04	0.89	2.14	-	3.02	16.22	-	0.05	98.80
1396.6	Half-Moon Island	Intermediate Argillic	53.60	21.07	0.23	4.09	0.07	4.96	2.57	0.54	0.46	10.65	0.80	-	-	0.12	99.16
1474.2	Buddington Peaks	Phyllic	66.27	14.54	1.11	3.99	0.03	0.03	1.00	0.61	8.16	-	3.22	-	-	0.08	99.04

Table 3.4B CHEMICAL ANALYSES OF "QUARTZ-PYRITE" ROCKS.

(B) TRACE ELEMENT DATA.

Alteration Type	Specimen No.	Location	Au*	Cd	Cr	Cu	Mo	Ni	Pb	Se	Sr	Te	V	Zn
Intermediate		Southern Fildes												
Argillic	1051.1A	Peninsula	35	3	10	21	25	28	27	370	97	39	nd	36
"	1064.1	"	41	4	15	167	24	20	28	14	51	20	23	58
Phyllic	1073.7	Stenhouse Bluff	32	1	10	141	17	13	19	181	1	21	nd	32
Advanced Argillic	1089.3	Northern Barton Peninsula	2	nd	5	26	19	37	nd	158	nd	8	nd	24
Phyllic	1337.6	Southern Barton Peninsula	27	5	15	47	21	21	8	36	3	16	nd	16
Propylitic	1352.1	North East Marion Cove	27	1	19	429	18	36	15	411	nd	21	13	22
Advanced Argillic	1359.1	Eastern Keller Peninsula	9	1	5	31	26	6	11	196	1	19	nd	10
"	1359.2	"	19	4	11	54	18	15	22	221	1	15	nd	62
"	1359.3	"	7	3	9	39	18	10	37	143	2	16	nd	36
"	1359.4	"	17	4	20	53	12	26	32	32	1	17	nd	82
"	1359.5	"	7	nd	20	74	22	32	43	20	2	36	nd	87
"	1359.6	"	20	3	15	18	12	16	40	63	1	23	nd	43
"	1359.7	"	14	4	17	26	14	13	38	32	2	16	nd	60
"	1359.8	"	28	3	18	54	16	18	32	157	1	5	nd	61
"	1359.9	"	25	2	20	31	11	24	32	145	1	12	nd	79
"	1359.10	"	27	nd	23	30	20	27	41	466	1	8	nd	76
"	1359.11	"	16	1	30	32	19	27	55	113	2	nd	nd	112
Intermediate Argillic	1396.6	Half-Moon Island	39	2	9	22	23	15	21	89	10	22	nd	26
Phyllic	1474.2	Buddington Peaks	28	3	15	72	17	18	18	404	nd	17	10	39

All figures are in parts per million (ppm)

* parts per billion (ppb)

Table 3.5 CHEMICAL ANALYSES OF PYRITE FROM "QUARTZ-PYRITE" ROCKS.

Alteration Type	Specimen No.	Location	Fe	S	Au*	Co	Cu	Mn	Ni	Pb	Se	Zn	Totals
Intermediate Argillic	1024.5	Fildes Peninsula	46.32	53.36	<1	230	96	2,713	32	8	575	58	99.68
"	1051.1A	"	46.41	53.38	14	140	110	200	<1	240	45	190	99.79
"	1064.1	"	-	-	<1	-	-	-	-	-	516	-	
Phyllic	1073.7	Stenhouse Bluff	46.45	53.41	30	-	864	-	60	-	30	-	99.86
"	1078.21A	Headland Opposite Dufayel Island	46.40	53.42	6	70	171	<1	<1	81	108	81	99.82
Phyllic	1082.1	Barton Peninsula	46.40	53.37	2	80	58	122	58	<1	422	382	99.77
Advanced Argillic	1089.3	"	45.28	52.64	140	160	210	164	51	211	30	22,080	97.92
Phyllic	1319.1	"	46.42	53.40	11	120	22	730	38	104	69	146	99.82
Propylitic	1352.1	"	46.42	53.22	9	210	572	1,052	104	51	93	108	99.64
"	1352.2	"	46.50	53.42	15	160	280	156	84	14	510	98	99.92
Advanced Argillic	1359.8	Keller Peninsula	46.41	53.42	22	50	198	34	<1	<1	80	81	99.83
"	1360.1	"	46.42	53.46	40	72	256	610	<1	304	42	98	99.88
Intermediate Argillic	1396.6	Half-Moon Island	46.40	53.40	19	80	42	2,486	20	67	30	144	99.80

* parts per billion (ppb)

All other trace elements in parts per million (ppm).

Table 3.6 REFLECTIVITIES AND HARDNESS VALUES OF OPAQUE MINERALS IN THE "QUARTZ-PYRITE" ROCKS.

PYRITE

Specimen No.	Location	Reflectivity (at 589 nm)	Vickers Hardness Number (100g load)
1024	Southern Fildes	49.2, 49.0 (pitted)	2128, 2205, 2205, 1764
1024.5	Peninsula	52.0, 50.4, 51.6	2090, 2205, 2128, 2018
1024.8C	"	49.2, 49.0, 50.1, 50.2	1917, 2018, 1854, 2128
1024.7	"	51.2, 51.2, 51.1	1984, 1854, 1917, 2090
1024.11	"	49.4, 50.4, 50.2	2090, 2205, 1323, 1984
1028	"	50.0, 50.0, 50.1	2018, 2018, 1951, 1951
1029.2	"	49.2, 49.0, 49.2 (pitted)	1382, 2054, 1951
1064.1	"	53.9, 52.8, 52.9	1951, 2018, 2054, 2018
1064.2	"	50.7, 49.0, 49.6, 50.2	2205, 1854, 1886, 2128
1067.1B	"	52.0, 53.2, 52.1	2205, 2205, 1951, 2018
1071.2	Dufayel Island	50.0, 49.6, 51.8	1825, 1170, 2018, 1825
1071.4	"	50.9, 49.2, 50.2	1917, 1656, 1532, 2167
1071.6	"	50.8, 50.6, 50.9	1708, 2205, 1487, 2167
1072.5	Precious Peaks	50.0, 50.0, 50.1	2128, 2205, 1886, 2205
1072.9B	"	51.6, 52.5, 51.8	1361, 2018, 2167, 2205
1073.1A	Stenhouse Bluff	49.7, 49.0, 49.6 (pitted)	1984, 1253, 2018, 2205
1073.1B	"	52.4, 52.0, 52.4, 50.7	2054, 2167, 1764, 2090
1073.6	"	50.4, 51.2, 50.3	1951, 1656, 1917, 2128
1075.1	Ullman Spur	51.8, 51.5, 51.6	2018, 2090, 2205, 1825
1075.12	"	51.5, 49.2, 50.8	2167, 1886, 2090, 1708
1078.18	Headland opposite	49.8, 49.1, 49.0 (pitted)	1220, 2090, 2167, 2018
1078.20B	Dufayel Island	50.7, 50.5, 50.6	1708, 2167, 2090, 1656
1078.21A	"	51.2, 51.2, 51.8	2018, 2167, 2090, 2167
1081.10	O'Caine Point	49.0, 49.4, (pitted)	1156, 1220, 2167, 1917
1081.11	Nelson Island	49.4, 49.4, 49.0 (pitted)	2205, 1202, 1825, 2054
1082.1	Noel Hill,	50.7, 51.0, 50.8	1629, 1737, 2090, 2054
1084.3	Barton Peninsula	51.9, 51.0, 51.0, 50.4	1951, 1825, 1984, 2090
1084.6	"	50.6, 51.0, 50.4	1604, 1323, 1854, 2054
1089.2	Northern Barton Peninsula	49.3, 49.9, 50.0	2128, 1532, 1951, 1382, 1793
1089.3	"	51.2, 50.0, 50.8	1532, 1886, 1984
1091.4	"	49.6, 50.0, 50.0	2054, 2205, 1984, 2090
1091.5	"	49.9, 50.0, 50.1	2128, 2205, 1656, 2128
1303	Central West	51.8, 50.9, 51.0	2205, 2054, 2205, 1764
1318.1	Barton Peninsula	50.2, 50.2, 50.8	1951, 2167, 1951, 2128
1319.1	"	49.8, 49.7, 50.0	1951, 1235, 1984, 2054
1351.2	North Eastern	50.7, 50.1, 50.6	1737, 2167, 2205, 1984
1351.4	Marion Cove	51.4, 52.6, 51.7	1917, 2167, 2090, 2054
1352.1	"	51.1, 50.0, 50.6	1532, 1465, 1681, 1487, 1854
1352.2	"	50.7, 51.2, 50.9	1825, 1917, 2167, 2205, 1737
1352.3	"	51.0, 50.0, 50.5	2205, 2167, 2205, 1984
1359.2	North East,	50.5, 49.9, 50.6	1951, 1186, 2128, 1917
1359.4	Keller Peninsula	49.4, 51.2, 50.8	1708, 1508, 1532, 2205
1359.6	"	52.7, 50.8, 51.5	1984, 1793, 1170, 2205
1359.8	"	52.0, 51.7, 51.8, 50.4	2128, 1580, 1854, 2018
1362.2	"	51.2, 51.1, 51.2	1656, 1854, 2205, 1604
1362.3	"	50.5, 50.8, 50.6	1956, 2128, 2018, 2018
1365.1	"	49.5, 49.0, 49.0 (pitted)	1917, 1402, 2054, 1343
1383.1	"	50.6, 51.5, 50.8	1764, 2205, 2205, 2018

//Continued.....

Table 3.6 (continued)

Specimen No.	Location	Reflectivity (at 589 nm)	Vickers Hardness Number (100g load)
1386.1	North East, Keller Peninsula	49.3, 49.7, 49.8 (pitted)	2054, 1956, 1487, 1604
1396.5	Half-Moon Island	50.6, 51.0, 50.8, 50.1	1465, 1886, 1764, 1656
1396.6	"	51.5, 52.0, 50.0, 53.0	1951, 1854, 1886, 1764
1398.1	"	52.4, 51.2, 51.8	1580, 1555, 1764, 1382
1509.1	"	52.5, 50.9, 51.4	1186, 1287, 1030, 1508
1347	Lavas, Barton	51.8, 50.5, 50.9	1917, 2018, 2054
1349.1	Peninsula	51.5, 50.6, 50.8	2054, 1951, 2054, 2128
PYRRHOTITE			
1082.1	Noel Hill, Barton Peninsula	R min 34.9, 34.5, 35.8 R max 39.6, 39.4, 39.2	322, 311, 374, 360
1084.3	"	R min 34.6, 34.8, 34.9 R max 40.1, 40.7, 40.6	324, 275, 382, 364
1303.2	"	R min 34.7, 34.8, 35.2 R max 39.8, 39.9, 40.1	380, 313, 353, 355
CHALCOPYRITE			
1082.1	Noel Hill, Barton Peninsula	40.0, 41.0, 40.8	248, 246, 284
HEMATITE			
1017.3E	Southern Fildes Peninsula	24.8, 23.4, 24.2, 23.5	1042, 871, 945
TENORITE			
1017.3E	Southern Fildes Peninsula		236

TABLE 3 : 7 CELL DIMENSIONS OF PYRITE FROM "QUARTZ-PYRITE" ROCKS

SPECIMEN NO.	LOCATION	a_o
1064.1	Southern Fildes Peninsula Intermediate Argillic Alt^n/	5.390
1078.21A	Headland Opposite Dufayel Island Phyllic Alt^n/	5.418
1352.2	North West Barton Peninsula Propylitic alteration	5.418
1359.8	East Keller Peninsula Advanced Argillic Alt^n/	5.405
1396.6	Half-Moon Island. Intermediate Argillic Alt^n/	5.407
STANDARD	J.C.P.D.S.	5.417

TABLE 3:8A MODAL ANALYSES OF "QUARTZ-PYRITE" ROCKS, (A) ADVANCED ARGILLIC ALTERATION.

Specimen Number	Location	Quartz	Alunite	Pyrophyllite	Kaolinite	Fluorite	Gypsum	Rutile	Native Sulphur	Diaspore	Resorbed Amphibole	Plagioclase	Carbonate	Pyrite	Total
1088.1	Northern Barton Peninsula	69.8	11.8	-	6.0	-	-	2.6	-	-	-	-	-	9.8	100.0
1089.2	Northern Barton Peninsula	25.3	-	62.1	-	2.8	-	0.5	-	-	-	-	-	9.3	100.0
1089.3	Northern Barton Peninsula	85.5	5.8	-	-	-	-	0.7	7.7	-	-	-	-	0.3	100.0
1091.4	Northern Barton Peninsula	56.0	-	-	38.6	-	-	0.9	-	-	-	2.1	-	2.3	99.9
1315.1	Northern Barton Peninsula	64.5	33.4	-	-	-	-	1.6	-	-	-	-	-	0.5	100.0
1315.3	Northern Barton Peninsula	34.2	63.0	-	<0.1	-	-	2.3	-	-	-	-	-	0.5	100.0
1315.9	Northern Barton Peninsula	92.9	2.3	-	<0.1	-	-	3.5	-	-	-	-	-	1.2	99.9
1315.12	Northern Barton Peninsula	96.3	0.6	-	1.3	-	-	1.5	-	-	-	-	-	0.3	100.0
1359.1	Keller Peninsula	82.6	7.2	-	6.8	-	-	0.4	-	-	-	-	-	3.0	100.0
1359.3	Keller Peninsula	91.0	-	-	0.7	-	6.4	1.3	-	-	-	-	-	0.5	99.9
1359.5	Keller Peninsula	88.8	4.1	-	3.6	-	-	0.8	-	-	-	-	-	2.7	100.0
1359.7	Keller Peninsula	66.2	29.7	-	0.9	-	-	0.3	-	-	-	-	-	2.8	99.9
1359.8	Keller Peninsula	35.4	40.8	-	16.5	-	0.3	0.4	-	<0.1	-	-	-	6.5	99.9
1359.10	Keller Peninsula	55.7	41.6	-	0.5	-	-	1.0	-	-	-	-	-	1.2	100.0
1362.1	Keller Peninsula	68.5	-	-	10.0	-	9.5	<0.1	-	0.2	10.8	-	-	0.9	99.9
1362.3	Keller Peninsula	43.8	36.7	-	13.0	-	5.8	0.2	-	-	-	-	-	0.4	99.9

All analyses determined on 1000 points.

Table 3.8B MODAL ANALYSES OF "QUARTZ-PYRITE" ROCKS (B) INTERMEDIATE ARGILLIC ALTERATION.

Specimen No.	Location	Quartz	Kaolinite	Muscovite	Rutile	Plagio-clase	Carbonate	Pyrite	Total
1024.8	Southern	12.9	22.3	-	1.6	37.5	24.2	1.5	100.0
1024.11	Fildes	22.0	26.0	-	<.1	21.6	28.2	2.2	100.0
1026.16	Peninsula	14.7	30.7	-	0.1	23.8	29.3	1.5	100.10
1028.00	"	36.2	17.4	-	<.1	17.5	27.0	1.9	100.00
1029.1	"	27.6	34.3	-	<.1	-	32.0	6.1	100.00
1051.1A	"	25.6	17.1	-	0.2	-	56.2	0.9	100.00
1051.2C	"	22.8	20.5	-	<.1	-	55.9	0.8	100.00
1064.1	"	12.7	35.7	-	2.8	10.4	36.7	1.7	100.00
1078.8A	Headland Opposite Dufayel Island	31.3	-	52.5	<.1	6.6	9.3	0.5	100.20
1382.2	Northern Keller Peninsula	22.2	-	53.4	0.2	6.1	17.2	1.0	100.10
1396.5	Half-	20.9	4.7	-	0.9	36.8	32.0	4.7	100.00
1396.6	Moon Island	50.2	26.3	-	1.3	-	18.7	3.5	100.00

All analyses determined on at least 1000 points.

TABLE 3:8C MODAL ANALYSES OF "QUARTZ-PYRITE" ROCKS,(C) PHYLLIC ALTERATION.

Specimen Number	Location	Quartz	Muscovite	Rutile	Plagioclase	Laumontite	Pyrite	Total
1072.7	Precious Peaks	26.3	8.4	1.3	-	62.5	1.4	99.9
1073.6	Stenhouse Bluff	40.7	55.7	< 0.1	0.2	-	3.4	100.0
1073.7	Stenhouse Bluff	40.1	55.8	< 0.1	0.6	-	3.5	100.0
1075.12	Ullman Spur	36.4	53.0	0.3	2.9	-	7.4	100.0
1078.21A	Headland Opposite Dufayel Island	57.7	18.6	< 0.1	-	-	23.7	100.0
1079.20	Crepin Point	58.3	39.0	< 0.1	-	-	2.7	100.0
1337.7	Southern Barton Peninsula	48.1	43.5	< 0.1	6.5	-	1.9	100.0
1337.8	Southern Barton Peninsula	52.3	40.0	< 0.1	7.3	-	0.4	100.0

All analyses determined on 1000 points.

TABLE 3:8D MODAL ANALYSES OF "QUARTZ-PYRITE" ROCKS, (D) PROPYLITIC ALTERATION.

Specimen Number	Location	Quartz	Muscovite	Rutile	Plagioclase	Uralite	Biotite + Chlorite	Tourmaline	Andalusite	Kaolinite	Carbonate	Epidote	Pyrite + Pyrrhotite	Amphibole	Total
1082.1	Noel Hill	35.1	55.1	< 0.1	-	-	-	-	-	-	-	-	9.8	-	100.0
1084.3	Noel Hill	33.3	50.4	< 0.1	3.4	-	-	-	-	-	-	-	12.9	-	100.0
1303.7	0.3 Km west of Noel Hill	61.7	33.5	< 0.1	-	-	-	0.5	-	-	-	-	4.2	-	99.9
1319.1	0.3 Km west of Noel Hill	31.6	52.0	< 0.1	8.0	-	-	-	-	-	-	-	8.3	-	99.9
1351.1	Eastern Marion Cove	25.7	-	< 0.1	53.2	-	5.6	-	-	-	10.9	1.7	1.4	1.6	100.1
1351.2	Eastern Marion Cove	44.4	15.3	< 0.1	28.9	-	5.3	-	-	-	3.9	0.1	2.0	-	99.9
1351.3	Eastern Marion Cove	38.2	9.5	0.1	35.6	0.6	11.4	-	-	0.9	0.5	0.5	1.3	1.2	99.8
1351.4A	Eastern Marion Cove	50.9	12.6	< 0.1	9.2	-	16.9	-	-	7.8	0.1	0.4	2.3	-	100.2
1351.4B	Eastern Marion Cove	26.5	22.9	0.1	17.3	-	19.5	-	-	10.4	-	0.3	3.1	-	100.1
1352.1	Eastern Marion Cove	35.5	36.1	< 0.1	-	-	2.1	3.4	17.5	-	-	-	5.4	-	100.0
1352.2	Eastern Marion Cove	70.1	23.1	< 0.1	0.1	-	0.3	1.5	-	2.9	-	0.1	1.9	-	100.0
1352.3	Eastern Marion Cove	53.5	28.8	< 0.1	2.2	3.0	2.7	1.1	-	-	7.7	0.1	0.7	-	99.8
1377.1B	Breccia Vein, Keller Peninsula	17.7	-	-	-	-	8.0	-	-	-	54.8	-	19.5 (Native Copper)	-	100.0

All analyses determined on 1000 points.

TABLE 3:9 MODAL ANALYSES OF OPAQUE PHASES IN THE JURASSIC LAVAS, TERTIARY INTRUSIVES AND " QUARTZ-PYRITE " ROCKS.

Specimen Number	Location	Rock Type	Pyrite	Pyrrhotite	Chalcopyrite	Bornite	Hematite	Magnetite	Ilmenite	Marcasite-Pyrite	Goethite	Rutile	Total
1082.1	Barton Peninsula	Propylitic Alteration	40.2	43.8	0.9	-	2.7	-	-	8.3	-	4.1	100.0
1084.3A	Barton Peninsula	Phyllic Alteration	16.2	76.2	0.2	-	7.3	-	-	-	-	-	99.9
1084.3B	Barton Peninsula	Phyllic Alteration	10.2	80.7	0.4	-	8.4	-	-	0.4	-	-	100.1
1089.3	Barton Peninsula	Advanced Argillic Alteration	99.9	-	-	-	-	-	-	-	-	0.1	100.0
1315.1	Barton Peninsula	Advanced Argillic Alteration	99.9	-	-	-	-	-	-	-	-	0.1	100.0
1319.1	Barton Peninsula	Phyllic Alteration	13.5	75.5	0.5	-	8.6	-	-	1.9	-	-	100.0
1359.6	Keller Peninsula	Advanced Argillic Alteration	98.0	-	-	-	1.8	-	-	-	-	0.2	100.0
1359.8	Keller Peninsula	Advanced Argillic Alteration	97.0	-	0.1	-	2.9	-	-	-	-	0.1	100.1
1017.3E	Fildes Peninsula	Intermediate Argillic Alteration	28.7	-	69.2	-	-	-	-	-	2.1	-	100.0
1067.1B	Fildes Peninsula	Intermediate Argillic Alteration	-	81.7(Tenorite)		-	10.8	-	-	-	7.6 (Chalcocite)		100.1
1079.14A	Crepin Point	Diorite	14.0	-	-	-	3.0	77.0	6.0	-	-	-	100.0
1353.2	Barton Peninsula	Granodiorite	3.4	-	-	-	4.5	80.7	11.4	-	-	-	100.0
1355.1	Barton Peninsula	Granodiorite	-	-	-	-	-	86.5	13.5	-	-	-	100.0
1396.6	Half-Moon Island	Diorite	2.9	-	-	-	6.5	45.6	44.9	-	-	-	99.9
1071.1	Dufayel Island	Andesite	74.4	-	9.9	-	6.5	-	-	-	-	9.2	100.0
1073.1B	Stenhouse Bluff	Andesite	38.3	-	2.5	-	5.8	50.8	2.5	-	-	-	99.9
1075.11	Ullman Spur	Andesite	-	-	-	-	7.1	92.9	-	-	-	-	100.0
1341.4	Barton Peninsula	Andesite	-	-	-	-	14.0	78.1	7.8	-	-	-	99.9
1347	Barton Peninsula	Andesite	76.7	-	18.8	0.8	-	-	-	-	-	3.6	99.9
1383.4	Barton Peninsula	Andesite	4.9	-	-	-	1.2	93.8	-	-	-	-	99.9

(All analyses determined on 1000 points).

TABLE 3:10A MODAL ANALYSES OF TERTIARY INTRUSIVES FROM THE SOUTH SHETLAND ISLANDS.

Specimen Number	Location	Quartz	Plagioclase	Orthoclase	Biotite	Chlorite	Amphibole+ Pyroxene	Muscovite	Hypersthene	Epidote	Carbonate	Opaques	Rock Type
1079.9	Crepin Point	11.2	62.8	2.1	-	-	16.6	-	-	0.5	-	6.8	Qtz-diorite
1079.13	Crepin Point	35.2	51.6	10.0	-	-	0.3	-	-	-	-	3.0	Qtz-diorite
1079.14A	Crepin Point	2.9	74.0	0.3	5.7	-	13.9	-	-	-	-	3.2	Qtz-diorite
1079.18	Crepin Point	6.0	71.6	1.1	2.3	-	16.6	-	-	-	-	2.4	Qtz-diorite
1083.6B	Barton Peninsula	16.8	58.5	1.3	0.2	0.9	12.7	5.2	-	0.9	-	3.5	Granodiorite
1318.1	Barton Peninsula	12.1	72.5	<0.1	-	0.2	5.7	-	-	1.9	-	7.6	Granodiorite
1350.1	Barton Peninsula	20.7	58.7	3.5	0.8	7.2	2.0	1.7	-	2.2	1.6	1.6	Granodiorite
1350.2	Barton Peninsula	25.1	52.1	2.5	<0.1	5.5	0.1	11.2	-	1.6	0.5	1.3	Granodiorite
1353.1	Barton Peninsula	15.1	69.4	0.7	4.2	-	7.0	0.5	-	1.4	-	1.7	Granodiorite
1356.2A	Barton Peninsula	3.5	76.0	1.2	11.4	0.2	-	-	4.8	-	-	2.7	Qtz-diorite
1356.2B	Barton Peninsula	1.1	74.3	0.2	14.2	0.4	-	-	2.8	2.4	-	4.6	Qtz-diorite
1358.1	Barton Peninsula	14.5	66.7	0.5	4.2	0.4	12.0	-	-	-	-	1.7	Granodiorite
1395.1	Half-Moon Island	16.9	45.0	0.2	-	-	18.9	16.4	-	-	-	2.8	Qtz-diorite
1398.1	Half-Moon Island	0.4	69.1	1.8	-	-	26.0	2.4	-	-	-	0.4	Qtz-diorite

(All determinations on 1000 points).

TABLE 3:10B MODAL ANALYSES OF VOLCANIC ROCKS, KING GEORGE ISLAND.

Specimen Number	Location	Quartz	Feldspar	Uralite	Amphibole	Chlorite	Glass	Muscovite	Rutile	Carbonate	Epidote	Opaques	Total	Rock Type
1054.1	Fildes Peninsula	0.2	48.7	18.2	2.7	-	29.8	-	<0.1	-	-	0.4	100.0	Andesite
1051.5	Fildes Peninsula	4.2	30.1	-	-	3.8	26.4	0.5	0.2	31.4	-	3.6	100.2	Andesite
1067.4	Fildes Peninsula	1.3	44.7	-	-	-	-	4.7	0.1	44.7	-	5.5	101.0	Andesite
1073.16	Stenhouse Bluff	-	54.7	-	-	17.6	-	18.0	<0.1	-	2.3	7.5	100.1	Rhyodacite
1075.11	Ullman Spur	6.1	30.4	-	-	6.0	49.9	4.7	1.4	-	<0.1	2.4	100.9	Andesite
1078.16	Headland Opposite Dufayel Island	1.6	25.3	-	-	1.6	51.1	6.1	0.2	12.6	<0.1	1.8	100.3	Andesite
1314.1	Barton Peninsula	5.9	26.7	1.3	-	8.9	40.7	15.0	0.2	-	-	1.5	100.2	Rhyolite
1324.1	Barton Peninsula	1.5	54.4	30.1	-	11.2	-	-	<0.1	-	0.5	2.9	100.6	Andesite
1337.1	Barton Peninsula	0.6	62.9	27.5	1.2	-	-	1.4	<0.1	-	0.3	6.1	100.0	Andesite
1361.1	Keller Peninsula	-	32.8	11.3	2.1	-	48.1	3.5	0.1	-	-	2.1	100.0	Andesite
1369.2	Keller Peninsula	8.6	5.2	-	-	0.5	33.8	2.9	<0.1	44.1	-	4.8	99.9	Andesite
1369.3	Keller Peninsula	10.0	17.4	39.9	-	4.6	25.1	0.6	<0.1	-	-	2.4	100.0	Andesite

(All determinations on 1000 points).

CHAPTER 4

COPPER DEPOSIT, NORTH OF CHARITY GLACIER, LIVINGSTONE ISLAND

4.1 Introduction

Livingstone Island, first discovered by William Smith in the brig "Williams" in February 1819 is the largest of the South Shetland Islands and lies at the southern end of the group (Fig. 4:1). Its precise location is between latitudes 62° 27' and 62° 48' south and longitudes 59° 45' and 61° 15' west.

Most of the early geological survey work on Livingstone Island was done in the first two decades of this century by Anderson (1906), Ferguson (1921) and Tyrrell (1921). Later more detailed work has been carried out since International Geophysical Year (1960) notably by Hobbs (1963), Araya and Herve (1966), Dalziel et al (1969 and 1972) and Valle et al (1975).

The area studied from early to late February 1976 lies in the south east part of the island between latitudes 62° 42' and 62° 44' south and longitudes 60° 18' and 60° 22' west (Fig. 4:1). The mineralisation in this area consists of a porphyry copper-molybdenum deposit that shows characteristic metalliferous sulphide zonation. The main sulphide minerals which occur in veinlets of random orientation are an inner zone of chalcopyrite, bornite, molybdenite and pyrite with an outer zone of galena, sphalerite and chalcopyrite. The mineralisation and associated igneous rocks are discussed below.

4.2 Field Relationships of Plutonic and Hypabyssal Rocks

A composite tonalitic pluton occurs north of Charity Glacier, Livingstone Island (Fig. 4:2, 4:3) which varies in composition from a coarse hornblende-rich diorite to a fine-grained tonalite. The earliest phase of intrusion in this polyphase plutonic episode is a

Table 4:2 Relationships of Igneous Rocks, North of Charity Glacier

(based on petrography)

State of Magma	Intrusive and/or mineralization	Tectonics
		SLIGHT THERMAL PULSE?
SOLID	MINERALIZATION AND ALTERATION	
SOLID	BRECCIA DYKES (HYDROTHERMAL)	
SOLID	? TONALITE SOUTH OF CHARITY GLACIER	
-?-?-?-?-?-	DOLERITE DYKES	
		--?---?---?---?---?---
MAGMA IN PROCESS OF CONGEALING	APLITE DYKES AND SHEETS	THERMAL AND TECTONIC STRESSES, NORTH OF CHARITY GLACIER CAUSE FOLIATION IN SYNPLUTONIC DYKES AND APLITE SHEETS.
MAGMA FLUID	SYNPLUTONIC DYKES	
MAGMA FLUID	TONALITE MAGMA	
MAGMA FLUID	DIORITE MAGMA	

dark green to black, hornblende-rich diorite, which is characterised by non-uniform composition and texture. It is generally non-foliated and coarse to medium-grained. Following this a light green-grey medium-grained tonalite was intruded. It contains dark greenish-grey ovoid to subspherical inclusions which have narrow gradational contacts with the enclosing plutonic rocks and appear to be partially resorbed fragments of andesitic lava. Xenoliths of the diorite occur in the tonalite near the junction of the two plutons. A fine-grained, light grey tonalitic phase occurs on the western margin of the outcrop and probably represents a third phase of plutonic activity, slightly earlier than the medium-grained phase, since its area of outcrop seems too wide to be a chilled margin. However, its fine-grain size may be due to fairly rapid cooling caused by its abutting against cold country rocks. In the southern part of the area near Charity Glacier, the medium and fine-grained tonalites show a foliation which strikes N30° E i.e. (NE-SW) and will be discussed later. The tonalites here consist of mafic and felsic bands (Hobbs, 1963), the main mafic mineral being biotite.

Intruded into the foliated tonalites, just north of Charity Glacier are a series of highly deformed and metamorphosed rocks previously regarded as "Basement Complex" fragments (Hobbs, 1963) occuring as xenoliths in the tonalite (False Bay Schists). Field mapping, however, has revealed their dyke-like form, generally trending NNE-SSW (Fig. 4:2). In places they consist of schistose xenolithic lenses in the form of pillow-like globules in a foliated, tonalitic host (plate 4:1). The central parts of these dyke-like masses consist of hornblende and plagioclase whereas the margins are mainly biotite and plagioclase. Slight segregation into felsic bands has occurred (Hobbs, 1963).

In places these dyke-like masses neck out along their length or pass upwards into pillow-like globules, surrounded by tonalite.

Intruded into the tonalites and "False Bay Schists" are a series of sub-horizontal sheet and dyke-like masses of white to pinkish-white quartz-feldspar-biotite aplites. They generally dip 10°- 20°SE and trend NE and NW (Fig. 4:8C), and vary from fine-grained orthoclase-rich aplite in the north to coarse-grained plagioclase-rich aplite in the south near Charity Glacier. Although the ratio of orthoclase to plagioclase decreases southwards, the total feldspar contentsof these rocks remain approximately constant (table 4:3). The aplites vary in thickness from 20 cm. in the north of the outcrop area to 1 - 2 cm. in the south, near Charity Glacier (1538). Included fragments of tonalite occur in these rocks, often with a contact zone of fine-grained aplitic material around them (1543). The aplites are commonest in the southern part of the area where they can constitute up to 20% of the rock volume. A possible feeder dyke has been located in this area (plate 4:2). Where the aplites are in contact with the tonalite wall-rock they frequently have a fine-grained chill zone about 0.5 cm. wide. In places cavities can be found in these aplites (1516) with quartz crystals projecting inwards from the edges, presumably indicating low confining pressures when the rocks were intruded. Immediately north of Charity Glacier, the aplites show evidence of slight folding, and an introduced schistosity shown by the subparallel alignment of biotite laths (1538, plate 4:3).

A phase of doleritic dyke injection occurred after the intrusion of the aplite sheets as clearly indicated by the failure of the aplites to cut these dykes (plate 4:4) and by the presence of xenoliths of aplite (1563.2, plate 4:5) and tonalite (1560) in these dolerite dykes,

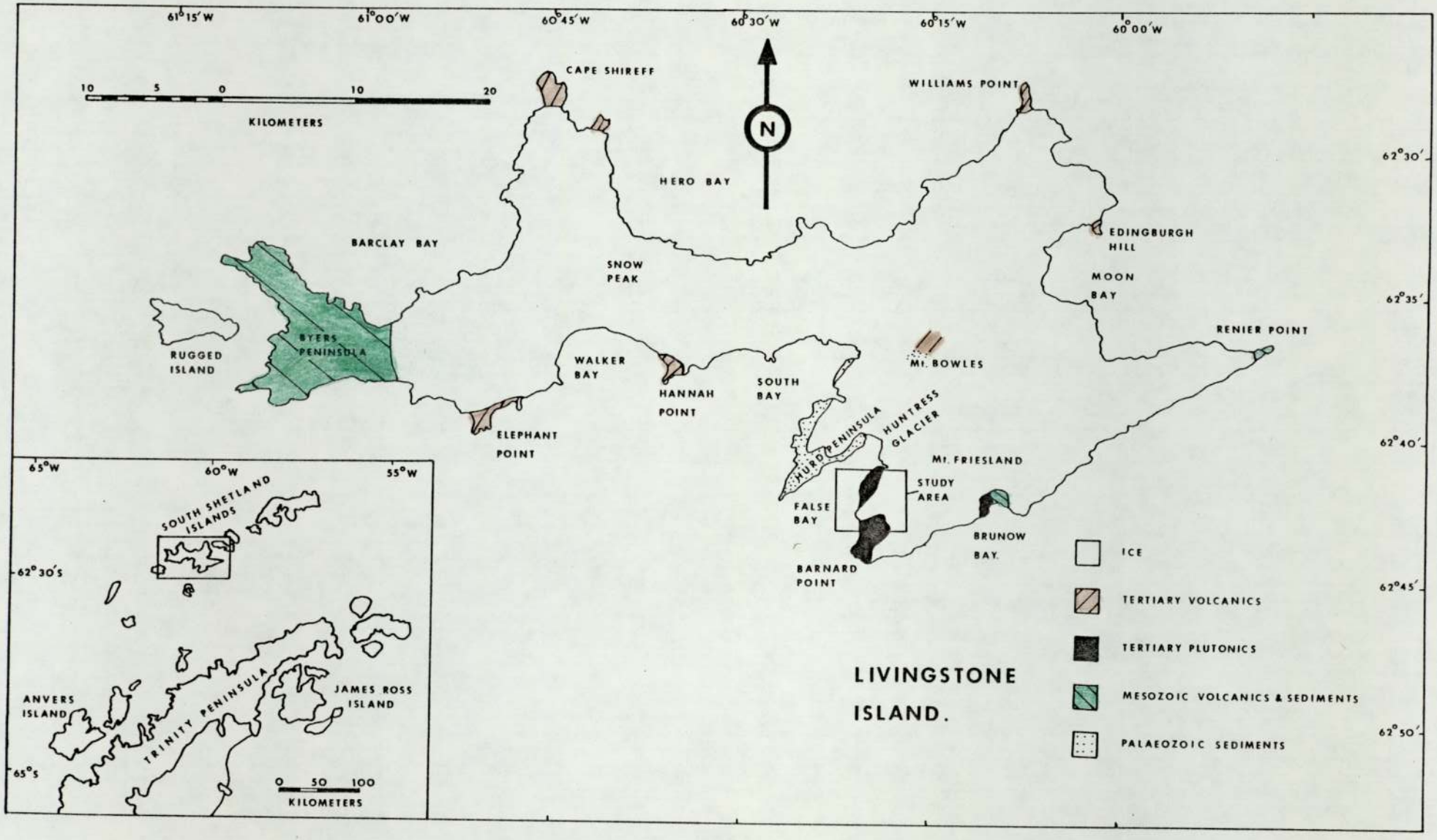

Fig 4:1 LIVINGSTONE ISLAND. INSERT SHOWS IT'S POSITION RELATIVE TO PENINSULA.(based on Hobbs 1963)

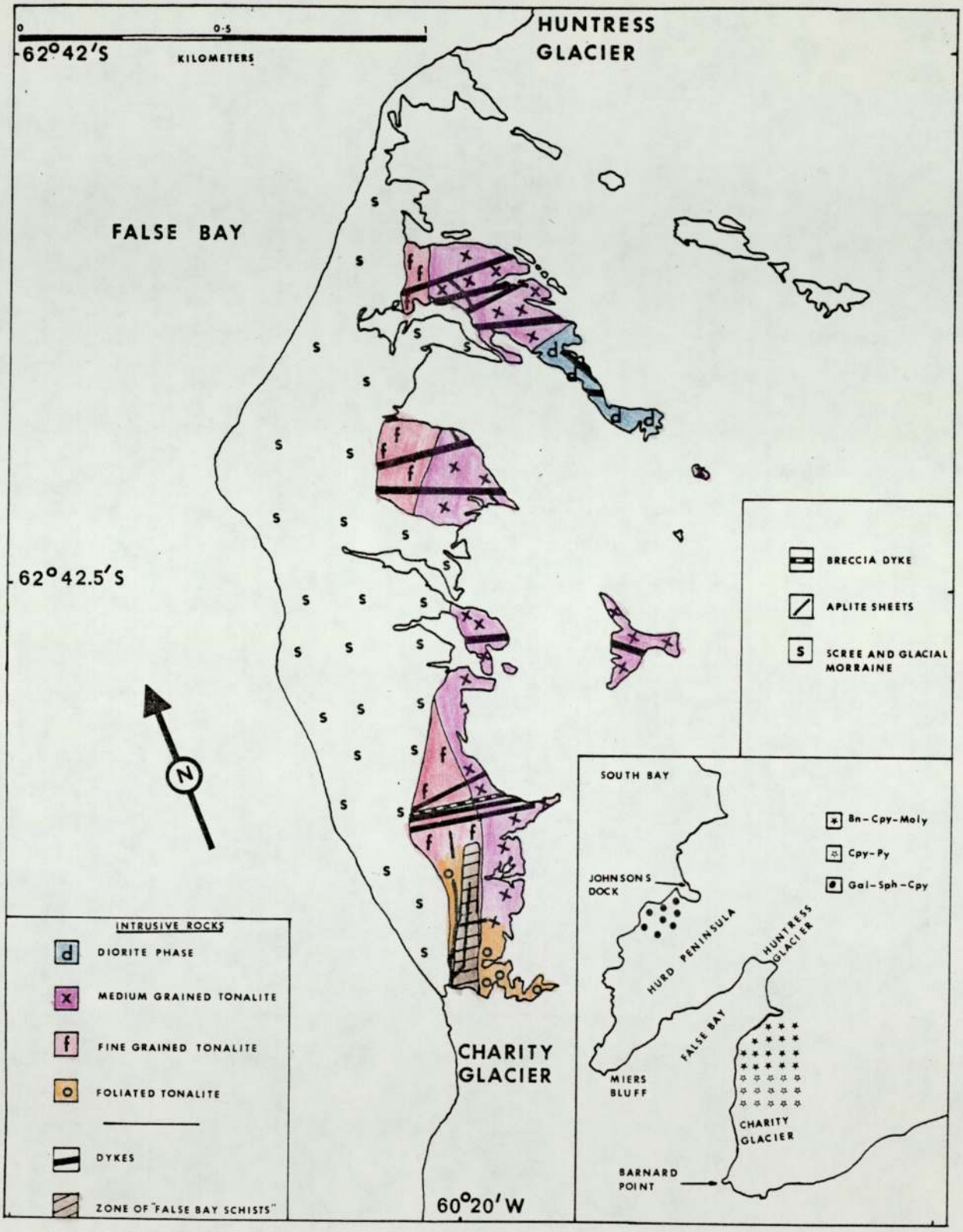

Fig 4:2 GEOLOGICAL SKETCH MAP OF AREA NORTH OF CHARITY GLACIER, LIVINGSTONE ISLAND. INSERT SHOWS METAL ZONATION IN FALSE BAY AREA (based on Vieira et al 1975).

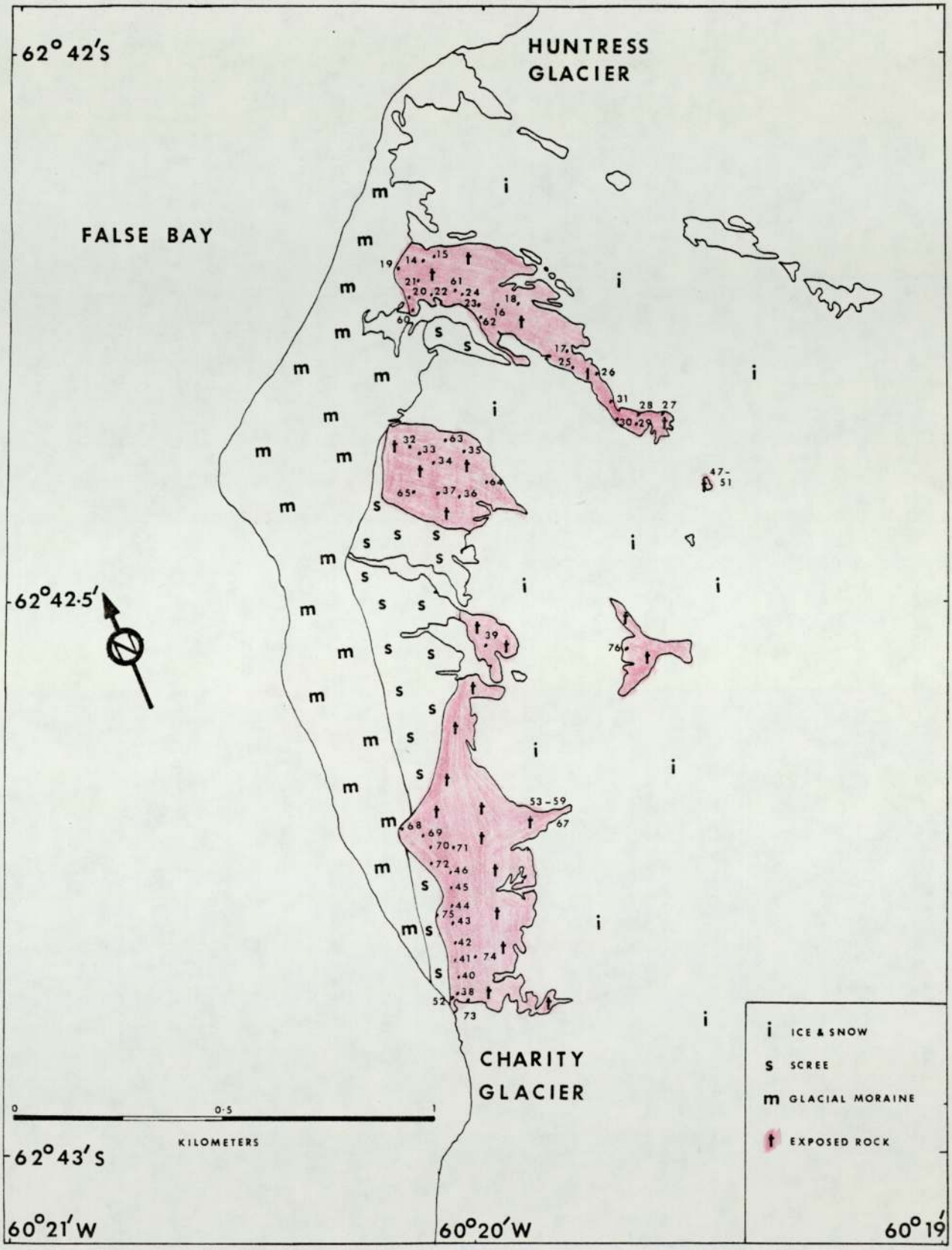

Fig4:3 SPECIMEN LOCATIONS NORTH OF CHARITY GLACIER.
(ALL ARE PREFIXED BY 15- -).LIVINGSTONE ISLAND.

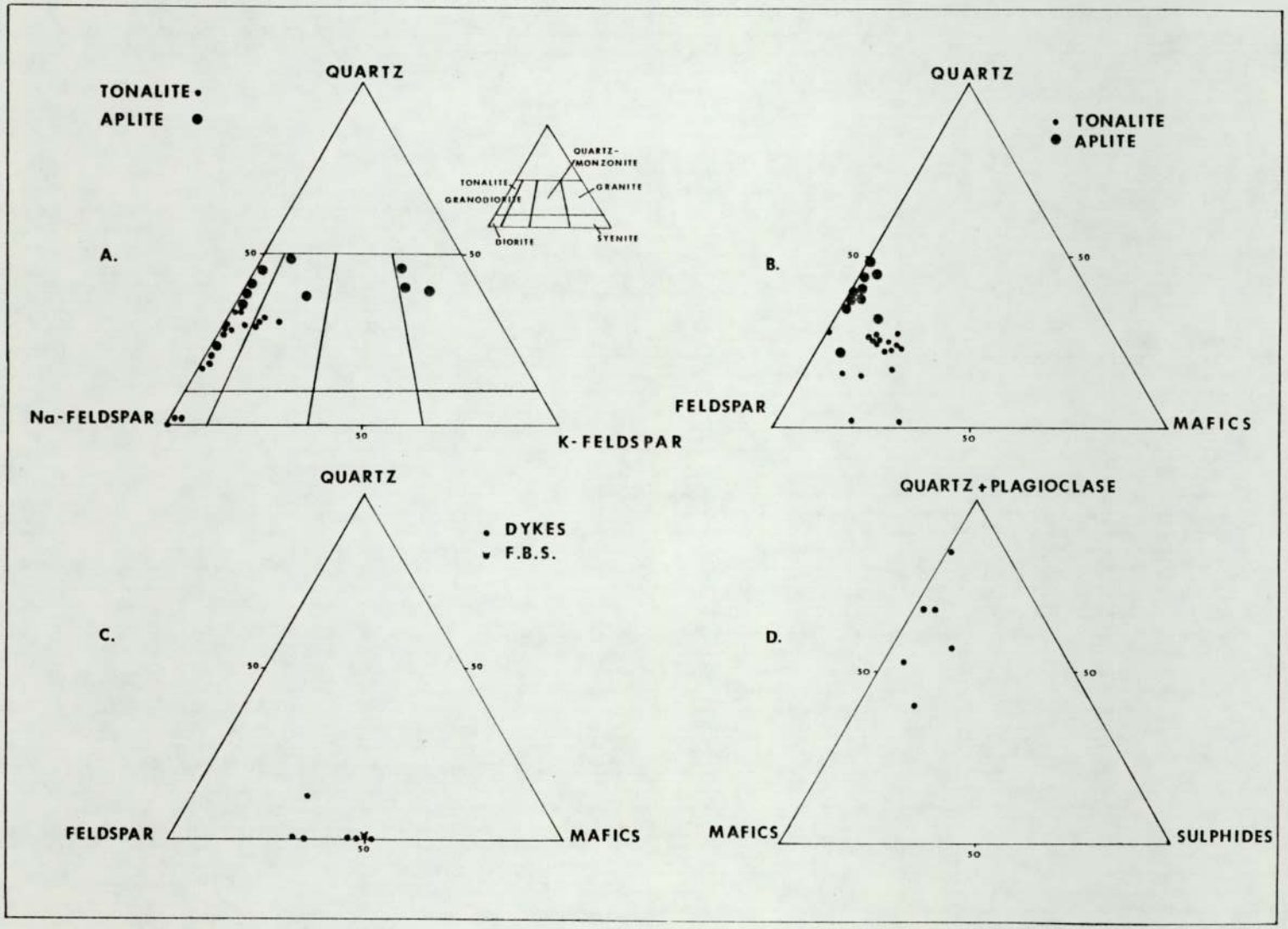

Fig 4:4 TERNARY DIAGRAMS OF MODAL DATA: A & B, TONALITES & APLITES; A, quartz–sodium feldspar–potassium feldspar, B; quartz–feldspar–mafics; C, quartz–feldspar–mafics FOR DYKES AND FALSE BAY SCHISTS (F.B.S.); D, quartz + plagioclase– mafics–sulphides FOR SULPHIDE BEARING VEINLETS. LIVINGSTONE ISLAND.

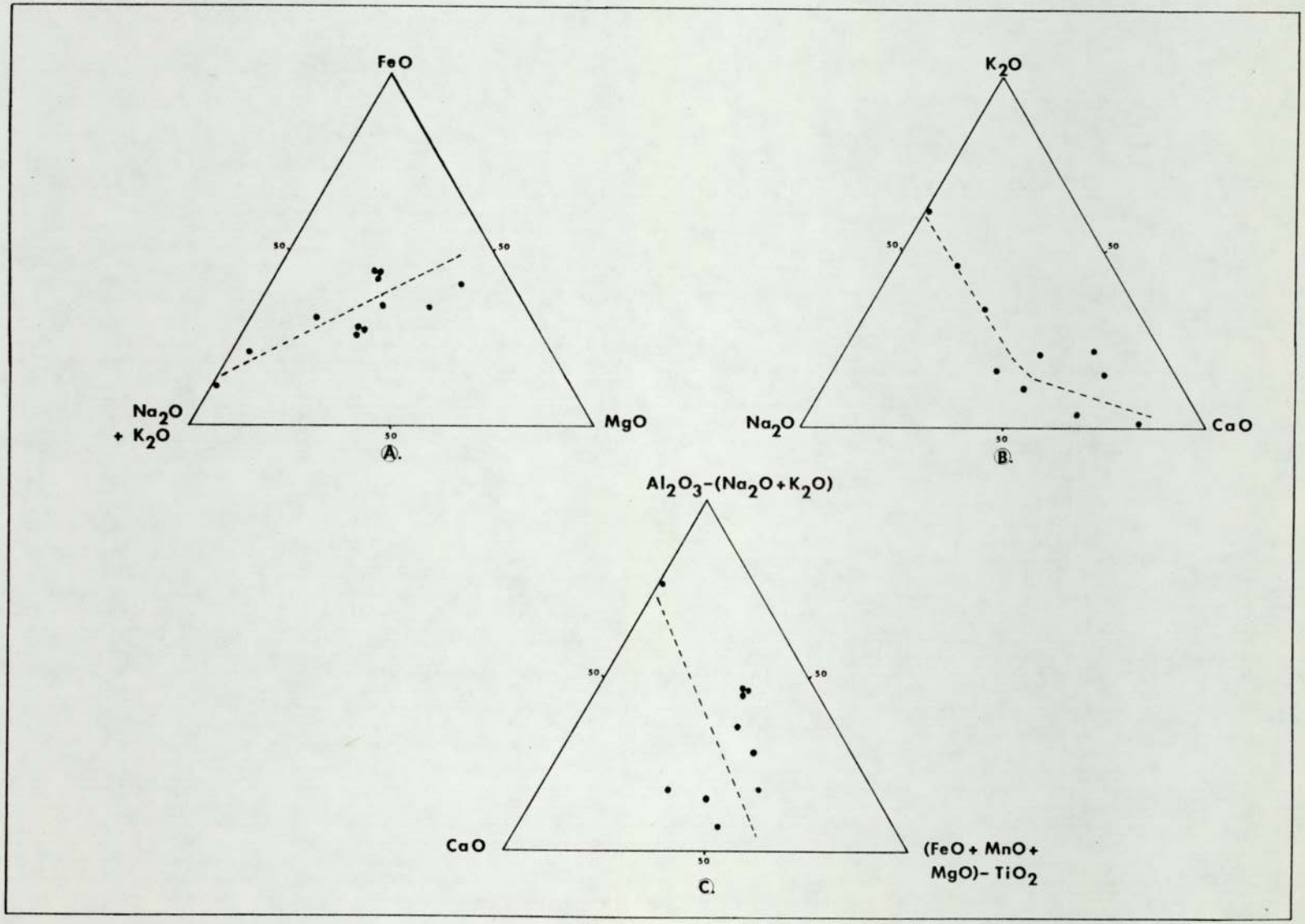

Fig 4:5 TERNARY PLOTS OF CHEMICAL DATA FOR TONALITES AND APLITES. LIVINGSTONE ISLAND.

A, $FeO-MgO-Na_2O+K_2O$; B, Na_2O-K_2O-CaO; C, $CaO-Al_2O_3-(Na_2O+K_2O)-(FeO+MnO+MgO)-TiO_2$.

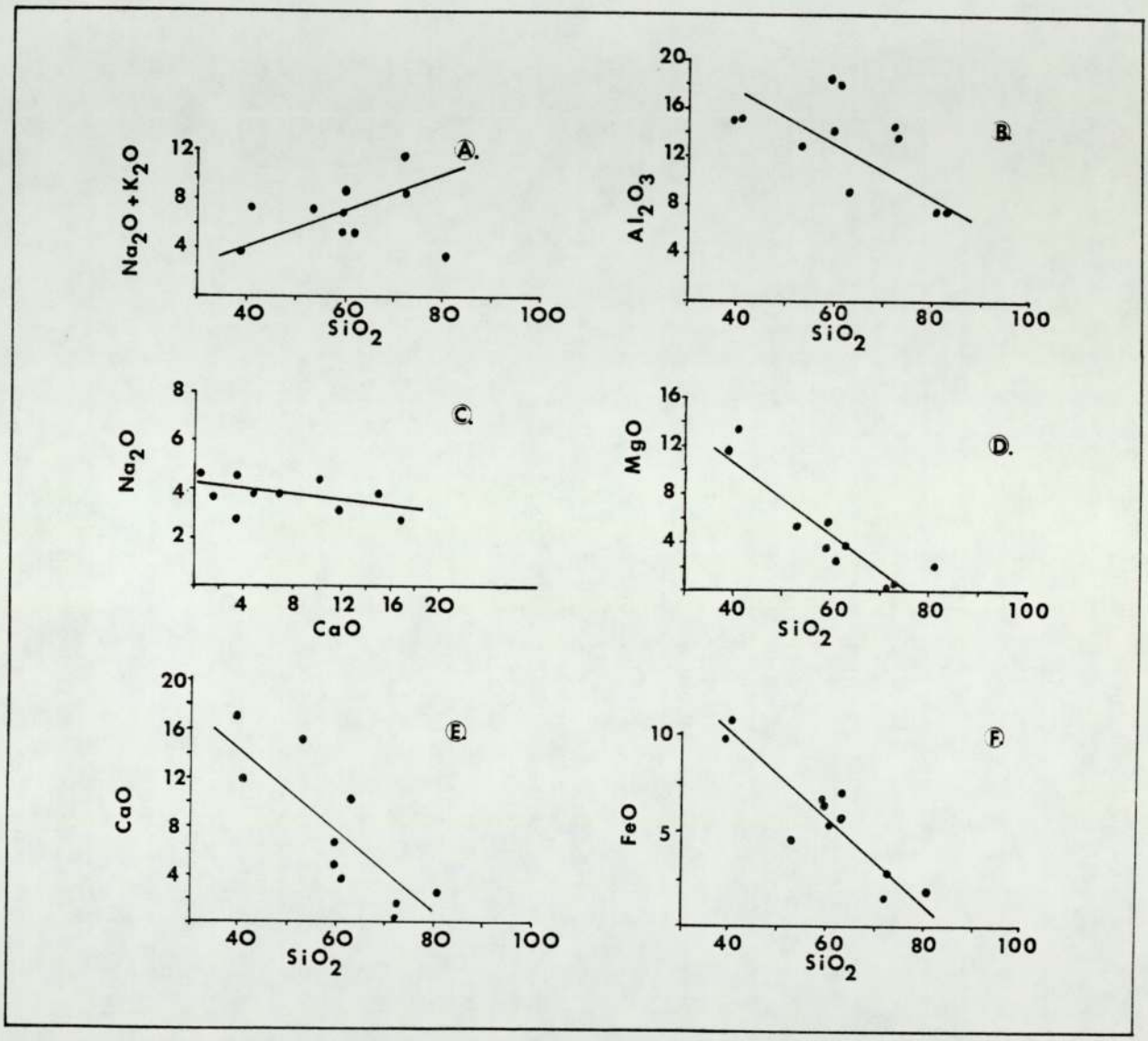

Fig 4:6 CHEMICAL VARIATION DIAGRAMS OF TONALITES & APLITES, NORTH OF CHARITY GLACIER, LIVINGSTONE ISLAND. Ⓐ, Na_2O+K_2O; Ⓑ, Al_2O_3; versus SiO_2; Ⓒ, Na_2O versus CaO; Ⓓ, MgO; Ⓔ, CaO; and Ⓕ, FeO; versus SiO_2.

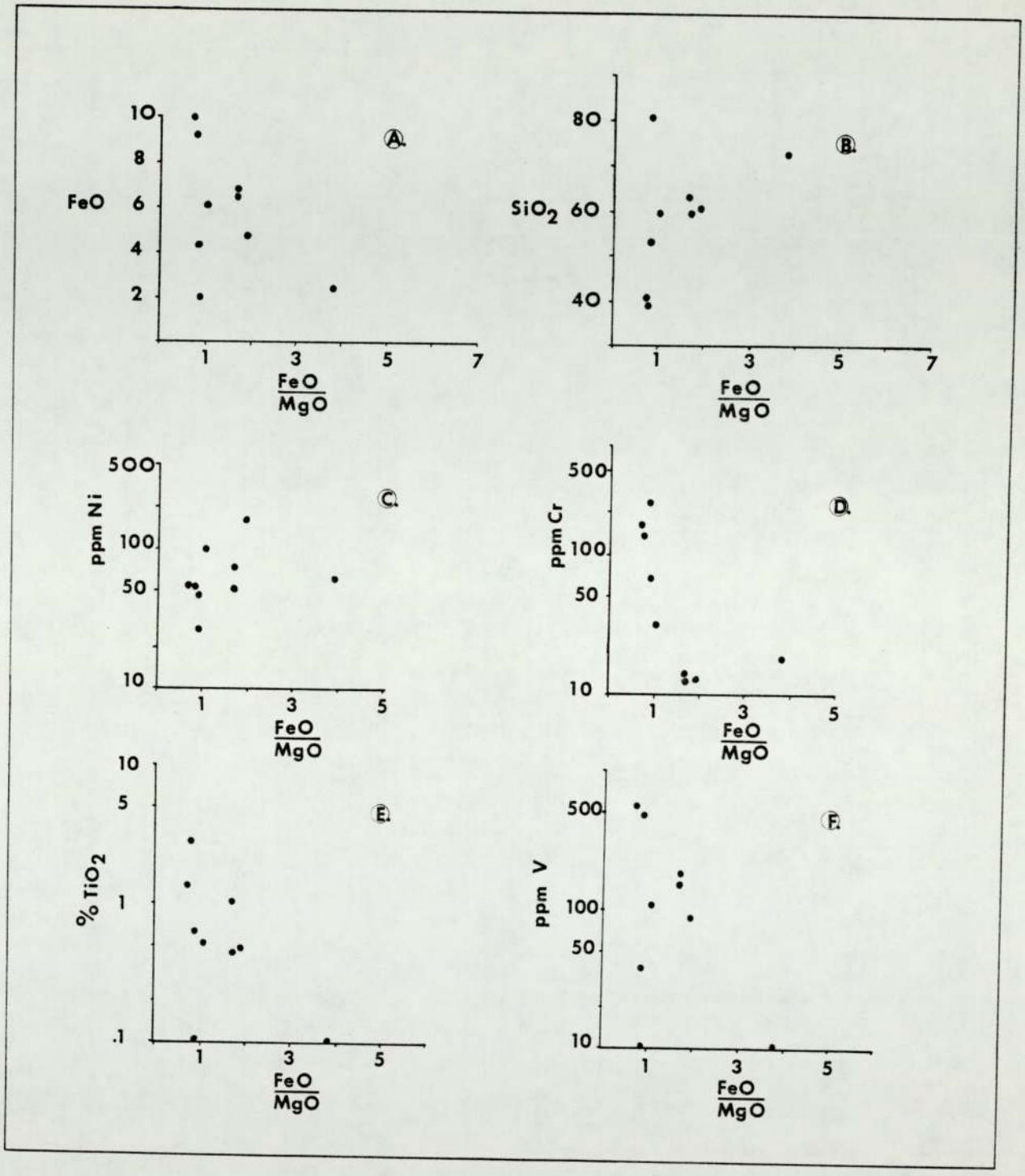

Fig 4:7 CHEMICAL VARIATION DIAGRAMS OF TONALITES AND APLITES, NORTH OF CHARITY GLACIER, LIVINGSTONE ISLAND. A, FeO; B, SiO_2; C, Ni; D, Cr; E, TiO_2; F, V; versus $\frac{FeO}{MgO}$ RATIO.

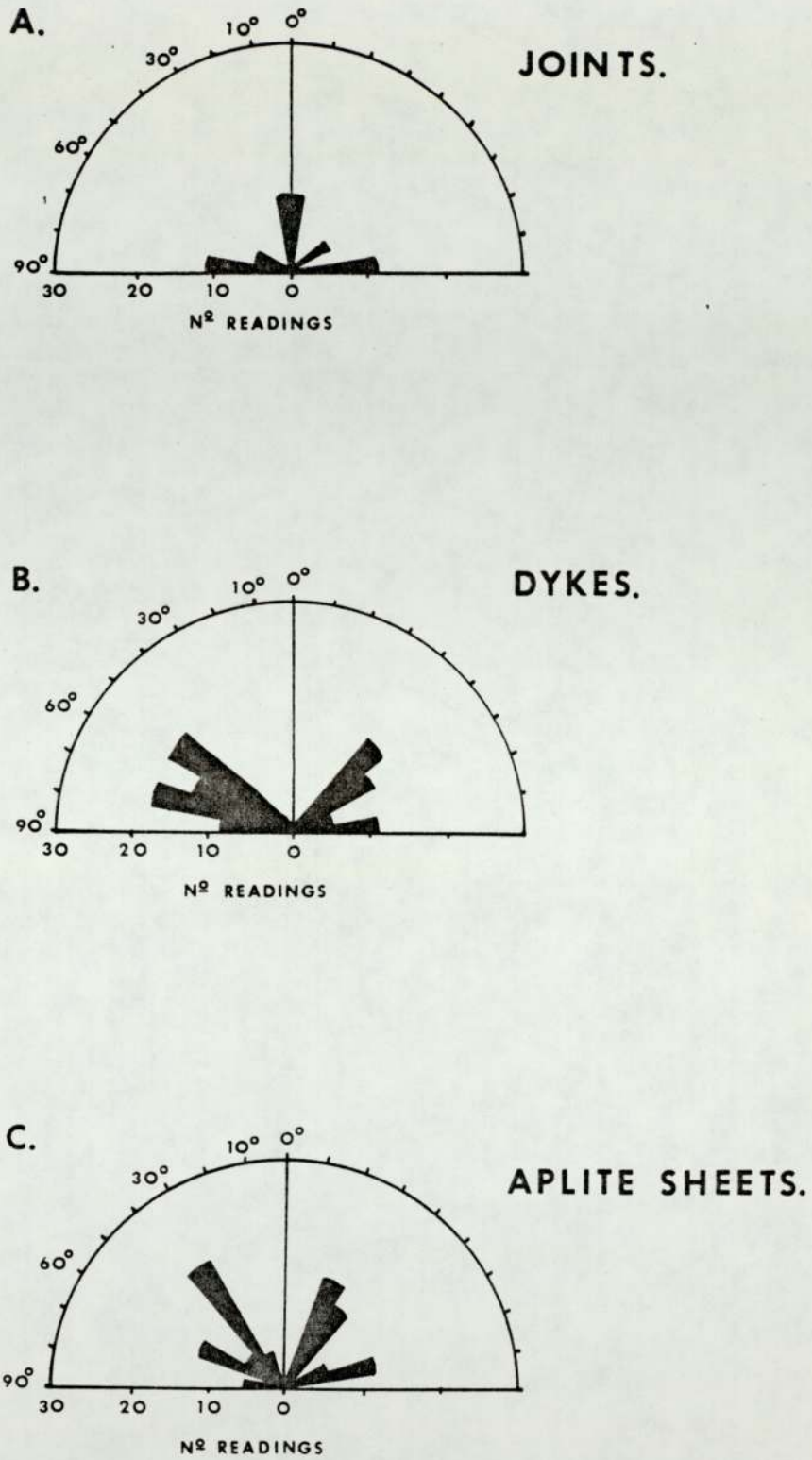

Fig 4:8 ROSE DIAGRAMS OF STRUCTURAL DATA. A, JOINTS IN PLUTONIC ROCKS; B, ORIENTATION OF DOLERITE DYKES; C, ORIENTION OF APLITE SHEETS. NORTH OF CHARITY GLACIER, LIVINGSTONE ISLAND.

although in places the dykes show boudinage structure, with the tonalite present in fractures in the dyke. Generally, the dolerite dykes are 1-4 m wide and trend NE-SW and NW-SE (Fig. 4:8B). The majority in the southern part of the area have been metamorphosed to hornblende-hornfels facies, although the intensity of this metamorphism decreases northwards away from Charity Glacier. There is a complete range of metamorphism from unaltered dolerite dykes to amphibolite. This suggests the process causing the alteration is not autometasomatism.

The latest phase of dyke intrusion appears to be narrow breccia dykes (20 cm. wide) which occur sub-parallel to the above dykes and probably have a hydrothermal origin. They often contain fragments of the nearby metamorphosed dykes (3-8 cm. maximum) and tonalites (1570.2) in a matrix of anhedral quartz, ferroandolomite and kaolinite. The whole dyke suite seems to have been intruded along regional extension fractures based on criteria by Ramsey (1967).

Joints

Mineralised joints and fractures generally have no specific directional components. The unmineralised joints, however, strike E-W and N-S (Fig. 4:8A) and are probably extension joints marking the position parallel to the direction of maximum principle compressive stress (based on Ramsey, 1967).

4.3 Petrography of Plutonic and Hypabyssal Rocks

4.3.1 Plutonic Rocks

Diorite

The dioritic phase consists of an hypidiomorphic mass of subhedral plagioclases (An_{50-45}, 5-0.2 mm.) showing normal and reverse zoning, with the calcic cores showing alteration to sericite, chlorite and epidote. Xenomorphic hornblende is the main phase (1528.1, 6-4 mm),

is later than plagioclase and contains poikilitic inclusions (<0.5mm) of biotite laths, colourless pyroxene (augite) and plagioclase. The hornblende, which is often zoned, shows alteration to pale green chlorite and epidote and in some instances seems to be replacing former augite. Interstitial granular sphene, zircon (<0.2 mm), anhedral carbonate (<0.5 mm) and epidote (1-0.4 mm) are also present (1530.1). Subhedral magnetite is present (<0.8 mm) showing alteration to hematite and is generally associated with chloritized hornblende crystals. Subhedral ilmenite is also present.

Modal analyses of the diorite indicates it consists of 27% plagioclase and 68% hornblende on average. Biotite, chlorite, pyroxene, sericite and magnetite are all <1.5% of the rock (table 4:3A).

Tonalites

a) Fine-Grained Phase

Petrographically, the rock consists of subhedral plagioclase laths (An_{45-35}) often zoned and showing slight alteration to sericite (2-0.2 mm). Interstitial quartz and orthoclase are present, often in myrmekitic intergrowths (1534). Subhedral biotite (2-0.1 mm) some of which is probably secondary (1540.1) and subhedral to anhedral hornblende (1.5 - 0.2 mm) often zoned due to replacement of pyroxene (plate 4:6) are present and usually show slight alteration to chlorite. Small amounts of sphene, euhedral apatite and granular zircon occur, along with rare blue-brown tourmaline (1568.1).

b) Medium-Grained Phase

This consists of zoned, subhedral plagioclase laths (An_{45-35}) showing alteration to sericite (1537.1B, 3-0.2 mm) with the basic cores containing inclusions of biotite and hornblende (1517.2). Interstitial anhedral quartz (3-0.1 mm) sometimes containing acicular rutile (1550.1) and anhedral orthoclase are also present, often in myrmekitic intergrowths

(1517.2). The mafic phases are subhedral biotite laths (5-0.1 mm) which often occur as inclusions in hornblende parallel to the cleavage (plate 4:7, 1555.2). The biotite commonly shows alteration to chlorite (1576.2) and some contain inclusions of quartz and feldspar. Some xenomorphic hornblende seems to be replacing plagioclase (2-0.1 mm). Granular zircon and rutile (<0.4 mm) are present associated with biotite, with sphene often present as a ring around magnetite. The opaque phases in this rock are subhedral magnetite, and subhedral ilmenite showing exsolution lamelli of hematite in two generations parallel to {0001}.

Modal analyses indicate quartz (13.5% - 27.3%) and plagioclase (44.8% - 66%) are the most abundant minerals, with smaller amounts of orthoclase (<6%) and hornblende (<20%). Biotite is normally less than 12%. The hornblende/biotite ratio varies between the igneous units, being >1 in the diorite and medium-grained tonalite, but <1 in the fine-grained phase. If the fine-grained phase has crystallized fairly rapidly, then this suggests that processes other than primary crystallization have produced hornblende in the other intrusives (table 4:3A).

4.3.2 Hypabyssal Rocks

"False Bay Schists"

The central parts consist, petrographically of xenoblastic hornblende, often in crystal aggregates and subhedral plagioclase, although quartz, orthoclase and minor biotite are also present. Biotite occurs in the hornblende usually having the same cleavage orientation (as it does in the tonalites). The edges of the dyke consists of biotite laths and plagioclase (1552.3). The biotite is usually bent and shows a slight foliation.

Aplite Dykes and Sheets

The aplites consist of a granular mass of anhedral quartz, often showing undulose extinction (2 - 0.1 mm), subhedral plagioclase (An_{20-10}, 8 - 0.2 mm), subhedral to anhedral orthoclase microperthite and minor microcline (1520.2). The earliest plagioclase crystals (which often show albite overgrowths) exhibit Carlsbad and multiple twinning, and in places have been partially resorbed by the melt, giving them a ragged appearance. Some myrmekitic intergrowths of quartz and feldspar occur. Plagioclase shows slight alteration to sericite but orthoclase seems fresh. Subhedral phlogopitic biotite laths (indicated by x-ray diffraction and electron microprobe) are present (1 - 0.2 mm) and are often slightly bent in the area around Charity Glacier where they possess a foliation (1538.7). Electron microprobe analysis indicates the phlogopitic biotite has an iron; magnesium; aluminium ratio of 28:54:18 (table 4:4), typical of metamorphic biotites as defined by Gower (1957). The ratio of 004-005 reflections indicate an iron content in octahedral sites of about 54% (based on data by Gower, 1957). Further north the mica is probably a true biotite as x-ray diffraction shows no {111} reflection. Subhedral magnetite (1520.4, 1544.1) and subhedral ilmenite (<0.1 mm) occur, usually showing partial alteration to hematite, although some hematite occurs along fractures in the biotite. Some ilmenite is also present in microfractures in the rock, (<0.3mm), and minor subhedral pyrite also occurs. Minor muscovite, rutile, epidote, apatite, zircon and sphene (1.5 - 0.2 mm) are present often associated with chalcopyrite (1536).

Modal analysis shows that quartz (48.6 - 22.3%), plagioclase (13.2 - 72%) and orthoclase (<.1 to 46.1%) are the major phases. Biotite is present at less than 11%, with the remaining minerals normally amounting to less than 4% of the aplites (table 4:3B).

Dolerite Dykes

The unaltered porphyritic dykes (1562.1) which occur in the north of the area (and are later than the consolidation of the tonalite) consist of a hypocrystalline mass containing "phenocrysts" of plagioclase (usually aggregates) and quartz (which has a reaction rim of pyroxene, plate 4:8). The phenocryst plagioclases, however, are considerably more sodic (An_{45-35}) than the groundmass plagioclases (An_{55-50}) and consequently the quartz and plagioclase are probably xenocrysts, similar to those found at Glass Mountain, California (Eichelberger, 1975). The presence of aplite and tonalite inclusions in these dykes confirms this.

Former olivine and pyroxene phenocrysts (3-1 mm) are present as talc, serpentine and tremolite pseudomorphs. The matrix consists of euhedral augite crystals and laths showing wavy extinction (0.5 - 0.1mm) and subhedral plagioclase (An_{55-50},1-0.2 mm). Interstitial between these phases is a fine-grained glassy phase that is difficult to identify. Iddingsite and zircon are also present.

The first signs of metamorphism are olivine and pyroxene phenocrysts showing alteration to talc, serpentine and tremolite (1537). With increasing metamorphic grade olivine and pyroxene are replaced by epidote, carbonate, hornblende and minor chlorite (1565.1). The most intense grades of metamorphism have produced alteration of the pyroxene to hornblende, usually as crystal aggregates (plate 4:9). Usually the groundmass ferromagnesian minerals seem to alter to hornblende before the phenocrysts. Groundmass plagioclase seems to recrystallize as albite-oligioclase, which shows slight alteration to sericite and carbonate. Hornblende shows slight alteration to chlorite, or more rarely biotite, with which it sometimes occurs in crystal aggregates

(1567.2). Minor anhedral quartz is present in the hornblende-rich varieties, usually showing undulose extinction.

The opaque phases in these dykes are euhedral magnetite (1 - 0.1 mm) often partially to completely pseudomorphed by hematite. Hematite and acicular rutile are common (1562.1). In the more altered dykes, euhedral pyrite (<0.7 mm) and minor anhedral chalcopyrite occur, showing alteration to goethite and chalcocite. Intergrowths of pyrrhotite and chalcopyrite occur as inclusions in some pyrites (1567.2).

Modal analyses show the unmetamorphosed dolerite dykes consist(table 4:3C) predominantly of plagioclase (60%) with pyroxene (15%) and olivine (12%). Quartz and magnetite are both less than 1.5%. The metamorphosed dykes consist of plagioclase (50%) and hornblende (40%). Smaller amounts (<5%) of biotite, chlorite, epidote, and pyroxene are also present.

In terms of their modal composition the "False Bay Schists" plot in a similar field to the metamorphosed dyke rocks (Fig. 4:4C), thus adding support for their proposed origin as synplutonic dykes.

Breccia Dykes (Hydrothermal)

These hydrothermal dykes consist of angular fragments of tonalites and other dykes in a matrix of anhedral quartz, minor kaolinite and interstitial ferroandolomite. The minerals in the rock fragments show sericitization and carbonitization with some being replaced by quartz. Anhedral rutile, subhedral magnetite (<0.5 mm) with inclusions of pyrite, along with chalcopyrite and bornite in simple intergrowths are present in these dykes.

Summary of Modal Analyses

Ternary plots of quartz-orthoclase-plagioclase for the diorites and tonalites (Fig. 4:4A) show that most of the rocks fall in a tight

cluster in the tonalite field, although some cross into the granodiorite field. Some of the highly differentiated aplites occur in the granite field and this adds support for the correlation of these rock bodies into a single differentiation process. A plot of quartz-feldspar-mafics (Fig. 4:4B) shows the decreasing proportion of mafic minerals and slight increase in quartz with progressive differentiation.

Each of the rock units occupies a distinct position on the various modal and chemical diagrams (Fig. 4:4, 4:5; table 4:3, 4:5). The data for the individual rock units generally form a broad belt indicating progressive differentiation; the mafic diorite intrusive being the least differentiated and the orthoclase-rich aplites the most. The magmatic episode displayed here is a sequence of plutonism, relatively late stage aplite dyke intrusion and emplacement of mafic dykes.

4.4 Geochemistry of the Intrusive Rocks

The major oxides SiO_2, Al_2O_3, CaO, MgO, FeO, Na_2O and K_2O and the minor oxides TiO_2 and MnO were determined for twelve igneous rocks; three aplites, seven tonalites and diorites and two dolerite dykes (table 4:5A). Eleven trace elements were also determined for these rocks (table 4:5B).

For the diorite phase silica varies between 39 and 41%, alumina is 14.76%, magnesia 13.5-11.8%, lime 11.9-16.84% and ferrous oxide 9.95-9.15%. The low silica and high magnesia and lime contents are probably associated with the fact that much of this rock is virtually mono-mineralic hornblende.

The tonalites vary from 53.52-63.42% silica and 8.59 - 18.86% alumina Lime varies from 15.01 to 3.5%, magnesia 2.46 - 5.83% and ferrous oxide about 6%. Sodium and potassium oxides are generally less than 4.6%.

The metamorphosed dolerite dykes contain 46-50% silica and 15.53-9.47% alumina Lime and magnesia vary from 17-9% with ferrous oxide about 7% and sodium and potassium oxides less than 4%. The dolerite dykes are, therefore, higher than the tonalites in magnesia, lime and manganese oxide.

The aplite dykes and sheets contain 72 - 80% silica, 13.57-14.34% alumina 0.19-1.51% lime, 0.4-0.6% ferrous oxide and 3.75-4.46% sodium oxide, with 4.52-7.27% potassium oxide. The aplite dykes and sheets are, therefore, higher than the tonalite pluton in sodium and potassium oxides and silica, and lower in magnesia, lime, alumina titania and manganese oxides.

The average levels of trace elements in the tonalites are Cr, 100 ppm; Ni, 60 ppm, both present mainly in hypersthene and clinopyroxene (Taylor et al, 1969), with V at 200 ppm present in magnetite and ilmenite. Mo (65 ppm), Cu (100 ppm), Pb (6 ppm), and Zn at 50 ppm are probably present as sulphide inclusions, notably molybdenite, chalcopyrite, galena and sphalerite (latter two undetected). Se at 300 ppm is substituting for sulphur in the sulphides, with Sr at 200 ppm substituting for Ca in plagioclase and amphibole.

Cr, Ni and Cu are higher than in the average granitic rock and were probably introduced by the mineralising fluids with V, Pb, Zn and Sr about the same as the average granitic rock (Sheraton and Black, 1969; Mason, 1952). The dolerite dykes are higher than the tonalites in Cr, Mo, Ni, Sr and Zn, with the aplites higher in Pb and Cu. These figures suggest that the amount of Pb and Cu has increased in the magma during crystallization, along with the major oxides, silica, sodium oxide and potassium oxide. The lower values of Cr, Ni and V in the aplites compared to the tonalites is due to the early precipitation

of magnetite during crystallization, and the lack of ferromagnesian minerals such as pyroxene in the aplites.

The major oxides have been plotted on silica variation diagrams (Fig. 4:6). Plotted against increasing silica, the oxides of the various igneous rocks exhibit a regular tend that is typical of the calc-alkaline rock series as defined by Miyashiro (1975). Ternary diagrams of selected chemical constituents FeO^*, $(Na_2O + K_2O)$, MgO; K_2O, Na_2O, CaO; and CaO, Al_2O_3- $(Na_2O + K_2O)$, $(FeO + MnO + MgO - TiO_2)$ (Fig. 4:5) also show trends typical of the calc-alkaline rock series as defined by Carmichael et al (1974), as do the behaviour of Ti, V, Cr and Ni (Fig. 4:7) relative to a differentiation index (FeO^*/MgO) (Miyashiro and Shido, 1975). The overall chemical behaviour shows similarities to the intrusive rocks of the Andes as defined by Dostal et al (1977). The data points of the igneous units defines an overall trend on the variation diagrams and ternary plots, the relative smoothness of which suggests that all the rocks are genetically related to a single magma series, similar to that defined by Carmichael et al (1974).

4.5 Mineralisation and Alteration

4.5.1 Field Relations of Mineralisation

Sparse sulphide mineral veinlets occur in the plutonic and hypabyssal rocks of this area, which are generally less than 5mm wide and have no specific preferred orientation. The mineralisation tends to occur on joint surfaces, which are often curved (1550), although occasionally mineralisation is present along other planes of weakness, specifically at aplite-tonalite junctions (1529, plate 4:10). Where the mineral veins cut the aplites, in the northern part of the outcrop area, favourable wall rock chemistry has caused sulphide precipitation (bornite, chalcopyrite and molybdenite) in the form of stringers (1574),

Table 4:9 Paragenesis of sulphide and gangue minerals in veinlets, north of Charity Glacier

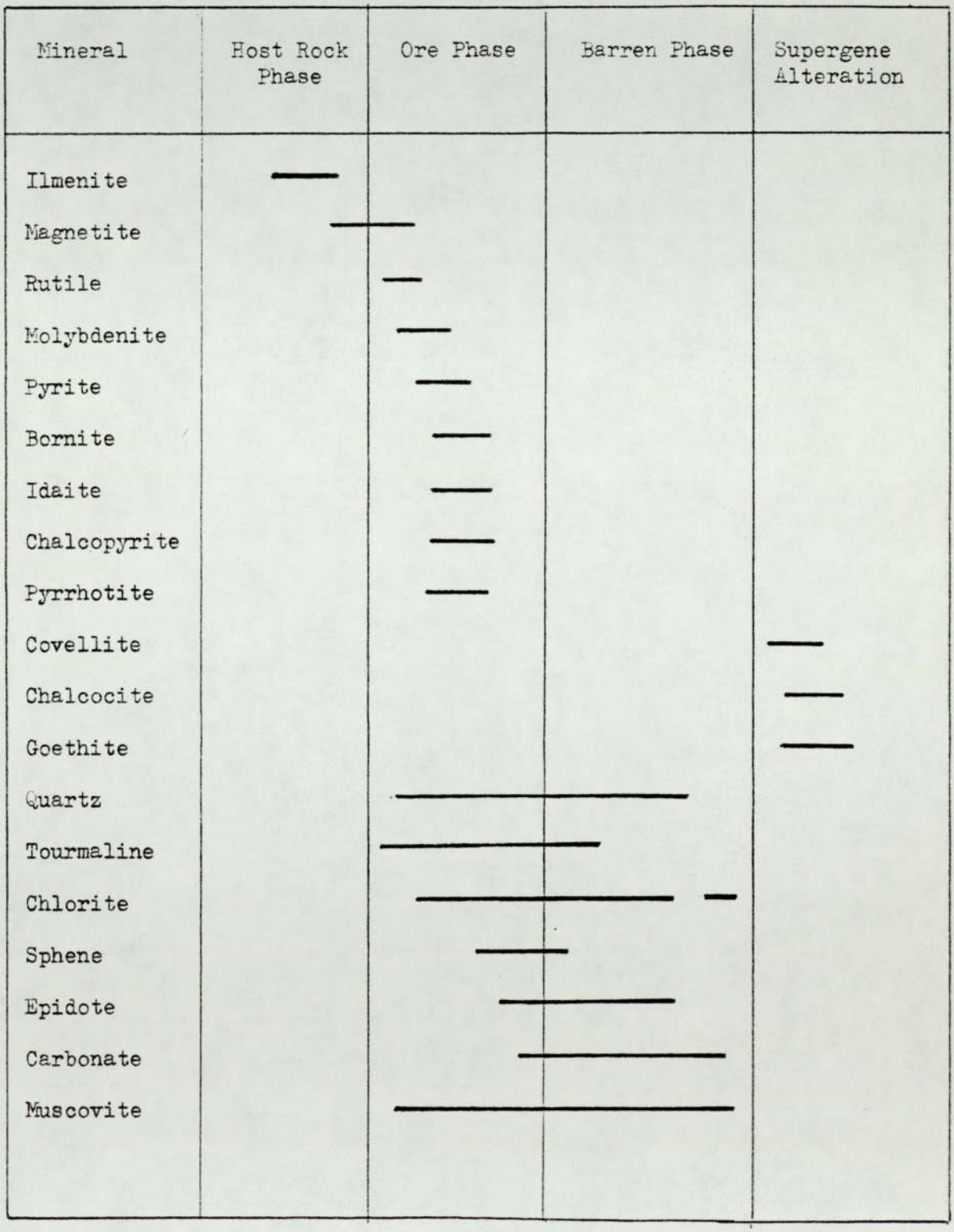

and pods (plate 4:11), the grain size of which is usually related to that of the host aplite. In the northern part of the area, veinlets of bornite, chalcopyrite and molybdenite predominate, although further south they consist mainly of chalcopyrite and pyrite (1539.1), with the sulphides normally concentrated at the edge of the vein, adjacent to the tonalite wall rock. Where the veinlets follow the junction between metamorphosed dykes and tonalite, the mineralisation is always concentrated on the tonalite side of the vein. In the aplite sheets, just north of Charity Glacier, chalcopyrite, pyrite and pyrrhotite occur, normally in fractures or small vug-shaped cavities (1538). Sparse molybdenite can be found on joints in the southern part of the area, but none has been found in polished section.

Numerous barren veinlets of quartz, chlorite, siderite and epidote also occur probably indicating two phases of mineralisation; an early sulphide bearing phase, and a later barren phase. A ternary plot of modal data (quartz + feldspar - sulphides - mafic minerals) show the mineral veinlets plot in a distinct field (Fig. 4:4D).

4.5.2 Paragenesis

The sulphide minerals are described in their presumed paragenetic sequence. This sequence has been deduced from textural evidence obtained from some one hundred polished and thin sections.

Ilmenite

Ilmenite in the mineral veins is probably a relict from the original tonalite, which has undergone alteration at the very edges of the mineral veins. The ilmenite tends to be anhedral and less than 0.6 mm in grain size. It is dull greyish white with a brownish tint and shows slight reflection pleochroism, which is more distinct in oil. It shows fairly strong anisotropy.

Rutile

Rutile is normally granular to anhedral with a grain size of less than 0.2 mm. It is probably derived from alteration of ilmenite, biotite or amphibole from the surrounding wall rock, and some rutile surrounds such ilmenite.

It is light grey in colour, and shows anisotropy which tend to be masked by the reddish brown internal reflections, these being more distinct in oil than air.

Magnetite

Magnetite is subhedral to euhedral with a grain size of less than 0.6 mm, and shows slight alteration to hematite. It seems to be the earliest hydrothermal opaque phase since it occurs as inclusions in bornite and molybdenite, although some is associated with altered amphiboles in the tonalite, and may be magmatic.

The magnetite is grey in colour with a slight brownish tint, and isotropic with a reflectivity at 589nm of about 20% (table 4:8A).

Molybdenite

The strongly anisotropic, subhedral molybdenite appears to be the earliest sulphide as bornite and chalcopyrite occur along fractures (plate 4:14). In places it seems to be associated with altered amphibole crystals, where it is disseminated at the sides of the veinlet. The molybdenite has a grain size of less than 1.2 mm and shows undulatory extinction. It has a distinct reflection pleochroism with measured reflectivities at 589 nm of a minimum 13% and maximum of 26%, and a Vickers Hardness Number at 10g load of between 69-102, which are within the accepted range for molybdenite as defined by Burke et al, (1971).

Bornite

Bornite tends to be anhedral with a grain size of less than 10 mm. It is pinkish brown in colour, and is mostly isotropic, but some is faintly anisotropic. Reflectivity measurements at 589 nm indicates the value for bornite is about 24%, which is slightly high and is probably due to very fine exsolution spindles and lamelli of chalcopyrite parallel to {100} (plate 4:12). Vickers Hardness Numbers for bornite are between 116-205 at 50g load, which are about normal for bornite. Bornite occurs in myrmekitic intergrowths with chalcopyrite usually of grain size less than 0.4 mm, (plate 4:13), and also seems to be replacing gangue. Some emulsion droplets of chalcopyrite occur in the bornite.

Idaite

Idaite, which is very similar to bornite optically, is orange-red in colour and anhedral in shape. It shows weak reflection pleochroism which is more distinct in oil than in air. Under crossed polars, however, idaite shows enormous anisotropy with the colours dark green to yellowish green, again more distinct in oil than air. It contains exsolution spindles and lamelli of chalcopyrite parallel to {111} (1520.5).

Pyrite

Pyrite seems paragenetically earlier than chalcopyrite, which often replaces it (plate 4:15). Pyrite is generally euhedral with a grain size of less than 1 mm. Pyrite is isotropic and pale yellow in colour, and often contains "emulsion droplets" of chalcopyrite and pyrrhotite (<0.4 mm, 1538). Inclusions of ilmenite and rutile occur (<0.42 mm) indicating the pyrite is later than these two phases.

Pyrite has a reflectivity at 589 nm of about 53%, and Vickers Hardness Number of 2205-1296 at 100 g load (table 4:8A) well within

the range for pure pyrite (Burke et al, 1971).

Chalcopyrite

This seems to be paragenetically the same age as bornite and is generally subhedral with a grain size of less than 1 mm. Chalcopyrite is yellow in colour and is isotropic or faintly anisotropic. It has a reflectivity at 589 nm of about 41% and Vickers Hardness Number of 286-209 (table 4:8A) which are within the accepted range for this mineral (Burke et al, 1971).

Where the chalcopyrite occurs in veinlets with pyrite (1539.1) it occurs along fractures in the pyrite (plate 4:15), and replaces the pyrite and gangue. Clearly it is paragenetically later than pyrite.

Chalcopyrite also occurs at the interface between pyrite and pyrrhotite, and along fractures and as emulsion droplets in these phases (1538).

Disseminated chalcopyrite and bornite occurs up to 5 cm from these veinlets in the northern part of the outcrop, but elsewhere minor amounts of disseminated chalcopyrite and pyrite occur in the host tonalite. At the edges of veinlets, chalcopyrite shows alteration to goethite, tenorite, chalcocite and colusite, although some shows alteration to covellite (1543.4A).

Pyrrhotite

Pyrrhotite occurs in the area north of Charity Glacier and has a grain size less than 20 mm. It is generally anhedral and occurs in simple intergrowths with, and along fractures in pyrite, and often contains emulsion droplets of chalcopyrite (plate 4:16). The pyrrhotite shows reflection pleochroism from reddish brown to creamy brown and shows strong anisotropy in air, which is even stronger in oil. Reflectivity of the pyrrhotite at 589 nm is about 37% with Vickers Hardness Number at

100g load of 306-328, (table 4:8A)

Etching with HI and XRD measurements have shown the pyrrhotite (table 4:1), consists of a flame-like intergrowth of monoclinic and hexagonal phases.

The pyrrhotite shows supergene alteration to a marcasite-pyrite like substance in a typical "birds-eye" texture.

Both pyrite and pyrrhotite seem to be replacing the quartz and feldspar gangue. The pyrrhotite-chalcopyrite-pyrite intergrowths may have resulted by exsolution on cooling of a single high temperature phase (Cabri, 1973).

Covellite

Covellite forms mainly by alteration of bornite or more rarely chalcopyrite due to supergene alteration, and normally is anhedral-subhedral with a grain size of less than 0.2 mm.

The covellite shows characteristic reflection pleochroism from dark blue to pale blue, and shows strong anisotropy, generally bright orange to copper brown.

Chalcocite

Chalcocite is generally anhedral with a grain size of less than 0.2 mm, and formed by supergene alteration of chalcopyrite, pyrite and bornite. Consequently it occurs along fractures or as replacements of these minerals.

The chalcocite is pale grey with a blueish tint, and very faintly anisotropic.

Goethite

Goethite occurs as a supergene replacement of pyrite, pyrrhotite and chalcopyrite, and also occurs along fractures in these sulphides.

The goethite is usually anhedral, with a grain size of less than 0.2 mm and is normally grey in colour. It shows anisotropy, although this tends to be masked by reddish internal reflections.

Tourmaline

Tourmaline is generally euhedral, and shows a dichroic colour zoning from brown to green (plate 4:18). Both sulphides and chlorite can be found along fractures in this mineral, and it appears to be the earliest gangue phase. Tourmaline crystals have a grain size of 1-0.1 mm and are often in close assocation with sulphides.

Quartz

Quartz (4-0.2 mm) is generally anhedral and frequently occurs as inclusions in the sulphides. It occurs at the margins of many veins, and shows undulose extinction.

Chlorite

There appears to be two phases of chlorite formation; an early pale yellow-green, subhedral phase (<1mm) which often occurs in radial clusters (plate 4:17) or microveinlets, and a later bright green chlorite which shows high relief, and which occurs in small veinlets cutting tourmaline. This late stage chlorite is replacing the earlier chlorite (1551.4). X-ray diffraction indicates the early chlorite in assocation with tourmaline is the 1b polymorph, but in veinlets lacking tourmaline it is the 1a polymorph. Some chlorite occurs in fractures in quartz (and may be replacing it) and as inclusions in some sulphides (1539.1). In the aplite sheets chlorite occurs in assocation with the sulphide "pods".

Epidote

Epidote (pistacite) is strongly pleochroic from bright yellow-green to pale green, and generally occurs in granular crystals (<0.5 mm). Some epidote is replacing chlorite, but is itself replaced by siderite and late stage chlorite.

Muscovite

Muscovite is invariably present in all veinlets, and tends to occur as colourless, subhedral (often radial) crystals. Veinlets of sericite cut clusters of chlorite (1539). X-ray diffraction suggests the main polymorph present is 2M, muscovite, but 1M muscovite is present in veins lacking tourmaline. Some muscovite seems to be replaced by chlorite (1539.1B).

Carbonate

Carbonate occurs as a late stage infilling to many veins and is frequently anhedral (<4mm). It also occurs along fractures in chlorite, and shows replacement by late stage chlorite. Carbonate can also be found around sulphides and some seems to be replacing early chlorite and sphene. Staining with ferrocyanide indicates it is siderite.

Accessory Minerals

Sparse, euhedral apatite is occasionally present in some veinlets (1529.1A) as is euhedral sphene (<2mm). Some sphene occurs around sulphides in the aplite sheets, indicating the secondary origin of the sulphides. Minor euhedral zircon is present in some veinlets (1539.1), as are albite, partially resorbed biotite and hornblende, the latter probably a relict from the surrounding tonalite.

4.5.3 Chemical Analyses of Sulphide Minerals

The sulphide minerals occurring in veinlets north of Charity Glacier have been analysed using atomic absorption spectrophotometry for various trace elements discussed below.

Pyrite contains 30-1766 ppb Au and less than 1 ppm Ni which is substituting for Fe in the pyrite lattice. Zn (62 ppm), Pb (<1ppm) and Cu (1022 ppm) are present as sulphide inclusions, although galena and sphalerite have not been detected, whereas chalcopyrite has.

Mn (1264 ppm) is probably present as inclusions of pyrolusite, with Se (61-85 ppm) substituting for sulphur. The levels of trace elements are in the range found for other pyrites (Ryall, 1977) although Cu and Mn are high (table 4:7).

Chalcopyrite and bornite heavy mineral seperates contain about 10 ppb Au, 1500 ppm Mn (probably present as pyrolusite) and 103 ppm Ni (substituting for Fe in the Cu-Fe sulphides). Pb (115 ppm) and Zn (160 ppm) are present as undetected sulphide inclusions (notably galena and sphalerite) with Se (30-4800 ppm) substituting for sulphur. These values are within the range of other chalcopyrites (Fleischer, 1955).

4.5.4 Alteration of Tonalites and Aplites around Mineral Veinlets

The tonalites and aplites show propylitic alteration around the mineral veinlets, as defined by Meyer and Hemley (1967).

The zoned subhedral plagioclase laths show alteration to 2M, muscovite in fairly large radial laths (1539.1), granular epidote, subhedral chlorite laths and anhedral siderite. Some plagioclase crystals show alteration to quartz. The calcic cores of the feldspars show more intense alteration than the sodic margins. Muscovite also occurs in radial clusters at the boundaries of quartz and feldspar in the aplites (1520.2). Poikilitic hornblende in the tonalites shows alteration to chlorite, siderite and quartz, although some show slight alteration to tourmaline and epidote. Where chlorite is present as a replacement of biotite, it generally contains myriads of small rutile needles. Biotite also shows slight alteration to quartz. Orthoclase in these rocks seems unaltered by the hydrothermal fluids (1520.5). Small quartz veins (<0.1 mm) cut plagioclase and hornblende (1551.6) as do carbonate veinlets, but carbonate seems best developed where these veinlets cut plagioclase crystals (1526.1). The carbonate

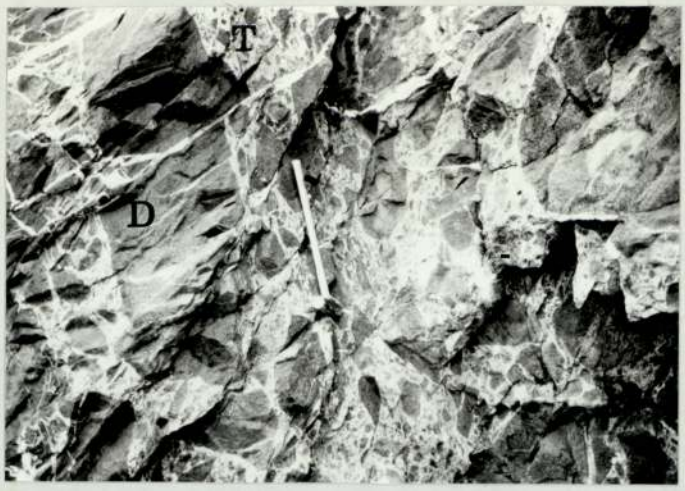

Plate 4:1 Pillow-like masses of syn-plutonic dykes, (D) disrupted by tectonic movements in a tonalitic host (T). 10 meters north of Charity Glacier, Livingstone Island (1552).

Plate 4:2 Aplite sheets (light grey), cutting tonalite host (dark grey). Note feeder? dyke. 0.3 km. north of Charity Glacier, Livingstone Island.

Plate 4:3 Coarse aplite showing subparallel alignment of biotite laths (black banding) in quartz and feldspar (white). Ten meters north of Charity Glacier, Livingstone Island (1538).

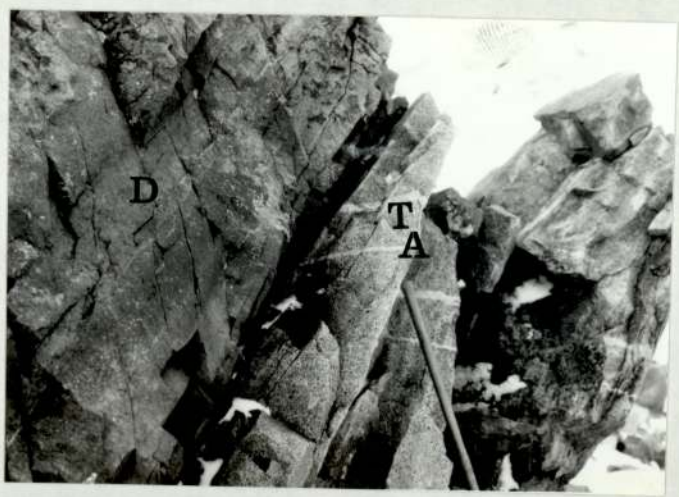

Plate 4:4 Aplite sheets (A) (white) cutting tonalite (T) (grey), which are truncated by a metamorphosed dyke (D) (dark grey, on left of plate). 1.2 km north of Charity Glacier, Livingstone Island (1537).

Plate 4:5 Xenolith of aplite occurring in metamorphosed, dolemitic dyke. 1.3 km. north of Charity Glacier, Livingstone Island (1563.2).

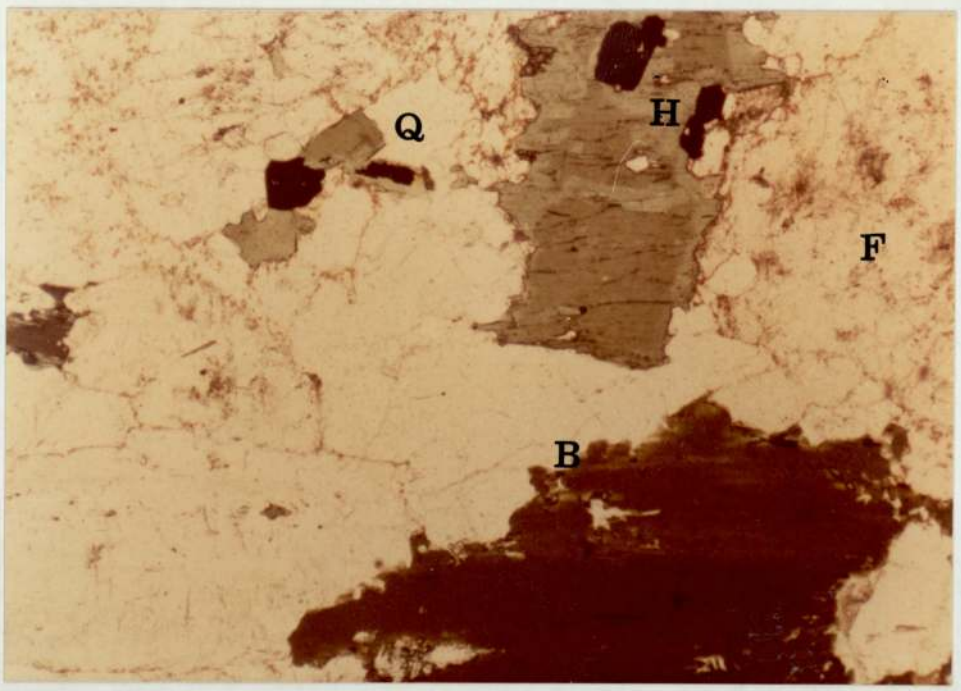

Plate 4:6 Anhedral quartz (colourless, low relief), feldspar (yellowish, low relief), biotite (dark brown) and amphibole (green). Black, euhedral opaques are magnetite. The amphibole shows colour zoning due to replacement of pyroxene (brownish green), and the overgrowth of later amphibole (green). Fine grained tonalite phase (1534). 1.3 km. north of Charity Glacier, Livingstone Island. Transmitted light, plane polarised light. X60. Amphibole (H), Quartz (Q), Feldspar (F), Biotite (B).

Plate 4:7 Anhedral quartz (colourless, low relief), feldspar (yellowish, low relief), with amphibole (green) containing biotite laths parallel to the cleavage (brown). Some biotite shows alteration to chlorite. Medium grained tonalite phase (1555.2). 0.5 km. north of Charity Glacier, Livingstone Island.

Transmitted light, plane polarised light, X60.

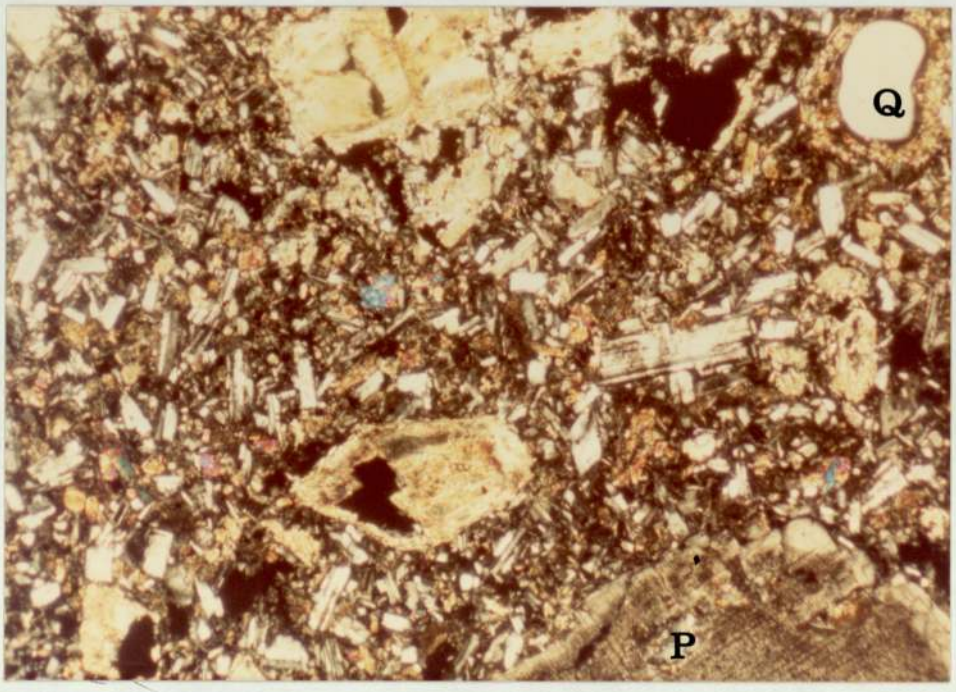

Plate 4:8 Porphyritic dolerite dyke. Groundmass consists of subhedral plagioclase laths (albite twinning) and augite granules (show second order blues, yellows and reds). Phenocrysts are serpentine and tremolite pseudomorphs after olivine and pyroxene. Xenocrysts of plagioclase (lower right of plate) (P) and quartz (upper right) (Q) with reaction run of pyroxene are present (1562.1). 2 km. north of Charity Glacier, Livingstone Island. Transmitted light, crossed polars, X40.

Plate 4:9 Hornblende, (green), after pyroxene?, in groundmass of albite-oligioclase (brownish) and hornblende, in metamorphosed dyke (1569.1). 0.5 km. north of Charity Glacier, Livingstone Island.
Transmitted light, plane polarised light, X40.

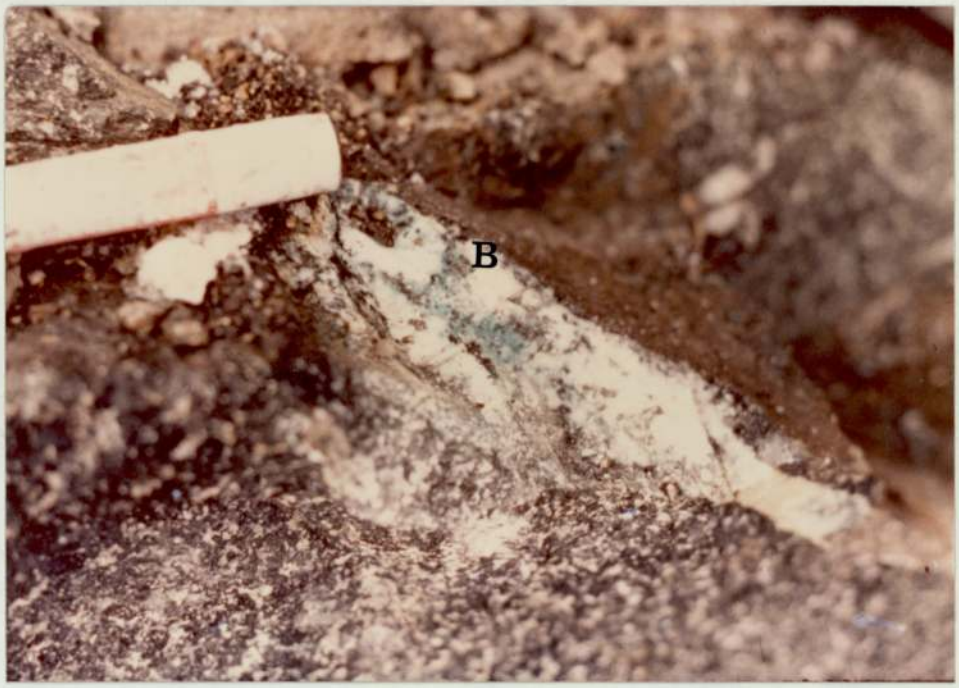

Plate 4:10 Bornite (B), (brown) showing oxidation to azurite (blue) at the junction between aplite sheet (white) and diorite (black). 2 km. north of Charity Glacier, Livingstone Island (1528).

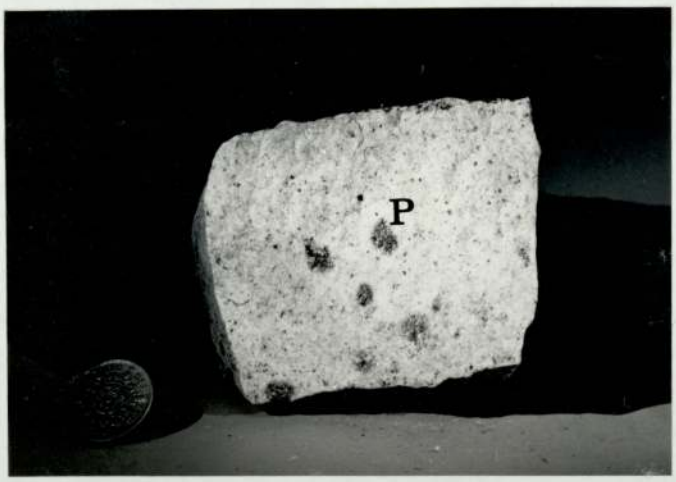

Plate 4:11 "Pods" of sulphides (P) (bornite, chalcopyrite and molybdenite), (grey) in aplite sheet (1520.5). 2.1 km. north of Charity Glacier, Livingstone Island.

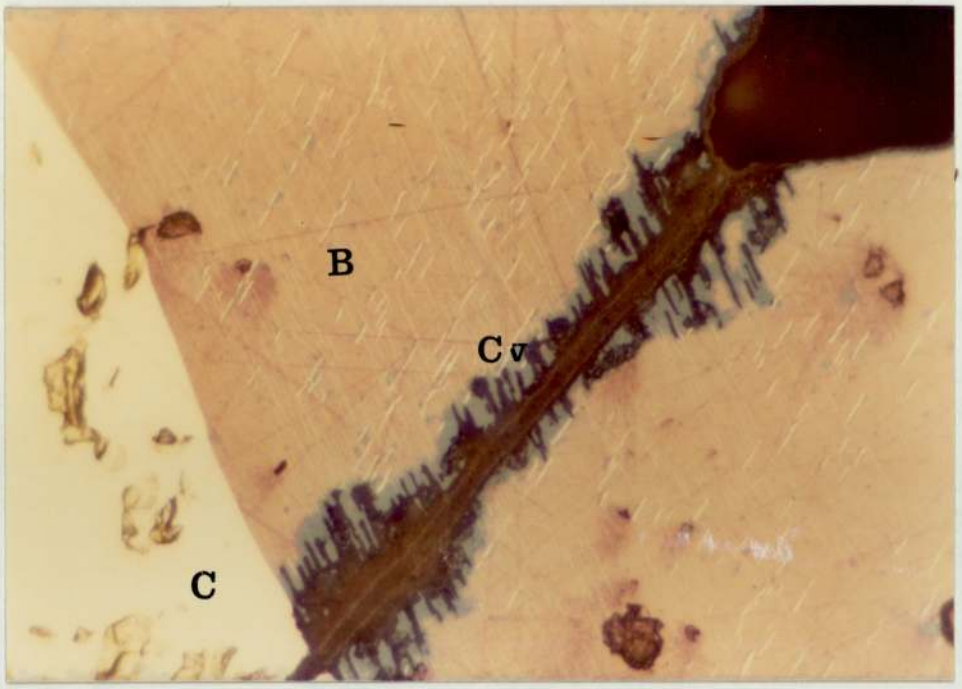

Plate 4:12 Bornite (B) (brown) showing exsolution spindles and lamelli of chalcopyrite, and alteration along fractures to covellite (Cv) (blue), in simple intergrowths with chalcopyrite (C) (yellow). (1520.5). 2.1 km. north of Charity Glacier, Livingstone Island. Reflected light, in oil, X160.

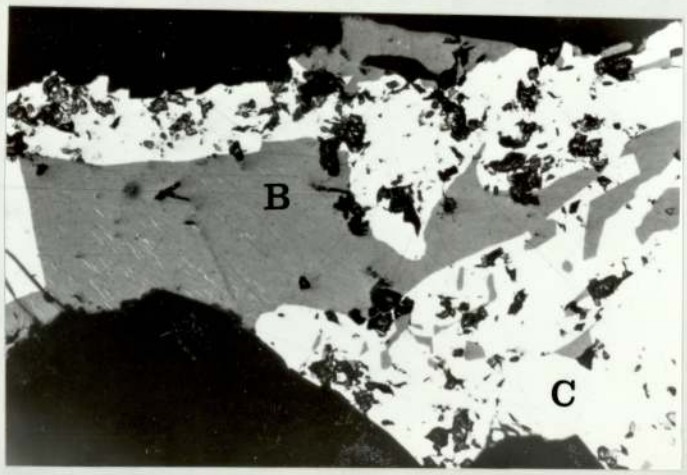

Plate 4:13 Bornite (B) (grey) in myrmekitic intergrowths with chalcopyrite (C) (white). Black is quartz and feldspar. (1520.2). 2.1 km. north of Charity Glacier, Livingstone Island. Reflected light, X60.

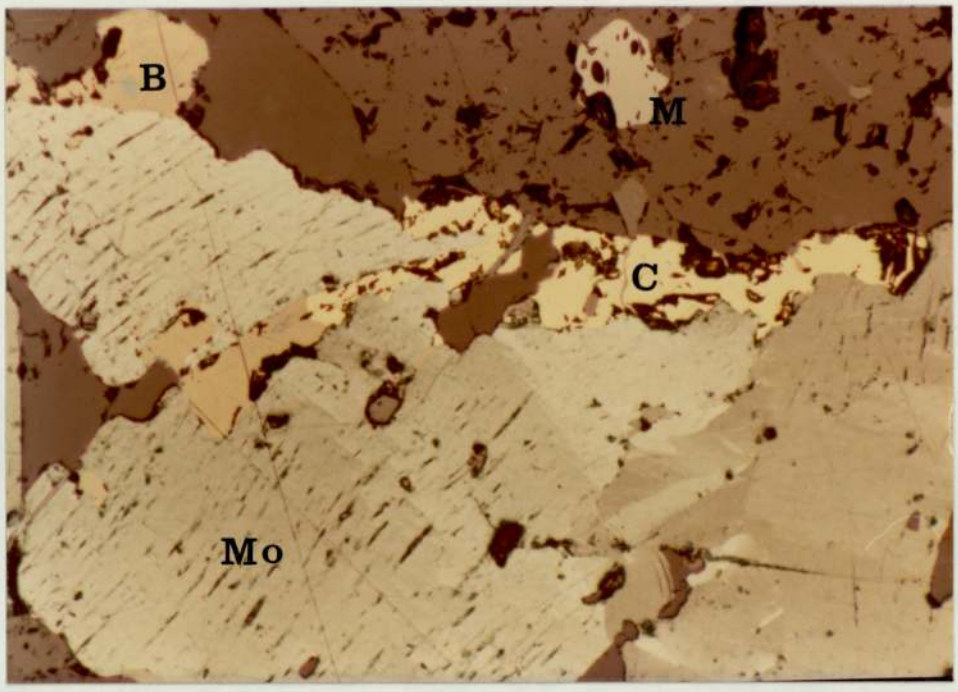

Plate 4:14 Molybdenite (Mo) (grey, various shades) showing pressure twinning, with bornite (B) (brown) and chalcopyrite (C) (yellow) along cleavages and fractures. Brownish grey mineral in upper part of plate is magnetite (M). Very dark brown is quartz and feldspar. (1520.5). 2.1 km. north of Charity Glacier, Livingstone Island. Reflected light X60.

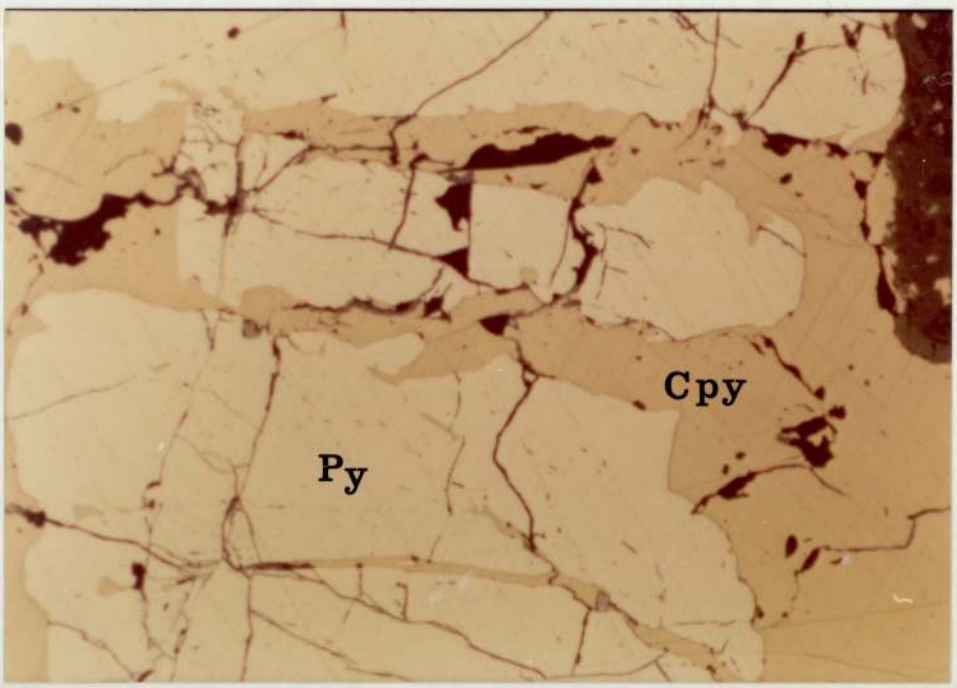

Plate 4:15 Pyrite (Py) (yellow) being replaced by chalcopyrite (Cpy) (deep yellow) along fractures (1543). 0.2 km. north of Charity Glacier, Livingstone Island. Reflected light, X120.

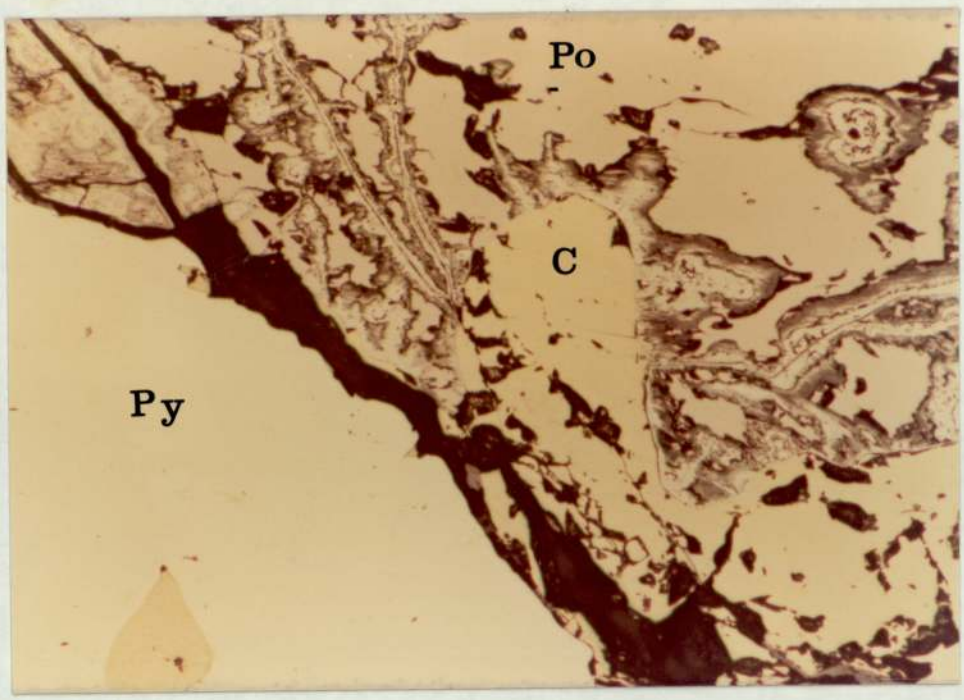

Plate 4:16 Pyrite (Py) (yellow), with pyrrhotite (Po) (brownish) showing characteristic "birds eye" texture due to weathering. Chalcopyrite (C) (deep yellow) occurs as inclusions in the pyrite and between pyrite and pyrrhotite. (1538.1). Ten meters north of Charity Glacier, Livingstone Island. Reflected light, X160.

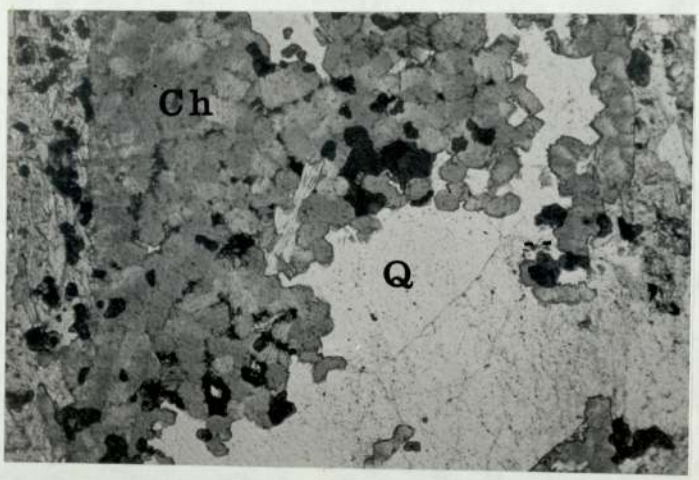

Plate 4:17 Chlorite (Ch) (shades of dark grey) in small clusters, quartz (Q) (colourless) and pyrite and chalcopyrite (black) in veinlet cutting tonalite. (1539.1). 1 km. north of Charity Glacier, Livingstone Island. Transmitted light, plane polarised light, X60.

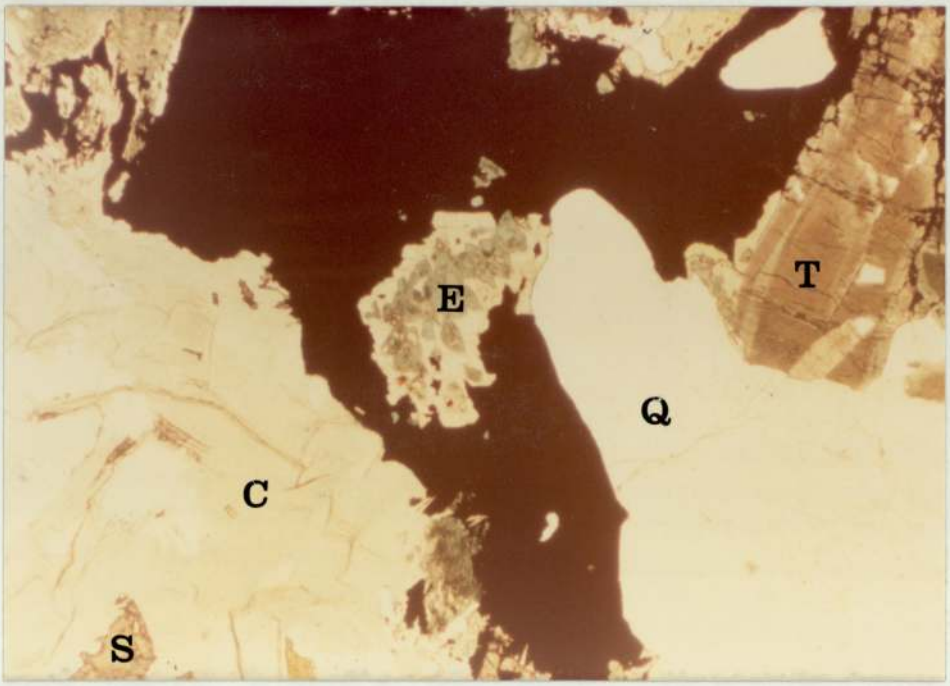

Plate 4:18 Veinlet cutting tonalite, 2.0 km. north of Charity Glacier, Livingstone Island (1550).

Minerals present are quartz (colourless, low relief), sulphides (black), chlorite (pale yellow-green, in bottom left of plate), epidote (yellow-green, in centre of plate), sphene (brownish yellow, bottom left) and tourmaline (bichroic brown to yellow, top right).

Transmitted light, plane polarised light, X60.

Tourmaline (T), Chlorite (C), Epidote (E), Quartz (Q), Sphene (S).

veinlets are later than the quartz veinlets.

4.6 Copper-Lead-Zinc Mineralisation on Mier's Bluff

Around the copper-molybdenum deposit north of Charity Glacier is a copper-lead-zinc deposit described by Valle et al (1975), located on north western Miers Bluff, in the flysch sequence (Dalziel, 1968) between Elephant Point and Johnson's Dock. This area was not visited by the author due to logistical problems.

The mineralisation here occurs in the form of veinlets and as disseminated sulphides associated with breccia dykes. The veinlets are generally thin and consist of barren quartz-carbonate veins, although some contain only quartz. These are cut by later carbonate veins. The veins containing sulphide mineralisation generally trend N-S and dip east, and formed by open space filling. Gangue minerals predominate over sulphides with the sulphide bearing veins paragenetically later than the barren veins. Breccia fragments (some composed of quartz-carbonate rock) have been found in these veins, although the majority are of the surrounding wall rock. Breccias formed by tectonic stresses have acted as porous hosts to mineralisation and are generally 10-30 meters thick, 300 meters long, trend N-S and dip 85° - 60° E. The intrusion of breccia seems to have been controlled by a zone of N-S faulting. The average size of the fragments is 5cm with quartz, carbonate and sulphides occurring in the open spaces around fragments. There seems to have been three periods of mineralisation with tectonic movements between each. The first phase of mineralisation is represented by quartz-carbonate and pyrite veins which were followed by a phase of tectonic movements which produced the breccias. Quartz, carbonate, sulphide mineralisation then occurred which was followed by a second phase of tectonic movement, itself followed by introduction of quartz-

carbonate veins.

Sulphide minerals include chalcopyrite, bornite, tennatite-tetrahedrite, sphalerite and galena. Chalcocite and covellite are also present and appear to have been deposited by hydrothermal solutions. The minerals generally show infill textures although galena shows some deformation. Supergene alteration minerals include malachite, azurite, cerussite, witherite, limonite, hematite, linearite and antilerite.

A phase of andesite dyke intrusion occurred after the mineralisation, which shows no preferred orientation. A later episode of fracturing has effected the Miers Bluff Series, mineral veins and andesitic dykes, which trend N70°W and N70°E.

4.7 Discussion of Igneous Activity, Rock Textures and Mineralisation

The earliest phase of intrusion north of Charity Glacier is a diorite rich in hornblende. It seems (Regan, 1976) that hornblende can appear in all stages of the evolution of basic rocks, as a cumulus phase, intercumulus phase or a product of late stage metasomatism due to introduction of water from external sources. The progressive replacement of pyroxene to form poikilitic hornblende (Bowes and Wright 1961) in the solid state is common to appanitic rocks. The presence of inclusions and pseudomorphs of pyroxene in the hornblendes in the diorite suggests that these solid state reactions may account for the high hornblende content of these rocks.

This was followed by intrusion of a separate pulse of tonalitic magma, rather than a surge in a single congealing pluton as indicated by xenoliths of diorite in the medium-grained tonalitic phase as shown in other plutons (Harry and Richey, 1963; Cobbins and Pitcher, 1972). At the western margins of the exposure a fine-grained phase was intruded, probably slightly earlier than the medium-grained phase, which in places

possesses a foliation (1540). The fine-grained nature of this rock was probably caused by the chilling effect of the cool, country rocks.

The hornblende/biotite ratio is higher in the other intrusives than the fine-grained phase, and may indicate the original tonalitic magma was richer in biotite than the medium-grained phase now indicates. Indeed, "generation of hornblende from pyroxene, in parallel with independent growth of hornblende and biotite may be an effect of advancing fractionation due to increasing water content" (Pitcher, 1978). In the area just north of Charity Glacier, the tonalite possesses a foliation, with mafic and felsic bands being common (Hobbs, 1963). Deformation of a partly consolidated syn-plutonic mush of crystals can give rise to this banding (Berger, 1971). This deformative force was probably due in part to regional stresses operating during batholithic emplacement, and strike sub-parallel to the Cordillera, as in South America (Dalziel, 1974).

The rocks previously regarded as the "False Bay Schists" appear in fact to be an early phase of doleritic dyke injection in a NNE-SSW direction. The disruption these dykes have undergone, and the strings of pillow-like globules (plate 4:3) in the tonalite suggest they are synplutonic dykes intruded into a semi-plastic host by comparison with other plutons (Roddick and Armstrong, 1959). There is some evidence of them having been disrupted while the host was still mobile, as in places they neck out along their length or pass upwards into pillow-like globules similar to synplutonic dykes in the Andes (Pitcher, 1978). The congealing pluton then thermally metamorphosed these dykes to hornblende-hornfels facies, although where the edges of the dyke were in contact with the tonalite, introduction of potassium and water has occurred, giving rise to a marginal phase of plagioclase and biotite

similar to that found in metamorphic terrains (Mernert, 1968).

These metamorphosed dykes have been intruded by aplite sheets which have also been slightly folded, with an introduced foliation of the phlogopitic biotite micas in the area just north of Charity Glacier. These aplites were probably intruded in the final stages of thermal and tectonic stresses that caused the foliation in the host pluton. These aplites seem to represent the end products of differentiation that produced tonalitic magma.

Following this was a further period of very early post-plutonic doleritic dyke intrusion (a common occurrence in Andean-type plutons, (Pitcher, (1978)), generally trending NW-SE and NE-SW, which contain xenoliths of tonalite and aplite. The presence of these xenoliths indicates these dykes are later than the "False Bay Schists" or aplites. The majority of the dykes have been metamorphosed, but the intensity of metamorphism decreases northwards away from Charity Glacier. The tectonic stresses that caused the foliation in the "False Bay Schists" were absent during the intrusion of the dolerite dykes. The decreasing intensity of metamorphism northwards may be due to there being more percolating fluids near the margin of the pluton, or the dykes get progressively younger northwards and, therefore, later in the cooling history of the pluton. Alternatively, the dykes may be contemporaneous and the magma congealed from north to south.

These metamorphic effects probably had some alteration action on the earlier diorites and tonalites and some xenomorphic hornblende may be secondary as in many Andean plutons (Berger, 1971). Their failure to recrystallise under metamorphism may be due to the system being closed to externally derived water (Kerrick, 1970). The intrusion of tonalite, aplite and associated dolerite dykes presumably

represents tapping at slightly different levels at different times of one common magma chamber, as in other calc-alkaline complexes (Carmichael et al, 1974).

Following the intrusion of dolerite dykes there was a period of porphyry copper style mineralisation which shows a sulphide zonation from bornite, chalcopyrite, molybdenite in the central area to chalcopyrite, pyrite, pyrrhotite in an intermediate zone, to an outer zone of galena, sphalerite, chalcopyrite, pyrite (Fig. 4:2 insert), typical of zonation in most porphyry copper deposits (Lowell and Guilbert, 1970; Sillitoe, 1972), which seems to depend on complex physicochemical factors (Barnes, 1962). The mineralisation here seems to be associated with the intrusion of small breccia dykes, which have undergone slight propylitic alteration, typical of porphyry copper deposits (Hollister, 1974). These seem to form by rapid faulting, thereby causing violent rock bursts (Mitcham, 1974), although little movement of the fragments usually occurs (Sillitoe, 1972). The paragenesis here shows some similarities to that in other porphyry copper deposits (Ray, 1914; Lowell and Guilbert, 1970), although molybdenum is slightly earlier than copper. The presence of pyrrhotite in this deposit, is however, unusual for this style of mineralisation as defined by Meyer and Hemley (1967), and may indicate a slight thermal pulse followed the mineralisation which produced pyrrhotite by thermal metamorphism of pyrite (Arnold, 1962), or the porphyry copper system had a low fs_2 and fo_2 (Meyer and Hemley, 1967). The occurrence of mineralisation in the metamorphosed dykes and not the fresh ones may mean the altered dykes were more porous to the mineralising fluids than the fine-grained dolerites, and, therefore, more receptive to mineralisation, or the fresh dolerite dykes are

slightly later than the mineralisation. Hypogene mineralisation in the intrusives is restricted to the margins of the mineral veins, although in places small amounts of disseminated pyrite and chalcopyrite are present. Extensive supergene sulphides (chalcocite blankets, etc.) seem to be absent here, and probably have been removed by glacial erosion. The small amounts of chalcocite, goethite and covellite probably represent recent supergene alteration.

TABLE 4:1 X-RAY DIFFRACTION DATA FOR PYRRHOTITES, NORTH OF CHARITY GLACIER

Specimen Number	$d_{(102)}$ in Å	N_{FeS}
1538	2.074	0.95
1538.1	2.074	0.95

(Values of N_{FeS} based on data by Yund and Hall, 1969).

TABLE 4:3A MODAL ANALYSES OF PLUTONIC ROCKS, NORTH OF CHARITY GLACIER, LIVINGSTON ISLAND.

Specimen Number	Location	Rock Type	Quartz	Plagioclase	Orthoclase	Hornblende	Biotite	Pyroxene	Opaques	Rutile	Zircon	Chlorite	Carbonate	Muscovite	Epidote	Total
1528.1	North east outcrop	Diorite	-	27.1	-	67.5	0.4	0.4	0.4	0.2	-	2.3	-	1.4	0.4	100.1
1514	North west outcrop	Tonalite	20.6	50.2	1.3	-	-	-	0.9	-	-	16.1	4.7	6.2	-	100.0
1517.1	Northern outcrop	Tonalite	21.5	44.8	6.1	9.5	5.9	-	1.3	-	-	2.8	0.2	7.7	0.3	100.1
1517.2	Northern outcrop	Tonalite	23.3	51.0	3.8	11.2	7.7	-	1.1	-	-	0.5	0.1	1.1	0.1	99.9
1526.1	North east outcrop	Tonalite	13.5	59.6	1.3	0.3	7.6	-	1.5	-	0.2 (Sphene)	-	15.2	0.8	0.1	100.1
1529.1A	North east outcrop	Tonalite	14.0	64.5	0.3	4.9	6.0	-	3.0	-	0.1 (Tourmaline)	2.0	0.6	4.4	0.1	99.9
1532	North central outcrop	Tonalite	25.5	47.5	12.1	6.2	7.0	-	0.5	0.2	-	0.3	-	0.6	-	99.9
1534	North central outcrop	Tonalite	26.4	53.3	8.4	4.1	7.3	-	0.6	-	-	<0.1	-	-	<0.1	100.1
1543.4	South outcrop	Tonalite	1.5	66.0	0.1	6.5	0.6	-	0.2	-	-	9.1	-	13.8	2.2	100.0
1547.1	North east outcrop	Tonalite	16.3	59.5	0.2	9.5	12.0	-	1.0	-	0.2 (Apatite)	0.6	-	0.5	0.3	100.1
1548.1	North east outcrop	Tonalite	24.4	59.3	0.4	6.6	7.0	-	1.0	-	-	0.3	0.1	0.7	0.2	100.0
1550.1	North east outcrop	Tonalite	27.5	53.0	0.6	9.1	7.2	-	1.0	0.2	0.1	0.7	0.3	0.3	-	100.0
1554.1	South east outcrop	Tonalite	1.5	51.5	1.2	20.2	-	-	2.0	0.2	0.1	5.8	0.2	16.7	2.6	100.0
1555.2	South east outcrop	Tonalite	23.9	55.6	0.6	8.9	5.2	-	0.8	0.1	-	2.7	-	2.0	0.2	100.0
1559.2	South east outcrop	Tonalite	21.9	57.1	0.2	9.7	5.4	-	0.4	-	-	1.5	0.9	2.8	0.1	100.0
1576.2	East central outcrop	Tonalite	27.3	53.4	0.1	9.5	7.8	-	1.3	0.2	0.1	<0.1	-	0.1	0.4	100.2

(All analyses determined on 1000 points).

TABLE 4:3B MODAL ANALYSES OF APLITE SHEETS, NORTH OF CHARITY GLACIER, LIVINGSTONE ISLAND.

Specimen Number	Location	Quartz	Plagioclase	Orthoclase	Biotite	Chlorite	Muscovite	Epidote	Opaques	Rutile	Zircon	Total
1520.2	North west outcrop	38.8	13.2	46.1	1.7	-	-	-	0.1	<0.1	0.1	100.0
1520.2	North west outcrop	44.9	17.0	36.0	0.7	0.2	0.2	-	0.7	<0.1	-	99.7
1520.5	North west outcrop	38.5	18.9	39.1	1.0	1.6	0.4	-	1.2	-	-	100.7
1536	Central outcrop	36.9	43.2	15.6	0.1	<0.1	-	-	3.8	<0.1	<0.1	99.6
1538.5	10m north of Charity Glacier	45.0	50.8	<0.1	3.6	<0.1	0.4	-	0.2	<0.1	-	100.0
1538.7	10m north of Charity Glacier	22.3	72.0	<0.1	5.3	<0.1	<0.1	-	0.1	<0.1	<0.1	99.7
1540.1	Southern outcrop	32.5	54.5	0.7	10.9	-	0.3	0.1	1.0	<0.1	-	100.0
1541.1	Southern outcrop	37.1	56.7	0.6	<0.1	0.6	5.0	-	<0.1	<0.1	<0.1	100.0
1564.1	Central outcrop	48.6	42.8	7.3	0.4	0.9	-	-	<0.1	<0.1	-	100.0
1568.1	South west outcrop	40.2	49.0	8.0	1.8	0.9	-	-	<0.1	<0.1	-	99.9

(All analyses determined on 1000 points).

TABLE 4:3C MODAL ANALYSES OF DYKE ROCKS, NORTH OF CHARITY GLACIER, LIVINGSTONE ISLAND.

Specimen Number	Location	Rock Type	Quartz	Plagioclase	Hornblende	Biotite	Chlorite	Epidote	Pyroxene	Serpentine (after Olivine)	Muscovite	Carbonate	Opaques	Fine Grained Matrix	Total
1552.3	20m north of Charity Glacier	"False Bay Schists"	-	49.5	-	50.1	-	0.1	-	-	-	-	0.3	-	100.0
1537	Central Outcrop	Metamorphosed Dyke	-	48.4	42.2	-	5.2	-	3.7	-	-	-	0.6	-	100.1
1560	North west Outcrop	Metamorphosed Dyke	<0.1	53.0	41.3	4.4	<0.1	0.8	-	-	-	-	0.4	-	99.9
1565.1	Central Outcrop	Metamorphosed Dyke	-	51.8	36.1	-	2.4	6.8	2.8	-	-	-	0.1	-	100.0
1567.2	South east Outcrop	Metamorphosed Dyke	12.7	55.1	23.4	4.4	<0.1	0.7	-	-	0.8	0.7	2.2	-	100.0
1569.1	South west Outcrop	Metamorphosed Dyke	-	34.8	65.2	-	-	-	-	-	-	-	-	-	100.0
1562.1	North west Outcrop	Dolerite Dyke	0.5	57.7	-	-	-	-	14.9	12.0	-	-	1.3	13.5	99.9
1570.2	South west Outcrop	Breccia Dyke	14.2	-	-	-	2.9	-	-	-	13.5	68.4	-	-	99.0

(All analyses determined on 1000 points).

TABLE 4 : 4A CELL DIMENSIONS OF PYRITE FROM MINERAL VEINLETS, NORTH OF CHARITY GLACIER

SPECIMEN NO.	LOCATION	CELL DIMENSION (a_o)
1538.3	20m north of Charity Glacier	ao = 5.394
1538.5	"	a_o = 5.399
1569.2B	South eastern outcrop	a_o = 5.384
Pure Pyrite	J.P.C.D.S.	a_o = 5.417

TABLE 4 : 48 ELECTRON MICROPROBE ANALYSIS OF BIOTITES FROM APLITE SHEETS, NORTH OF CHARITY GLACIER.

	SPECIMEN NO.	LOCATION	SiO_2	Al_2O_3	FeO	MgO	K_2O	TOTAL
1	1538.5A	20 metres north of Charity Glacier	45.35	16.26	12.81	14.16	10.42	99.00
2	1538.5B	"	43.00	17.13	12.48	13.80	12.60	99.01

MOLE PERCENTAGES OF METALS IN OCTAHEDRAL SITES IN BIOTITES FROM APLITE SHEETS, NORTH OF CHARITY GLACIER

	SPECIMEN NO.	LOCATION	Fe	Mg	Al
1	1538.5A	20 metres north of Charity Glacier	27.51	54.42	18.07
2	1538.5B	"	27.63	54.60	17.76

Biotite formula :-

1. $K_{1.85}\ (Mg_{2.95},\ Fe_{1.50},\ Al_{0.99})_{5.44}\ (Al_{1.68},\ Si_{6.32})_{8.00}\ O_{20}\ (OH)_4$

2. $K_{2.28}\ (Mg_{2.91},\ Fe_{1.48},\ Al_{0.95})_{5.34}\ (Al_{1.91},\ Si_{6.09})_{8.00}\ O_{20}\ (OH)_4$

Table 4.5A CHEMICAL ANALYSES OF MAJOR OXIDES IN INTRUSIVE ROCKS, NORTH OF CHARITY GLACIER, LIVINGSTONE ISLAND.

Specimen No.	Location	SiO_2	Al_2O_3	TiO_2	FeO	MgO	CaO	Na_2O	K_2O	MnO	S	Totals
APLITES												
1520.2	North west, outcrop	72.00	14.34	0.10	1.48	0.43	0.19	4.46	7.27	0.006	-	100.27
1538.5	20m north of Charity Glacier	72.84	13.57	0.10	2.43	0.64	1.51	3.75	4.52	0.034	-	99.39
1543.1A	Southern outcrop	80.53	7.74	0.10	2.00	2.29	2.68	2.73	0.99	0.024	-	99.08
DIORITES												
1528.1	North eastern	39.63	14.76	2.84	9.96	11.80	12.84	2.95	5.91	0.132	0.027	100.85
1530.1	outcrop	40.89	14.76	1.35	9.15	13.42	11.90	3.07	4.13	0.121	0.030	98.82
TONALITES												
1513	North west outcrop	63.42	8.59	1.02	6.57	3.89	10.02	4.46	0.91	0.020	0.060	98.96
1532	North central outcrop	60.70	18.17	0.47	4.76	2.46	3.50	4.56	4.20	0.089	0.047	98.96
1543.4	Southern outcrop	53.52	12.83	0.63	4.36	5.17	15.01	3.89	3.45	0.072	0.030	98.96
1547.1	North east, outcrop	59.92	14.06	0.53	6.10	5.83	6.29	3.84	2.68	0.083	0.055	99.39
1553.2	South east, outcrop	59.24	18.86	0.43	6.48	3.79	4.84	3.87	1.13	0.095	0.054	98.79
AVERAGE GRANODIORITE (Taylor & White, 1966)		66.9	15.7	0.6	3.8	1.6	3.6	3.8	3.1	0.06		
DYKE ROCKS												
DOLERITE DYKES												
1562.1	North west outcrop	46.27	9.47	1.04	7.19	14.21	17.05	3.58	0.29	0.16	-	99.26
METAMORPHOSED DYKE												
1565.1	Central outcrop	50.30	15.53	1.62	6.98	9.47	9.03	3.52	2.92	0.117	-	99.49

Table 4.5B CHEMICAL ANALYSES OF TRACE ELEMENTS IN INTRUSIVE ROCKS, NORTH OF CHARITY GLACIER, LIVINGSTONE ISLAND.

Specimen No.	Location	Au*	Cr	Cu	Mo	Ni	Pb	Se	Sr	Te	V	Zn
APLITES												
1520.2	north west outcrop	36	11	120	33	69	16	48	27	14	10	12
1538.5	20m north of Charity Glacier	36	18	340	54	63	5	nd	48	14	10	12
1543.4A	southern outcrop	34	68	640	29	27	20	213	79	21	6	17
DIORITES												
1528.1	north eastern	44	162	70	37	54	13	262	211	49	490	55
1530.1	outcrop	58	138	100	35	54	11	381	256	49	560	40
TONALITES												
1513.1	north west outcrop	57	24	90	61	51	2	102	178	nd	187	55
1532	central outcrop	40	13	10	64	167	2	295	97	nd	88	42
1543.4	southern outcrop	68	233	140	84	47	8	115	198	29	37	33
1547.1	north east outcrop	56	31	320	72	100	6	453	224	14	108	33
1553.2	south eastern outcrop	52	24	530	58	73	nd	335	132	26	152	46
average granodiorite (Taylor & White, 1966)			30	25	1	15	15	440			75	
DYKES												
DOLERITE DYKES												
1562.1	north western outcrop	50	217	40	101	53	2	nd	232	21	144	50
METAMORPHOSED DYKES												
1565.1	central outcrop	42	248	20	73	148	4	368	195	26	160	60

Note: All figures are in parts per million (ppm), except Au* which is in parts per billion (ppb).

TABLE 4:6A MODAL ANALYSES OF ALTERATION VEINLETS ASSOCIATED WITH THE MINERALIZATION NORTH OF CHARITY GLACIER, LIVINGSTONE ISLAND.

Specimen Number	Location	Quartz	Plagioclase	Chlorite	Epidote	Muscovite	Sphene	Tourmaline	Amphibole	Carbonate	Opaques	Total
1524.1	North west outcrop	48.3	31.2	1.7	12.1	6.1	-	-	-	-	0.5	99.9
1539.1	Southern, central outcrop	36.4	20.0	24.5	-	13.7	-	-	-	3.5	1.9	100.0
1539.1	Southern, central outcrop	33.1	3.3	39.5	-	8.9	0.2	-	-	2.7	12.6	100.3
1539.1B	Southern, central outcrop	49.7	4.2	25.0	-	5.7	0.1	-	-	0.8	14.5	100.0
1551.4	Extreme north east outcrop	47.7	4.4	13.9	0.5	1.1	0.1	16.6	2.2	8.9	4.7	100.1
1551.6	Extreme north east outcrop	67.3	0.4	9.3	1.5	0.5	1.1	13.6	0.4	0.5	5.2	99.8

All analyses determined on 1000 points

TABLE 4:6B MODAL ANALYSES OF SULPHIDE AND OXIDE OPAQUE MINERAL ASSEMBLAGES IN MINERAL VEINLETS, NORTH OF CHARITY GLACIER, LIVINGSTONE ISLAND.

BORNITE-CHALCOPYRITE-MOLYBDENITE ASSEMBLAGE:

Specimen Number	Location	Bornite	Chalcopyrite	Molybdenite	Idaite	Magnetite	Covellite	Pyrite	Pyrrhotite	Hematite	Chalcocite	Goethite	Pyrite-Marcasite	Total
1520.2	North west outcrop	64.3	20.3	9.6	2.7	1.9	0.8	-	-	-	0.3	-	-	99.9
1520.5A	North west outcrop	76.3	14.2	-	2.3	-	4.6	-	-	-	2.6	-	-	100.0
1520.5B	North west outcrop	31.1	4.8	51.5	11.6	-	1.0	-	-	-	-	-	-	100.0
1520.5C	North west outcrop	59.0	25.8	0.9	1.9	1.9	2.9	-	-	-	9.5	-	-	101.9
1530	North east outcrop	62.4	4.4	-	3.0	25.5	1.7	-	-	-	3.0	-	-	100.0
1536	North central outcrop	6.3	83.9	-	0.7	-	0.9	-	-	-	8.2	-	-	100.0
1550.1	North east outcrop	87.4	-	-	-	3.4	6.1	-	-	1.1	1.1	-	-	99.1
1551A	North east outcrop	90.9	-	-	0.3	0.8	8.0	-	-	-	-	-	-	100.0
1551B	North east outcrop	79.2	-	3.3	0.3	-	14.5	-	-	-	2.7	-	-	100.0
1551.4A	North east outcrop	83.9	-	-	0.6	8.1	6.0	-	-	-	1.5	-	-	100.1
1551.4B	North east outcrop	82.8	0.7	-	-	9.8	3.6	-	-	-	2.9	-	-	99.8

(All analyses determined on 1000 points).

TABLE 4:6C MODAL ANALYSES OF SULPHIDE AND OXIDE OPAQUE MINERAL ASSEMBLAGES IN MINERAL VEINLETS, NORTH OF CHARITY GLACIER, LIVINGSTONE ISLAND.

PYRITE-PYRRHOTITE-CHALCOPYRITE ASSEMBLAGE:

Specimen Number	Location	Rock Type	Bornite	Chalcopyrite	Magnetite	Covellite	Pyrite	Pyrrhotite	Hematite	Chalcocite	Goethite	Pyrite-Pyrrhotite	Total
1538.1	20m north of Charity Glacier	Aplite	-	2.3	-	-	27.7	44.9	-	-	3.2	21.9	100.0
1538.2	20m north of Charity Glacier	Aplite	-	4.9	-	-	94.6	0.4	-	-	-	-	99.9
1539.1	Central outcrop	Aplite	-	86.3	-	-	1.3	-	-	-	12.4	-	100.0
1543.1A	South outcrop	Aplite	-	83.5	-	-	0.6	-	-	15.9	-	-	100.0
1543.4	South outcrop	Aplite	-	93.1	-	-	6.2	-	-	-	0.7	-	100.0
1543.4A	South outcrop	Aplite	-	83.2	-	-	16.6	-	-	-	0.2	-	100.0
1545.2	South outcrop	Aplite	-	41.7	-	-	33.3	-	-	25.0	-	-	100.0
1574.1	South outcrop	Aplite	-	72.5	-	-	21.3	0.2	-	-	6.0	-	100.0
1567.2	South outcrop	Dyke Rock	0.5	20.0	2.9	-	71.7	3.7	-	1.1	-	-	99.9
1532	North, central outcrop	Tonalite	-	1.9	85.3	-	-	-	12.7	-	-	-	99.9
1553.2	South eastern outcrop	Tonalite	-	14.6	70.8	-	5.2	-	-	9.3	-	-	99.9
1559.2	South eastern outcrop	Tonalite	-	0.9	71.8	-	-	-	27.3	-	-	-	100.0

(All determinations on at least 1000 points).

TABLE 4 : 7 CHEMICAL ANALYSIS OF SELECTED SULPHIDE SEPARATES NORTH OF CHARITY GLACIER

SPECIMEN NO.	LOCATION	MINERAL	Fe	S	* Au	Cu	Mn	Ni	Pb	Se	Zn
1536	Southern outcrop	Py	-	-	30	-	-	-	-	85	-
1538.5	20m north of Charity Glacier	Py	46.42	53.40	1,766	1022	1264	1	1	61	62
1539.1	Southern, central outcrop	Cpy	-	-	40	-	1184	1	115	30	57
1551.4	Extreme northeast outcrop	Bn + Cpy	-	-	1	-	2220	103	1	4800	160
1574.1	Southern outcrop	Cpy	-	-	6	-	530	37	1	1923	10

NOTE: All figures for the trace elements are in parts per million (ppm) * ppb

Table 4.8A REFLECTIVITIES AND HARDNESS VALUES FOR SULPHIDE MINERALS, NORTH OF CHARITY GLACIER, LIVINGSTONE ISLAND.

Specimen No.	Location	Host Rock Type	Reflectivity at 589 nm	Vickers Hardness No.	load (grams)
PYRITE					
1538.1	20m north of Charity Glacier	Aplite sheet	54.2, 53.8, 53.1	1984, 1253, 1681, 1793	100
1538.5		Aplite sheet	52.6, 52.9, 52.6	1508, 2018, 1854	100
1543	Southern outcrop	Tonalite	52.9, 53.2, 53.0	1681, 1865, 1656	100
1543.4	Southern outcrop	Tonalite	52.0, 51.0, 51.7, 52.0	1580, 2205, 2128	100
1567.2	South east outcrop	Dyke Rock	53.1, 52.5, 52.9, 53.5	1984, 1296, 1912	100
1574.1	Southern outcrop	Aplite sheet	50.8, 52.8, 51.9, 51.5	1656, 2205, 2205	100
PYRRHOTITE					
1538.1	20m north of Charity Glacier	Aplite sheet	37.3, 36.3, 36.6, 37.5	320, 328, 324, 306	100
CHALCOPYRITE					
1520.2	North west outcrop	Aplite sheet	41.8, 41.8, 39.3, 42.1	250, 268, 243, 268	100
1536	North, central outcrop	Aplite sheet	41.8, 40.3, 37.6	227, 236, 230	100
1538.5	20m north of Charity Glacier	Aplite sheet	41.8, 41.9, 42.0, 40.7	238, 223, 209, 243	100
1539.1	Central outcrop	Tonalite	36.2, 37.1, 36.9, 39.2, 40.4	227, 286, 243, 259	100
1543.1A	Southern	Tonalite	36.9, 37.6, 37.1	241, 277, 263, 238	100
1543.4A	outcrop	veinlet	40.4, 40.6, 42.0, 39.5	277, 250, 275, 261	100
1574.1	Southern outcrop	Aplite sheet	42.0, 42.5, 43.0, 42.5	268, 238, 225	100
BORNITE					
1520.2	North west outcrop	Aplite sheet	25.3, 25.7, 26.4, 24.6	124, 123, 117, 146	50g
1550.1	Extreme north -	Tonalite	22.4, 23.1, 23.6, 24.0	184, 178, 205	50g
1551	east outcrop	Tonalite	24.3, 24.1, 23.3, 23.5	117, 124, 131, 126	50g
1551.4	" "	Tonalite	23.8, 24.7, 23.7, 22.7	125, 116, 146, 126, 135	50g
MAGNETITE					
1576.3	Eastern outcrop	Tonalite	19.9, 20.6, 20.5	-	

TABLE 4 : 8 B REFLECTIVITIES AND HARDNESSES OF SULPHIDE MINERALS, NORTH OF CHARITY GLACIER

SPECIMEN NO.	LOCATION	ROCK TYPE	REFLECTIVITY AT 589mm	VICKERS HARDNESS NUMBER	LOAD
	MOLYBDENITE				
1520.2	North west outcrop	Aplite Sheet	Rmax 25.9,26.1,28.0,24.5 Rmin 13.9,12.3,12.9,11.6	69.8,101.8,84.5 71.6	10g
1550.1	North east outcrop	Tonalite	Rmax 24.0,27.2,25.8 Rmin 12.7,13.4,13.9	70.2,102,85.3 70.6	10g

CHAPTER 5

MINERALISATION IN THE SOUTH SHETLAND ISLANDS

The South Shetland Islands lie to the north west of the Antarctic Peninsula between latitudes 62° and 63°S and longitude 62° and 57°W. From north to south they are King George, Nelson, Robert, Greenwich, Half-Moon and Livingstone Islands (Fig. 5:4). The majority of the islands have extensive ice caps, with minor areas of exposed rock present in coastal regions, although the exposed rock only amounts to about 5% of the surface area of the islands.

5.1 Occurrences of Mineralization in the South Shetland Islands.

5.1.1 Livingstone Island

Red and green jasper is present in veinlets cutting Tertiary lavas (Hobbs, 1963) on Hannah Point. Chalcopyrite is present in the ?Jurassic lavas at Renier Point in the south-eastern corner of the island (Smellie, J.L., per . comm).

5.1.2 Half-Moon Island

Sparse veinlets of quartz-bornite-chalcopyrite which trend 028° and 330° and are usually 3 cm. wide cut the ?Jurassic lavas in the north east and south east corner of the island. They consist of anhedral quartz (<0.25 mm), with fine-grained interstitial kaolinite, and some ferroandolomite porphyroblasts (1501). The introduction of carbonate is paragenetically later than quartz as veinlets of carbonate cut these quartz veins. The composition of the carbonate is identical to that in the "Quartz-Pyrite" rocks and is probably associated with this late-stage alteration, and, therefore, the quartz veins are earlier than this alteration.

Pale green subhedral chlorite and granules of epidote are associated with the sulphides in the quartz veinlets, the veinlets often having a

halo of sericitised wall rock around them. Anhedral bornite and chalcopyrite (<0.1 mm) are sparsely scattered through the veinlets, and often occur in simple intergrowths, with minor idaite also present. Bornite contains exsolution spindles and lamelli of chalcopyrite parallel to {111} (plate 5:1B, 1506.1), and shows supergene alteration to covellite, chalcocite and cuprite (1501). Minor anhedral rutile and pyrite also occur, with subhedral magnetite showing replacement by hematite (plate 5:1A). Magnetite shows replacement by hematite in the surrounding lavas.

5.1.3 Greenwich Island

Veins varying in width from 1 to 2.5 m and containing chalcopyrite in a gangue of ankerite, barite, calcite, quartz and magnetite, have been found on Greenwich Island (Mueller, 1963). Native copper, however, occurs in glacial erratics on nearby Dee Island (1008.1, plate 5:2).

5.1.4 Robert Island

Native copper has been reported from Coppermine Cove in the north west corner of the island by old whalers during the last century, but the occurrence on Dee Islands suggests this also may have been glacial erratic material as none has since been found in situe (Davies, R.E.S., per comm).

5.1.5 Nelson Island

Veinlets of pyrite and quartz cut the ?Jurassic lavas at O'Caine Point and are less than 6mm wide. They consist of euhedral quartz and pyrite, with the pyrite concentrated at the edges of the veinlet along with fine-grained quartz (plate 5:3). Euhedral quartz occurs in the central parts of the vein with ferroancalcite and calcite filling the interstices between the quartz crystals (1081.10). In places the veinlets contain brecciated wall rock fragments less than 3mm in size.

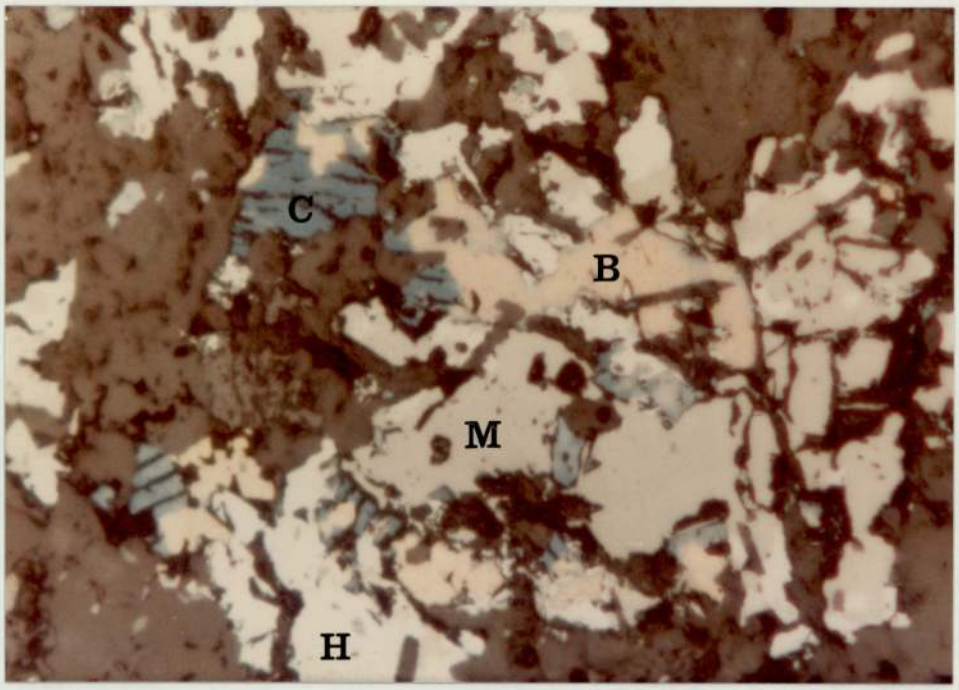

Plate 5:1A Magnetite (grey), hematite (light grey) with bornite (orange) showing alteration to covellite (blue) in quartz vein cutting pre-Andean lavas on Half-Moon Island. (1501). Reflected light, X60. Magnetite (M), Hematite (H), Bornite (B) and Covellite (C).

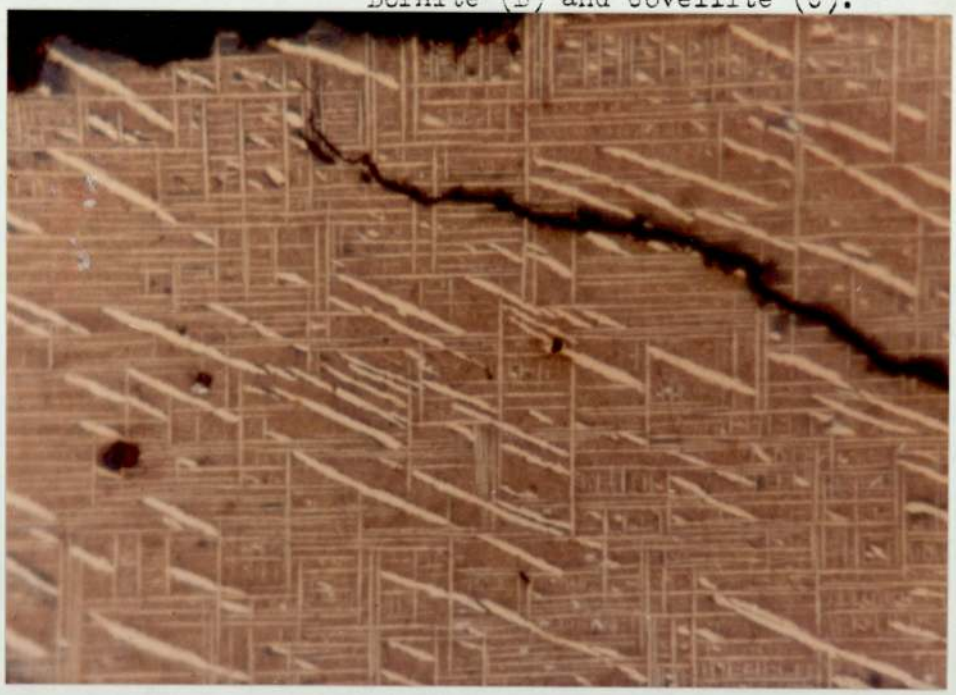

Plate 5:1B Bornite (brown) showing exsolution spindles and lamelli of chalcopyrite (yellow). Bornite shows alteration to covellite (blue) along fractures. In quartz vein cutting pre-Andean lavas, Half-Moon Island. (1506). Reflected light, in oil, X180.

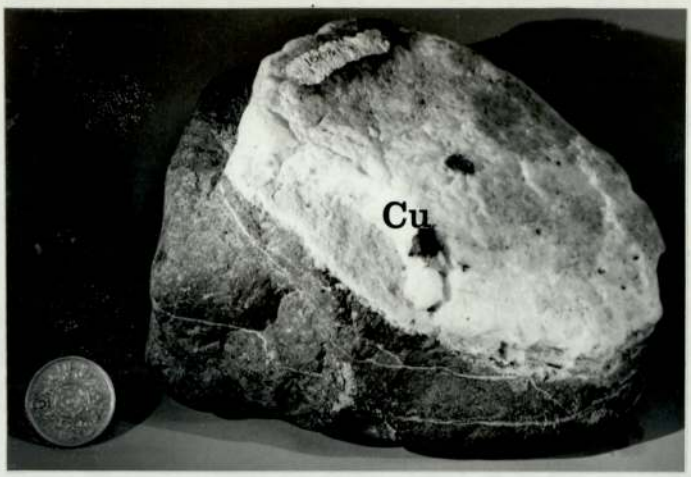

Plate 5:2 Native copper (black) in quartz. Glacial erratic, Dee Island (1008.1). Copper (Cu).

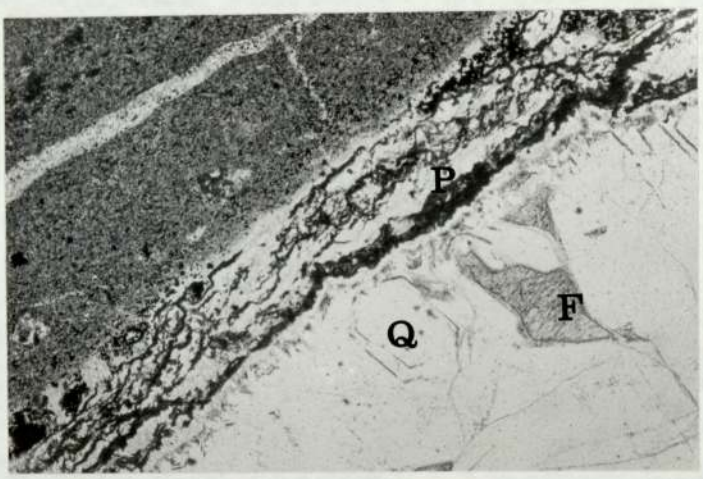

Plate 5:3 Quartz (Q) (euhedral, colourless, low relief), ferroancalcite (F) (colourless high relief) and pyrite (P) (black, near edges of veinlet) in veinlet cutting lavas. O'Caine Point, Nelson Island (1081.10). Transmitted light, plane polarised light, X60.

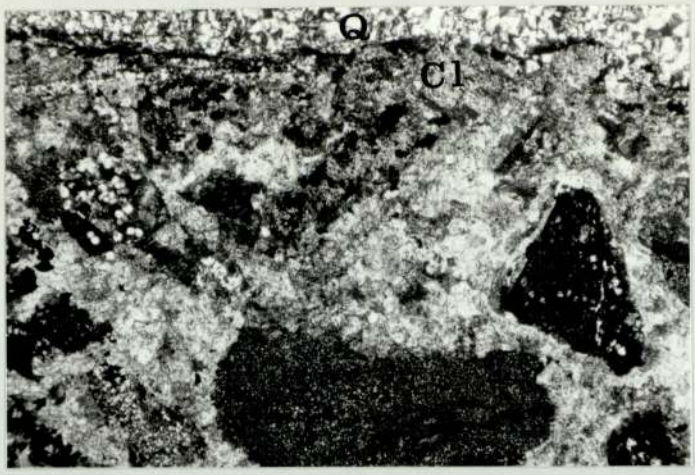

Plate 5:4 Breccia vein cutting lavas, southern Keller Peninsula, King George Island. Groundmass consists of chlorite (grey) and quartz (white) with a zone of microcrystalline quartz occurring at the edges of the breccia vein. Fragments in the vein are of lavas and "Quartz-Pyrite" rock (1377.1B). Transmitted light, crossed polars, X60. Chlorite (Cl) Quartz (Q) Rock Fragments (R).

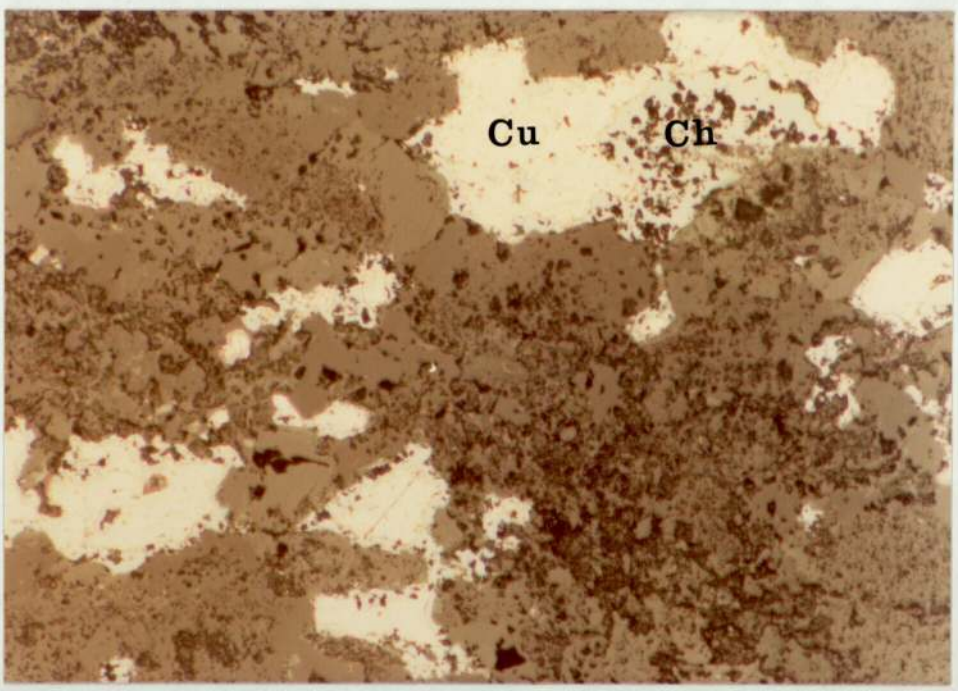

Plate 5:5 Native copper (bright orange) showing alteration to chalcocite (grey) in breccia vein, southern Keller Peninsula, King George Island (1377.1B). Reflected light X60. Copper (Cu), Chalcocite (Ch).

5.1.6 King George Island

Small breccia veinlets composed of anhedral quartz, ferroandolomite (<2.0 mm) and chlorite (plate 5:4) and containing clasts of lava and "Quartz-Pyrite" rock occur on the southern ridge (1377.1B) and south east shore (1381) of Keller Peninsula. At the edges of the veinlets native copper occurs (<0.1 mm, Plate 5:5) which shows alteration to chalcocite. In places the native copper seems to be an overgrowth on acicular hematite.

5.1.7 Elephant Island Group

Chromium (as chromite) nickel and cobalt have been recorded on Aspland Island (Kossack, 1955). Chromite has also been recorded on Gibbs Island (Tyrrell, 1921). Azurite stains have been found on Mount Houlder, Elephant Island (Wordie, 1921) with asbestos and graphite recently reported from the same island (Rowley and Pride, 1977).

5.2 Discussion of the "Quartz-Pyrite" Rocks of the South Shetland Islands

The "Quartz-Pyrite" rocks of the South Shetland Islands are a series of andesitic volcanics and tonalitic plutonic rocks that have been altered by the passage of hydrothermal solutions. Broadly, they can be grouped into four alteration assemblages; advanced argillic (quartz-alunite-kaolinite-pyrite), intermediate argillic (quartz-carbonate-kaolinite-pyrite), phyllic (quartz-muscovite-pyrite) and propylitic alteration (quartz-chlorite-muscovite-epidote-tourmaline-pyrite). These rocks are generally of irregular shape, and pass into unaltered andesitic lavas over a distance of 0.2 - 10 meters. The "Quartz-Pyrite" alteration shows many similarities to the low termperature epithermal-solfataric alteration associated with the late stage hydrothermal

fluids derived from crystallizing granitic rocks (White, 1957), typical of geothermal areas (Raymahashay, 1968). These rocks show a close spacial relationship to the Tertiary plutons.

5.2.1 Solfataric-Epithermal Deposits

Mineralogically, solfataric and epithermal deposits are similar, the difference between the two styles of deposit being that solfataric alteration occurs near the surface (up to 300 meters depth) of the volcanic pile, whereas epithermal alteration takes place at slightly greater depth. Solfataric alteration is, therefore, transitional to epithermal.

In volcanic spring systems, wall rock near the surface shows little or no alteration unless leached by sulphuric acid above the water table, whereas rocks at depths greater than 100 feet are in contact with thermal solutions and shows some evidence of alteration (White, 1957). Most alteration is in the form of irregular shaped fissures or small veins.

Epithermal alteration is generally found in calc-alkaline rocks and is of the vein type which normally occupy faults, although some form complex stockworks with intricate branching (Schmitt, 1950). Stockworks and pipes are also present. Drusy cavities, comb, colloform and crustiform textures and intermineral breccias are features suggesting low confining pressures; and shallow depths of emplacement are typical (Sillitoe, 1977). The brecciated nature of many deposits may be related to the fact that an explosive origin seems likely for many solfataric vents (Marker and White, 1975), although some may be formed by shrinkage of colloidal silica gel and not tectonic processes (Talliaferro, 1934).

This mineralization is genetically related to the late stages of activity of stratovolcanoes, although it is common for mineralisation to utilise structural channelways produced up to 15 my earlier, commonly during episodes of caldera development (Lipman et al, 1976). Indeed,

faults up which these solutions moved to form epithermal deposits are often associated with caldera collapse (Stoki and Konelay, 1974).

Propylitic alteration affects the volcanics (which become dull green and tough) in the vicinity of the veins, with haloes of phyllic alteration around many veins (Sillitoe, 1977).. Minerals common to this alteration assemblage are chlorite, epidote, calcite and other carbonates, pyrite, tourmaline and rarely albite (Schmitt, 1950). Zeolites are deposited no more than several hundred meters below the surface and are common in hot spring deposits, although they are rare in epithermal deposits (Schmitt, 1950). Other alteration assemblages include silica-alunite-kaolinite alteration which is the result of H_2S reacting with oxygen saturated groundwater and forming sulphuric acid. The quartz-sericite alteration indicating accumulation of quartz and potassium normally forms a 0.3-3 meter sheath both sides of the vein (Schmitt, 1950). Pipe-like deposits of advanced argillic alteration often pass downwards into zones of phyllic alteration (Burbank, 1950), the muscovite content usually being formed under alkaline conditions (Deer et al, 1966).

Andesites during the alteration process first show decomposition of feldspar phenocrysts (especially those rich in anorthite), with plagioclase becoming turbid and replaced by kaolinite. Mafic minerals are then replaced by chlorite (Naboko, 1959).

Meteoric water is a major component in epithermal ore fluids (Schmitt, 1950) and a circulating system of heated meteoric water is generally formed in porous rocks following the intrusion of plutonic bodies (Steven and Eaton, 1975).

5.2.2 Significance and Typical Mineralogy of Epithermal-Solfataric Deposits

The mineral assemblages present in these rocks which are characteristic of this type of alteration are described below:-

Alunite typically forms by sulphuric acid leaching of feldspar (Steiner, 1953) usually between 90° - 180°C (Holler, 1967), the sulphuric acid being generated by oxidation of H_2S by oxygen saturated groundwater (Allen and Day, 1935). Alunite can also form by direct precipitation in crater lakes and hot springs (Slansky, 1975), and up to 400-500 meters beneath the volcanic surface (Sillitoe, 1975). Alunite and natroalunite are important prospecting guides because of their association with base and precious metal deposits (Cunningham and Hall, 1976) and porphyry copper prospects (Knight, 1976). Kaolinite can form congruously with alunite (Raymahashay, 1968) although pyrophyllite often forms in preference to kaolinite below 200°C, if the fluid phase is saturated with quartz, although decreasing temperature favours the precipitation of alunite over silicate minerals (Knight, 1977). Anhydrite tends to be a major phase in these deposits, which normally hydrates to gypsum (Birnie and Hall, 1974).

Native sulphur often replaces opalized volcanic rocks at depth (up to 300 meters) beneath the surface of solfataras (Mukaiyama, 1970) and can fill cavities left by leached feldspar phenocrysts (Raymahashay, 1968). Sulphur can also occur adjacent to fractures often replacing the more permeable horizons (Mukaiyama, 1970). Native sulphur deposits associated with solfataric activity can pass transitionally downwards into Pb/Zn mineralisation, and pass upwards into manganese mineralisation (Sillitoe, 1975; Goossens, 1972).

Pyrite can form by leaching of iron and replacement of magnetite in altered lavas, by hydrothermal solutions, by direct precipitation (Arnorsson et al, 1973) or by reduction of alunite (Butter, 1965). Tenorite, hematite, jarosite, gypsum and fluorite have also been found in solfatarically altered rocks (Naboko, 1959) as have epidote and laumontite(generally below 600 meters depending on the geothermal gradient) (White and Sigvaldason, 1963; Sigvaldason, 1963). Manganese, tungsten, barium, mercury, arsenic, gold and silver are metals associated with solfataric deposits (White, 1957) where deposition of the precious metals is related to changes in a number of physicochemical factors (Seward, 1973). Replacement of plagioclase by calcite or siderite has been noted in alkaline alteration assemblages (Steiner, 1953) and CO_2 is a major constituent of volcanic gases especially at a late stage in the volcanic cycle (Giggenbach, 1976; Markhinim and Bozhkova, 1976). The alteration of tuffs to carbonate rich assemblages probably occurred by introduction of CO_2 and Ca (Steiner, 1953), although much Ca was probably leached from plagioclase (Rabone, 1975).

5.2.3 Comparison of Epithermal-Solfataric Alteration with the "Quartz-Pyrite" Rocks

The "Quartz-Pyrite" rocks shows many similarities to epithermal-solfataric alteration, among which are the brecciated nature of many deposits, and breccia fragments in quartz veins on Dufayel Island, both indicating the deposits formed under low pressure.

Where alteration occurs around faults as on southern Barton Peninsula, the andesite lavas show phyllic alteration up to ten meters either side of the faults. Most alteration, however, is of an irregular nature and tends to occur around irregular shaped fissures or small veins. Alteration seems more extensive in porous and tuffaceous rocks

than in blocky lavas. Some veins show comb and crustiform textures; for example, southern Dufayel Island. On Barton Peninsula some of the fractures utilised by the hydrothermal solutions may be caldera faults.

Propylitic alteration is widespread in the ?Jurassic volcanics which are dull green and hard. The propylitic alteration is more intense in the vicinity of areas of phyllic alteration. Minerals present in areas showing intense propylitic alteration are quartz, chlorite, epidote, muscovite, tourmaline, pyrite and pyrrhotite.

Around areas of intermediate argillic alteration zeolites (stilbite natrolite and apophyllite), ferroandolomite, ferroancalcite and cryptocrystalline quartz are present in vesicles in the lavas and suggests that this alteration took place at a high level in the volcanic pile. Quartz-alunite-kaolinite-pyrophyllite-pyrite assemblages (advanced argillic alteration) suggests leaching by sulphuric acid, with the native sulphur present in these deposits indicating they formed at depths less than 300 - 500 meters. The sulphur often occurs in lath-shaped cavities left by leached feldspar phenocrysts.

Pyrite in these deposits can pseudomorph magnetite, but most is pyritohedral and probably formed by direct precipitation, although in areas of advanced argillic alteration it is often associated with alunite and fluorite (occasionally).

5.2.3 Conclusions about "Quartz-Pyrite" Rocks

These areas of "Quartz-Pyrite" alteration are spatialy related to Tertiary plutons, which seem to have acted as a heat source to provide a circulating, heated, meteoric water system, which percolating along fractures in the country rock produced the "Quartz-Pyrite" alteration.

The metal content of these rocks is low, although the sulphur content is relatively high. Sulphur, therefore, seems to have been introduced by the hydrothermal solutions whereas most of the iron was probably derived from the original lavas. No trace of significant manganese mineralisation has been found in the South Shetland Islands, and it has probably been removed by erosion. The high zinc (22,000 ppm) values in pyrite in areas of advanced argillic alteration suggest Pb/Zn or precious metal mineralisation may lie at depth by comparison with deposits in the Andes (Sillitoe, 1975).

The low grade propylitic alteration of the ?Jurassic lavas was probably associated with the circulating, meteoric water system. Where the water was at the deepest, least oxidised level strong propylitic alteration occurred, although the presence of tourmaline and daphnite suggest there may have been some introduction of juvenile fluids based on work by Sheppard (1977). As the water passed upwards through the highly oxidised andesitic lavas, phyllic alteration occurred. Introduction of oxygen saturated groundwater oxidised the H_2S present in the fluids to sulphuric acid and advanced argillic alteration occurred. By comparison with deposits in the Yellowstone Park (Keith and Muffler, 1978), the areas of intermediate argillic alteration (carbonate-rich assemblages) may have originated in the upper parts of tuffaceous rocks in zones where boiling groundwater was present, and CO_2 was lost during this boiling process.

The "Quartz-Pyrite" deposits seem to represent volcanogenic alteration zones formed during the development of andesitic stratovolcanoes, which are often associated with the development of porphyry copper deposits and Pb/Zn mineralization (Branch, 1976; Fig 5:1).

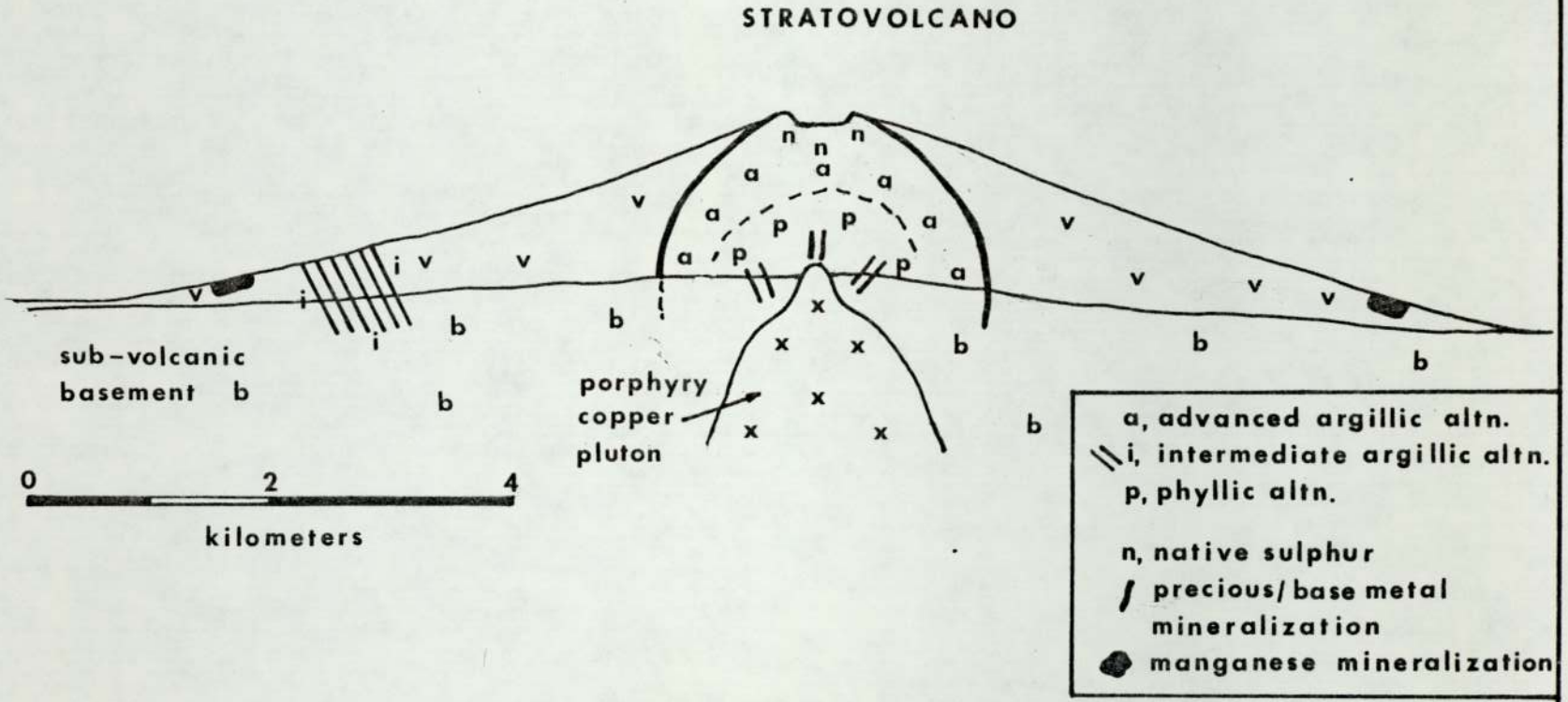

Fig5:1 DIAGRAM SHOWING RELATIONSHIP OF 'QUARTZ-PYRITE' ALTERATION TO PORPHYRY COPPER MINERALIZATION, KING GEORGE ISLAND. (after Sillitoe 1977)

5.3 Copper Deposit, North of Charity Glacier, Livingstone Island

The copper deposit, north of Charity Glacier, Livingstone Island occurs in a composite tonalitic pluton. The earliest phase of plutonic activity was the intrusion of a hornblende-rich diorite, which was followed by a fine-grained tonalite and then a medium-grained tonalite. Synplutonic dykes were then intruded into the medium-grained tonalite, and tectonic stresses present in the final phases of intrusion have introduced a schistosity into these rocks. Aplite sheets were then intruded into these dykes and plutonic rocks, and are most abundant in the southern part of the area. A later phase of dolerite dyke intrusion then occurred, which in the southern part of the complex shows metamorphism to hornblende hornfels facies.

Hydrothermal breccia dykes were then intruded which were followed by porphyry copper style mineralisation. The mineralisation which occurs mainly in veinlets of random orientation is zoned from a central core of bornite-chalcopyrite- molybdenite to chalcopyrite-pyrite-pyrrhotite to an outer zone of chalcopyrite-galena-sphalerite.

5.3.1 Porphyry Copper Mineralisation

Porphyry copper deposits are magmatic-hydrothermal deposits frequently centered on a prophyritic intrusive plutonic rock, forming part of a composite intrusion (Lowell and Guilbert, 1970). They consist of disseminated and stockwork veinlet sulphide (Cu and Mo) mineralisation, emplaced into host rocks that have been altered by hydrothermal solutions into roughly concentric zoning patterns, generally at depths of 1,000-1,500 meters(Nielsen, 1968). These deposits are often bounded by regional faults (Lowell and Guilbert, 1970), and the mineralisation is controlled mainly by faulting in the Andes (Hollister, 1975).

Porphyry copper deposits are a normal facet of calc-alkaline magmatism, the magmas from which they come are derived by partial melting of oceanic crustal rocks on underlying subduction zones at the elongate compressive junctions between lithospheric plates (Sillitoe, 1972; Mitchell and Bell, 1973; Sawkins, 1972). These deposits form during a series of discrete pulses perhaps correlatable with changes in the relative rates and directions of motion of the lithospheric plates (Sillitoe, 1977). The linear metallogenetic belts in Chile which may be due to shifting loci of magma and included metal generation on a subduction zone, seem to be independent of control by tectonic lineament intersection (Sillitoe, 1972), although Pitcher (1978) suggests the main control of batholithic emplacement is structural.

The most common types of intrusive rock associated with continental porphyry coppers are granodiorite and quartz-monzonite (Stringham, 1966; Creasey, 1966; Hollister, 1974; Lowell and Guilbert, 1970). In contrast, porphyry copper deposits in island arc environments are often associated with tonalites (Wolf, 1973; Cox et al, 1973), generally of irregular-elongate shape and often stock-like (Lowell and Guilbert, 1970). This suggests the intrusions are compositionally more primitive than their cratonic counterparts and involvement of epi-crustal material in the development of these magmas is, therefore, restricted. Consequently, they contain relatively small amounts of potassium feldspar (Kesler et al, 1975) and are often hypidiomorphic (Patten et al, 1973). Aplite dykes and sheets are characteristic of the porphyry copper and molybdenum deposits in Perú and North America (Hollister, 1975) and often represent a link between magma and ore (Lutton, 1952).

Vapour fractionation as a method of separating economic elements from tonalite magmas occurs over a greater pressure and depth range than for quartz-monzonite (Whitney, 1977). Vapour derived from a crystallizing silicic intrusive plays an important role in the generation of disseminated copper deposits (Burnham, 1967). Thus ore deposits associated with tonalites may extend to greater depths than with quartz-monzonite magmas (Whitney, 1977).

Hydrothermal fluids in island arc porphyry copper environments are often deficient in sulphur. Iron can be retained in biotite, chlorite and magnetite, instead of reacting to form pyrite (Bowen et al, 1977). Some sulphur for the sulphides may have been derived by chloritization of biotite by hypogene fluids (Banks, 1973) or released from biotite in the magmatic stage (Lovering et al, 1970).

Hydrothermal alteration zones associated with porphyry copper environments are characteristically concentrically zoned from a potassic core to phyllic, argillic and finally propylitic zones (Lowell and Guilbert, 1970). The potassic alteration zone seems to be due to the highest temperature magmatic fluids, with the phyllic, argillic and propylitic alteration caused by a superimposed, circulating, hot water system fed by meteoric and connate water (Lowell and Guilbert, 1970). The dioritic model of Hollister (1975) suggests that alteration zones associated with tonalitic intrusives consist of a potassic core surrounded only by a propylitic periphery (chlorite-sericite or chlorite-epidote) as a result of the effect of the more basic tonalite (as opposed to the acid monzonites) reacting with the hydrothermal fluids.

The metalliferous mineralisation shows zonation from a low sulphide, chalcopyrite-pyrite-molybdenite core, through a high sulphide, pyrite-chalcopyrite shell to a chalcopyrite-galena-sphalerite periphery.

Disseminated sulphides are present in the core of these deposits, and veinlets are predominant in the peripheral zones (Lowell and Guilbert, 1970).

5.3.2 Comparison of the Deposit North of Charity Glacier, with other Porphyry Copper Deposits

The deposit, north of Charity Glacier is bounded by regional faults (Ashcroft, 1972; Hobbs, 1963) typical of this type of deposit, although the mineralisation is controlled by extension joints and fractures rather than by faulting as in the Andes.

The composition of intrusive rocks in this area shows trends similar to those found in island arcs by comparison with Kesler et al (1975), although the aplite sheets range into the granite field, and are characteristic of porphyry copper deposits. This plus the fact that the South Shetland Islands were probably part of the Antarctic Peninsula prior to the opening of the Bransfield Strait (Barker and Griffiths, 1972) and have a continental basement (Ashcroft, 1972) suggests the plutonic rocks and consequently the associated porphyry copper deposits are transitional between continental and island arc types.

The area north of Charity Glacier seems to represent the propylitic zone of such a deposit (quartz-chlorite-sericite-epidote alteration) with the potassic core probably lying at depth (Fig. 5:2). Probably the chief departure of this deposit from the typical diorite model (Hollister, 1975) porphyry copper deposit is the relatively low grade of mineralised rock and the presence of molybdenite as a major sulphide. The relative paucity of sulphides in this deposit may indicate the hydrothermal fluids were deficient in sulphur. The patterns of alteration and mineralisation are typical of these concentrically zoned deposits (Fig. 4:2) and the sparseness of breccia dykes is also characteristic.

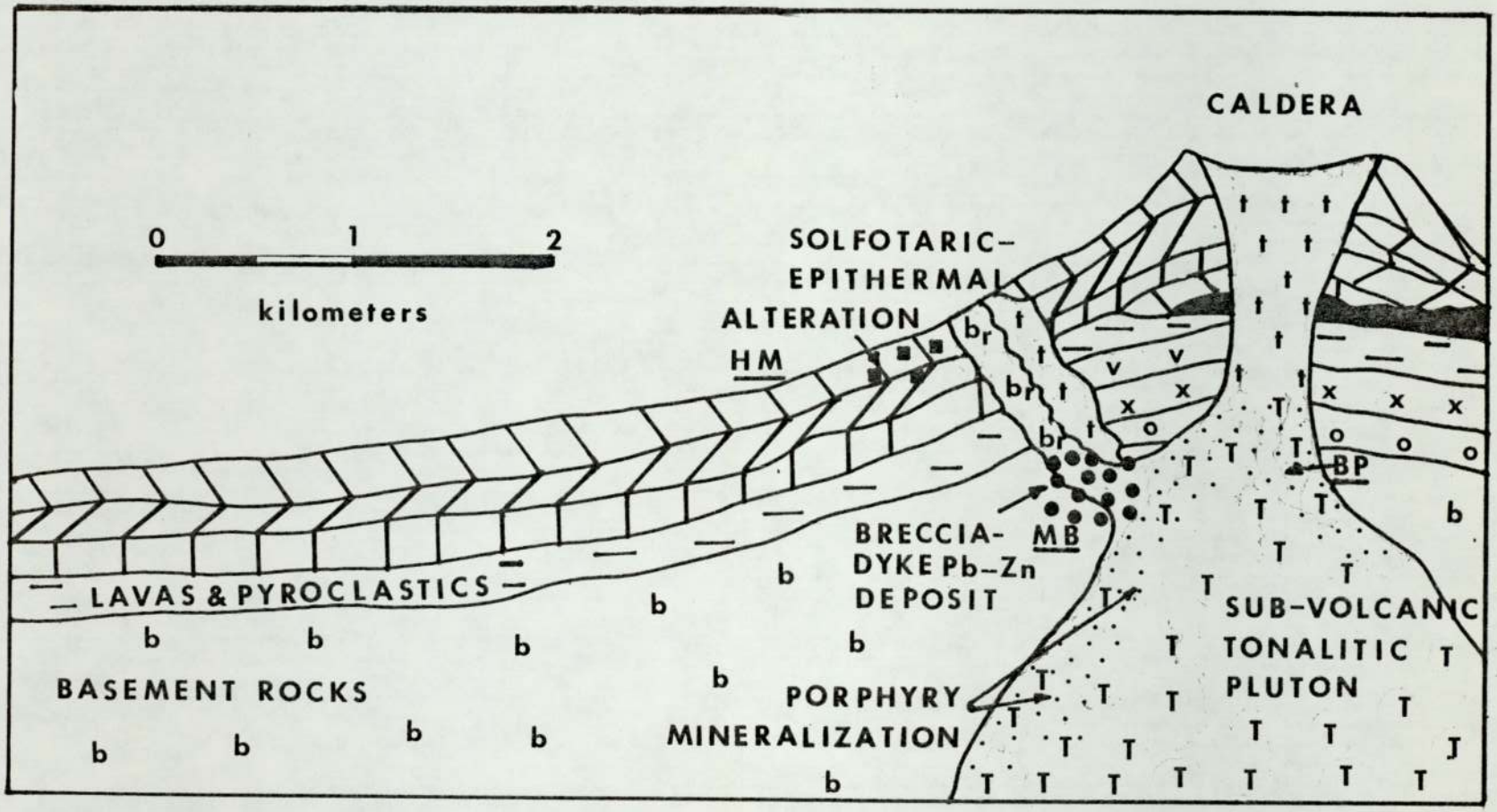

Fig 5:2 SCHEMATIC DIAGRAM OF THE GENESIS OF MINERAL DEPOSITS ON LIVINGSTONE ISLAND. BP, BARNARD POINT COPPER DEPOSIT; MB, MIERS BLUFF Pb–Zn DEPOSIT; HM, HALF MOON ISLAND LOW TEMPERATURE ALTERATION. (AFTER SILLITOE 1977).

5.3.3 Conclusions about the Copper Deposit, North of Charity Glacier

Using the Lowell and Guilbert (1970), Hollister (1975), Sillitoe (1973) and James (1971) models we can speculate on the location of higher grade mineralisation. The associated and slightly older breccia dykes are similar in petrology and age to those that preceeded mineralisation in the typical porphyry copper deposits of the Circum-Pacific belt. The alteration and mineralisation assemblages also have many similarities in petrology and chemistry. The coarseness of the quartz veins, the presence of magnetite and the lack of significant potassic alteration suggests a site marginal to a higher grade deposit (Fig. 5:2).

This complex, therefore, probably represents the outer solid shell which later ruptured to produce a porphyritic-aphanitic texture in the subsequently crystallized rocks as in other deposits (Neilson, 1968). Volatiles released by the quenching magma migrated outwards along joints and planes of weakness in the very north of the area causing alteration and mineralisation as a result of gradients from near magmatic temperatures to the relatively cool wall rocks. Thus erosion has not removed any significant ore deposit and richer deposits may lie beneath the present erosion surface or adjacent to the copper deposit described.

5.4 Comparison of Metalliferous Mineralisation in the South Shetland Islands with that in other Island Arcs

To the north of the South Shetland Islands lies a deep trench down which oceanic crust has been subducted for at least the last 20 my (Herron and Tucholke, 1976) and which is bounded at the northern and southern margins by the Shackleton and Hero fracture zones respectively. A marginal basin has developed to the south east of the Islands (Barker and Griffiths, 1972) which underlies the Bransfield Strait and has separated the South Shetland Islands from the Antarctic Peninsula.

The majority of the known mineralisation in the South Shetland Islands seems to be associated with the emplacement of tonalite to granodiorite plutons of early Tertiary age (40-57 my). The association of the mineralisation with the subduction of the south eastern Pacific sea floor beneath the South Shetland trench and the opening of the Bransfield Strait seems certain, and is fairly typical of volcanic island arcs with a marginal basin (Fig. 5:3). No distinct metallogenetic zoning pattern is evident in the South Shetland Islands as in the Andes, probably due to the high erosional level of many plutonic intrusions.

Ophiolites

Ophiolites are an assemblage of basic and ultrabasic rocks consisting of (from bottom to top) tectonized peridotite, layered cumulates ranging from dunite and peridotite to olivine gabbro, to trondjemites above which is a sheeted dyke complex which merges into pillow lavas and dykes. Sediments normally lie on top of the succession.

These bodies of rock are regarded as slices of oceanic lithosphere that have been tectonically emplaced into island arcs (Hutchinson, 1975) by a process known as obduction (Coleman, 1971; Gass, 1977), during which slices of oceanic crust and upper mantle can be emplaced in the island arc during the final stages of subduction of ocean floor (Dewey and Bird, 1971). Ophiolites can also occur in elongate belts at the junction of two plates in a suture zone or thrust onto the subducting plate together with the magmatic arc rocks, (Mitchell and Bell, 1973). Obduction normally occurs during a reversal of plate motion and can also be accompanied by the emplacement of glaucophane schists (Gass et al, 1975).

The South Shetland Islands are in a tectonic environment suitable for the emplacement of ophiolites, and the presence of dunite-sepentinite

bodies on Gibbs Island (Tyrrell, 1945) and the presence of chromium (as chromite), cobalt and nickel on Gibbs and Aspland Island suggest ophiolites or podiform chromite complexes (as defined by Thayer, 1964) may be present. The Cornwallis Island "granite", which is a trondhjemite (Baker and Rex, 1973) may represent a sodium rich granite which are often associated with ophiolite complexes (Gass et al, 1975). Chromium bearing dunite bodies often contain platinum in economic quantities (Razin, 1976).

The presence of sodic amphibole schists (glaucophane-crossite) on Smith Island indicates obduction has occurred on the South Shetland Islands, in the late Tertiary (90 my, Davies, R.E.S., per comm.), which is probably connected with the opening of the Bransfield Strait.

Porphyry Copper and Molybdenum Deposits

These deposits are common in island arc environments (Mitchell and Bell, 1973), and often occur at the summit or around the margins of stocks or small plutons intruded beneath contemporaneously erupted volcanic rocks.

A porphyry copper-molybdenum deposit with peripheral Pb/Zn mineralisation has been found on south eastern Livingstone Island. The hydrothermal fluids that produced this deposit were probably sulphur deficient judging by the abundance of magnetite, biotite and chlorite in the host intrusive and the relative sparseness of disseminated sulphide minerals.

The abundant areas of low temperature epithermal alteration on King George Island suggests porphyry copper deposits may be present at depth, based on models by Sillitoe (1977). The presence of native sulphur and alunite on King George Island, however, suggests the

fluids here were sulphur rich and high grade porphyry copper deposits may lie at depth. Native sulphur typically occurs in island arc environments (Horikoshi, 1976).

Mercury and porphyry copper mineralisation may be connected (White et al, 1971), cinnabar and quicksilver ores being formed in vapour dominated reservoirs above boiling brine zones in which porphyry coppers are formed. If mercury deposits are present in the South Shetland Islands they should lie stratigraphically above porphyry copper deposits (Fig. 5:3).

Gold is often associated with granodiorite plutons in island arcs, generally in quartz veins (Sawkins, 1972), the gold generally being present in sulphides and tellurides. Gold can be associated with thick successions of andesitic lavas and metasedimentaryrocks and can be associated with caldera boundary faults (Denholm, 1967). Gold analyses of sulphides and lavas on King George Island show the values are not higher than the average andesitic rocks.

Besshi Sulphide Deposits

Besshi type sulphide deposits occur in the Sanbagawa metamorphic belt in Japan and are associated with intermediate to basic submarine volcanism. Sediments associated with these deposits are mainly carbonaceous mudstones, quartzites and clastic limestones of deep water facies. These copper-pyrite deposits are formed as part of island arc volcanism adjacent to a continent in a tensional tectonic environment (Mitchell and Bell, 1973), and can occur in glaucophane schists (Isihara, 1978).

Glaucophane schists occur on Smith Island and these contain lenses rich in opaque minerals. These are mainly subhedral hematite, but anhedral chalcopyrite and euhedral pyrite are also present. This may

indicate lavas and sediments containing iron and sulphides were metamorphosed to produce these rocks, and may represent a very low grade Besshi sulphide deposit.

Kuroko Deposits

Kuroko Deposits are predominantly massive stratiform sulphide ores with an underlying stockwork and root zones of vein type copper, lead and zinc (Colley, 1976) occurring in submarine volcanic rocks, formed in shallow marine environments (Horikoshi and Satu, 1970). They are generally associated with clastic dacitic or andesitic volcanics and formed due to fluids emanating from rhyolite domes intruded into these rocks during the last stages of volcanism. The intrusion of these rhyolite-dacite domes and flows being followed by phreatic explosions (Horikoshi, 1969). The major constituents of these deposits are pyrite, chalcopyrite, sphalerite, galena, barite and quartz commonly showing a vertical zonation. Gypsum or anhydrite commonly occur as separate bodies around these ore bodies.

The South Shetland Island appear to be in a similar geological environment to Japan in that the island arc is backed by a continent and itself lies on Continental crust (Ashcroft, 1972) and could be a suitable environment for the formation of Kuroko ores.

Skarn Deposits

Skarn deposits occur around granotoid intrusives in calcareous rocks or limestones as replacement Pb-Zn-Ag deposits. In non-calcareous rocks quartz rich vein deposits occur containing either W-Sn-Cu or Mo-Pb-Zn. Since calcareous rocks are absent in the South Shetland Islands it is unlikely that Skarn deposits are present here.

Stratabound manganese deposits are often related to submarine volcanism (Isihara, 1978; Kesler, 1978) and could be present in the South Shetlands.

Sn, Bi, Mo, W and F mineralisation may be present on the Antarctic Peninsula, opposite the South Shetland Islands as it is elsewhere in island arcs backed by a continental landmass (Garsen and Mitchell, 1977), and indeed, fluorite has been recorded on the Oscar II Coast (Fleet, 1968).

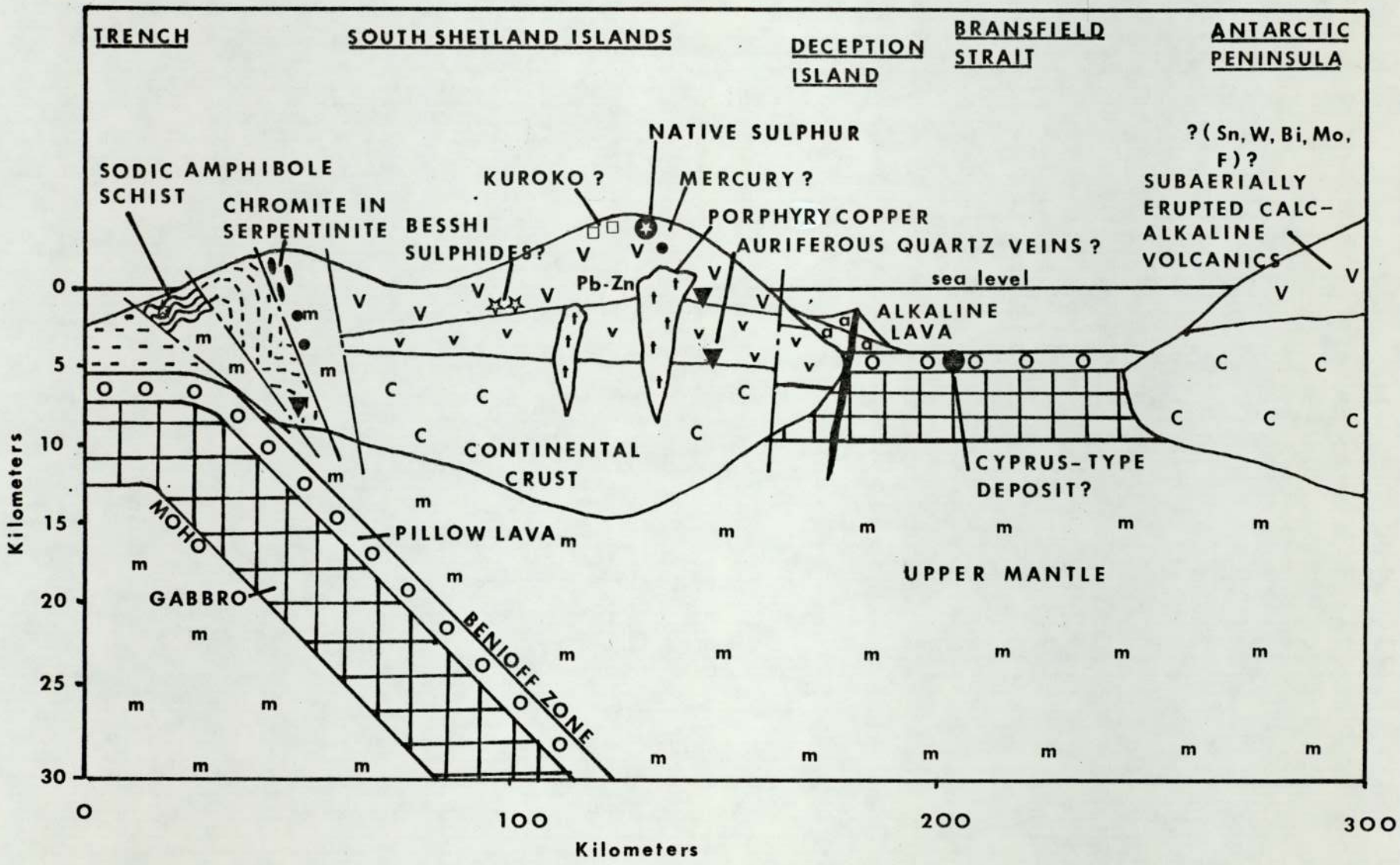

FIG.5:3 SCHEMATIC DIAGRAM OF METALLIFEROUS MINERALIZATION IN THE SOUTH SHETLAND ISLANDS. THE MINERALIZATION SEEMS TYPICAL OF THAT FOUND IN ISLAND ARCS WITH A BACK ARC BASIN BEHIND A CONTINENT. (AFTER GARSON AND MITCHELL 1977).

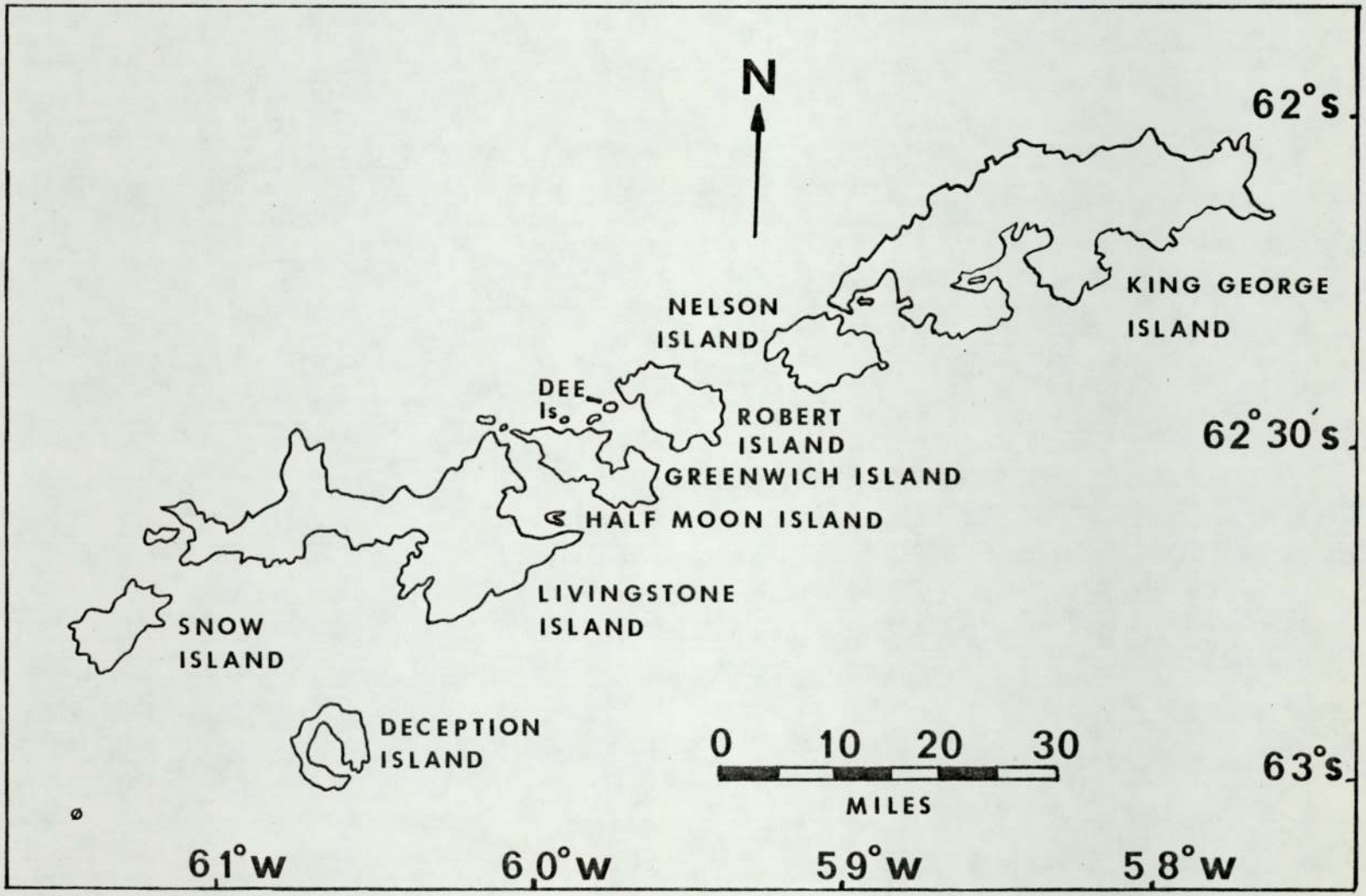

FIG. 5:4, MAP SHOWING THE POSITION OF THE SOUTH SHETLAND ISLANDS.

CHAPTER 6

MINERAL DEPOSIT AT ARGENTINE ISLANDS NORTH EAST GRAHAM LAND

6.1 Introduction

The Argentine and Anagram Islands are situated off the north east coast of Graham Land, between latitude 65° 12' and 65° 16' south and longitude 64° 13' and 64° 20' west. The majority of the islands have a permanent ice cover, but during the summer months many of the northward facing slopes are ice and snow free.

The first geological reconnaissance of the Argentine Islands was carried out by the British Graham Land Expedition (1934-37) when they wintered on Winter Island. A British base was established on Galindez Island in 1954, the first geological survey of the Islands being undertaken by G. J. Roe during 1958-59. Later work on the geology was carried out by Elliot (1964) and Fraser (1965). The field work associated with the present study of the mineralisation was undertaken from January to February, 1977.

The Argentine and Anagram Islands (Fig. 6:1) are composed entirely of igneous rocks (Elliot, 1964; Fraser, 1965) ranging from Jurassic volcanics on the Islands to the east of the Argentine Islands Group, and plutonic rocks of Tertiary age in the western part. The Anagram Islands are composed of Tertiary plutonic rocks. Where the calc-alkaline andesites and pyroclastic rocks of the Jurassic volcanic suite are adjacent to the plutonic rocks they have been metamorphosed and metasomatised. The volcanic rocks have also been intruded by pre-Andean dykes and sills.

The Tertiary Andean Intrusive Suite which intrudes the Jurassic volcanics is represented mainly by tonalites and granodiorites, but ranges from gabbro to quartz-monzonite. The granodiorites on the Barchan Islands

Fig. 6:6 General Geology of the Argentine Islands

(after Elliot, 1964; Fraser, 1965).

AGE	ROCK TYPE	TECTONICS
RECENT to PLEISTOCENE	RAISED BEACHES, GLACIAL DEPOSITS	
		FAULTING?
	TERTIARY LAVAS	
	POST-ANDEAN DYKES	
	MINERALIZATION AND ALTERATION	
	QUARTZ-MAGNETITE VEINS	
TERTIARY		FAULTING
	TUFFS	
	QUARTZ-MONZONITE VEINS	
	PLUTONIC ROCKS { GRANODIORITE, TONALITE, GABBRO	
	PRE-ANDEAN DYKES	
UPPER JURASSIC	CALC-ALKALINE LAVAS, TUFFS AND BRECCIAS	

have been invaded by quartz-magnetite veins (Fig. 6:3) with molybdenum and copper mineralization present on sheet joints in the Forge Islands. The presence of the quartz-magnetite veins and molybdenum mineralisation suggest the Argentine Islands represent the basal part of a porphyry molybdenum deposit.

The plutonic rocks and quartz-magnetite veins are intruded by post-Andean dykes.

The igneous rocks and associated mineralisation are discussed below:

6.2 Field Relations of the Igneous Rocks

The oldest rocks in the Argentine Islands are a series of calc-alkaline volcanics of Jurassic age (Elliot, 1964). These generally grey to black rocks vary from trachytic and porphyritic andesites to dacite breccias and crystal tuffs. In places the brecciated tops of lava flows are exposed on Skua (S8) and Winter Islands. The rocks are well jointed, but do not show distinct layering or bedding, although some subhorizontal joints in the lavas on Skua Island may be bedding joints.

Breccias and tuffs are present on Galindez, Uruguay and Grotto Islands and are generally light grey to grey in colour. On Grotto Island, the tuffs show evidence of being almost vertical, although elsewhere the bedding is subhorizontal. Fragments in these rocks are generally andesites and silicified tuffs, although quartzites have also been found. On Galindez Island areas of breccia occur which are roughly circular in outline and may represent old volcanic vents.

Intruded into these lavas and breccias are microdiorite dykes and sills of variable thickness which are pre-Andean in age. They generally have chill contacts 0.5 mm wide of glass, but there is often some degree of brecciation at the contact (Elliot, 1964).

Where the lavas and pyroclastics have been intruded by Tertiary plutons, for example in the Barchan Islands, they have been thermally metamorphosed to a crumbly, fine-grained plagioclase-amphibole-biotite hornfels which shows mafic and felsic banding, with slight foliation in places. The pre-Andean dykes also show the effect of magmatic and hydrothermal alteration, and where they are in the contact metamorphic aureole of the plutonic rocks they show alteration to hornblende-plagioclase hornfels.

Intruded into the Jurassic volcanics are a series of plutonic rocks (dated by K/Ar methods at 54-57 m.y.; Rex. 1976), which range from gabbro to quartz-monzonite, although on the Argentine Islands, tonalites and granodiorites are the most abundant rock types. The earliest phase of plutonic activity is represented by xenoliths of olivine and hypersthene gabbros in banded gabbros on the Anagram Islands (Fraser, 1965).

The banded gabbro itself occurs in an elongate zone to the northeast of Nob Island about 0.5 km. wide, and shows rhythmic banding of dark gabbroic and light anorthositic layers which are usually vertical or steeply dipping, and which according to Fraser (1965) originated by forced flow of a crystal mush and pseudosedimentary deposition. The gabbro has undergone late stage magmatic alteration and cavities and vugs are present containing plagioclase, hornblende, epidote, magnetite, pyrite and chalcopyrite (A2). Veinlets of hornblende with epidote and pyrite cut the gabbro (3 - 0.5 cm wide). The gabbro is also intruded by aplite sheets (less than 0.5 m wide).

Xenoliths of the banded gabbro occur in the surrounding tonalites, and where the gabbro is in contact with the tonalites, the junction is generally well defined. In the Argentine Islands, no contacts are visible between the various phases of tonalite and granodiorite. The

plutonic rocks in the Argentine Islands are white to light grey in colour, and are generally medium-grained, leucocratic rocks.

Later quartz-monzonite veins cut these plutonic rocks, with a pink, almost circular quartz-monzonite intrusive approximately ten meters wide cutting the granodiorite on the Forge Islands (Fig. 6:1), although elsewhere the veins are less than 50 cm wide. These rocks appear to represent the final phase of plutonism.

Greenish-grey, post-Andean dykes intrude the Jurassic lavas, plutonic rocks and quartz-magnetite veins (plate 6:1), and are mainly microgabbroic and microdioritic (Elliot, 1964). They often have a porphyritic texture and strike east-west.

The latest phase of volcanic activity is represented on Irizar Island by porphyritic andesites and augite microdiorites of Tertiary age (Elliot, 1964) (Fig. 6:6).

6.3 Petrography of the Igneous Rocks on the Argentine and Anagram Islands.

6.3.1 Jurassic Volcanics

The petrography of these lavas has been described by Elliot, (1964) as consisting of subhedral plagioclase phenocrysts (An_{30-40},) less than 1mm, which show alteration to epidote, chlorite, sericite and calcite, set in a matrix of plagioclase (An_{28-36}) which sometimes show subparallel alignment. Minor anhedral quartz is present in the groundmass, often with interstitial amphibole and biotite which shows alteration to chlorite. The biotite is probably secondary, having formed by low grade thermal metamorphism. Chlorite and epidote occur surrounding magnetite. Minor euhedral apatite also occurs. Subhedral magnetite and ilmenite showing resorption and alteration to hematite and rutile, with minor chalcopyrite (less than 0.62 mm) showing alteration to chalcocite are the opaque

phases in the lava. Inclusions of pyrite occur in some magnetites (less than 0.01 mm).

The tuffs, however, show "porphyritic" texture with crystals of plagioclase and quartz in a fine-grained quartzo-feldspathic matrix. Chlorite and epidote are common, the epidote apparently occurring in two generations; an early phase affecting the lavas which occur as fragments in the tuffs, and a later, less intense phase that affected the groundmass of the tuffs (S8B). Pyrite is present in the matrix of the rocks, but only rarely in the clasts.

6.3.2 Pre-Andean Dykes

The petrology of these rocks has been discussed in detail by Elliot (1964), and have been shown to consist of phenocrysts of plagioclase and amphibole in a groundmass of plagioclase laths. Amphibole often contains remnant cores of augite.

6.3.3 Plutonic Rocks

1. Banded Gabbro

The petrology of this rock has been discussed in detail by Fraser (1965), with the present study investigating the secondary alteration.

Petrographically, the rock consists of subhedral plagioclase feldspar (An_{50-55}) which shows slight alteration to muscovite, epidote and carbonate, although some early plagioclase seems to be replaced by later sodic plagioclase (A8). Some interstitial orthoclase is also present. Pale green to colourless, subhedral amphibole is present (less than 3mm) containing inclusions of euhedral augite, and may be replacing plagioclase in places (A1). Amphibole shows alteration to carbonate, quartz and chlorite, with biotite and some augite also showing replacement by chlorite. Augite also shows alteration to green and brown hornblende, although the minor hypersthene present shows more

extensive alteration. Subhedral olivine also occurs, often surrounded by a reaction rim of hypersthene, and showing alteration to serpentine.

The primary minerals in the gabbro, dominantly plagioclase and pyroxene show simple igneous textures, with adcumulus growth of plagioclase and intercumulus growth of hornblende. The gabbro also shows good examples of igneous lamination and primary igneous layering, all evidence of a cumulate type crystallization in a magma chamber.

Optical studies and electron microprobe data (table 6:1) show two phases of magnetite formation are present in the rock. The early euhedral magnetite which occurs in simple intergrowths with ilmenite (A8) and contains exsolution lamelli of ilmenite parallel to $\{111\}$, shows replacement by amphibole and probably formed during crystallization of the gabbroic magma. Later subhedral magnetite occurs, often surrounded by biotite and muscovite which seems to have formed by the action of late stage magmatic fluids (Fraser, 1965). Small veinlet-like masses of magnetite occur in fractures in the rock and show alteration to hematite along $\{111\}$. The secondary magnetite does not contain ilmenite exsolution lamelli. Subhedral rutile is also present.

Pyrite occurs as inclusions in some magnetites, and along cleavages in the amphiboles. Subhedral chalcopyrite (less than 0.3 mm) showing marginal alteration to covellite and chalcocite, and anhedral pyrite containing "emulsion droplets" of pyrrhotite (less than 0.01 mm) are also present.

2. Aplite Veins cutting the Banded Gabbro

The aplites consist of an inequigranular mass of anhedral quartz, subhedral plagioclase feldspar (An_{45-30}, less than 0.8 mm) showing alteration to epidote and muscovite. Subhedral chlorite (replacing biotite) is often associated with carbonate although Fraser (1965) also

describes prehnite. Minor zircon is also present, with small veinlets of muscovite and epidote traversing the rock (less than 0.1 mm). The opaque phases are anhedral ilmenite showing alteration to rutile, subhedral magnetite and anhedral pyrite.

3. Tonalites and Granodiorites

These rocks generally consist of an hypidiomorphic mass of anhedral to subhedral plagioclase (An_{40-30}) which often show zoning from a calcic core (An_{46}) to a sodic margin (An_{25}), anhedral quartz and minor anhedral orthoclase. Clusters of quartz and biotite occur interstitially, which seem to be replacing feldspar and amphibole (H33.1). In places graphic intergrowths of quartz and feldspar occur, the quartz frequently showing undulose extinction. Orthoclase is generally perthitic and sometimes poikilitically encloses plagioclase, and often replaces it (as first seen by Elliot, 1964). Xenocrysts of plagioclase containing pyroxene and amphibole are present.

Hornblende is the predominant ferromagnesian mineral, containing inclusions of augite, although Elliot (1964) described rare hypersthene. Biotite and hornblende show alteration to chlorite, epidote, sphene and carbonate. Minor zircon, apatite and rutile are also present (less than 0.3 mm). At the margins of the pluton a chill zone is present consisting of subhedral biotite, anhedral quartz and subhedral plagioclase (H55.1).

Opaque minerals present are acicular to subhedral ilmenite (less than 0.35 mm, B3A) in simple intergrowths with euhedral magnetite. The magnetite contains exsolution lamelli of ilmenite parallel to $\{111\}$, "emulsion droplets" of pyrite and pyrrhotite (B19), and shows slight alteration to hematite along fractures. Some ilmenite contains hematite exsolution lamelli (B19). The magnetite and ilmenite frequently have a halo of chlorite and carbonate. Minor amounts of euhedral pyrite are

present showing marginal alteration to goethite, which are in simple intergrowths with pyrrhotite and chalcopyrite (B18), with the chalcopyrite showing alteration to chalcocite.

4. Quartz-Monzonite Veins

These rocks consist of spherical myrmekitic intergrowths (8mm) of quartz and feldspar which are clearly visible in the hand specimen. The centres of these intergrowths are fine-grained and composed of plagioclase and quartz, with the coarser peripheries consisting of orthoclase and quartz. The quartz in each intergrowth is optically continuous.

The groundmass consists of subhedral plagioclase showing alteration to chlorite, muscovite and epidote (especially the calcic cores). Some brown hornblende (less than 1.2 mm) and subhedral biotite (less than 3.0 mm) are present, although the biotite is usually replaced by chlorite. Some amphibole shows slight alteration to biotite. Minor zircon (less than 0.2 mm) and acicular rutile occur in the quartz, with siderite often along cleavages in the chlorite (F8A).

Euhedral magnetite (less than 0.45 mm) and subhedral ilmenite occur in simple intergrowths, often surrounded by epidote, siderite and chlorite, with magnetite showing alteration to hematite along fractures. Inclusions of pyrite occur in the magnetite and minor chalcopyrite is present showing alteration to chalcocite.

Modal analysis of the plutonic rocks of the Argentine Island Group (table 6:3) have been obtained in the present studies, and using these in collaboration with Elliot (1964) and Fraser (1965) data, it is clear these rocks form part of a normal calc-alkaline trend (Fig. 6:2B). A plot of quartz-feldspar-mafics (Fig. 6:2A) shows the increasing proportion of quartz and decreasing proportion of mafics as differentiation progresses.

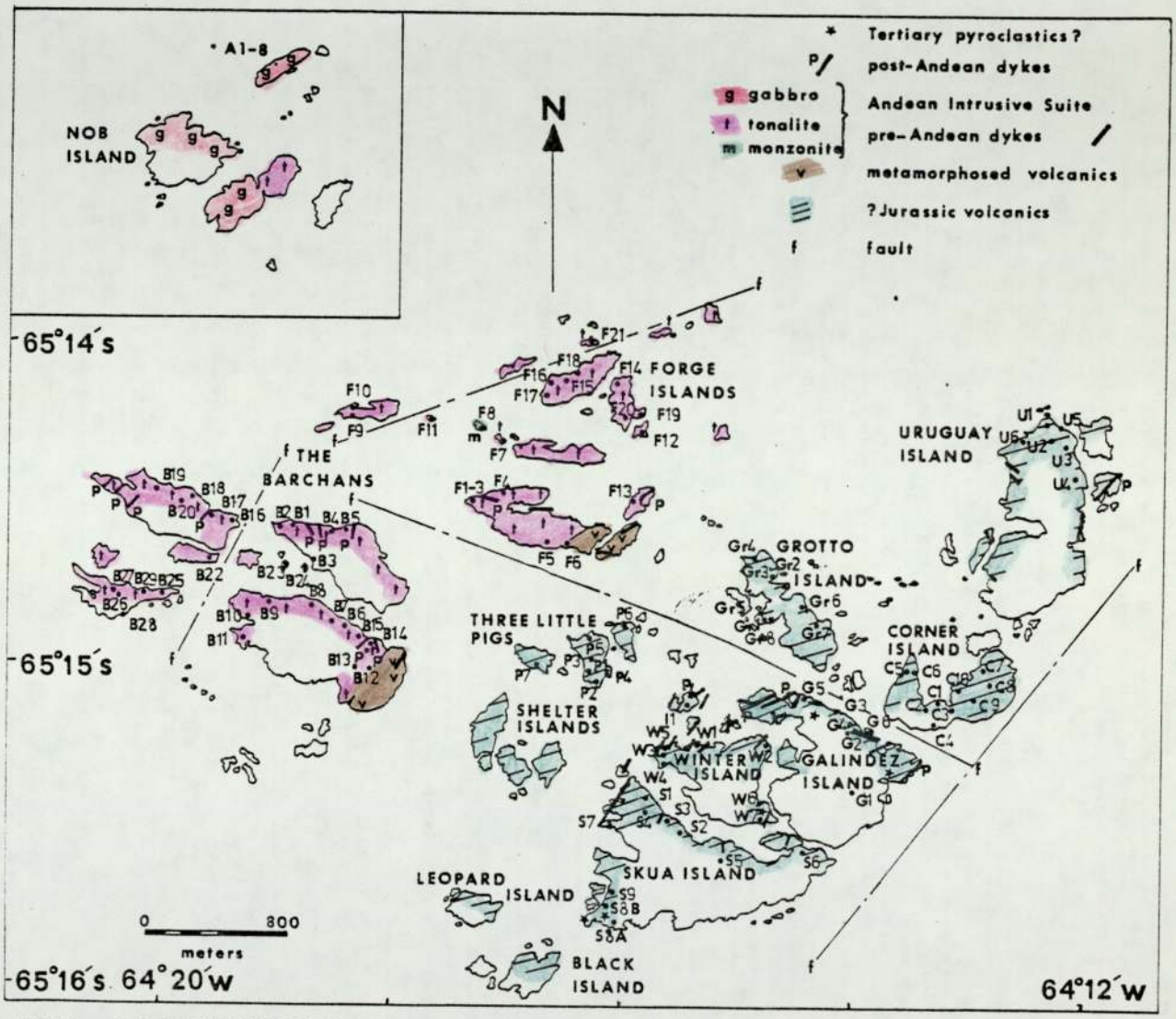

FIG.6:1 SPECIMEN LOCATIONS AND GENERAL GEOLOGY, ARGENTINE ISLANDS, GRAHAM LAND. (based on field work and data of Elliot(1964) and Fraser(1965)). INSERT SHOWS ANAGRAM ISLANDS.

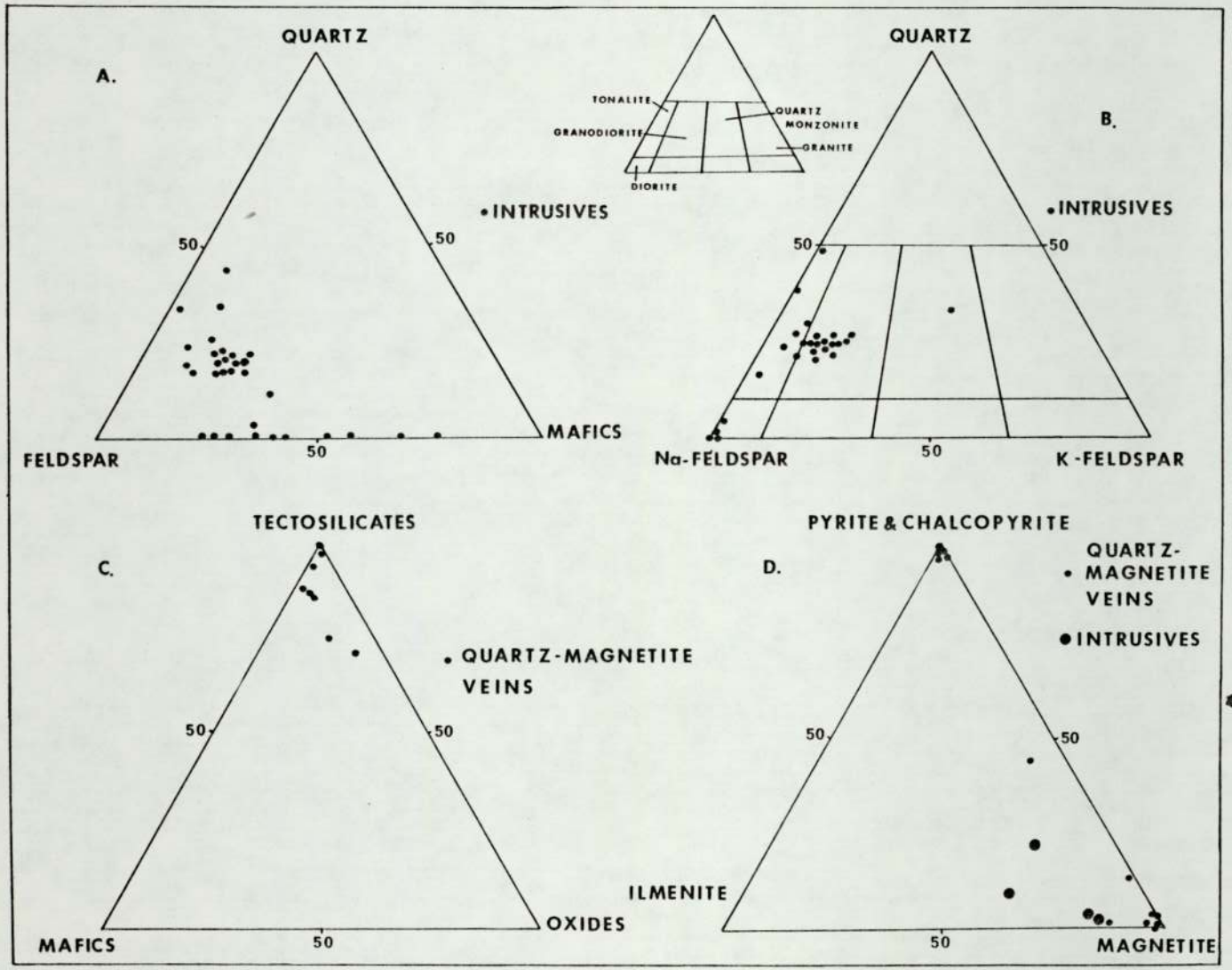

Fig.6:2 TERNARY DIAGRAMS OF MODAL DATA, ARGENTINE & ANAGRAM ISLANDS, GRAHAM LAND. A, quartz-feldspar-mafics; B, quartz-sodium feldspar-potassium feldspar (FOR PLUTONIC ROCKS); C, PLOT OF tectosilicates (quartz and feldspar)-mafics (hornblende, chlorite and epidote)-oxides (magnetite and hematite) IN QUARTZ-MAGNETITE VEINS; D, RATIO OF ilmenite-magnetite-pyrite and chalcopyrite IN QUARTZ-MAGNETITE VEINS AND PLUTONIC ROCKS.

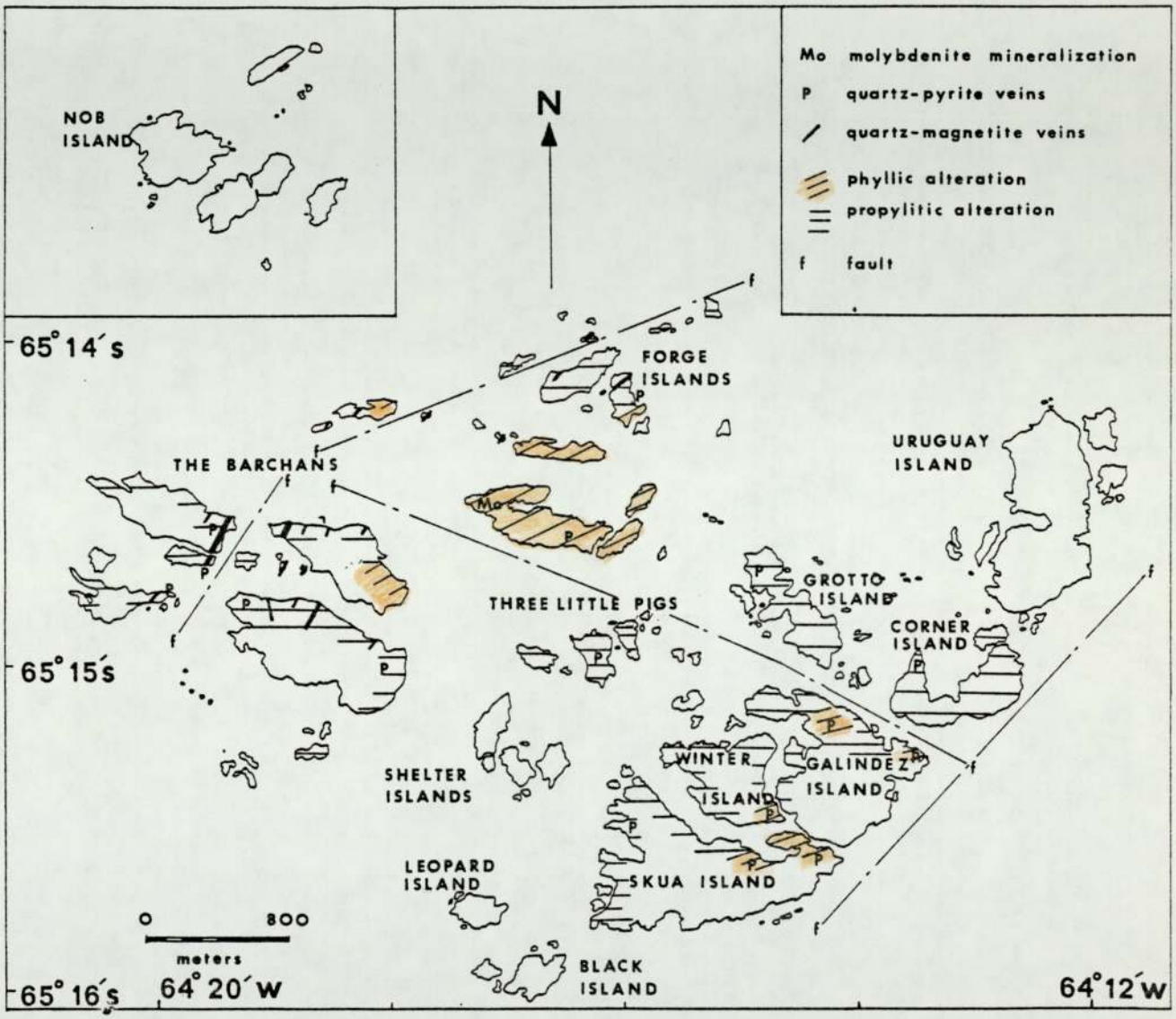

FIG 6:3 DIAGRAM OF MINERALIZATION AND ALTERATION IN THE ARGENTINE AND ANAGRAM ISLANDS.(INSERT SHOWS ANAGRAM ISLANDS).

ALTERATION: PROPYLITIC, Pr; PHYLLIC, \\; POTASSIC, =; t, TONALITE.

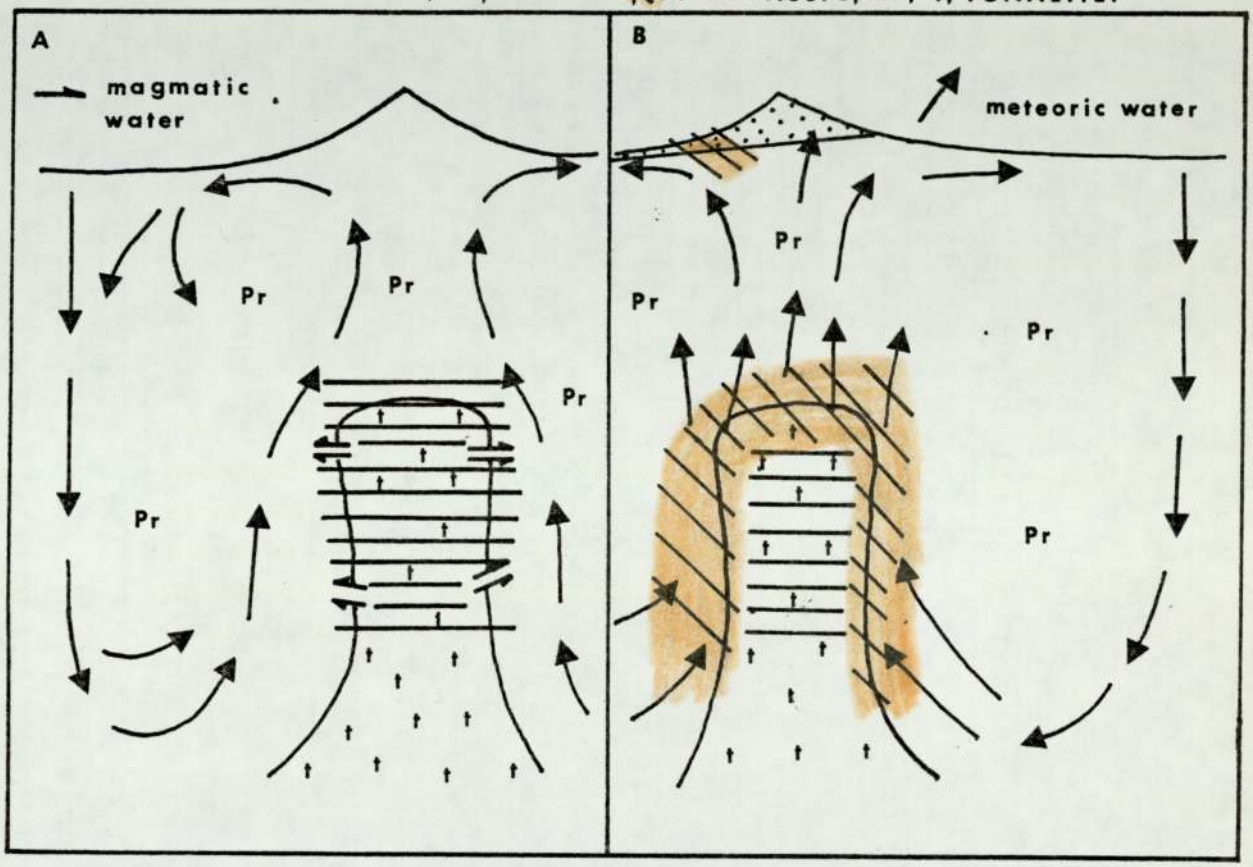

FIG.6:4 HYPOTHETICAL MODEL OF PORPHYRY SYSTEM, ARGENTINE ISLANDS.

A; EARLY STAGE
Intrusion of molten magma. Crystallization produced magmatic -hydrothermal fluids that caused potassic alteration. Circulating groundwater system established causing propylitic alteration of ?Jurassic lavas.

(after Sheppard, 1977)

B; LATE STAGE
Extrusion of tuffs occurs (dotted). As magma cools the meteoric-hydrothermal system encroaches upon the waning magmatic-hydrothermal part of the system, and phyllic alteration is produced at the interface of the two. Low temperature phyllic alteration affects tuffs. Metals introduced at this stage.

6.3.4 Post-Andean Dykes

Elliot (1964) subdivided these dykes into microgabbroic and microdioritic.

The microgabbroic group tend to be porphyritic with phenocrysts of plagioclase and pyroxene in a groundmass of plagioclase, pyroxene and magnetite with rare amphibole. Some xenocrysts of plagioclase and quartz are present derived from the granodiorites. Plagioclase shows alteration to chlorite, sericite, epidote and carbonate, with pyroxene replaced by chlorite, calcite and epidote. Mineral aggregates occur in these dykes composed of plagioclase, amphibole, augite and chlorite, which represent water rich pockets that crystallized after the dykes.

The microdiorites tend to be aphanitic with an intergranular to trachytic groundmass. Plagioclase (An $_{44-30}$) and augite are present with some amphibole and minor interstitial quartz. Plagioclase and pyroxene show alteration to epidote, sericite, carbonate and chlorite, with vesicules in some rocks infilled with epidote, chlorite, quartz, carbonate and pyrite, and occasionally actinolite.

6.4 Mineralisation and Alteration

6.4.1 Quartz-Magnetite Veins

1. Field Relationships of Quartz-Magnetite Veins

Quartz-Magnetite veins varying in width from ten meters to ten millimeters are present on the Barchan and Forge Islands, in the Argentine Island Group (Fig. 6:3 , plate 6:2).

They seem to represent fault zones that have been filled with brecciated wall rock, the quartz and magnetite being deposited in the interstices between the fragments. The fragments of granodiorite are generally angular, but never less than three centimeters in size.

Most have a bleached margin around them. Smaller veinlets of quartz and magnetite invade the granodiorite around these larger veins, occurring mainly along sheet joints (B2).

Magnetite is often concentrated near the margins of the veins, frequently in a symmetrical manner (plate 6:3), and often shows a multicoloured lustre (plate 6:4). The veins trend in a direction parallel to, and either side of a major fault zone that crosses the central part of the Argentine Island Group. In places late stage post-Andean dykes cut the quartz-magnetite veins (plate 6:1).

2. Petrography of the Quartz- Magnetite Veins

The quartz-magnetite veins consist of an inequigranular mass of anhedral to subhedral quartz showing undulose extinction (less than 10 cm, B16D), often with a zone of fine-grained quartz at the edges of the vein adjacent to the wall-rock. Some early quartz-crystals show overgrowths of a later phase of quartz deposition (F15), although some could be a replacement after feldspar. Some microveinlets of quartz cut the earlier quartz crystals (F9). At the edges of some veins (B17) orthoclase perthite, albite and quartz occur in myrmekitic intergrowths (plate 6:5) some of which contain acicular rutile. Minor chlorite (1a) and epidote are present in small veinlets (less than 0.1 mm), with some chlorite having bent lamelli (B23). Euhedral epidote and quartz occur in vugs (plate 6:6). Both green and brown amphibole occur in these veins, where abundant it is green, and where sparse generally brown. Frequently the amphibole has siderite and chlorite along the cleavages (B14), with siderite also present in cleavages in the chlorite. Biotite crystals occur in the granodiorite perpendicular to the contact of the quartz-magnetite veins, with partially resorbed relicts of the same crystal present in the veins themselves (B23), indicating some replacement

of the granodiorite by the hydrothermal solutions has occurred. 1M muscovite and zircon are also present.

Magnetite is the major opaque mineral in these veins and is often surrounded by subhedral epidote (F9, plate 6:7A and 6:7B), with chlorite laths, siderite and epidote occurring in cavities in the magnetite (F15). Magnetite is interstitial between quartz crystals (B20), and shows slight replacement of quartz. In rare instances the subhedral magnetite shows fine exsolution lamelli of {0001} plates of ilmenite parallel to {111} (F14). "Emulsion droplets" of pyrite (B16) and more rarely chalcopyrite, bornite and pyrrhotite (B2) are present in the magnetite. The slightly anisotropic magnetite (B2 and B16) often shows alteration along {111} to hematite (plate 6:8), especially around fractures, although in places it is almost completely altered to hematite with small islands of magnetite surrounded by hematite (B2). Subhedral chalcopyrite relicts occur in the hematite from the original magnetite.

3. Alteration of Granodiorites around the Quartz-Magnetite Veins

The plutonic rocks which have been intruded by these quartz-magnetite veins show alteration of plagioclase feldspar to 1M muscovite, quartz (F9) and epidote (some being clinozoizite). Anhedral quartz has been introduced interstitially to the feldspars. Biotite laths occur showing alteration to chlorite (1a), quartz and siderite (B23), initially along cleavage planes, but directly adjacent to the veins complete replacement has taken place. Hornblende shows alteration to chlorite, epidote and siderite, with orthoclase showing alteration to chlorite, epidote and siderite also. Some hornblende shows alteration to biotite. Epidote usually occurs in association with chlorite, and in small microveinlets with quartz and chlorite traversing the rock (F15, B20), with minor rutile also present (F9).

Anhedral chalcopyrite has been introduced into the alteration zone in simple intergrowths with bornite (which show alteration to covellite, F17), although some idaite showing exsolution spindles and lamelli of chalcopyrite parallel to {100} (less than 0.2 mm) is also present. Chalcopyrite shows alteration to covellite and chalcocite (F9). Magnetite is present in these alteration zones (less than 2.4 mm) containing inclusions of idaite, chalcopyrite and pyrite (less than 0.6 mm). Subhedral pyrite also occurs (less than 0.05 mm) (B2D) and often contains "emulsion droplets" of chalcopyrite and pyrrhotite in simple intergrowths (B8, B22), which were probably originally chalcopyrrhotite, and inclusions of magnetite and covellite (after chalcopyrite). The pyrites frequently have an inclusion rich rim and an inclusion free centre, and show slight alteration to geothite. The subhedral magnetites and ilmenites from the granodiorites show partial alteration to hematite and rutile.

4. Chemical and Modal Analyses of magnetites from the Plutonic Rocks and Quartz-Magnetite Veins

Chemical analysis of magnetites from the plutonic rocks and quartz-magnetite veins from the Argentine and Anagram Islands has been achieved by Atomic Absorption Spectrometry using the method of Zussman (1967) and electron microprobe analysis by the method of Carmichael, (1967).

(a) Plutonic Rocks

The chemical analyses indicate the magnetites in the banded gabbro on the Anagram Islands contains approximately 0.2% TiO_2, 0.15% Cr_2O_3, 0.10% MnO, 1.0% V_2O_5 with the iron calculated as Fe_3O_4. (table 6:1). As the rocks become more acidic (gabbro to granodiorite to quartz-monzonite) the overall content of trace elements decreases, although the relative importance of MnO to other trace elements increases (table 6:2).

The temperatures of formation of magnetite in these rocks were calculated using the method of Buddington and Lindsley (1964). The results suggest the magnetites in the gabbro from the Anagram Islands formed at less than 600°C, clearly indicative of their secondary origin, although co-existing magnetite and ilmenite formed during magma crystallization indicate a temperature of formation of 900 - 1000°C. Manganese distribution may also be plotted as a function of equilibrium temperature (Buddington and Lindsley, 1964). Plotted on a graph of % MnO in ilmenite against % MnO in magnetite, the data places the magnetite in the gabbro in the field of acid plutonics. This is presumably due to the fact that the temperature of the late stage magmatic fluids that deposited the magnetite were near to the liquidus temperature for water saturated granites. The data also suggests the granodiorites crystallised about 700 - 800°C and the quartz-monzonite crystallised at less than 700°C.

(b) Quartz-Magnetite Veins

The magnetites in the quartz-magnetite veins contain less than 0.1% TiO_2, Cr_2O_3 and V_2O_5 and about 0.2% MnO and Al_2O_3. Pb is undetectable by electron microprobe methods (table 8:4). The data of Buddington and Lindsley (1964) suggests the magnetite formed at less than 500°C. Cell dimensions (ao = 8.385), reflectivity values (R_{589nm} = 19%) and Vickers Numbers at 100g load (578 - 1202) are well within the range for pure magnetite (Burke, et al, 1971).

Trace elements in the magnetites (table 6:4) are; Ni (100 ppm), Cr (10 ppm) and V (320 ppm) which are substituting for iron, and 180 ppm Mo, 15 ppm Cu, 80 ppm Zn and 8 ppm Pb present as inclusions of sulphides in the magnetite (probably submicroscopic). Se (360 ppm) and 30 ppm Te are substituting for sulphur in the sulphide inclusions. Sr (4 ppm) is probably associated with small inclusions of feldspar in the magnetite.

Modal analyses (table 6:7, Fig. 6:2C) of the quartz-magnetite veins shows quartz to be the major constituent (30.1 - 99.5%) with orthoclase perthite (0 - 42.5%) and plagioclase (0 - 28%) present. Magnetite varies from (0.3 - 22.0%) with chlorite (0 - 6.5%), epidote (0 - 6.7%) and muscovite (0 - 5.2%). Amphibole, siderite, zircon, rutile and biotite are all present in quantities less than 0.4%.

Modal ratios of the opaque phases (table 6:8, Fig. 6:2D) in the quartz-magnetite veins suggests magnetite (48.3 - 99.1%) is the main phase with hematite (0 - 80.3%) and pyrite (0.2 - 6.1%) also present. Chalcopyrite, bornite and pyrrhotite varies from 0 - 5% and goethite 0 - 5.6%. A comparison with the intrusive rocks show magnetite (59.6 - 84%) and ilmenite (0 - 30.8%) are the main phases.

Chemical analyses of the quartz-magnetite veins (table 6:9) indicate silica at 97% is predominant (as quartz) with magnesia, lime, potassium oxide, alumina, manganese oxide and titania all less than 0.1%. Sodium oxide at 2% and magnetite at 0.6% are the main metallic oxides. Sodium oxide, lime, alumina and potassium oxide are present in feldspar, magnesia in chlorite and epidote, and titania in rutile. Manganese oxide is present in magnetite. Trace element studies (table 6:9) indicate that virtually all those studied are less than 10 ppm, with Cr, Ni and V substituting for iron in magnetite, and Cu, Pb and Zn present as sulphide inclusions, particularly chalcopyrite, galena and sphalerite. Mo at 100 ppm is present as molybdenite. Se and Te are substituting for sulphur in the sulphides, with Sr substituting for Ca in feldspar.

6.4.2 Field Relationships of Molybdenite and Related Mineralisation

Molybdenite mineralisation occurs on the largest of the Forge Islands, specifically in the north western corner (Fig. 6:3). The molybdenite mineralisation cuts the quartz monzonite veins, but not the post-Andean dykes. The molybdenite occurs mainly on sheet joints in the granodiorite

Figure 6:5 Paragenesis of ore and gangue minerals, Argentine Islands.

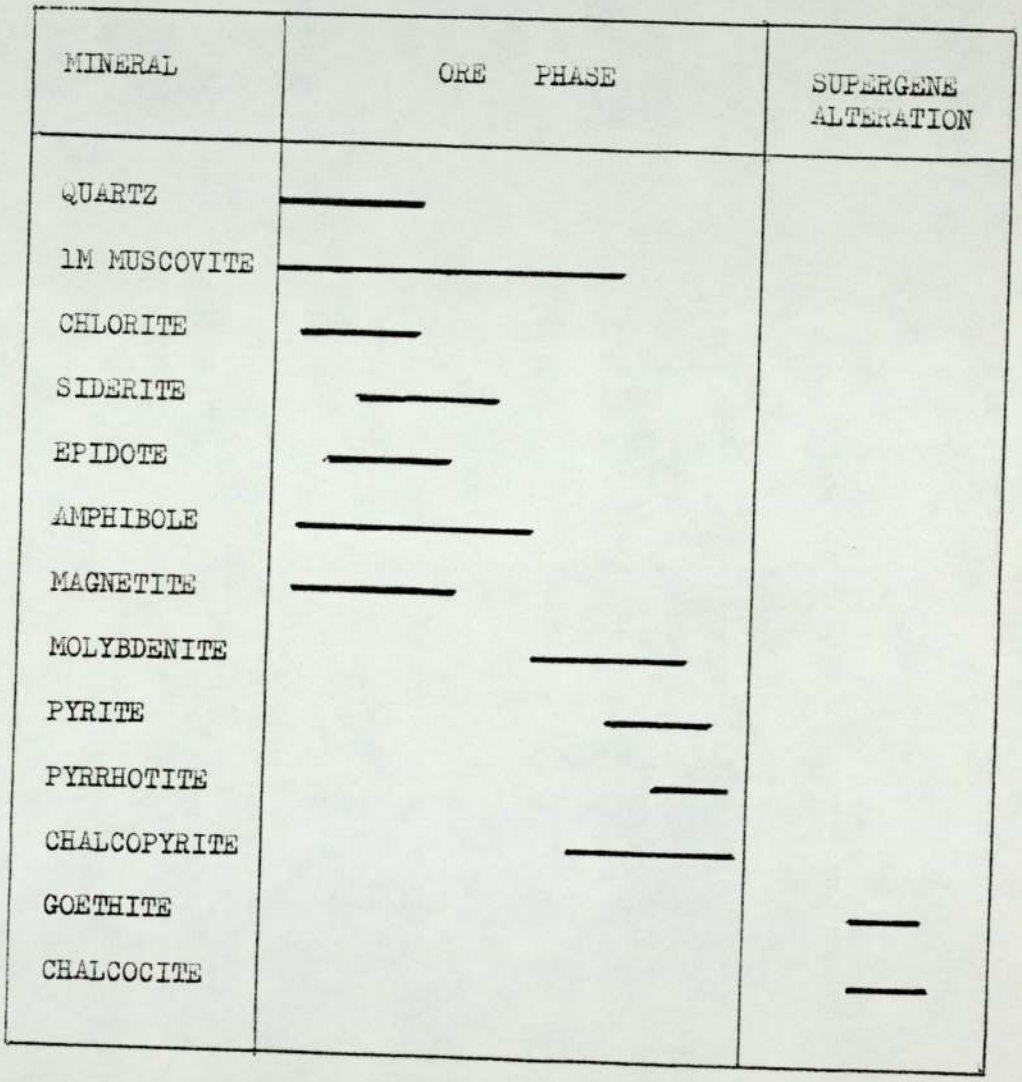

(plate 6:9) (in assocation with quartz and chalcopyrite), which are about four millimeters wide and dip 20°N and trend ENE-WSW. This mineralisation only outcrops over an area of about two hundred square meters, with the veins an average of several meters apart.

Surrounding the molybdenite mineralisation are veinlets of quartz and pyrite which cut the granodiorite (plate 6:10) and quartz-magnetite veins, and seem to be genetically the same age as the molybdenite. Where the veins are present in the Jurassic lavas, for example the three Little Pigs, epidote also occurs in assocation with the quartz and pyrite.

6.4.3 Paragenesis

The minerals are discussed in their assumed paragenetic sequence, this being deduced by the study of approximately twenty thin and polished sections.

Quartz

This is the earliest mineral in the veinlets, and tends to be anhedral to subhedral. It also occurs as inclusions in molybdenite and pyrite.

Muscovite

Subhedral 1M muscovite occurs at the edges of the molybdenite veins (F2G) and as inclusions in the molybdenite and pyrite.

Molybdenite

Molybdenite is normally subhedral (less than 2mm), although many of the laths are bent and show pressure twinning (F2A). X-ray diffraction indicates it is the 2H polymorph. The mineral shows distinct reflection pleochroism and strong anisotropy. It is grey to silvery grey in colour, with undulatory extinction in crossed polars. The reflection pleochroism is more distinct in oil.

Pyrite

Euhedral pyrite (less than 5mm) which is pale yellow and isotropic contains inclusions of quartz, pyrrhotite, chalcopyrite, rutile, epidote, chlorite and euhedral magnetite, which it is replacing (B22, P1). Around fractures the pyrite shows alteration to goethite and lepidochrocite. Reflectivity values at 589nm range from 50.9 to 52.9% and Vickers Hardness Numbers at 100g load are 1629-2205 and are within the range for pure pyrite (Burke, et al, 1971) (table 6:6).

Chemical analyses of the pyrite has been achieved using Atomic Absorption Spectroscopy, which shows the pyrite contains 40 ppm Co, <1ppm Ni, (substituting for iron), 140 ppm Cu, 50 ppm Zn and <1ppm Pb (present as sulphide inclusions) and 200 ppm Se which is substituting for sulphur (table 6:10, F9, F20). The pyrite also contains about 1000ppm Mn (pyrolusite?). These values are within the range of normal pyrites (Fleischer, 1955). The Co/Ni ratio which is greater than one (1) indicates the pyrite had a volcanogenic origin (Loftus-Hills and Solomon, 1969).

Chalcopyrite

Subhedral chalcopyrite is present in association with molybdenite and seems paragenetically later. Reflectivity values at 589 nm are 39.8 to 41.5 and Vickers Hardness Numbers at 100g load are 218 to 225 are well within the range for chalcopyrite (Burke, et al, 1971).

6.5 Alteration Effects of the Mineralising Solutions

6.5.1 Alteration of Jurassic lavas and Pyroclastics

Irregular shaped areas of hydrothermally altered pyroclastics occur on Galindez, Winter and Skua Islands some of which may be old volcanic vents filled with pyroclastic debris.

Plate 6:1 Post-Andean dyke cutting quartz-magnetite vein and granodiorite, Barchan Islands, Argentine Islands. (B17).

Plate 6:2 Quartz-magnetite veins cutting granodiorite, north east Barchan Island. Note the brecciated fragments of granodiorite in the quartz veins, which appear to have originated by faulting. B2. Argentine Islands.

Plate 6:3 Quartz-magnetite vein cutting granodiorite, Barchan Islands. Note that the magnetite (black) is concentrated symmetrically in a zone close to the margins of the vein (B2), Barchan Island, Argentine Islands.

Plate 6:4 Edge of quartz-magnetite vein, Barchan Islands. Note the magnetite (black) has an irridescent, multicoloured lustre. B2. Argentine Islands.

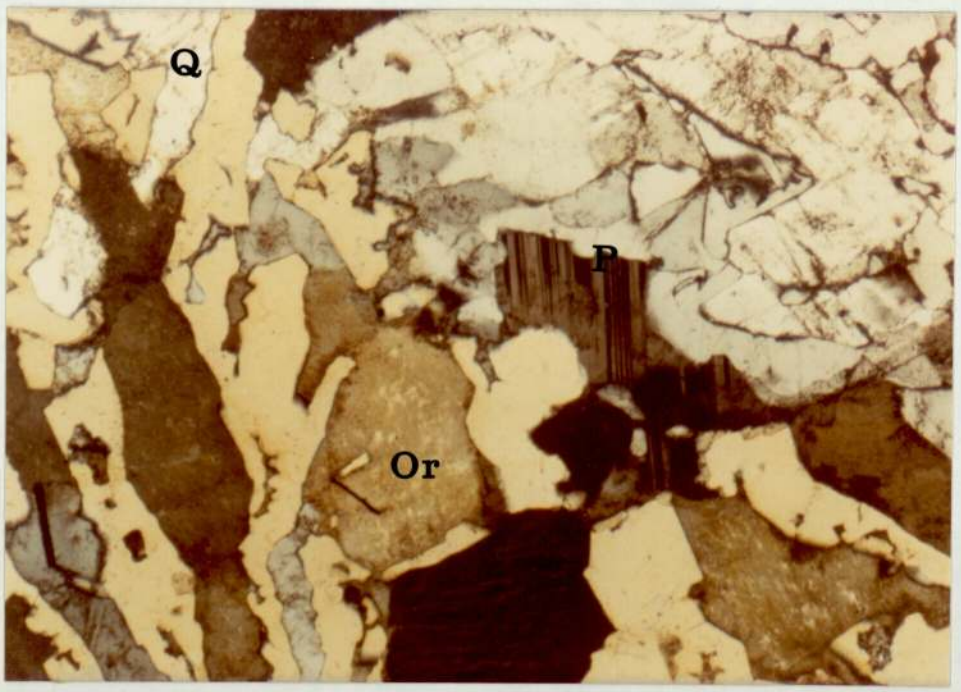

Plate 6:5 Quartz (greyish white and yellowish), plagioclase feldspar (white-grey, showing albite twinning) and orthoclase perthite (dark yellow) in myrmekitic intergrowths. At edge of quartz-magnetite vein, Barchan Islands, Argentine Islands (B17). Transmitted light, crossed polars, X60. Quartz (Q), Plagioclase (P), Orthoclase (Or). (Slide has been stained with cobaltinitrite).

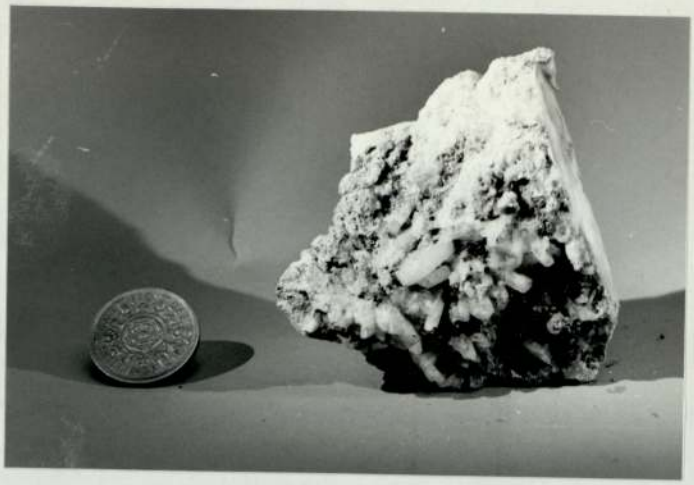

Plate 6:6 Quartz (white) and epidote (grey, granular) in vug-like cavities in quartz-magnetite veins, Barchan Islands, Argentine Islands.

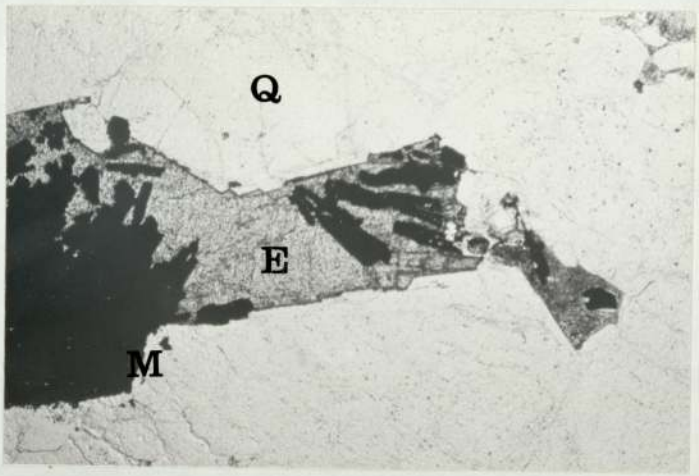

Plate 6:7A Magnetite (black) surrounded by epidote (dark grey, high relief) and quartz (light grey, low relief). Transmitted light, plane polarised light, X60. F9. Forge Islands, Argentine Islands. Quartz (Q), Epidote (E), and Magnetite (M).

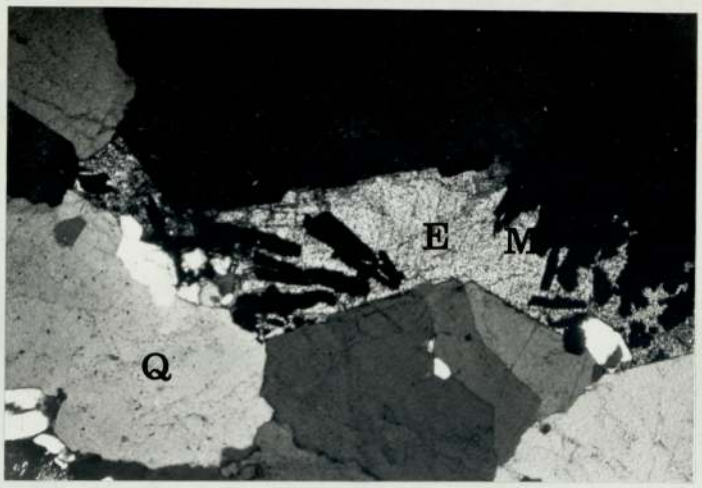

Plate 6:7B Magnetite (black), surrounded by epidote (whiteish grey, high relief) and quartz (shades of grey). Note the anhedral to subhedral nature of the quartz.

Transmitted light, crossed polars, X60. F9.

Forge Islands, Argentine Islands. Quartz (Q), Epidote (E), and Magnetite (M).

Plate 6:8 Magnetite (grey) showing alteration along fractures to hematite (light grey). B2.

Reflected light X 100. Barchan Islands, Argentine Islands.

Plate 6:9 Molybdenite (Mo) (silvery grey) occurring on sheet joints in granodiorite on the north western corner of the largest Forge Island. Also occurring in association with the molybdenite is quartz (white) and chalcopyrite (not visible in plate). F1. Argentine Islands.

Plate 6:10 Pyrite (Py) (yellow) showing oxidation to goethite, in veinlet of quartz, cutting granodiorite on the Barchan Islands. B22. Argentine Islands. These veins are peripheral to the molybdenite mineralisation.

Petrographically, the rocks consist of microcrystalline quartz, frequently containing acicular rutile and interstitial 1M muscovite (G6). Some quartz phenocrysts occur showing radial extinction, with partially resorbed subhedral plagioclase feldspar replaced by 1M muscovite along fractures and in the calcic cores of zoned crystals (W2). Minor amounts of kaolinite and chlorite are present, probably replacing former ferromagnesian minerals, with some zircon granules (less than 0.1 mm). Former amygdales are infilled by quartz and epidote.

Euhedral pyrite occurs disseminated through the groundmass of the altered rocks and contains inclusions of epidote (Gr 3), 1M muscovite, rutile and pyrrhotite (G6), although subhedral pyrrhotite occurs showing alteration to a marcasite-pyrite like substance often in simple intergrowths with pyrite (Gr 3).

Modal analyses (table 6:11) indicate the rocks consist predominantly of quartz (38 - 58%) and 1M muscovite (30 - 51%), with pyrite (2.5 - 8.3%), and plagioclase (0.7 - 5.6%). Chlorite and epidote are present, normally less than 4%.

Chemical analyses (table 6:12) indicates the rocks consist of 64% SiO_2 (present mainly as quartz), 17% Al_2O_3, 1.12% Na_2O and 8.5% K_2O (present as muscovite). CaO (0.07%) and MgO (0.35%) are probably associated with plagioclase and epidote, with the TiO_2 (0.57%) mainly rutile. The rocks also contain 4% FeO and 3.60% S present as pyrite with MnO (0.03%) represented as pyrolusite. Analysis of trace elements indicates that, Cr, Ni and V are less than 30 ppm and probably substituting for iron in pyrite. Cu, Mo, Pb and Zn are also less than 30 ppm, and present as small amounts of sulphide (mainly chalcopyrite, molybdenite, galena and sphalerite). Se (440 ppm) and Te (less than 30 ppm) are substituting for sulphur in pyrite. Cd and Sr (less than 30 ppm) are

substituting for Ca in plagioclase.

Using the models of Meyer and Hemley (1967) and Lowell and Guilbert (1970) this appears to represent phyllic alteration.

Around quartz-pyrite veinlets, the Jurassic lavas show propylitic alteration, with the matrix being replaced by quartz (less than 0.3 mm) and euhedral epidote, with coarse-grained quartz replacing former feldspar phenocrysts. The quartz often contains acicular rutile, with inclusions of quartz occurring in some epidotes. Chlorite replacing biotite is common.

6.5.2 Alteration of Tertiary Plutons

The granodiorite plutons of the Argentine Islands show evidence of potassium silicate alteration. Plagioclase feldspar shows replacement by orthoclase, quartz, sericite, epidote and biotite, with late stage clusters of biotite and quartz interstitial to the feldspars. Amphibole shows alteration to biotite and chlorite, with the chlorite itself being replaced by siderite and epidote. Small veinlets of siderite traverse the rock (H96.1).

Low grade phyllic alteration has been superimposed on the potassic alteration in the Forge Islands (Fig. 6:4, 6:3), where the fluids that produced the molybdenum mineralisation have permeated the granodiorite. Plagioclase, orthoclase, biotite and amphibole show alteration to muscovite directly adjacent to these veins, although biotite also shows alteration to chlorite.

6.6 Discussion of the Igneous Textures in the Plutonic Rocks of The Argentine and Anagram Islands

The sequence of intrusion of plutonic rocks in the Argentine and Anagram Islands appears to be gabbro, tonalite, granodiorite and quartz-monzonite, in common with most intrusive complexes in an Andean type

plate margin (Pitcher, 1978).

Hornblende, which appears as a secondary mineral in the banded gabbros, can appear in all stages of the evolution of gabbros (Mullan and Bussell, 1977), as a cumulus or intercumulus phase, or more commonly as a product of late stage metasomatism resulting from a build up of water during crystallisation of a magma. The introduction of magnetite, pyrite, chalcopyrite and brown hornblende associated with the alteration of plagioclase to epidote, clinozoisite and hornblende, and alteration of olivine to talc and pyroxene to hornblende is a characteristic of appanitic rocks the world over (Bowes and Wright, 1960; Joplin, 1959). This type of amphibolitization is due to penetration of water rich volatiles frequently associated with late stage brecciation, formed during the crystallization of water rich gabbroic magmas (Elsdon, 1972). Some of the water associated with these fluids has come from external sources (as in the Andes, Regan, 1976). One possible source of the volatiles is the tonalites which followed the intrusion of the gabbro, although these were probably undersaturated with water, and there is no simple spatial or temporal relationship of amphibolization to the tonalite-gabbro contact as first noticed by Fraser(1965). The gabbro may, therefore, have absorbed water from the country rocks during its final emplacement into the volcanic cover, and expelled this fluid during the final stages of crystallization. Thus the alteration of the banded gabbro is associated with late stage magmatic aqueous fluids expelled from the crystallizing gabbro, rather than injected residual fluids as suggested by Fraser (1965). Chemical data from the magnetites in this rock suggests the fluids had a temperature of less than 600°C.

The banded gabbro seems to have been preceded by the intrusion of hypersthene and olivine gabbros since inclusions of these occur in the banded rock (Fraser, 1965). The banded gabbro was followed by the intrusion of tonalitic to granodioritic bodies, and sill like masses of aplite cut the banded gabbro on the Island to the north east of Nob Island.

The majority of the plutonic bodies in the Argentine Islands are biotite-hornblende granodiorites and tonalites, and the lack of clear contact zones between the phases of plutons in these rocks suggest they were intruded by internal surges of magma within a single congealing pluton as in the coastal batholiths of Peru (Cobbing and Pitcher, 1972). The simplicity of textures and uniformity of grain size in these rocks clearly indicates they crystallized from magmas, although basic cores of plagioclase (An_{50}) overgrown by rims of An_{23} suggest rapid changes in physical conditions due probably to the magma containing suspended crystals at the time of its emplacement. The presence of inclusions of pyroxene in hornblende in these rocks may be due to the fact that pyroxene, which appears early in the sequence of crystallization, is generally converted to amphibole. This normally occurs in parallel with independent growth of hornblende and biotite due to increasing water content as a result of advancing fractionation (Pitcher, 1978).

The pink quartz-monzonite dykes occuring on the Forge Islands containing spherical myrmekitic intergrowths, characteristic of eutectic crystallization, probably represent the end result of the differentiation process in the Argentine Islands.

6.7 Discussion of the Mineralisation in the Argentine Islands

The molybdenite mineralisation in the Argentine Islands bears many similarities to that found in porphyry copper-molybdenum deposits elsewhere in the Circum-Pacific belt (Lowell and Guilbert, 1970; Hollister, 1975). Molybdenite occurs as vein fillings in sheet joints associated with chalcopyrite and quartz in an hypidiomorphic, granodiorite pluton. Although minor amounts of disseminated sulphides occur in the granodiorite, the majority are probably of magmatic affiliation, for example "emulsion droplets" of sulphides in magnetite. Comparison with other porphyry copper-molybdenum systems suggests this represents the central part of the deposit (Lowell and Guilbert, 1970).

Surrounding the molybdenite core are veinlets of quartz containing pyrite and minor pyrrhotite and chalcopyrite, indicative of a sulphide zonation. Indeed the alteration zones also suggest that the central molybdenite mineralisation has associated halos of phyllic alteration, where the feldspars in the host intrusive have been sericitised and veinlets of quartz and 1M muscovite traverse the host intrusive.

Associated with the quartz-pyrite veinlets, however, are halos of propylitic alteration, with the feldspars and ferromagnesian minerals showing alteration to siderite, chlorite and epidote. Both these alteration types seem to be superimposed on an early, magmatic potassium silicate alteration, where they affect the granodiorites (Fig. 6:4). Typically, the potassium feldspar in the rock is a cloudy pink colour in hand specimen.

Although the granodiorite is the host intrusive rock for the molybdenite, the spatial distribution of the mineralisation itself, seems more closely related to the quartz-monzonite dykes. These bodies appear slightly earlier than the mineralisation, and are more numerous

in the area where the molybdenite occurs, than elsewhere in the island group. Many seem to show weak propylitic alteration, typical of porphyry copper deposits elsewhere (Lowell and Guilbert, 1970).

The presence of two phases of epidotization in the pyroclastic rocks of Galindez and Skua Islands with the clasts more heavily epidotized than the porous matrix, suggests they must have been deposited in the terminal phases of the process which produced the epidotization of the calc-alkaline lavas. This view is only consistent if the tuffs were erupted co-magmatically with the intrusion of the granodiorite to quartz-monzonite bodies (Fig. 6:4). Indeed extrusion of large amounts of pyroclastic material from volcanic vents is favourable to porphyry mineralisation, since pyroclastic eruptions derived from a crystallising intrusive, generally cause partial destruction of the intrusive structure and increase the potential for disseminated mineralisation (Whitney, 1977).

The heated, aqueous fluids which caused the epidotization were probably derived by interaction of meteoric groundwater with saline fluids evolved from the crystallising magma, using comparisons with other deposits (Hemley and McNabb, 1978).

The areas of phyllic alteration in the lavas of Galindez, Winter and Skua Islands, seem to be concentrated in what appear to be igneous breccias or old volcanic vents. In other Circum-Pacific areas these zones act as guides to concealed porphyry copper systems (Gilmour, 1977). The phyllic alteration seems to be typical low temperature, hydrothermal alteration, probably associated with the residual fluids derived from the molybdenum mineralisation. A further indication that the phyllic alteration amd molybdenum mineralisation are related is the similarity in mineralogy, in that 1M muscovite and pyrite containing emulsion droplets of pyrrhotite and chalcopyrite occur in both areas.

The quartz-magnetite veins seem to occur around major fault zones running NE-SW and NW-SE across the Argentine Islands, and indeed appear thickest where the faults intersect near the Barchan Islands (Fig. 6:3). This suggests the faults acted as channelways for the passage of the hydrothermal fluids, although petrographic data indicates some replacement of the surrounding granodiorite has occurred as well as simple fracture infilling. Quartz-magnetite-amphibole veins are commonly associated with the outer, basal zones of porphyry copper-molybdenum deposits (Lowell and Guilbert, 1970), commonly forming at a temperature of less than 600°C (Cox et al, 1975).

The lack of significant sulphides in this deposit suggests the fluids responsible for the mineralisation were either sulphur deficient, or the sulphur was in a highly oxidised state. In such cases in other porphyry deposits the iron is then usually deposited as magnetite rather than pyrite (Hollister, 1975), which may account for the abundance of quartz-magnetite veins in the Argentine Islands. A supergene sulphide blanket is clearly absent in the Argentine Islands, but may have been present in Tertiary times, and has since been removed by Pleistocene glacial erosion. In conclusion, therefore, it seems that the Argentine Islands represent a faulted, porphyry molybdenum deposit.

The intrusive activity began in the early Tertiary (57-54 my)with the emplacement of a calc-alkaline plutonic complex ranging from gabbro to granodiorite into Jurassic lavas. A phase of quartz-monzonite dykes and small irregular shaped bodies were then intruded into the plutonic complex in the vicinity of the Forge Islands. The fluids derived from the crystallisation of these bodies produced a central molybdenite mineralisation, and surrounding quartz-pyrite mineralisation, with veins of quartz and magnetite at depth, along with characteristic

phyllic and propylitic alteration. Following the mineralisation was a period of injection of microgabbroic and microdioritic post-Andean dykes. (Fig. 6:4).

TABLE 6 : 1 ELECTRON MICROPROBE ANALYSIS OF MAGNETITES FROM BANDED GABBRO, ANAGRAM ISLANDS.

SPECIMEN NO.	LOCATION	Fe_3O_4	FeO	TiO_2	MnO	Cr_2O_3	V_2O_5	Total
A8	Island to the north east of Nob Island							
magnetite		98.48	-	.167	.107	.167	.588	99.51
magnetite	"	97.93	-	.649	.140	.143	1.377	100.2
magnetite	"	97.28	-	.177	2.275	.171	1.236	101.14
magnetite	"	78.00	-	15.692	1.173	.102	2.961	97.93
ilmenite	"	-	43.26	50.614	2.275	.162	6.542	102.85

TABLE 6 : 2 ELECTRON MICROPROBE ANALYSIS OF MAGNETITES FROM GRANODIORITE AND QUARTZ -MONZONITE, ARGENTINE ISLANDS

SPECIMEN NO.	LOCATION	Fe_3O_4	TiO_2	MnO	Cr_2O_3	V_2O_5	Total
F2F	FORGE ISLANDS						
Granodio-rite		93.20	6.110	.169	.038	.255	99.77
F8A	FORGE ISLANDS	97.89	.503	.253	.063	.567	99.28
Quartz-Monzonite	"	97.93	.405	.211	.055	.550	99.15

TABLE 6:3 MODAL ANALYSES OF PLUTONIC ROCKS, ARGENTINE AND ANAGRAM ISLANDS.

Specimen Number	Location	Rock Type	Quartz	Plagioclase	Orthoclase	Chlorite	Epidote	Green Hornblende	Brown Hornblende	Biotite	Pyroxene	Olivine	Carbonate	Opaques	Total
A1	Anagram Islands	Banded Gabbro	-	75.6	-	-	-	7.6	0.2	0.2	11.2	0.8	-	4.4	100.0
A8	Anagram Islands	Banded Gabbro	-	58.0	-	-	-	28.4	2.0	-	6.1	-	-	5.5	100.0
A3	Anagram Islands	Aplite Vein	43.4	44.8	1.4	5.3	3.4	-	-	-	-	-	0.9	-	99.2
F8A	Forge Islands	Quartz-Monzonite	32.8	28.0	35.6	0.8	0.2	0.1	-	1.2	-	-	-	1.3	100.0

(All analyses determined on 1000 points).

TABLE 6:4 ELECTRON MICROPROBE AND ATOMIC ABSORPTION ANALYSIS OF MAGNETITES FROM QUARTZ-MAGNETITE VEINS, ARGENTINE ISLANDS.

Specimen Number	Location	Method of analysis	SiO_2	Al_2O_3	MgO	CaO	TiO_2	Fe_3O_4	MnO	Au	Cr	Cu	Mo	Ni	Pb	Se	Sr	Te	V	Zn	Total
B2A*	Barchan Islands	AA	8.86	0.14	0.043	.006	.033	90.76	.15	44	9	10	146	78	8	368	4	50	338	90	99.99
B2	Barchan Islands	EM	-	-	-	-	.081	98.26	.38	-	164	-	-	-	nd	-	-	-	184	-	98.72
B2	Barchan Islands	EM	-	-	-	-	.081	99.04	.41	-	164	-	-	-	-	-	-	-	370	-	99.53
B2	Barchan Islands	EM	-	-	-	-	.071	98.41	.30	-	164	-	-	-	-	-	-	-	159	-	98.80
B2	Barchan Islands	EM	-	0.20	-	-	.058	98.42	.19	-	212	-	-	-	nd	-	-	-	168	-	98.87
B16*	Barchan Islands	AA	17.00	.27	0.086	.005	.100	82.33	.11	44	10	20	215	133	8	364	3	29	300	60	99.93
B16	Barchan Islands	EM	-	-	-	-	.032	99.04	.32	-	80	-	-	-	-	-	-	-	184	-	99.40
B16	Barchan Islands	EM	-	-	-	-	.049	98.11	.21	-	164	-	-	-	-	-	-	-	280	-	98.37
B16	Barchan Islands	EM	-	0.16	-	-	.023	98.69	.18	-	246	-	-	-	-	-	-	-	80	-	99.06
B16	Barchan Islands	EM	-	-	-	-	.065	99.19	.20	-	205	-	-	-	nd	-	-	-	28	-	99.45

AA= atomic absorption analysis, EM= electron microprobe analysis.

Trace elements are in parts per million (ppm), except Au which is in parts per billion(ppb).

Major oxides are in weight percent. -means not analysed, nd none detectable.

B2A* and B16* were analysed by AA analysis on bulk samples and the high silica values are probably due to quartz contamination from the quartz vein.

TABLE 6 : 5 CELL DIMENSIONS OF MAGNETITE

SPECIMEN NO.	CELL DIMENSIONS
B2	a_o = 8.381
B8	a_o = 8.380
B16	a_o = 8.392

Table 6.6 REFLECTIVITY AND HARDNESS VALUES FOR OPAQUE MINERALS, ARGENTINE AND ANAGRAM ISLANDS.

	Specimen No.	Location	Reflectivity (at 589 nm)	Vickers Hardness Number (at 100g load)
		MAGNETITE		
A	**GABBRO**			
	A8	ANAGRAM ISLAND	19.6, 20.0, 19.3, 19.1	598, 623, 616
B	**QUARTZ-MAGNETITE VEINS**			
	B2	BARCHAN ISLANDS	19.2, 20.5, 18.6, 19.0, 19.5	616, 583, 605, 623, 634, 682
	B8		18.7, 18.6, 18.3	634, 682, 641
	B16	BARCHAN ISLANDS	18.8, 19.3, 18.9	578, 731, 709
	B20	BARCHAN ISLANDS	18.1, 18.8, 19.2	648, 695, 634
	F9	FORGE ISLANDS	18.7, 18.8, 19.1, 18.5	682, 641, 688, 623, 641, 578
	F14		18.9, 19.2, 19.1	832, 731, 891
	F15	FORGE ISLANDS	18.8, 18.6, 19.8	1055, 1202, 1186
	F17	FORGE ISLANDS	18.8, 19.0, 19.0	1030, 1017, 824
	F21	FORGE ISLANDS	19.0, 18.6, 18.6	1069, 862, 1055
		ILMENITE		
A	**GABBRO**			
	A8	ANAGRAM ISLAND	19.5, 19.8, 19.6, 19.5	796, 871
		PYRITE		
A	**GABBRO**			
	A8	ANAGRAM ISLAND	50.2, 51.6, 50.8	2025, 1984, 2054
	QUARTZ-MAGNETITE VEINS			
	B20	BARCHAN ISLANDS	51.4, 52.2, 50.9	1708, 1629, 1629
	B19		49.9, 50.2, 51.0	2025, 1984, 2054
	F20	FORGE ISLANDS	52.0, 51.8, 51.9	2054, 1984, 2205
C	**QUARTZ-PYRITE VEINS**			
	B22	BARCHAN ISLANDS	52.4, 52.8, 52.9	2054, 2205, 1984
	P1	THREE LITTLE PIGS	51.8, 51.6, 52.0	2054, 2205, 2054
		CHALCOPYRITE		
	QUARTZ-MAGNETITE VEINS			
	B20	BARCHAN ISLANDS	41.5, 40.3, 39.8	218, 225, 218

TABLE 6:7 MODAL ANALYSIS OF QUARTZ-MAGNETITE VEINS, ARGENTINE ISLANDS.

Specimen Number	Location	Quartz	Orthoclase	Plagioclase	Chlorite	Epidote	Hornblende	Carbonate	Biotite	Zircon	Rutile	Muscovite	Opaques	Total
B14	Barchan Islands	30.1	37.5	28.0	3.0	1.1	-	-	-	-	-	-	0.3	100.0
B16D	Barchan Islands	99.5	-	-	-	-	-	-	-	-	-	-	0.5	100.0
B17	Barchan Islands	45.3	42.5	10.5	0.2	0.2	0.4	-	-	-	-	-	0.9	100.0
B20	Barchan Islands	83.1	2.2	-	1.5	5.2	-	0.3	-	-	-	5.2	2.5	100.0
B23	Barchan Islands	81.0	5.3	1.9	6.5	2.5	-	0.2	-	-	-	0.9	1.8	100.1
F9	Forge Islands	66.6	0.7	5.0	2.0	3.1	-	0.3	-	0.2	0.1	-	22.0	100.0
F15	Forge Islands	85.4	1.5	-	3.0	6.7	-	0.3	-	-	-	0.4	2.7	100.0
F21	Forge Islands	75.0	-	-	4.2	5.1	-	-	-	-	-	0.6	14.4	99.3

(All analyses determined on 1000 points).

TABLE 6:8 MODAL ANALYSES OF OPAQUE PHASES FROM PLUTONIC ROCKS AND QUARTZ-MAGNETITE VEINS, ARGENTINE ISLANDS.

Specimen Number	Location	Rock Type	Magnetite	Hematite	Ilmenite	Pyrite	Chalcopyrite	Bornite	Pyrrhotite	Goethite	Chalcocite	Total
A3	Anagram Islands	Gabbro	60.8	-	30.8	6.9	1.5	-	-	-	-	100.0
A8	Anagram Islands	Gabbro	59.6	-	17.7	7.1	14.2	-	-	-	1.4	100.0
B18	Barchan Islands	Granodiorite	81.4	-	15.1	3.5	-	-	-	-	-	100.0
F1	Forge Islands	Granodiorite	83.8	-	14.7	1.5	-	-	-	-	-	100.0
B2	Barchan Islands	Quartz-magnetite vein	94.7	4.3	-	0.8	0.2	-	-	-	-	100.0
B2	Barchan Islands	Quartz-magnetite vein	90.9	8.2	-	0.6	0.2	-	-	-	-	99.9
B2	Barchan Islands	Quartz-magnetite vein	97.9	1.2	-	0.8	0.2	-	-	-	-	100.1
B16	Barchan Islands	Quartz-magnetite vein	89.2	10.7	-	0.2	-	-	-	-	-	100.1
B16	Barchan Islands	Quartz-magnetite vein	19.0	80.3	-	0.5	0.2	-	-	-	-	100.0
B20	Barchan Islands	Quartz-magnetite vein	48.3	7.6	-	40.7	3.4	-	-	-	-	100.0
F9	Forge Islands	Quartz-magnetite vein	87.1	-	-	6.1	5.0	1.8	-	-	-	100.0
F15	Forge Islands	Quartz-magnetite veins	99.1	-	-	0.9	-	-	-	-	-	100.0
B22	Barchan Islands	Quartz-pyrite vein	-	-	-	94.0	1.6	-	3.2	1.1	-	99.9
B20	Barchan Islands	Quartz-pyrite vein	3.7	-	-	46.8	48.5	-	0.3	0.7	-	100.0
G6	Galindez Island	Quartz-pyrite vein	-	-	-	98.4	0.5	-	1.1	-	-	100.0
P1	Three Little Pigs.	Quartz-pyrite vein	-	-	-	93.8	0.2	-	0.4	5.6	-	100.0

(All analyses determined on 1000 points).

TABLE 6:9 CHEMICAL ANALYSES OF QUARTZ-MAGNETITE VEINS ON THE ARGENTINE ISLANDS, AND GABBRO ON THE ANAGRAM ISLANDS.

Specimen Number	Location	SiO_2	Al_2O_3	TiO_2	MgO	CaO	FeO	Na_2O	K_2O	MnO	Au*	Cr	Cu	Mo	Ni	Pb	Se	Sr	Te	V	Zn	Total
F6C	Forge Islands (contains feldspar)	58.10	11.98	0.28	0.05	20.78	3.00	2.02	3.60	0.054	42	7	6	106	24	5	124	202	66	150	10	99.86
B17	North west Island in Barchan Island Group	97.50	0.02	nd	0.02	0.01	0.62	1.69	0.02	0.027	nd	10	5	90	1	nd	nd	1	nd	nd	14	99.91
B2	Largest of the Barchan Islands	96.40	0.02	0.07	0.02	0.01	0.62	2.75	0.02	0.017	nd	9	6	118	nd	nd	106	1	nd	nd	6	99.93
A8	Gabbro, Anagram Islands	50.14	10.50	2.34	6.64	11.49	14.50	4.09	0.14	0.14	54	13	300	18	69	25	623	158	20	1380	70	99.98

Major oxides are in weight percent. Trace elements are in parts per million (ppm) except Au* which is in parts per billion (ppb)

TABLE 6 : 10 CHEMICAL ANALYSES OF PYRITE SEPARATES FROM QUARTZ PYRITE VEINS AND AREAS OF PHYLLIC ALTERATION

Specimen No.	Location	Fe	S	Au	Co	Cu	Mn	Ni	Pb	Se	Zn	Totals
QUARTZ-PYRITE VEINS												
F9	FORGE	46.45	53.38	13	50	92	1156	<1	<1	30	29	99.94
F20	ISLANDS	46.42	53.39	40	30	80	779	< 1	<1	430	23	99.88
AREA OF PHYLLIC ALTERATION IN PYROCLASTIC ROCKS												
G8	GALINDEZ ISLAND	46.41	53.37	<1	140	14	10,240	60	74	185	38	100.80

TRACE ELEMENTS ARE IN PPM.

(except Au which is in parts per billion)

TABLE 6:11 MODAL ANALYSIS OF AREAS OF PHYLLIC ALTERATION ON THE ARGENTINE ISLANDS.

Rock Type	Specimen Number	Location	Quartz	Muscovite	Plagioclase	Chlorite	Epidote	Pyrite	Total
Phyllic alteration of pyroclastics	G6	Galindez Island	58.0	30.6	5.6	-	3.3	2.5	100.0
Phyllic alteration of pyroclastics.	W2	Winter Island	38.4	50.8	0.7	1.7	-	8.3	99.9

All analyses determined on 1000 points.

TABLE 6:12 CHEMICAL ANALYSIS OF AREA OF PHYLLIC ALTERATION, GALINDEZ ISLAND, ARGENTINE ISLANDS.

(A) MAJOR OXIDES:

Rock Type	Specimen Number	SiO_2	Al_2O_3	TiO_2	MgO	CaO	FeO	Na_2O	K_2O	MnO	S^{2-}	H_2O-	Total
Phyllic alteration of pyroclastics	G6	63.90	17.08	0.57	0.35	0.07	3.98	1.12	8.84	0.03	3.60	0.12	99.66

(B) TRACE ELEMENTS:

(All trace elements in parts per million-ppm, except Au* which is in parts per billion-ppb).

Specimen Number	Au*	Cd	Cr	Cu	Mo	Ni	Pb	Se	Sr	Te	V	Zn
G6	30	3	7	19	15	7	23	441	1	18	nd	14

CHAPTER 7

COPPER DEPOSIT ON HORSESHOE ISLAND, MARGUERITE BAY.

7.1 Introduction

Horseshoe Island is situated at the north eastern margin of Marguerite Bay, between Pourquoi Pas and the Graham Land Peninsula. Its precise location is between latitudes 62° 21' and 67° 05' west and longitudes 67° 48' and 67° 54' south. An old British base is situated on the northern coast of the Island, to the north of Lystad Bay, although no published literature has appeared on the geology of the island.

The northern arm of the island is composed of two major rock types, these being a dark olivine gabbro and a coarse, pink potassic granite. The two intrusions are bounded by a linear ENE-WSW trending fault. Following the intrusion of the gabbro there occurred a phase of alteration caused by late stage magmatic fluids, which lead to the introduction of magnetite and brown hornblende into the gabbro. Mineralisation of the gabbro then followed which seems to have been associated with the pink granite. The mineralisation in the gabbro is also present on small islands in Lystad Bay where it has been intruded by bosses of pink granite. Disseminated chalcopyrite and pyrite is present in the gabbro and the deposit seems to be a porphyry copper similar to Ray, Arizona, in that the copper is concentrated in the basic rock.

On the southern arm of the island, areas of phyllic alteration are present which were caused by low temperature hydrothermal fluids, and seem to be related to the mineralisation process. The mineralisation

and associated igneous rocks are discussed below.

7.2 Field Relationships of the Igneous Rocks

The dark grey olivine gabbro to orthogabbro is present on the northern arm of the island (Fig. 7:1), and its exposed area is about four square kilometers. The rock is generally medium-grained (plate 7:3) and is relatively homogeneous, in that it does not appear to vary in grain size over the outcrop area. Malachite staining is common on the gabbro, especially in cracks and fractures which occur on sheltered surfaces (plate 7:1). Chemical and petrographic analysis indicate the rock is a gabbro (table 7:1).

The gabbro has been invaded by veins of white to light grey aplitic (granodioritic) material which in places has given the rock a brecciated appearance (plate 7:2), and suggests the aplites were intruded at a relatively high level. The aplites seem to run parallel to the fault separating the granite and gabbro, but only intrude the gabbro. Faulted against the gabbro is a coarse, pink granite. The rock is homogeneous and non-foliated with orthoclase and quartz clearly visible in hand specimen. The fault trends ENE-WSW (075°) and form a remarkably sharp contact between the two rock types. Bosses of the granite intrude the gabbro on islands in Lystad Bay (Fig. 7:1).

Quartz-albitite dykes which trend NNW-SSE (160°) and vary in width from one to four meters, intrude the granite, aplite veins and gabbro. They are frequently stained with pyrolusite, and have been dated by K/Ar methods at 90 my (Grikurov et al, 1966).

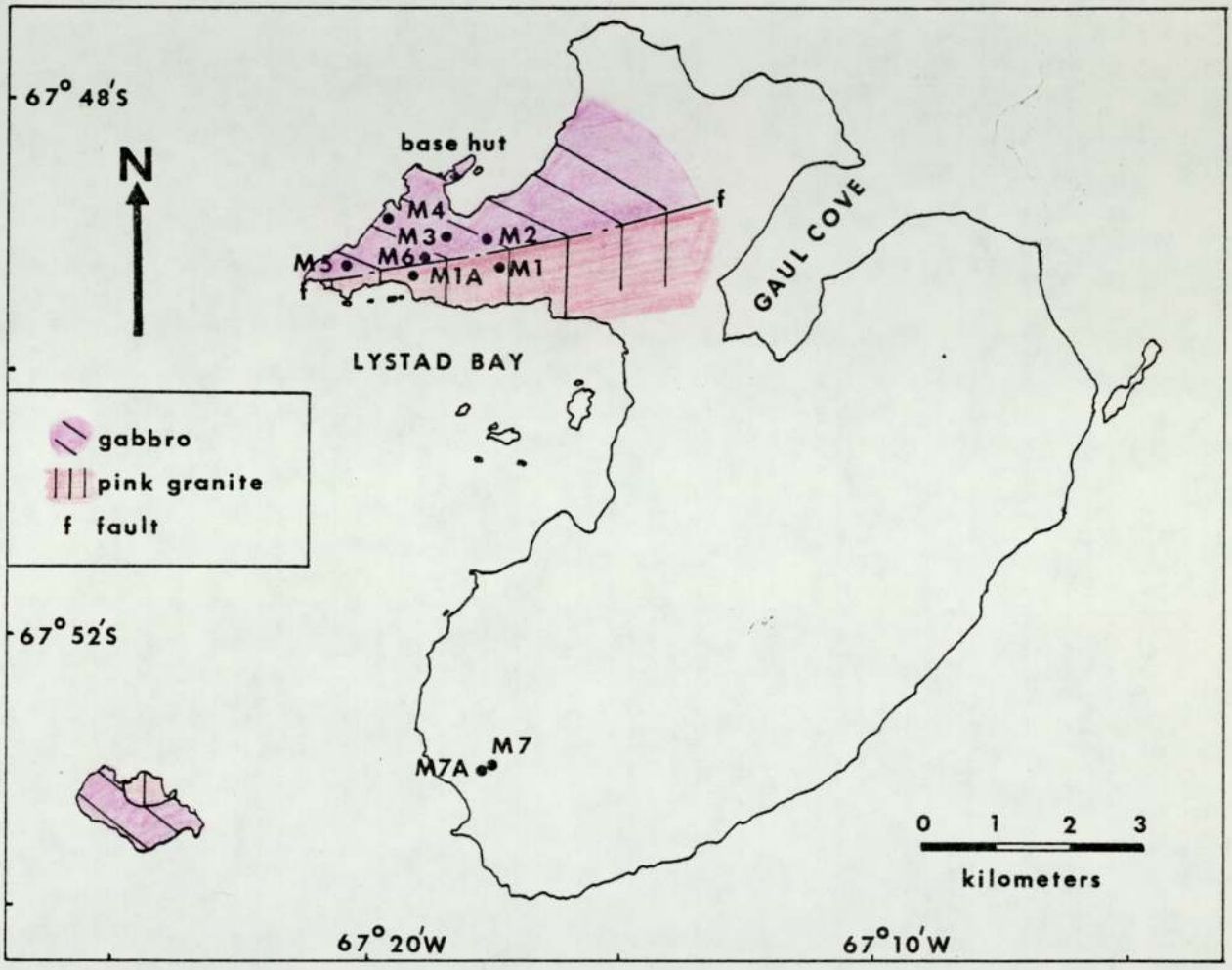

FIG.7:1 SPECIMEN LOCATION AND GENERAL GEOLOGICAL MAP OF HORSESHOE ISLAND, MARGUERITE BAY.

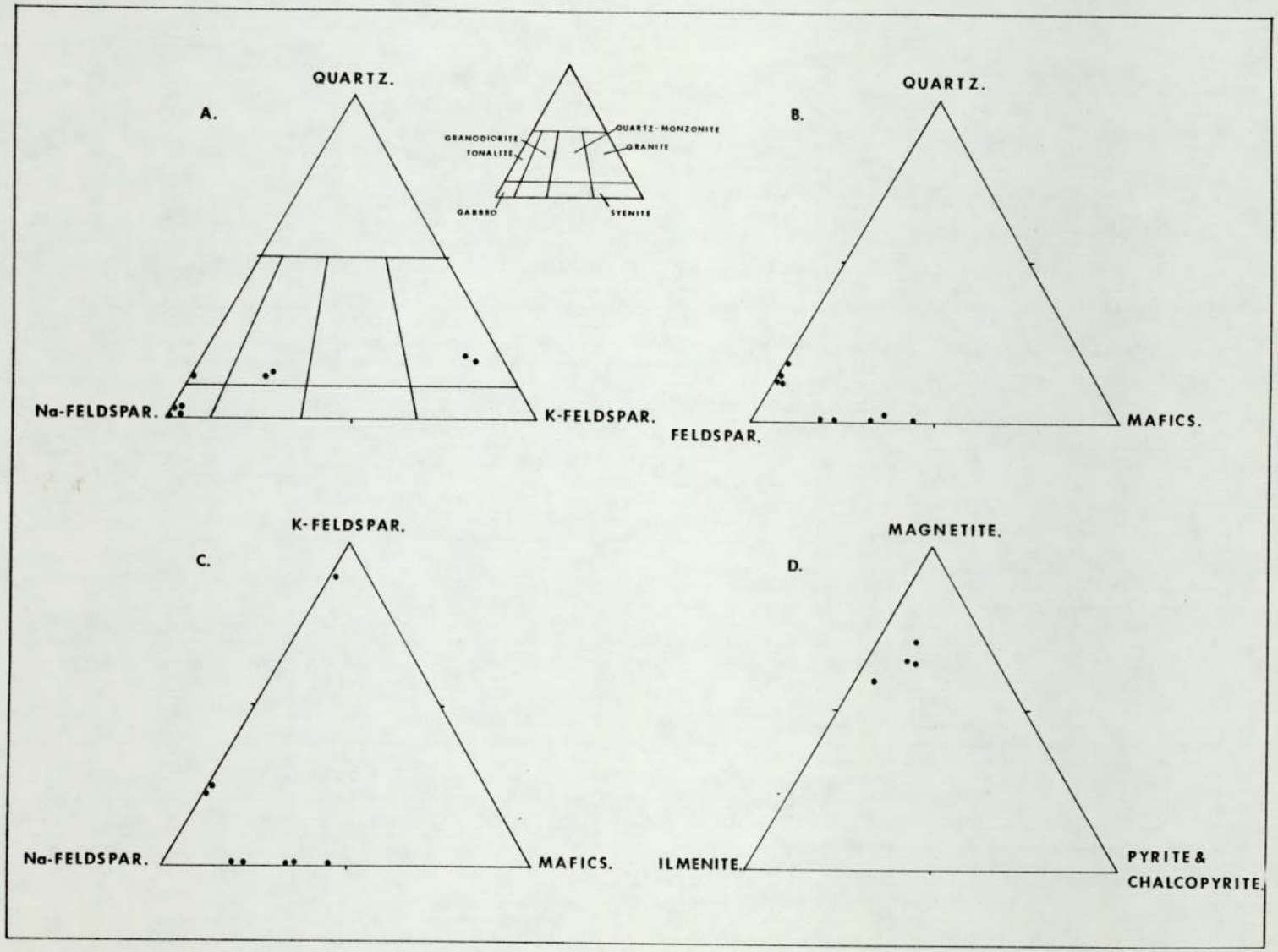

Fig 7:2 TERNARY DIAGRAMS OF MODAL DATA, HORSESHOE ISLAND. A, B & C GABBRO & GRANITE, A, quartz-sodium feldspar-potassium feldspar; B, quartz-feldspar-mafics; C, sodium feldspar-potassium feldspar-mafics; D, RATIO OF OPAQUE PHASES IN THE GABBRO, magnetite-ilmenite-pyrite & chalcopyrite.

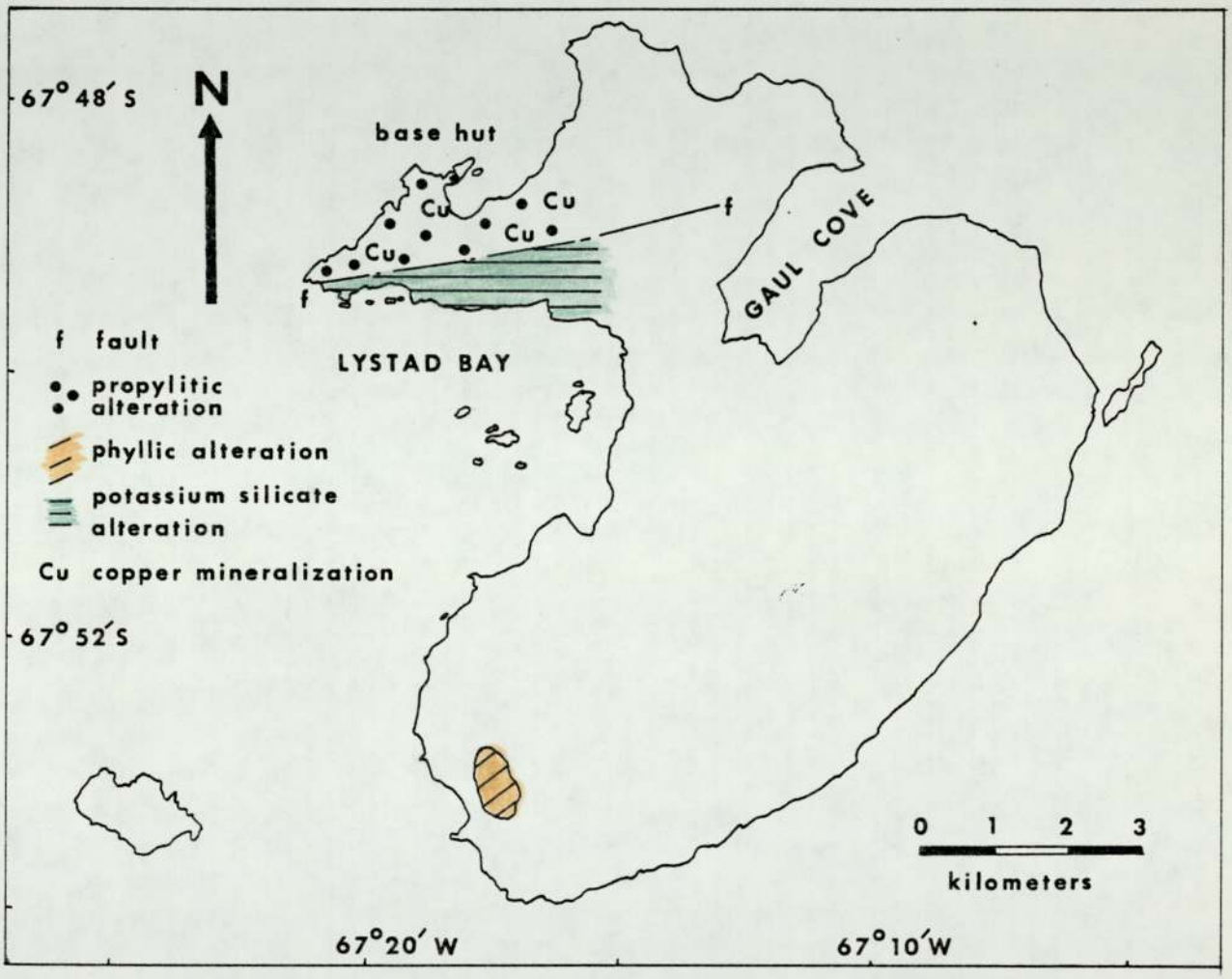

FIG.7:3 ALTERATION AND MINERALIZATION ZONES, HORSESHOE ISLAND, MARGURITE BAY.

7.3 Petrology of the Intrusive Rocks

7.3.1 Gabbro

The gabbro consists petrographically of a medium-grained, hypidiomorphic mass of subhedral plagioclase fledspar (An $_{50-60}$, <4mm) and titaniferous augite. Euhedral olivine is also present, but is frequently pseudomorphed by talc and tremolite. The plagioclase is frequently zoned with the calcic cores showing alteration to muscovite, siderite, epidote and chlorite (M3). Some rare interstitial orthoclase and quartz occur, normally in close proximity to the intruded aplite veins. A euhedral, slightly pleochroic pyroxene (pale brown to pale blue-green <2mm) is present which often shows simple and multiple twinning and wavy extinction. The mineral has a large 2V, extinction angle of 36° - 45°, is biaxial positive and length slow, properties which suggest it is titaniferous augite. In places euhedral olivine is present (plate 7:4), but is generally pseudomorphed by tremolite, talc, iddingsite, antigorite and magnetite (M5). The magnetite is often found along former fractures in the olivine. Where fresh olivine occurs, the optical properties suggest it is chrysolite, and the mineral often contains inclusions of plagioclase (<0.4 mm, M6) and frequently has a reaction rim of hypersthene (M6). Plagioclase, olivine and augite are often poikilitically enclosed by brown, euhedral hornblende (plate 7:5), although some green hornblende is also present (<3mm). In rare instances the brown hornblende shows alteration to chlorite, epidote, uralite and muscovite generally along fractures. Some veinlets of brown hornblende traverse the plagioclases (M3). Chlorite and sphene occur surrounding magnetite and ilmenite and sometimes replace plagioclase and augite along fractures and cleavages. Siderite and muscovite also occur associated with chlorite. Uralite shows slight alteration to chlorite.

Euhedral apatite is also present (<1mm) and occasionally contains spherical inclusions of carbonate (M3). Intergranular epidote and siderite also occur (<0.5 mm) with interstitial biotite (probably secondary <1.5 mm) present as an overgrowth on magnetite and ilmenite, but also as a replacement of pyroxene and hornblende. Such features as the progressive replacement of pyroxene to form poikilitic hornblende is characteristic of hornblende gabbros and appinitic rocks generally (Bowes and Wright, 1960; Joplin, 1959). Biotite can form by direct precipitation or as a result of increasing water content in the magma (Pitcher, 1978).

The oxide opaque minerals tend to be interstitial between the silicate phases although inclusions are common in the brown hornblende. They consist largely of euhedral-subhedral magnetite which contains {0001} plates of ilmenite exsolved parallel to {111} and subhedral ilmenite which seems slightly resorbed by brown hornblende. Exsolution lamelli of hematite also occur. Magnetite and ilmenite occur in simple intergrowths. Ilmenite shows alteration to rutile and hematite, with magnetite altering to hematite along {111} or more rarely to chlorite. Reflectivities at 589 nm (magnetite 19%, ilmenite 18.7%) and Vickers Hardness Numbers (magnetite 668 - 934, ilmenite 702 - 981, table 7:5) are within the range for the pure minerals. Magnetite appears to have formed during a phase of late stage magmatic alteration as its temperature of formation appears to be about 600°C (using the data of Buddington and Lindsley, 1964). The earliest phase of chalcopyrite and pyrite formation is associated with this process also as inclusions of these sulphides occur in the magnetite. The paragenetically earlier, and in places slightly resorbed ilmenite is probably a precipitate from the original magma and its slight alteration to rutile may have been

caused by aqueous solutions at 200 - 650°C (based on Karkhanavala and Momin, 1959). Rounded inclusions of chalcopyrite, bornite and pyrite occur in the magnetite and ilmenite as emulsion droplets (< 0.08 mm, plate 7:5, M5).

Modal analyses of the gabbro (table 7:2) indicate plagioclase feldspar is the main phase (42 - 60%) with titaniferous augite usually constituting from 7 - 34% of the rock. Brown hornblende forms between 7.4 to 11%, with magnetite and ilmenite forming 5.6 - 11.3% of the rock. Green amphibole and chlorite constitute 4% and 5% of the rock respectively with all other components (quartz, orthoclase, olivine, apatite) constituting less than 5% of the rock. Modal analysis of the opaque minerals indicates magnetite (54 - 65%) and ilmenite (19 - 38%) are the main phases. Pyrite forms between 5 and 12% of the opaques with chalcopyrite (0.5 - 2%). Chalcocite and cuprite form less than 3% (Fig. 7:2D, table 7:3).

7.3.2. Aplite Veins

Petrographically, the aplite veins consist of an inequigranular mass of subhedral plagioclase feldspar (An_{40-45}, <1.8 mm), often zoned (M4). Most show slight alteration to muscovite and quartz. Interstitial orthoclase perthite (<1.5 mm) and anhedral quartz showing undulose extinction are also present. There are minor amounts of green hornblende (<1mm) frequently associated with magnetite and showing slight alteration to chlorite. Some intergranular epidote, zircon (<0.4 mm) and siderite (<0.2 mm) also occur.

Modal analyses show the rock contains plagioclase feldspar (60%), orthoclase (19%) and 13% quartz (table 7:2), and indicate a granodioritic composition. Other components constitute less than 5% of the rock.

Plate 7:1 Olivine gabbro (dark grey) with green malachite stains, mainly in fractures. The light grey rock cutting the gabbro is aplite.

Northern Horseshoe Island, Marguerite Bay (M4).

Plate 7:2 Gabbro (dark grey) cut by aplite veins (white). The brecciated appearance of the gabbro is typical.

Horseshoe Island, Marguerite Bay (M4).

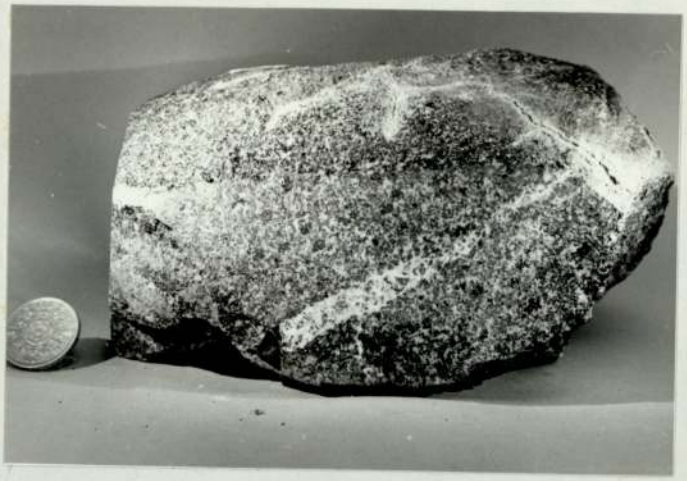

Plate 7:3 Hand specimen of gabbro, cut by small aplite vein (white) and malachite stains (greyish white) on top surface of specimen. Note medium grained texture. White crystals in gabbro are plagioclase, black; hornblende, dark grey; augite. M4A. Horseshoe Island, Marguerite Bay.

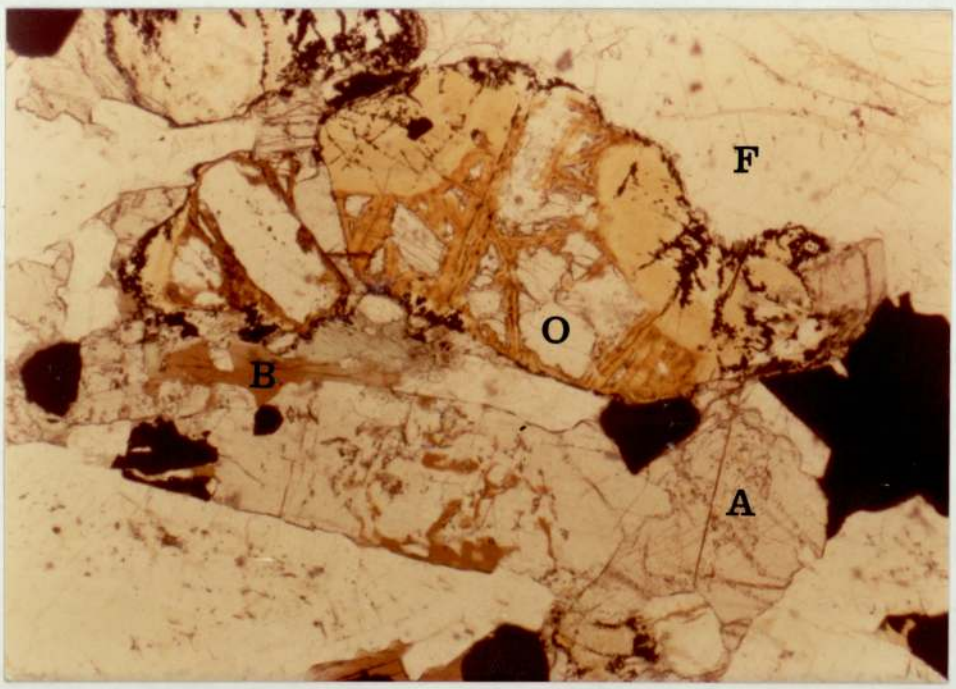

Plate 7:4 Plagioclase feldspar (white, low relief), titaniferous augite (pale brown, high relief), olivine (colourless, high relief), showing alteration to iddingsite and tremolite, and magnetite (black). Pyroxene shows alteration to brown hornblende. Gabbro, Horseshoe Island, Marguerite Bay. M6, plane polarised light, transmitted light, X60. Feldspar (F), Augite (A), Olivine (O) and Amphibole (B).

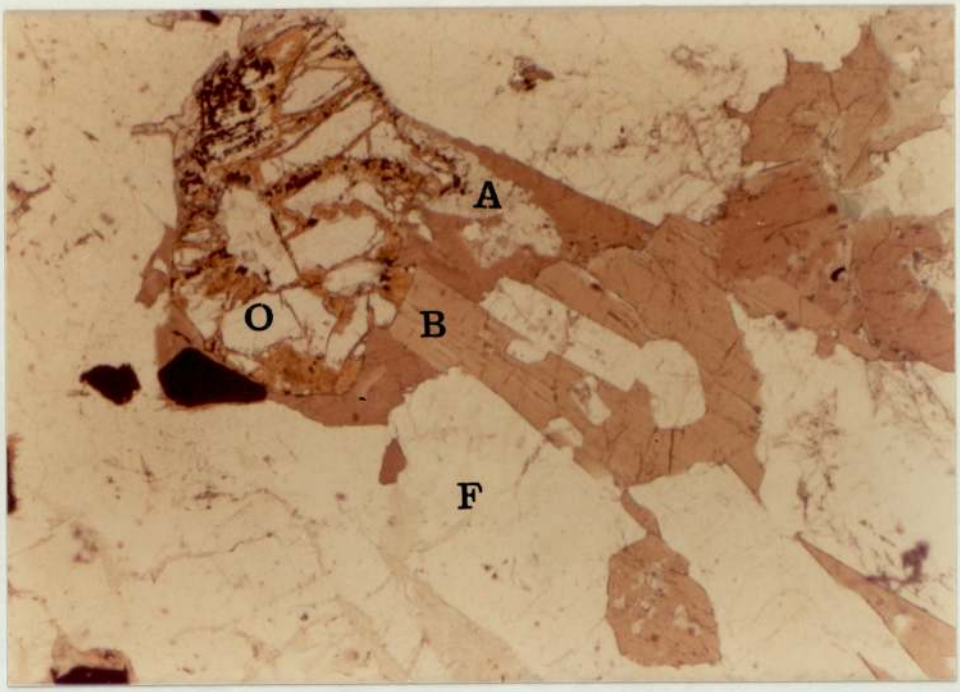

Plate 7:5 Plagioclase (white, low relief), olivine (white, high relief) and titaniferous augite (pale brown, high relief) poikilitically enclosed and replaced by brown hornblende. M6. Gabbro, Horseshoe Island, Marguerite Bay. Plane polarised light, transmitted light X60. Plagioclase (F), Hornblende (B), Olivine (O), and Augite (A).

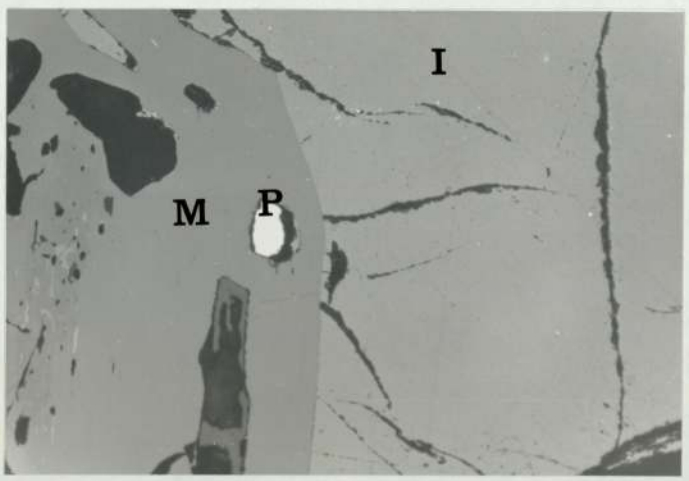

Plate 7:6 Ilmenite (light grey) and magnetite (darker grey) with inclusions of pyrite (white) and plagioclase (black). Reflected light X160. M5. Gabbro, Horseshoe Island, Marguerite Bay. Ilmenite (I), Magnetite (M), Pyrite (P).

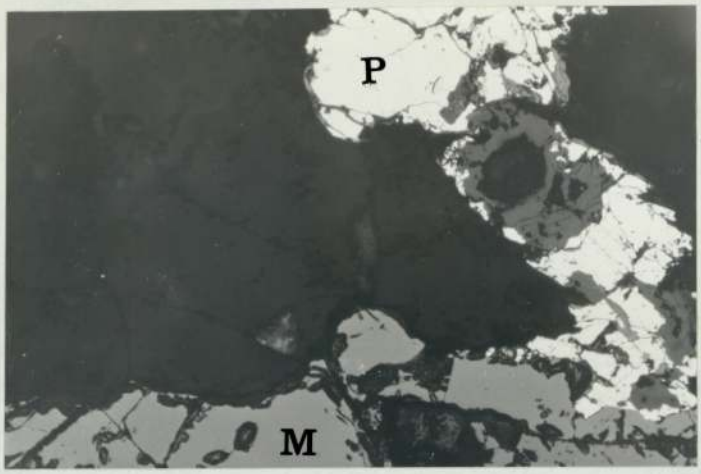

Plate 7:7 Magnetite (M) (grey) and pyrite (P) (white). Gabbro, Horseshoe Island, Marguerite Bay. Reflected light, X160. M4.

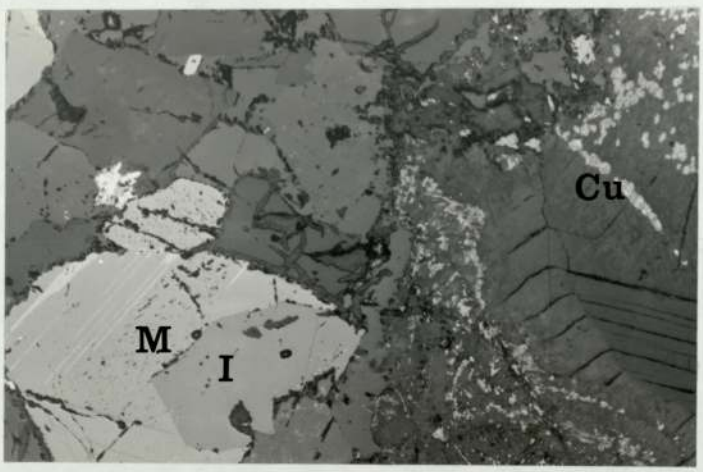

Plate 7:8 Magnetite (M) (light grey) with ilmenite exsolution lamelli, and ilmenite (I) (dark grey) in simple intergrowths. Cuprite (medium grey) occurs along cleavages in hornblende crystal (top right of plate). White mineral is pyrite. M5. Horseshoe Island, Marguerite Bay. Reflected light X100. Cuprite (Cu).

Plate 7:9 Area of phyllic alteration (whitish yellow) in gneissose granite, Southern Horseshoe Island, Marguerite Bay. Note pale yellow altered granite (G) and darker yellow altered dyke (D) (top centre of plate).

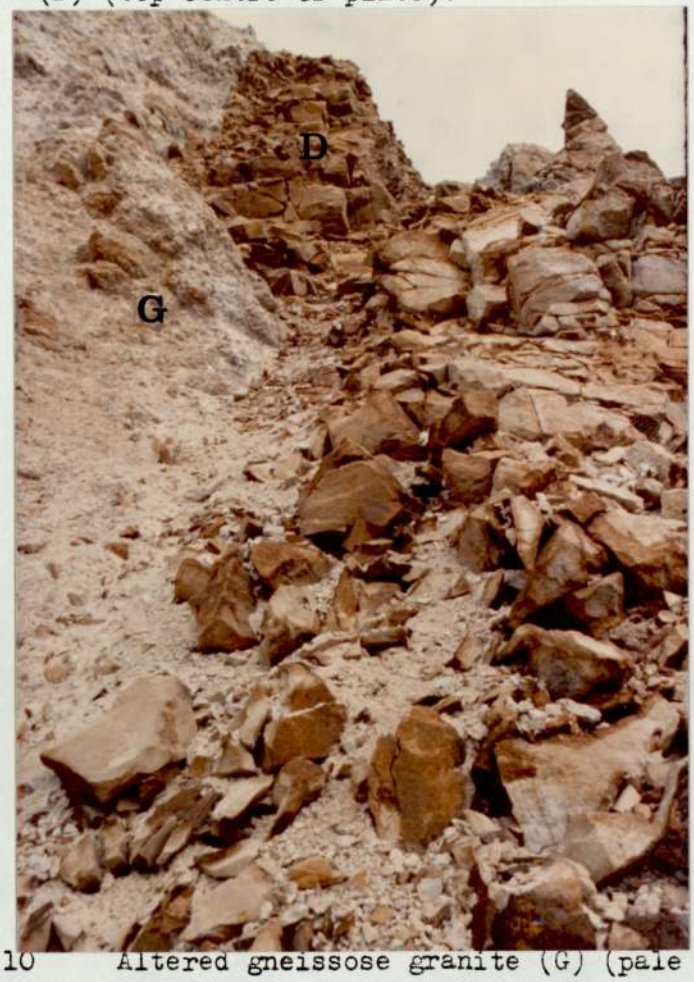

Plate 7:10 Altered gneissose granite (G) (pale yellow) traversed by altered dyke rock (D) (dark yellow). Dyke is about 3 meters wide. Horseshoe Island, Marguerite Bay, M7 & M7A.

Plate 7:11 Thin section of granite showing phyllic alteration. Large quartz crystals (dark grey to white) are pseudomorphs after feldspar. Groundmass consists of subhedral $2M_1$ muscovite (showing second order yellows and reds) and anhedral quartz (white). Later granular quartz veinlets cutting large quartz crystals. Black is pyrite. M7. Horseshoe Island. Transmitted light, crossed polars, X60.

7.3.3. Pink Granite

The granite consists of an inequigranular mass of orthoclase perthite (<4mm), anhedral microcline, subhedral plagioclase (An_{8-14}, <2mm) and interstitial anhedral quartz showing undulose extinction. Some of the plagioclases are zoned, with the calcic cores often showing alteration to muscovite. Some orthoclase shows relict zoning from former plagioclases indicating orthoclase has replaced plagioclase. Small veinlets of potash feldspar traverse the rock (M1A). Subhedral amphibole occurs showing alteration to biotite (<2mm) although alteration of amphibole and biotite to chlorite is common, with siderite granules often present in association with chlorite. Small (<0.3 mm) euhedral zircons are common, and have brown, radioactive halos where they occur in feldspars. Some zircon is present as inclusions in subhedral magnetite and ilmenite. Magnetite and ilmenite are often present in simple intergrowths and can be associated with amphibole or surrounded by chlorite. Small veinlets of magnetite traverse the granite (M1). Minor anhedral rutile is present (<0.2 mm), and small veinlets of quartz, pyrite, clinozoisite and epidote (<0.2 mm) traverse the rock also.

Modal analyses show the granite consists of potassium feldspar (orthoclase and microcline) 67%, quartz 17% and plagioclase 7% indicating the rock is a true granite. All other components make up less than 6% of the rock.

7.3.4. Dykes

Petrographically, these rocks consist of phenocrysts of subhedral albite (<2mm) which show slight alteration to muscovite and chlorite, in a groundmass of albite laths (some in radial clusters) and interstitial quartz (<1mm). Acicular apatites occur (<0.5mm) with rare

biotite and hornblende showing alteration to chlorite. Small amounts of euhedral zircon are present. Subhedral magnetite (<0.5 mm) showing slight alteration to hematite, with inclusions of pyrite is present, which is often surrounded by chlorite laths.

Modal analysis shows these rocks are composed almost exclusively of plagioclase (85%) and quartz (13%). Amphibole, epidote and magnetite form less than 2%.

7.3.5 Ternary Plots of Modal Data

Plotted on a ternary diagram (Fig. 7:2A) (quartz-plagioclase-orthoclase) the modal analyses indicate the intrusive rocks form part of a broad differentiation trend from gabbro to granite, typical of the calc-alkaline suites as defined by Carmichael et al, (1974). A plot of quartz-feldspar-mafics shows the decreasing proportion of mafic minerals and increasing amount of quartz during differentiation (Fig. 7:2B). A plot of plagioclase-orthoclase-mafics shows the increasing proportion of potassium feldspar and decreasing mafics during differentiation (Fig. 7:2C).

7.3.6. Chemical Analysis of the Gabbro

Chemical analysis of the gabbro is given in table 7:1 and indicates it is a true gabbro based on Carmichael et al (1974). Trace element analyses show the rock contains 21 ppm Cr, 163 ppm Ni, and 92 ppm V; these elements probably being present mainly in magnetite, ilmenite and pyroxene (Taylor et al, 1969). Cu at 24 ppm is present as chalcopyrite with Mo 4ppm, Pb 26ppm and Zn 65ppm probably present as submicroscopic sulphides. Se at 660 ppm and Te at 24 ppm are present substituting for sulphur in the sulphides. Sr at 246ppm is probably substituting for Ca in the feldspars and pyroxenes.

Comparison of these figures with those for average basaltic rocks suggests V and Cr are slightly low and Ni slightly higher than average, based on data by Taylor et al, (1969). The V and Cr are probably low because much of the magnetite present in the rock is of late magmatic derivation, and, therefore, lower in V and Cr than magmatic magnetites. The high Ni may be associated with the large amounts of titaniferous augite.

7.3.7 Chemical Analysis of the Magnetites from the Gabbro

Electron microprobe analysis of the magnetites in the gabbro was achieved using the method of Carmichael (1968). Details of this method are given in the appendix. These analyses (table 7:4) indicate the magnetites in this rock contain about 1.5% V_2O_5, 0.2% MnO, 0.5% Cr_2O_3, 3% TiO_2 and 95% Fe_3O_4. In view of the fact that these magnetites co-exist with ilmenite, the data of Buddington and Lindsley (1964) and Elsdon (1972) can be applied to obtain an approximate temperature of formation. These analyses suggest a temperature of formation for the magnetites of between 500 - 670°C, characteristic of metamorphic-granitic rocks. This data strongly suggests the magnetites formed or at least re-equilibrated during a phase of late stage magmatic alteration at relatively high temperatures, which also lead to the formation of brown hornblende as in gabbros in Greenland (Elsdon, 1977).

7.4 Mineralisation and Alteration

7.4.1 Field Relationships of Mineralisation

Green malachite staining is abundant only over the surface of the gabbro, generally in small fractures on sheltered surfaces. Near the junction of the gabbro and granite, limonite staining is predominant. The gabbro contains goethite and chalcocite, formed by alteration of chalcopyrite and pyrite, and presumably represents a supergene alteration

Figure 7:3 Paragenesis of minerals in Gabbro, Northern Horseshoe Island

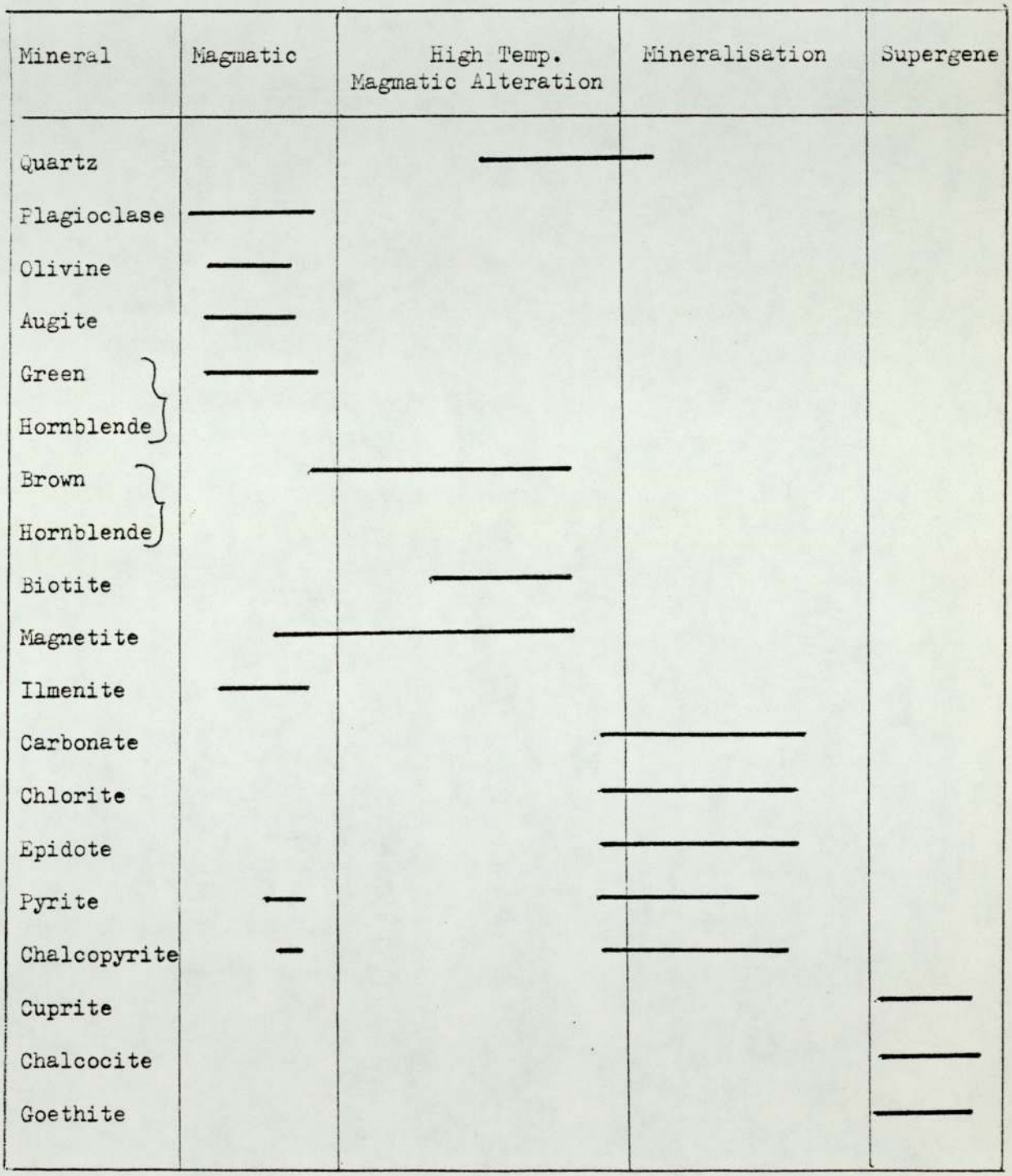

zone. Fieldwork also suggests the disseminated copper sulphide mineralisation occurs only in the gabbro. The aplite veins and granite seem devoid of sulphide mineralisation (Fig. 7:3).

7.4.2 Paragenesis

The sulphide minerals associated with the mineralisation process are discussed in their assumed paragenetic sequence. This sequence was deduced from textural evidence from some fifteen polished and thin sections.

Pyrite

Pyrite seems to be the earliest sulphide and is generally subhedral-anhedral (<1.4mm, plate 7:7). Pyrite is isotropic to faintly anisotropic and pale yellow in colour with a reflectivity of 52.5% (at 589nm) and a Vickers Hardness Number of 1487-2205 (at 100g load) which are within the range for pure pyrite (Burke et al, 1971). The pyrite contains inclusions of plagioclase and seems partially resorbed by the silicate phases (table 7:5).

A later phase of euhedral pyrite occurs which contains emulsion droplets of chalcopyrite (<0.01 mm).

Chalcopyrite

Subhedral chalcopyrite is present (<0.1mm) and is generally yellow in colour and isotropic to anisotropic. It shows marginal to complete alteration to chalcocite, tenorite and occasionally, bornite. The ratio of chalcopyrite to pyrite in the gabbro is about 4 to 5.

Chalcocite and Cuprite

Chalcocite is anhedral and pale bluish grey in colour and isotropic. Cuprite is also anhedral, whiteish grey with a bluish tint, with red internal reflections and showing anisotropy. Chalcocite occurs as pseudomorphs after chalcopyrite or as a marginal replacement of this

sulphide. Cuprite, however, occurs along cleavage planes in the brown hornblende (M5, plate 7:8) as lattice shaped replacements.

Goethite

Goethite is generally anhedral and grey in colour. It shows some anisotropy, but this is masked by reddish internal reflections.

7.4.3 Hydrothermal Alteration

The gabbro shows some introduction of secondary quartz with amphibole and biotite showing alteration to chlorite and epidote (mainly along fractures and cleavages). Disseminated epidote and siderite are present as veinlets consisting of quartz, epidote and pyrite. Plagioclase (especially the calcic cores of zoned crystals) shows alteration to muscovite and chlorite which also occur along cleavages in augite and as a halo around magnetite and ilmenite. The mineralogy of this alteration type seems typical of propylitic alteration (Meyer and Hemley, 1967).

The pink granite shows characteristic potassium silicate alteration (as defined by Meyer and Hemley, 1967) and veinlets of orthoclase traverse the rock (M1A). Orthoclase also replaces plagioclase, with relict zoning present in orthoclase from former plagioclase. Amphibole shows alteration to biotite. Biotite and amphibole show alteration to chlorite also.

7.5 Phyllic Alteration on South West Horseshoe Island

7.5.1 Field Relationships of Phyllic Alteration

On the south western part of Horseshoe Island, irregular shaped areas of yellowish-white hydrothermally altered rock occur in gneissose granitic country rock (Hawkes, per. comm.) (plate 7:9, Fig. 7:3). Late stage dykes about one to three meters wide which cut the country rock also show phyllic alteration in places (plate 7:10). However, fine-

grained areas of unaltered country rock occur in these zones of phyllic alteration, normally four by three meters in size. This alteration seems to be related to the mineralisation on the northern arm of the island.

7.5.2 Petrography of Rocks showing Phyllic Alteration

The altered granite (M7) consists of anhedral to granular quartz (2 - 0.1 mm) showing undulose extinction, some of which seems to be replacing former feldspar phenocrysts. In places a second phase of quartz occurs as small (<0.1 mm) anhedral, interlocking crystals along fractures in the larger quartz phenocrysts. The matrix of the rock consists of fine-grained anhedral quartz (<0.1 mm) parts of which appear optically continuous, and subhedral $2M_1$ muscovite although rare kaolinite also occurs (plate 7:11). Clusters of $2M_1$ muscovite seems to be replacing former ferromagnesian minerals. Some granules of zircon and anhedral rutile (<0.1mm) are present and are probably relicts from the original granite.

The altered dyke consists petrographically of subhedral plagioclase laths (1 - 0.1 mm, M7A) partially to completely replaced by quartz and $2M_1$ muscovite. Some secondary anhedral to subhedral quartz is present (<0.1 mm) along with $2M_1$ muscovite laths (<0.1 mm) and intergranular jarosite comprising the groundmass.

Subhedral pyrite is the major sulphide present in these rocks and often contains emulsion droplets of pyrrhotite and inclusions of quartz, muscovite and rutile. The pyrite is fresh and unaltered. Minor amounts of anhedral hematite also occur. The pyrite is pale yellow and isotropic to slightly anisotropic and has a reflectivity (at 589 nm) of about 53% and Vickers Hardness Number (at 100g load) of 1437-2205 (table 7:8A), and are within the range for pure pyrite (Burke, et al, 1971).

Cell dimensions of the pyrite ^{a}o = 5.343 (pure pyrite ao = 5.417, JCPDS) is close to the accepted value (table 7:8B).

Modal analyses of these altered rocks (table 7:6) suggest muscovite (36 - 51%) and quartz (22 - 49%) are the major phases present in these rocks. In some (M7A) plagioclase forms 42% of the rock. Pyrite and rutile are invariably present, normally less than 1%.

7.6. Chemical Analysis of Rocks showing Phyllic Alteration and of Sulphide Mineral Seperates from these Rocks.

Chemical analyses of the rocks showing phyllic alteration (table 7:9) has been achieved using atomic absorption spectrophotometery. These results indicate the rocks contain between 64 and 72% SiO_2, 13% Al_2O_3, 6.6% Na_2O, 4% K_2O, 0.5% MgO and 0.5% CaO with 3% FeO and 0.2% TiO_2. These values are similar to those found in areas of phyllic alteration in the South Shetland Islands (this thesis).

The silica is present mainly as quartz, with alumina sodium and potassium oxides present as muscovite, with lime present in plagioclase, ferrous oxide in pyrite and titania present in rutile.

Levels of trace elements (table 7:9B) are also similar to the "Quartz-Pyrite" rocks of the South Shetland Islands. Cr (5ppm), Ni (6ppm) and Mo (26ppm) are probably present in pyrite. Cu at 20ppm is present as minor chalcopyrite with Pb (18ppm) and Zn (20ppm) probably present as submicroscopic galena and sphalerite. Se (30ppm) and Te (15ppm) is substituting for sulphur in pyrite.

Chemical Analysis of Pyrite.

Chemical analysis of pyrite from these areas of phyllic alteration (table 7:7) has been achieved using atomic absorption photometery. Seperation of the pyrite from the silicate phases was achieved using heavy liquids (bromoform). Pyrite was examined in polished section and

was found to be pure, and no other significant phases were present.

These analyses indicate the pyrite contains 120ppm Co and 70ppm Ni probably substituting for iron. These figures indicate a Co/Ni ratio of greater than one, and suggests the pyrite had a volcanogenic origin (Loftus-Hills and Solomon, 1969). Se (500ppm) is substituting for sulphur with Zn (58ppm) and Pb (5ppm) probably present as submicroscopic inclusions of galena. These values are approximately those of average pyrite (Ryall, 1977; Fleischer, 1955).

7.7 Summary of Igneous Activity at Horseshoe Island, and Comparison with other Literature

Field-work combined with petrographic and chemical data indicate the sequence of intrusion of plutonic and hypabyssal rocks on Horseshoe Island is gabbro, aplite veins, granite and albitite dykes.

Basaltic magmas are relatively common at an early stage in plutonic cycles in continental margin environment (Carmichael, et al, 1974), especially the Andean type (Pitcher, 1978), and the gabbro at Horseshoe Island appear to be the earliest phase in this polyplutonic episode. The primary mineral assemblage of the gabbro is dominated by plagioclase and pyroxene, and in the Andes rocks of this type frequently exhibit simple igneous textures, with adcumulus growth of plagioclase and intercumulus growth of hornblende (Regan, 1976) as at Horseshoe Island. Amphibolisation associated with late stage explosive brecciation and penetration by water rich volatiles are common in gabbroic rocks (Regan, 1976), and the early crystallisation of brown hornblende and widespread alteration derived from the magma itself, clearly indicates the gabbroic magma at Horseshoe Island had a high water content, which built up during crystallization (based on work by Mullan and Bussell, 1977) and probably also had a high $Fe^{III} : Fe^{II}$ ratio by comparison with rocks in Greenland

(Elsdon, 1977). Post-consolidation amphibolisation reactions in the solid state leading to heterogeneous meladiorite occur in gabbroid rocks (Pitcher, 1978), and may partly explain the apparent replacement of pyroxene by brown hornblende on Horseshoe Island (plate 7:4 and 7:5).

Closely associated with this process at Horseshoe Island as in the Andes is net veining by leuco-granite implying that it was brecciation which permitted the penetration of volatiles (Pitcher, 1978) responsible for the metasomatism on Horseshoe Island, although there is some evidence that introduction of water from external sources may be responsible for this process in some gabbroic rocks (Regan, 1976; Elsdon, 1977).

The pink granite seems to be the latest phase of plutonic activity, typical of calc-alkaline rock suites (as defined by Carmichael et al, 1974). A phase of quartz-albitite dykes were then intruded into these consolidated, plutonic masses, a feature typical of late stage batholithic emplacement in the Andes (Pitcher, 1978).

7.8 Summary of Mineralisation and Alteration at Horseshoe Island

Limited field-work due to logistical problems has allowed a preliminary interpretation of the mineralisation on Horseshoe Island. A phase of iron and copper sulphide mineralisation occurred after the intrusion of the aplite veins, and is concentrated mainly in the gabbro. This field data suggests the mineralisation is probably derived from the pink granite. The main sulphides present are chalcopyrite, pyrite and bornite, the bornite probably forming by incipient alteration of chalcopyrite. The deposit shows many similarities to that of the Ray Deposit in Arizona as described by Phillips et al, (1974), in that magnetite has envelopes of sphene, biotite and chlorite.

The late stage magmatic autometasomatism of the gabbro shows similarities to the propylitic alteration derived from the granite, and great care was needed to distinguish between the two. However, the alteration of biotite and hornblende to chlorite, and the small veinlets of quartz, epidote and pyrite are typical of propylitic alteration as defined by Meyer and Hemley (1967). The basic nature of the gabbro, and its reactions with hydrothermal fluids suggests a phyllic and argillic zone may be lacking in this deposit, as it often is in other basic intrusives, such as tonalites and diorites (Hollister, 1975).

The phyllic alteration on the southern arm of the Island appears to be typical of low temperature alteration associated with the peripheral zone of porphyry copper deposits as described by Sillitoe, (1973), as in the South Shetland Islands (this thesis).

The granite is most likely to be the source of the hydrothermal fluids that produced the disseminated sulphide mineralisation in the gabbro, since granites are more likely to produce vapour containing economic elements than gabbro (Whitney, 1977). A study of the alteration assemblages indicates that the granite is part of the potassic core, upfaulted against the propylitic zone by an ENE-WSW trending fault that runs across the northern arm of the Island. The fluids emanating from the granite were probably low in sulphur, and consequently not all the iron in the gabbro has been consumed to produce pyrite and much has been retained in the form of magnetite, amphibole and chlorite as in other porphyry copper deposits (Bowen, et al, 1977; Hollister, 1975). The lack of significant amounts of sulphide mineralisation in the potassic core is typical of porphyry copper deposits (Lowell and Guilbert, 1970). The small amounts of supergene sulphides and oxides in the gabbro tend to be mainly malachite,

although close to the fault contact between the granite and gabbro, limonite is the main supergene mineral, and suggests a zoning in the copper:iron ratio over the outcrop area of the gabbro.

Using the models of Lowell and Guilbert (1970), James (1971), Hollister (1975) and Sillitoe (1973)one can speculate on the position of the Horseshoe Island deposit in relation to other porphyry copper deposits. Since the bulk of the sulphide mineralisation associated with porphyry copper deposits is usually associated with the phyllic zone, or in deposits lacking such a zone, the junction of the propylitic and potassic zones (Bowen et al, 1977), then the Horseshoe Island deposit probably represents a site marginal to a high sulphide, low copper zone.

TABLE 7 : 1 PARTIAL CHEMICAL ANALYSIS OF GABBRO FROM NORTHERN HORSESHOE ISLAND.

Oxide	per cent
SiO_2	45.50
Al_2O_3	10.40
TiO_2	2.92
MgO	6.73
CaO	16.48
Na_2O	3.92
K_2O	0.21
FeO	14.20
MnO	0.13

MAJOR ELEMENTS

TOTAL = 100.49.

element	ppm.
Au	58 ppb
Cr	21
Cu	24
Mo	4
Ni	163
Pb	26
Se	660
Sr	246
Te	24
V	92
Zn	65

TRACE ELEMENTS

TABLE 7:2 MODAL ANALYSES OF INTRUSIVE ROCKS FROM NORTHERN HORSESHOE ISLAND, MARGUERITE BAY.

Specimen Number	Rock Type	Quartz	Plagioclase	Potash Feldspar	Augite	Hypersthene	Biotite	Olivine	Green Hornblende	Brown Hornblende	Chlorite	Epidote	Carbonate	Apatite	Magnetite +Ilmenite	Muscovite	Tremolite	Total
M3	Gabbro	-	44.2	-	11.8	-	-	0.3	4.5	10.9	7.3	0.1	1.1	4.1	10.7	4.7	0.4	100.1
M4	Gabbro	0.9	42.2	0.4	23.6	-	-	-	3.8	9.9	8.3	0.2	-	-	10.9	-	-	100.2
M4A	Gabbro	0.2	51.3	-	24.1	0.4	0.6	0.2	4.0	8.0	0.9	-	-	0.2	8.8	-	1.4	100.1
M5	Gabbro	-	43.8	-	34.0	-	-	0.2	1.3	7.4	1.1	-	-	-	11.3	0.4	0.8	100.3
M6	Gabbro	-	59.9	-	7.3	0.9	0.4	4.9	2.2	8.0	3.5	-	0.2	1.0	5.6	0.1	5.9	99.9
M4	Aplite vein	13.3	60.0	19.2	-	-	-	-	4.0	1.1	0.6	-	-	-	1.7	-	-	99.7
M4A	Aplite vein	12.6	61.2	18.5	-	-	-	-	4.3	1.2	0.4	-	-	-	1.8	-	-	100.0
M1A	Granite	16.7	7.1	67.4	-	-	0.6	-	5.2	-	0.2	1.6	-	0.4	0.9	-	-	100.1
M2	Albitophyre Dyke	13.0	85.1	-	-	-	-	-	1.0	-	-	0.4	-	-	0.5	-	-	100.0

(All analyses determined on 1000 points).

Table 7.3 MODAL ANALYSES OF OPAQUE PHASES IN GABBRO, NORTHERN HORSESHOE ISLAND.

Specimen No.	Location	Magnetite	Ilmenite	Pyrite	Chalco-pyrite	Cuprite	Chalcocite
M4	Northern Horseshoe Island	64.1	22.2	12.0	-	-	1.7
M4A		70.6	18.9	7.3	1.2	1.2	0.9
M4A	Northern Horseshoe Island	53.8	37.6	5.0	0.5	0.8	2.3
M5	Northern Horseshoe Island	65.0	23.6	5.9	1.7	2.9	0.9

All analyses determined on at least 1000 points.

TABLE 7 : 4 CHEMICAL ANALYSES OF MAGNETITES FROM GABBRO, HORSESHOE ISLAND, MARGUERITE BAY (by electron microprobe method)

SPECIMEN NO.	LOCATION	Fe_3O_4	TiO_2	MnO	Cr_2O_3	V_2O_5	Totals
M4A	Northern Horseshoe Island	89.38	6.600	0.210	0.12	1.44	97.75
M4A	"	93.00	2.620	0.200	0.11	1.36	97.29
M4A	"	95.56	2.770	0.200	1.00	1.37	100.89

TABLE 7 : 5 REFLECTIVITY AND HARDNESS VALUES FOR OPAQUE MINERALS IN GABBRO, NORTHERN HORSESHOE ISLAND

SPECIMEN NO.	LOCATION	REFLECTIVITY (AT 589mm)	VICKERS HARDNESS NO. (100g load)
MAGNETITE			
M4	Northern Horseshoe Island	19.0,18.8,18.2,20.1,19.7	695,796,709,763,772,695
M4A		19.0,19.5,19.5,19.1,19.9	716,756,747,934,853,702
M5	"	18.6,18.6,18.6,20.0,19.0	668,781,772,814,695,740
ILMENITE			
M4	Northern Horseshoe Island	17.2, 18.0	871, 702
M4A		17.7, 19.3, 20.4	740, 740, 981, 934
M5	"	19.8, 18.7	871, 981
PYRITE			
M4	Northern Horseshoe Island	52.6,52.6,52.7,52.3	1487,2205,1656,2086,1737

Table 7.6 MODAL ANALYSES OF AREA OF PHYLLIC ALTERATION, SOUTHERN HORSESHOE ISLAND.

Specimen No.	Location	Quartz	Plagioclase	Muscovite	Rutile	Pyrite
M7 altered granite	South west Horseshoe Island	48.6	-	50.9	< .1	0.6
M7A altered dyke	South west Horseshoe Island	21.7	42.3	35.8	< .1	< .1

All analyses determined on at least 1000 points.

TABLE 7 : 7 CHEMICAL ANALYSES OF PYRITE FROM AREAS OF PHYLLIC ALTERATION, SOUTHERN HORSESHOE ISLAND
(using atomic absorption methods)

SPECIMEN NO.	LOCATION	* Au	Co	Ni	Se	Pb	Zn
M7	Southern Horseshoe Island	1	120	38	516	1	46
M7		1	620	256	69	2	68
M7A	"	1	210	104	111	5	58
M7A	"	2	160	84	510	7	16

All values in parts per million (ppm) except Au *
which is reported in parts per billion (ppb)

Table 7.8A REFLECTIVITY AND HARDNESS VALUES FOR PYRITE IN AREA OF PHYLLIC ALTERATION, HORSESHOE ISLAND.

Specimen No.	Location	Reflectivity (at 589 nm)	Vickers Hardness Number (100g load)
M7	Southern	52.8, 53.1, 53.1	1681, 1361, 1992
M7	Horseshoe	52.3, 50.8 50.5	1681, 1170, 1984
M7A	Island	52.1, 50.9, 51.7	1404, 1950, 1945

Table 7.8B CELL DIMENSIONS OF PYRITE FROM AREA OF PHYLLIC ALTERATION, SOUTHERN HORSESHOE ISLAND.

Specimen No.	Location	a_o
M7	Southern Horseshoe	5.343
M7A	Island	5.398

Pure Pyrite $a_o = 5.417$

TABLE 7:9 CHEMICAL ANALYSES OF AREAS OF PHYLLIC ALTERATION, SOUTHERN HORSESHOE ISLAND.

Specimen Number	Rock Type	SiO_2	Al_2O_3	TiO_2	FeO	MnO	MgO	CaO	Na_2O	K_2O	S^{2-}	H_2O-	Au*	Cd	Cr	Cu	Mo	Ni	Pb	Se	Sr	Te	V	Zn	Total
M7	Altered granite	63.92	23.11	0.05	1.63	0.002	0.30	0.12	0.34	10.90	0.46	0.18	28	2	3	20	13	8	12	15	nd	19	nd	8	100.92
M7A	Altered dyke	71.94	13.18	0.15	2.87	0.001	0.05	0.04	6.63	3.93	0.82	0.27	22	1	6	19	26	2	26	46	nd	13	nd	32	99.88

Major element analyses are in weight percent. Trace element analyses are in parts per million (ppm), except Au* which is in parts per billion (ppb).

CHAPTER 8

COMPARISON OF KNOWN METALLIC MINERAL OCCURRENCES IN THE ANDES AND SOUTH AFRICA WITH THOSE LIKELY TO BE FOUND IN THE ANTARCTIC PENINSULA

8.1 Introduction

Since the Andes and Antarctic Peninsula are geologically similar (Dalziel, 1974) then ore deposits found in both areas should be of a similar style. In the following discussion of the mineralisation, deposits found in the Andes are described and similar geological environments in which they could be found in the Antarctic Peninsula are suggested. The discussion is divided into two parts; pre-Gondwanide deposits (similar to those found in the Geological Basement of the Andes and Southern Africa) and post-Gondwanide deposits, similar to the post-Palaeozoic ore deposits of the Andes. Since most ore deposits are less than 2km. in outcrop (those associated with plutonic intrusions) then such deposits are unlikely to be easily found due to the vast cover of ice on the Antarctic Peninsula. However, the length of strike of rocks on the Antarctic Peninsula may be such that some deposits may be located in ice free areas. Most deposits found on islands on the west coast of the Antarctic Peninsula are of relatively high level, and suggested no more than 2km. of rock has been eroded from the off-lying islands. In the South Shetland Islands the general erosional level is probably 0.5 - 1km. (as indicated by the presence of high level hydrothermal alteration), although in the Elephant Island area where there has been extensive faulting, the chromite deposits suggest a deep level of erosion.

8.2 Pre-Gondwanide Ore Deposits

Prior to the break up of Gondwanaland in the late Mesozoic, South America, Africa, India, Australia and Antarctica were part of the same super continent (Barker and Griffiths, 1977). Ore deposits found in pre-Mesozoic rocks in the other continents should, therefore, also be present in the Antarctic. The relatively small outcrop areas of pre-Gondwanide rocks in the Antarctic Peninsula (Trinity Peninsula and northern Palmer Land), however, makes it unlikely that major ore deposits will be found here. In the Andes ore deposits found in these "Basement Rocks" include an assemblage of post-magmatic ore deposits of Sn, W and rare metals (Be, Li, Ta and U) (Angelelli et al, 1970). Most of the Sn and W bearing quartz veins are of small size, but complex pegmatites are often sources of Be and Li. Base and precious metal veins and stratabound deposits occur, but are not as important as the ones of Andean age. Archean granite-greenstone belts occur in northern Palmer Land (Anckorn, 1975). Elsewhere Cr, Ni, Cu, Au and asbestos have been discovered in these deposits where ultramafic and mafic components are present, although Sb, Au and smaller amounts of Hg, barite, Cu-Pb-Zn and massive sulphides occur in chemical sediments. These probably represent terminating cycles of volcanism (Anhaeusser, 1976). Intrusions of similar size to the Bushveld have been found in East Antarctica (Dufek Mountains), and elsewhere these large basic bodies are major suppliers of the world's Cr, Ni, Cu, Fe, V and platinoids.

8.3 Post-Gondwanide Ore Deposits

Following the fragmentation of Gondwanaland in the Mesozoic, subduction and the related magmatism were in evidence along the western Antarctic Peninsula. The subducted crust dipped eastwards beneath the Antarctic Peninsula. Ore deposits formed during this period were

related to this magmatism which is tectonically and stratigraphically similar to the Andean margin of South America. The ore deposits formed in the Antarctic Peninsula are, therefore, likely to be similar to those in the Andes as suggested by Ericksen, (1976). The styles of ore deposits are discussed below using a general model of Andean deposits which is (from west to east), contact metasomatic iron deposits, vein type copper-gold and silver deposits, stratiform copper and manganese deposits, porphyry copper-molybdenum deposits, polymetallic deposits and tin-tungsten deposits. Areas of similar geological environments in the Antarctic Peninsula are given, but it is not suggested ore deposits found in these environments in the Andes will necessarily be found there.

Contact Metasomatic Iron Deposits

These deposits occur mainly in meta-andesitic rocks which are present as roof pendants or at the contacts of granodiorite to tonalite batholiths of middle Cretaceous age in the Andes. Some contain up to 100 million tons of 60% iron ore, for example Romeral and El Tofo in central Chile. The iron occurs as lenses, irregular bodies or veins of magnetite with associated specularite and apatite (Ruiz et al, 1965). If this style of deposit is present in the Antarctic Peninsula, then a geologically similar environment probably occurs on the western side of the Peninsula around Tertiary plutons on Anvers and nearby Islands.

Copper-Gold and Silver Vein Type Deposits

In the Andes these deposits generally occur peripheral to or within Cretaceous batholithic intrusions (Gross, 1975), associated with calc-alkaline rocks, and frequently occur in the same belt as porphyry copper deposits, but at a higher structural level in the volcanic pile (Hutchinson and Taylor, 1978). Gold occurs (mainly as tellurides) in chalcopyrite-pyrite-specularite veins which also contain minor lead, zinc, cobalt and

molybdenum. Silver deposits also occur in the batholithic belt of Chile with the mineralisation present in calcareous rocks, and only rarely in the intrusives themselves. Silver is present mainly as sulphosalts with minor cobalt, nickel, lead and zinc, normally in a quartz, barite, calcite gangue (Ruiz et al, 1965). Notable deposits in this group are Chanarcillo, Acari and La Higuera in Central Chile. Favourable environments for these deposits on the Antarctic Peninsula are in and around the Tertiary plutonic rocks on the Danco Coast, Anvers Island and the Marguerite Bay area.

Stratiform Copper Deposits

This type of deposit consists of finely disseminated chalcocite, bornite, and chalcopyrite, usually with a significant silver content which is found interbedded with calc-alkaline (mainly acidic) volcanic rocks or with intercalated sediments of Jurassic, Cretaceous or Tertiary age (Ruiz et al, 1971). Gangue and alteration minerals are sparse with genetically related intrusives apparently absent. In the Andes these deposits are present in the porphyry copper belt in lavas that are broadly co-magmatic with the spatially related batholiths, for example El Salado in South Central Chile. Frequently, they are concentrated in amygaloidal or brecciated upper parts of andesite lava flows. Where they occur in sedimentaryrocks, the indications are that they accumulated in reducing conditions, and are broadly syngenetic with the enveloping volcanic rocks (Stole, 1965; Ripley et al, 1977). Deposits of this type could be present in the Upper Jurassic or Tertiary lavas that were erupted co-magmatically with related plutonic rocks in the Antarctic Peninsula, for example the South Shetland Islands, Danco Coast and the Graham Coast, Graham Land.

Stratiform Manganese Deposits

Manganese oxides occur intercalated with Lower Cretaceous submarine volcano-sedimentry sequences, often interbedded with water-lain arenaceous volcanic rocks (volcanogenic sandstones). The manganese was of syngenetic origin and was deposited from volcanic emanations under shallow marine conditions (Aguirre and Mehech, 1964). Ferruginous chert and copper mineralisation are also locally associated with these deposits. A notable deposit in the Andes is Corral Quernado. Waterlain arenaceous volcanic rocks are present in the Antarctic Peninsula interbedded with the Jurassic volcanic rocks, and environmentally favourable areas include Adelaide Island, South Shetland Islands and the Graham Coast.

Tourmaline Breccia Pipes

Copper bearing tourmaline breccia pipes are closely related to porphyry copper deposits. (Sillitoe and Sawkins, 1971) and are genetically connected to Tertiary plutons of granodioritic composition, but in Chile are located to the west of the large porphyry copper deposits, notable deposits including Disputada and Turmalina in southern central Chile. The mineralisation occurs in subcircular, near vertical pipes consisting of quartz-tourmaline-pyrite-chalcopyrite mineralisation acting as a cement to angular fragments of the host rocks. Gold, tungsten and molybdenum can be important by products. Pipes usually occur in clusters of up to one hundred, and probably form by a collapse mechanism. The occurrence of quartz-tourmaline-chalcopyrite-pyrite erratics on Doumer Island indicates these deposits may be present on the island or surrounding areas.

Porphyry Copper-Molybdenum Deposits

These low grade, disseminated copper deposits are generally centered on composite stocks or related to the late phases of large plutons. Small, high level stocks showing a porphyritic texture and tonalite-monzonite composition are generally favourable hosts for such mineralisation in the Andes (Sillitoe, 1973). Centered on these stocks are concentric zones of potassic, phyllic and occasionally argillic alteration with an extensive outer zone of propylitic alteration which can be used as exploration guides to these deposits (Lowell and Guilbert, 1970). Disseminated chalcopyrite and molybdenite occurs in the host intrusive, generally in the phyllic zone. Halos of Pb-Zn-Ag mineralisation are uncommon around these deposits in the western part of Chile, for example El Salvador and El Teniente. Further east, however, where the porphyry copper deposits occur in the polymetallic belt, they have halos of Pb-Zn-Ag mineralisation (Sillitoe, 1976), notable deposits among this type are Michiquillay in Peru and Paramillos in Argentina. Porphyry molybdenum deposits are less common in the Andes than in western North America, although several important occurrences are known in South America (Los Loros in Chile) (Sillitoe, 1973).

Porphyry copper and molybdenum deposits have been found on the Antarctic Peninsula, along the western coast of Graham Land at Argentine Island and Anvers Island. In the South Shetland Islands (Livingstone Island) the porphyry copper-molybdenum deposit at Charity Glacier has a polymetallic Pb-Zn-Ag halo . Molybdenum is common in all examined deposits. Other areas, notably Anvers Island show extensive alteration zonation characteristic of porphyry copper mineralisation. The known porphyry copper-molybdenum deposits on the Antarctic Peninsula occur in a longitudinal belt which runs along the west coast of Graham Land, probably with a maximum width of 150km.

Polymetallic Deposits

These Cu-Pb-Zn-Ag deposits are associated with small isolated stocks ranging in composition from diorite to adamellite. Host rocks to these deposits in the Andes are marine sedimentary rocks containing some limestones but some are calc-alkaline lavas of Tertiary age. Some deposits occur in veins, notably El Tontal in Argentina, whereas others are of the contact metasomatic type, for example Antamina in Peru, and still others are a combination of the two types, notably Morococha in Peru. The vein type is more common in volcanic rocks and the skarn ore bodies are localised in calcareous rocks (Bellido and de Montrevil, 1972). Porphyry Pb-Zn-Ag deposits have been described in southern Bolivia (San Cristobal) occurring as disseminations and breccia.infillings (Jacobson et al, 1969). Other elements frequently associated with these deposits, notably Cerro de Pasco in Peru are Sn, Cd, I, Se, Te, Hg, Bi and Ge. The main metals found in these deposits are Cu, Pb, Zn and Ag and some districts show a metallogenetic zonation (Petersen, 1970). These deposits occur in a belt running approximately N-S through eastern Chile and Argentina.

Veins of Pb-Zn-Ag mineralisation found in association with intermediate plutonic rocks, have been described on the Danco Coast (Vieira et al, 1978) and Livingstone Island in the South Shetland Islands (Valle et al, 1975) with Zn mineralisation recorded at Postillion Rock in Neny Fjord (Hoskins, 1963). These occurrences suggest that a polymetallic belt, running approximately N-S is present in the Peninsula, with the Grandier Channel as its westward limit.

Volcanogenic Iron Deposits

Magnetite-hematite deposits of volcanogenic origin have been described by Park (1961) and Ruiz et al (1965), notable among which is El Laco in Chile. This deposit consists of iron oxides with minor apatite and actinolite occurring as flows and feeder structures related to andesitic volcanoes of Pleistocene age (Frutos and Oyarzun, 1975). Magnetite-hematite flows of presumed Pleistocene age have been described on Brabant Island (Vieira et al, 1978) which appear to be identical to those in the Andes mentioned above.

Red Bed Copper and Uranium Deposits

Red bed deposits are generally stratiform, lens-shaped bodies occurring in bleached sandstone or conglomerate beds. Minerals normally found in these deposits include chalcocite, native copper and hematite accompanied by minor Pb, Ag, V and U. Notable deposits in the Andes are Corocoro and El Cucho in Chile in molasse type sequences. The source of the metals appear to be interbedded tuffs and lavas, or the Red Beds themselves, some being rich in volcanic components (Petersen, 1965; Papenfus, 1931). Hematised sandstones of Cretaceous age occur in northern Palmer Land, which from the petrographic and field descriptions appear to be red beds (Anckorn, 1975) and could contain the above type of mineralisation.

Tin-Tungsten and Tin-Silver Deposits

The tin-tungsten vein deposits of the eastern Bolivian cordillera occur at the contact of batholithic intrusions and to some extent in them, and are mainly Mesozoic in age. Notable deposits include Milluri and Araca. The veins consist mainly of quartz, cassiterite, wolframite and scheelite, (Ahlfeld and Schneider-Scherbina, 1964). The tin-silver deposits of southern Bolivia appear to be spatially

related to subvolcanic dacitic to quartz-latite stocks (for example Avicaya and Colquechaca) and are late Tertiary in age (Turneaure, 1960). Veins of this type sometimes occur superimposed on porphyry tin deposits (Ahlfeld and Schneider-Scherbina, 1964). Porphyry tin deposits have been described in the Andes (Oruro and Chocaya in southern Bolivia) (Sillitoe et al, 1975).

Tin mineralisation of unusual occurrence is present on the Peninsula on Alexander Island. Veinlets of ? cassiterite, penninite, quartz and albite occur in hornfelsed sedimentary rocks adjacent to Cretaceous plutonic intrusions. However, if tin mineralisation is present along the Antarctic Peninsula itself it seems most likely to occur along the eastern side of Graham Land where fluorite mineralisation has already been recorded on the Bowman and Wilkins Coast (Fraser and Grimley, 1972) and the Oscar II Coast (Fleet, 1968). Fluorite normally occurs behind the tin-tungsten mineralisation in an Andean type plate margin (Garson and Mitchell, 1977).

Carbonatites

When South America and Africa seperated in the Gondwanaland break-up, intrusion of carbonatites accompanied rifting in areas either side of the rift zone due to changes in the spreading rate during the development of the Atlantic Ocean (Macintyre, 1977). Intrusion of carbonatites may have occurred in the Antarctic (most probably East Antarctica) where such rifting was also present.

Residual and Alluvial Deposits

Lateritic and Bauxitic deposits have been found in the Andes (Goossens, 1972) but are unlikely to be present in the Antarctic Peninsula, since being porous and soft and occurring at a relatively high level, they will probably have been removed by glacial erosion. Since the end of the Pleistocene ice age, temperatures have been too

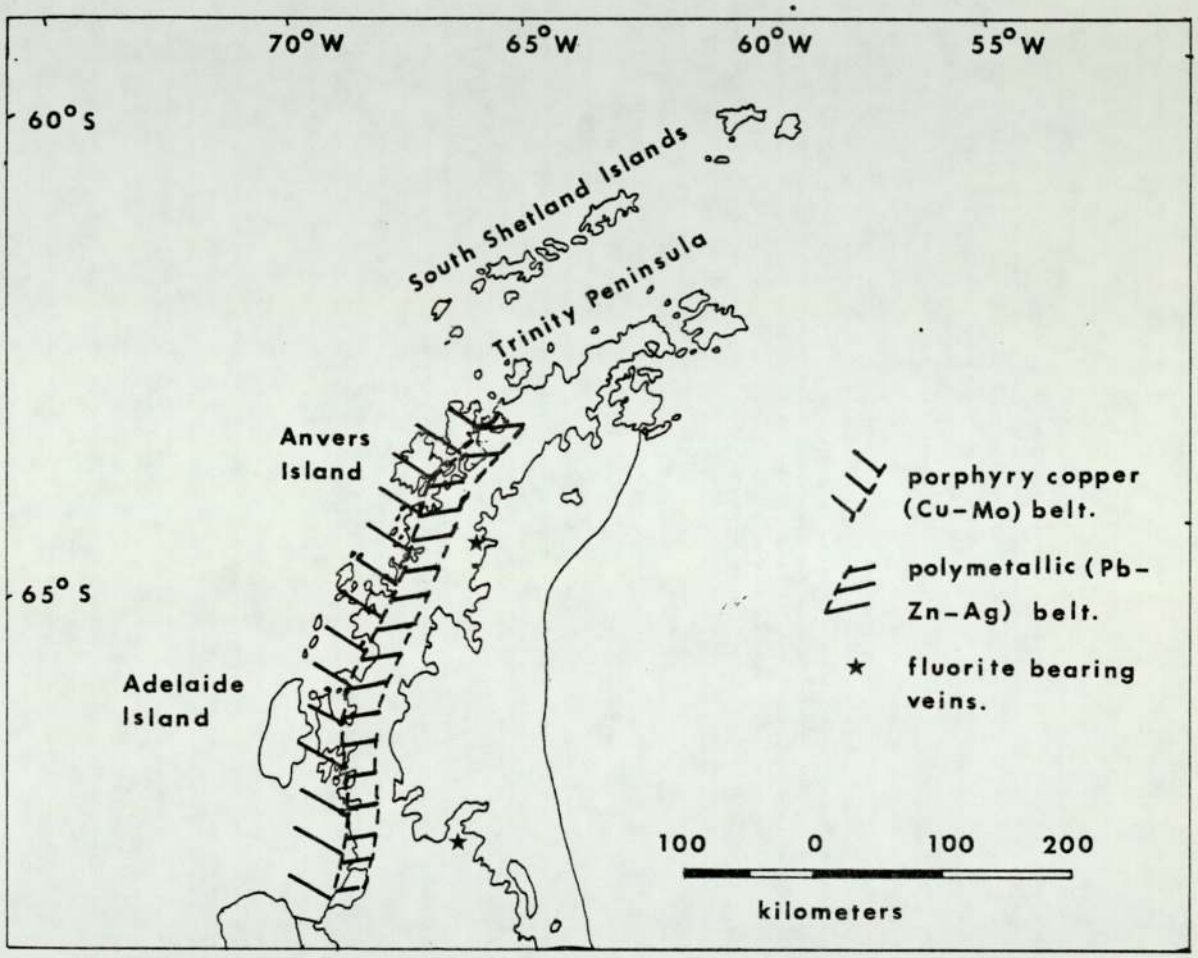

FIG.8:1 DIAGRAM SHOWING METALLOGENETIC BELTS IN THE WESTERN ANTARCTIC PENINSULA.

low for significant deposits to have formed in the recent past.

8.4 Zonation

Zonation of metals in the Antarctic Peninsula is not clear mainly due to the limited data available at present. However, preliminary work does suggest that there is a broad east to west metal zonation, with a porphyry copper-molybdenum belt running approximately N-S from Anvers Island to the Wordie Ice Shelf area, which is followed inland by a polymetallic lead, zinc, copper silver belt (Fig. 8:1). Only further detailed work can elucidate the precise boundaries of these belts which may be complex due to changes in the underlying subduction zone, by comparison with the Andes (Sillitoe, 1976).

8.5. Lineaments

Lineaments and intersections of lineaments have been suggested to be responsible for localizing igneous activity and producing patterns of mineralisation, especially in the cordillera of the Western U.S.A. (Kutina, 1969; Jerome and Cook, 1967; Heyl, 1972), although some authors reject their significance (Gulluly, 1976). Inevitably, faults, fractures and drainage patterns are the only features visible on the surface which could account for the localisation of ore deposits and intrusives. In North America, however, geophysical evidence tends to confirm the existence of deep linear trends that reflect basement structures (Stewart et al, 1977) and those important for metallogeny often date far back in geological time and have been repeatedly re-activated (Billingsley and Locke, 1941).

In the Antarctic Peninsula, faults and fractures are the only visible guide to possible ore deposits, since drainage patterns have not had time to develop, and were they to do so they would be guided by the glacial topography. The transverse faults on the sea floor

(Herron and Tucholke, 1976) north west of the Antarctic Peninsula, presumably continue down the Benioff zone, where the sea floor has been subducted, and these may have acted as channelways for fluids percolating up through the mantle into the crust. Evidence for this is found in the fact that all the known ore deposits on the Antarctic Peninsula occur (to within 50km.) of the region where these faults would underlie Graham Land, on the subducted crust, notable among which are Anvers Island and Marguerite Bay. Indeed, the largest of these faults (Tula Fracture Zone) passes under northern Palmer Land approximately at the point where the Antarctic Peninsula widens in area, and should be a favourable region of mineralisation.

8.6 Source of the Metals

Ore forming elements can be derived from above or below the Moho (Krauskopf, 1967) or by single or multiple stage processes involving pre-enrichment of crustal rocks (Krauskopf, 1971). Lowell (1974) has suggested that in North America metals may originate from copper rich parts of the Pre-Cambrian crust in which massive sulphides occur, and that these metals have produced the Laramide porphyry copper deposits. Garson and Mitchell (1977) suggest that extraction of copper from pre-ore rocks intruded by calc-alkaline plutons is achieved by a circulating meteoric water system, with the plutons simply acting as "heat engines". In magmatic arcs related to subduction processes, the ore metals are thought to have originated with the magmas which formed as partial melts from subducted oceanic crust and sediments (Hollister, 1975; Sillitoe, 1972), from the overlying upper mantle or by partial melting of lower continental crust, with or without significant differentiation or contamination. There is now evidence for metal accumulation or enrichment at mid-ocean ridges, for example the East Pacific Rise or

Red Sea (Ridge, 1973; Bonatti et al, 1976) which have presumably come directly from the upper mantle. These metals are also contained in sediments or manganese nodules which are taken down the Benioff Zone and the metals then expelled in hydrothermal fluids due to heating of the decending plate (Mitchell, 1977). The association of most ore deposits with acid intrusives in the Antarctic Peninsula suggested ore forming fluids originated from them during crystallisation. Indeed, felsic magmas can contain up to 10% water (Burnham, 1967). Sillitoe (1971) has suggested that most fluids come from the mantle and that areas of continental crust overlying such "anomalous" mantle should be rich in ore deposits. Mantle cells and the circulation of material in the mantle, probably plays a large part in the generation of metal bearing fluids (Walker, 1972).

The sulphur also present in association with these metals was probably derived as residual aqueous fluids from the crystallising silicic intrusives, or by leaching of pre-ore rocks by circulating meteoric water (Garson and Mitchell, 1977) or possibly by late stage leaching of biotite in the host plutons (Banks, 1973). It is probable that the ore deposits on the Antarctic Peninsula are related to the metal distribution in the subducted oceanic crust as in the Andes (Sillitoe, 1973), the mineralisation originating from metal rich muds, Cyprus-type massive sulphides or copper rich tholeiites decending along the Benioff Zone. Evidence from magnetite-hematite flows in Chile, and the presence of numerous porphyry molybdenum deposits in continental North America and not in Island Arc environments indicated some metals are derived by re-mobilisation of continental crust (Sillitoe, 1976). The presence of abundant molybdenum in the porphyry copper-molybdenum deposits of the Antarctic Peninsula may indicate that continental crust,

which probably underlies this region may have played a large part in the derivation of the ore forming fluids as well as the generation of the host plutonic bodies.

8.7 Age of Mineralisation

From a preliminary study of the metalliferous mineralisation in the Western Antarctic Peninsula, all the known ore deposits occur in association with granitoid plutonic rocks which range in age from 100 - 40 my (Rex, 1976). This indicates the ore deposits are late Cretaceous to early Tertiary although the plutonic bodies found on the Antarctic Peninsula range from Upper Jurassic to late Tertiary (Rex, 1976). These facts suggest that the known ore deposits formed during a distinct metallogenetic epoch, related to subduction of the southeast Pacific Plate beneath the Antarctic Peninsula and that generation of metals was produced by a process related to but not identical with partial melting that produced the felsic magmas. Deposits not directly related to plutonism on the Antarctic Peninsula, for example the magnetite-hematite flows of Brabant Island have been assigned a Pleistocene age (Vieira et al, 1978), although with little supporting evidence for such a conclusion.

APPENDIX I

A.1 SAMPLE SELECTION AND PREPARATION FOR CHEMICAL ANALYSIS

Specimens were selected for analysis which showed few signs of weathering. Sections of the samples were then cut using a 12" diamond saw, and the edges removed and discarded. Thus only the inner, unaltered parts of the specimens were used for analysis.

The samples were then crushed, into 0.5 cm (on average) fragments using a jaw crusher with hardened steel jaws, which was mounted in a dust extraction cabinet. The crushed rock was collected on a fibre glass tray and placed into labelled polythene sample bags.

Approximately 500g of sample was taken from the material collected in the jaw crusher and ground, in 200g lots, in a 'Tema' swing mill equipped with a 100 ml tungsten carbide grinding barrel.

The samples were reduced to 60 - 200 mesh by grinding for 30 seconds. The sample was then split using a stainless steel sample splitter, and 200 g of this was taken and re-ground for $2\frac{1}{2}$ minutes in the 'Tema' mill to reduce the average grain size to below 200 mesh. The samples were then sieved to 200 mesh and stored in labelled polythene bags.

The 'Tema' mill barrel and grinding rings were cleaned between each specimen by washing in warm tap water, and dried with a compressed air jet.

The sample splitter was cleaned using a compressed air jet in a dust extraction cabinet.

A.2 SAMPLE PREPARATION FOR ELECTRON MICROPROBE ANALYSIS

Polished and thin sections (ground with $\frac{1}{4}\mu m$ paste) were coated with a thin layer of carbon (50 - 100 Å) to provide electrical conductivity of the specimen. The carbon coating was produced by

isolating the specimen in a vacuum and striking an electrical arc between two carbon electrodes. An arc of 4 - 5 seconds produced a layer of carbon of suitable thickness on the specimen.

APPENDIX 2

A.2.1. CHEMICAL ANALYSIS

2.1.1 SAMPLE DISSOLUTION

a) Andesite lavas, Tertiary plutonic rocks and "Quartz-Pyrite" Rocks

Major Elements

A metaborate fusion method was used for the determination of major elements in these rocks (Si, Al, Ti, Ca, Mg, Fe, Na, K and Mn).

0.1g of sample was added to about 1g of lithium metaborate in a graphite crucible. The sample was mixed thoroughly and then heated to 1000°C in a muffle furnace for fifteen minutes. When fusion was complete, the molten mass was poured into dilute HCl (15% v/v HCl), and the solution was agitated on a magnetic stirrer until all the metaborate had dissolved. The solution was diluted to 200 mls and then filtered into plastic containers for storage. A blank solution was used to determine the levels of impurities in the chemicals used in the dissolution of these rocks.

The diluted solutions were used directly for the determination of Si and Al, and diluted five times for the determination of Ca, Mg, Ti, Fe, Na, K and Mn. Calculation of the weight per cent element in the original rocks were as follows:-

$$\text{Wt.\% element} = \frac{\text{ug/ml solution x dilution factor x 0.02}}{\text{gm sample}}$$

These figures were converted into % oxides by multiplication by the relevant factor $\frac{M\ O}{M}$ where M is the metal and O is oxygen.

Trace Elements

To 1g of the powdered rock sample in a teflon beaker was added 10 mls of conc. HF, followed by 20 mls of conc. HCl and 15 mls of conc. HNO_3. The sample was allowed to dissolve, and then heated to dryness on a water bath. 5mls of perchloric acid were then added and the sample heated on a hot plate until fumes of Cl_2O_7 were evolved. Once this fuming stopped, and all fluorides had been volatilised the beaker was allowed to cool. The residue was then dissolved in 20 mls of 50% HCl and heated until dissolution was complete. The solution was filtered and diluted to 100 mls.

$$\text{Wt.\% element} = \frac{\text{ug/ml of solution} \times 0.01 \times \text{dilution factor}}{\text{grams of sample}}$$

$$\text{ppm element} = \text{Wt.\% element} \times 10^4$$

Elements determined by this method were Cd, Cr, Cu, Mo, Ni, Pb, Se, Sr, Te, V and Zn.

b) Sulphide Minerals

To 0.3g of the powdered sulphide 10 mls of 10% tartaric acid were added and 6 mls of conc. HNO_3. The solution was left to stand at room temperature overnight, and then heated on a steam bath for 2 - 3 hours until the precipitate of sulphur turned white. The residue was filtered and washed, the filtrate being collected in a 100 ml volumetric flask and diluted to the set volume. A blank solution containing only the chemical reagents was also analysed.

Elements determined on pyrite, chalcopyrite and bornite were Co, Cu, Mn, Ni, Pb, Se and Zn.

$$\text{ppm element} = \frac{\text{ug/ml in sample} \times 10^2}{\text{grams of sample}}$$

c) Gold Analysis on Rocks and Sulphides

To 10g of the powdered sample in a beaker was added 25 mls of conc. HCl, and after digesting for 15 minutes on a hot plate, a further 15 mls of conc. HNO_3 were also added. After 25 minutes digestion, 25 mls of conc. HCl and 25 mls of water were added and the solution boiled to expel oxides of nitrogen. The solution was cooled, filtered and diluted to 100 mls in a volumetric flask.

$$\text{ppb Au} = \frac{\text{ug/ml of solution} \times 10^4}{\text{grams of sample}}$$

d) Magnetite

To 0.5 g of magnetite were added 25 mls of conc. HCl, and the sample allowed to dissolve by heating on a hot plate. Once solution was complete, the iron was oxidised to Fe^{III} by dropwise additions of conc. HNO_3 until the frothing ceased. The solution was diluted to 100 mls and filtered into a plastic container.

$$\text{Wt.\% element} = \frac{\text{ug/ml of solution} \times 0.01 \times \text{dilution factor}}{\text{grams of sample}}$$

$$\text{ppm element} = \text{Wt.\%} \times 10^4$$

2.1.2 ATOMIC ABSORPTION ANALYSIS

In all of the present work a Perkin Elmer model 460 double beam, atomic absorption spectrophotometer (A.A.S.) equipped with a chart recorder read out was used.

In A.A.S. analysis there are a number of interferences that produce a non-linear calibration curve of concentration against absorbance. The two types relevant to the present work are ionisation interference and matrix interference.

In ionisation interference the population of neutral atoms of a given element in the flame (absorbing atoms) is influenced by the concentration of other more easily ionised elements. Also ionisation of a particular element can occur which reduces the population of neutral atoms leading to reduced sensitivity. This can be overcome by adding an excess of an easily ionised element that is completely ionised in the flame. Sodium citrate was added as an ionisation supressor.

Matrix interference has the effect of increasing the absorption of a particular element due to salts in solution drying out in the flame to form solid particles. These particles produce an apparent effect by physically obstructing the light beam. This was overcome by dilution of the solution to reduce the concentration of the matrix or using standards of similar matrix.

Matrix interferences occurred only with trace elements, these being Cu, Ni, Zn, Pb and Sr. Si, Al and Fe were determined directly against an aqueous standard without dilution.

Standard metal solutions were prepared from "spec-pure" compounds dissolved in A.R. acid to produce a concentration of 1000ppm, except Si where a concentration of 4,000ppm was used. The standard compositions are given below:-

Standards of the trace elements (Cu, Ni, Sr, Pb and Zn etc.) were prepared with a concentration of 100ppm. These 100ppm standards were prepared as required from 1,000ppm standards by dilution.

	compound used	solvent	conc.
Si	SiO_2	water	4,000
Al	Al metal	1% HCl	1,000
Ti	Ti metal	50% HCl	1,000
Mg	Mg metal	1% HCl	1,000
Ca	Ca CO_3	1% HCl	1,000
Fe	Fe metal	2.5% HNO_3	1,000
Mn	Mn metal	1% HCl	1,000
Na	Na Cl	water	1,000
K	K Cl	water	1,000
Au	Au metal	5% HCl	1,000
Cd	Cd metal	1% HCl	1,000
Co	Co metal	1% HCl	1,000
Cr	$K_2Cr\ O_4$	water	1,000
Cu	Cu metal	1% HNO_3	1,000
Mo	$(NH_4)_6\ Mo_7\ O_{24}.4H_2O$	1% NH_4OH	1,000
Ni	Ni metal	1% HNO_3	1,000
Pb	Pb $(NO_3)_2$	1% HNO_3	1,000
Se	Se metal	10% HCl	1,000
Sr	Sr $(NO_3)_2$	1% HNO_3	1,000
Te	Te metal	1% HCl	1,000
V	V metal	1% HNO_3	1,000
Zn	Zn metal	1% HCl	1,000

Instrument Settings

Instrument settings used in the present work were taken from the 1976 edition of the Perkin-Elmer Atomic Absorption Handbook. The settings varied from element to element and are given below:-

	flame	wavelength	slit width
Si	N_2O/C_2H_2	251.6 nm	0.2 nm
Al	"	309.3 nm	0.7 nm
Ti	"	365.3 nm	0.2 nm
Mg	Air/C_2H_2	285.2 nm	0.7 nm
Ca	"	422.7 nm	0.7 nm
Fe	"	248.3 nm	0.2 nm
Mn	"	279.5 nm	0.2 nm
Na	"	589.6 nm	0.7 nm
K	"	766.5 nm	2.0 nm
Au	"	242.8 nm	0.7 nm
Cd	"	228.8 nm	0.7 nm
Co	"	240.7 nm	0.2 nm
Cr	"	357.9 nm	0.7 nm
Cu	"	324.8 nm	0.7 nm
Mo	N_2O/C_2H_2	313.3 nm	0.7 nm
Ni	Air/C_2H_2	232.0 nm	0.2 nm
Pb	"	283.3 nm	0.7 nm
Se	"	196.0 nm	2.0 nm
Sr	"	460.7 nm	0.7 nm
Te	"	214.3 nm	0.2 nm
V	N_2O/C_2H_2	318.4 nm	0.7 nm
Zn	Air/C_2H_2	213.9 nm	0.7 nm

At least three standard concentrations were used for each analysis. Standards were run before and after each set of unknowns, with no more than nine unknowns being run between the sets of standards. Blank solutions were used to correct for matrix absorption. Corrections for blank absorbance and matrix effects were made by the A.A.S. machine before printing the concentration values.

Accuracy of the method

Rock standards were used in the determination of these results, which have a similar composition to the analysed rock specimens. An aplitic granite (Q.M.C.11) was used as standard for tonalite analysis and a dolerite (Q.M.C.13) was used as a standard for the calc-alkaline lavas and "Quartz-Pyrite" rocks. All these results were within ± 6% of the accepted values (see below):-

Q.M.C. 11 (aplitic granite)		Result	Q.M.C. 13 (dolerite)	Result
SiO_2	75.45	74.40	49.65	49.00
Al_2O_3	13.94	14.00	13.07	12.90
TiO_2	0.04	0.02	2.66	2.70
Fe_2O_3	0.53	0.48	16.25	16.30
MnO	0.03	0.04	0.23	0.30
MgO	0.095	0.10	4.20	4.10
CaO	0.80	0.76	8.21	8.30
Na_2O	4.60	4.40	2.92	2.88
K_2O	4.32	4.42	1.45	1.50

Trace elements (ppm)

	Q.M.C. 11	Result	Q.M.C. 13	Result
Co	3	4	32	38
Cr	4	6	24	20
Cu	9	10	180	190
Ni	8	10	14	10
Pb	80	100	10	8
Sr	200	180	260	270
V	15	16	400	420
Zn	20	18	100	130

2.2 X-RAY DIFFRACTION ANALYSIS

X-ray diffraction analysis was used to determine the nature of various mineral phases encountered in the present work.

The particular X.R.D. machine used was a Philips 1130 X-ray generation unit, coupled with a P W 1370 goniometer controller and a 800300 recorder.

For the mineral determinations the sample was scanned from between 2°- 80° 2θ generally at $\frac{1}{2}^{\circ}$ per minute, with the graph paper on the chart recorder moving at 10 mm per minute.

During the determinations, the recorder was set at the following:- time constant 0.4 sec., lower level 2.1, window 1.5, and attenuation X3.

The Cu tube which operated at 40 ku and 40 ma was used as the X-ray source for non-ferrous minerals, whilst the Co tube which operated at 30 kv and 30 ma was used for the identification of ferrous minerals.

The samples for analysis were ground in an agate mortar until fine enough to be placed into the aluminium holder used in the XRD machine.

2.3. POINT COUNTING

A Swift automatic point counter was used to determine the proportion of minerals in both polished and thin sections.

The point counter had a N-S movement of 0.16 mm and an E-W movement of 0.3 mm.

All determinations were carried out using at least 1,000 points.

2.4 REFLECTIVITY MEASUREMENTS OF OPAQUE MINERALS

A Reichert Zetopan microscope fitted with a sepectral reflectometer was used to determine the reflectivities of the opaque minerals in the rocks under study. All measurements were carried out at 589 nm.

Once placed under the microscope and focused, the aperture was

reduced until only the mineral for identification was in view, and then a determination done. The reading for the unknown mineral was then compared with two Zeiss standards; SiC (reflectivity of 20.6% at 589 nm) and W Ti C (reflectivity of 48.7% at 589 nm), which were placed under the microscope objective without altering any settings.

2.5 INDENTATION MICROHARDNESS

A Vickers M73 mircrohardness tester was used for these determinations. Using a X40 objective, the reading at the filar micrometer plane is X120, and this reading was calibrated using a stainless steel microgrid with 0.1 mm divisions. The reading was adjusted by means of a graduated eye-piece draw tube.

The relationship between Vickers Hardness Number (VHN) and micrometer reading is as follows:-

$$V.H.N. = \frac{1854 \times P}{d^2} \ Kg/mm^2$$

where P = load applied in grammes and d = average length of the diagonal in microns.

2.6 ELECTRON MICROPROBE ANALYSIS

Electron microprobe analysis of magnetites from the Argentine Islands and biotites from Charity Glacier, Livingstone Island have been achieved using a Microscan V.

The specimen current for each sample was 0.5×10^{-7} ma, at a voltage of 15 kv for the magnetites and 20 kv for the analysis of biotites. The pure metal standards were used for each element, except sulphur where pyrite was used as the standard. Crystals used in each counter and Bragg angle of counter to the specimen for each element is listed below:-

Element	Crystal	Bragg Angle
Fe	Li F	57° 29'
Mn	Li F	62° 56'
Pb	Li F	33° 56'
Ni	Li F	48° 38'
Ti	P E T	36° 39'
Cr	P E T	30° 21'
V	P E T	36° 39'
S	P E T	75° 49'
K	P E T	50° 40'
Al	R.A.P	37° 14'
Si	R.A.P	31° 40'
Mg	R.A.P	44° 30'

Li F Lithium fluorite

P E T Pentethylratrol

R.A.P Rubidium acid thalate.

A correction factor was applied to the counts obtained for the specimen and standard for lost counts due to atomic number, absorption and fluorescence corrections.

(dead time)

where % element = $\left(\frac{\text{counts for specimen + dead time}}{\text{counts for standard + dead time}}\right)$ x 100

The figures were then put in a computer programme and corrections made for matrix factors due to the standard and sample being in different atomic matrics, and, therefore, having different absorption factors. The computer programme was provided by J. Ashworth.

REFERENCES

1. ADIE, R.J. (1953) — The rocks of Graham Land. Univ. Cambridge Ph.D Thesis. 259 pp.

2. ADIE, R.J. (1954) — The Petrology of Graham Land 1:- The Basement Complex, early Palaeozoic plutonic and volcanic rocks. Falkland Islands Dependencies Surv. Sci. Rept., No.11 22 pp.

3. ADIE, R.J. (1955) — The Petrology of Graham Land 11:- The Andean Granite-Gabbro intrusive suite. Falkland Islands Dependencies Surv. Sci. Rept., No. 12 39 pp.

4. ADIE, R.J. (1957) — The Petrology of Graham Land 111:- The metamorphic rocks of the Trinity Peninsula Series. Falkland Islands Dependencies Surv. Sci. Rept., No. 20 26 pp.

5. ADIE, R.J. (1964) — Geologic History in Priestley, R., Adie. R.J., and Robin, G.deq., eds. Antarctic Research: London, Butterworths, p. 118-162.

6. ADIE, R.J. (1972) — Evolution of volcanism in the Antarctic Peninsula, in Adie. R.J., ed. Antarctic Geology and Geophysics: Oslo, Universitetsforlaget, p. 137-142

7. ADIE, R.J. (1972) — The Geochemistry of Graham Land. in Adie. R.J., ed. Antarctic Geology. Cape Town, North-Holland Amsterdam. p. 541-550.

8. AGUIRRE, L., and MEHECH, S. (1964) — Stratigraphy and mineralogy of the manganese sedimentary deposits of Coquimbo Province, Chile: Econ. Geol., 59 p. 428-442.

9. AHLFELD, F. and SCHNEIDER-SCHERBINA, A., (1964) — Los yacimientos minerales y de hidrocarburos de Bolivia: La Paz, Depto. Nacional de Geologia, Bolivia 5 388 pp.

10. AITKENHEAD, N. (1965) — The Geology of the Duse Bay-Larsen Inlet area, north-east Graham Land. British Antarctic Survey Sci. Rept., 51 62 pp.

11. ALLEN, E.T., and DAY, A.L. (1935) — Hot Springs of the Yellowstone National Park: Carnegie Institute Washington Publication no. 466

11a. ANCKORN, J.F. (1975) — The Geology of N. E. Palmer Land, Antarctica, MSc. Thesis, Univ. of Birmingham.

12. ANDERSSON, J.G. (1906) On the Geology of Graham Land. Uppsala Univ. Geol. Inst. Bull., 7 p. 19-71.

13. ANDERSON, C.A. (1935) Alteration of the lavas surrounding the Hot Springs in the Lassen Volcanic National Park. American Mineralogist 20 p. 240-252.

14. ANDERSON, A.T. (1968) Oxidation of the La Blache Lake titaniferous magnetite deposit, Quebec. Journ. Geol., 76 p. 528-541

15. ANGELELLI. V., FERNANDEX LIMA, J.C., HERRERA, A., and ARISTARAERI. L., (1970) Descripcion del mapa metalogenitico de la Republica Argentina. Minerales metaligerous: Buenos Aires, Direc. Nacional de Geologio y Mineria, 193 pp.

16. ANHAEUSSER, C.R. (1976) Archean Metallogeny in Southern Africa, Econ. Geol., 71 p. 16-43.

17. ARAYA, R., and HERVE, F., (1966) Estudio geomorfologies y geologico en las Islas Shetland del Sur, Antarctica. Publnes Inst. Antarctico Chile No. 8 p. 1-15

18. ARNOLD, R.G., (1962) Equilibrium relations between pyrrhotite and pyrite from 325°- 743°C. Econ. Geol., 57 p. 72-90.

19. ARNORSSON, S., HAWKES, H.E., and TOOMS, J.S. (1973) Present day formation of pyrite in hot springs in Iceland. Trans. Inst. Mining. Metallurgy Section B. 76 p. B115-B117.

20. ASHCROFT, W.A., (1972) Crustal Structure of the South Shetland Islands and Bransfield Strait. British Antarctic Survey Sci. Rept., 66 43 pp.

21. AYLING, M.E., (1977) The Geology of the "St. Valentines" area and related observations in the Batterbee Mountains, Palmer Land. Univ. Birmingham Ph.D. Thesis.

22. BANKS, N.G., (1973) Biotite as a source of some of the sulphur in porphyry copper deposits. Econ. Geol., 68 p. 697-702.

23. BAKER, P.E., (1970) Plate tectonics of the Scotia Sea region. Nature 228 p. 1293-1296.

24. BAKER, P.E., (1972) Recent Volcanism and Magmatic Variation in the Scotia Arc, In; Adie, R.J., ed. Antarctic Geology and Geophysics: Oslo. Universitetsforlaget p. 57-60

25. BARKER, P.F., and GRIFFITHS, D.H. (1972) The evolution of the Scotia Ridge and Scotia Sea. Philos. Trans. Roy. Soc. London. Series A., 271 p. 151-183

26. BAKER, P.E., (1974) Volcanism and Plate Tectonics in the Antarctic Peninsula and Scotia Arc. International Symposium on Volcanology. Santiago, Chile. Institute Geographico. Militar. p. 1-9.

27. BARKER, P.F., and GRIFFITHS, D.H. (1977) Towards a more certain reconstruction of Gondwanaland. Philos. Trans. Roy. Soc. London B279 p. 143-159.

28. BAKER, P.E., and REX, D.C., (1973) Age and petrology of the Cornwallis Island granodiorite. British Antarctic Survey Bulletin 32 p. 55-62

29. BARTON, C.M. (1963) Geology of King George Island, South Shetlands. Ph.D. Thesis. Univ. Birmingham.

30. BARTON, C. M. (1964) The Geology of the South Shetland Islands III. The Stratigraphy of King George Island. British Antarctic Survey Sci. Rept., 44 33 pp.

31. BARNES, H.L. (1962) Mechanisms of mineral zoning. Econ. Geol., 57 p. 30-37.

32. BARROW, J. (1931) Introductory note (to an article on the Islands of Deception). Roy. Geog. Soc., 1 p. 62.

33. BAYLY, M.B., (1957) The Geology of the Danco Coast, Graham Land. Falkland Islands Dependencies Survey Preliminary Rept., No. 1 33 pp.

34. BELL, C.M., (1973) Geology of parts of Alexander Island. Univ. Birmingham Ph. D. Thesis.

35. BELL, C.M. (1973) The Geology of the Beethoven Peninsula, south western Alexander Island. British Antarctic Survey Bulletin 32 p. 75 - 84.

36. BELL, C.M. (1973) The Geology of southern Alexander Island. British Antarctic Survey Bulletin 33 p. 1-16.

37. BELL, C.M., (1974) Geological observations in northern Alexander Island. British Antarctic Survey Bulletin 39 p. 35-44.

38. BELLIDO, E., and de MONTREUIL, L. (1972) Aspectos generales de la metalogenia de Peru; Lima, Servicio de Geologia y Mineria Geologia Economica, No. 1 149 pp.

39. BERGER, A.R., (1971) The origin of banding in the main Donegal Granite, north west Ireland. Geol. Journ., 7 p. 437-58.

40. BIBBY, J.S. (1961) The Geology of Escurra Inlet and Point Thomas, Admiralty Bay, King George Island, South Shetlands. Falkland Islands Dependencies Survey, Preliminary Rept., No. 8.

41. BIBBY, J.S. (1960) The Geology of Joinville Island. Falkland Islands Dependencies Survey, Preliminary Rept., No. 7.

42. BIBBY, J.S. (1961) The Geology of James Ross Island and the Bald Head - Crystal Hill - Church Point area, Trinity Peninsula, Graham Land. Falkland Islands Dependencies Survey Preliminary Rept., No. 9.

43. BIBBY, J.S. (1966) The stratigraphy of part of north east Graham Land and the James Ross Island Group. British Antarctic Survey Sci. Rept., 53 37 pp.

44. BILLINGSLEY, P. and LOCKE, A. (1941) Structure of ore districts in the continental framework. Trans. American Inst. Min. Metall. Engrs. 144 p. 9 - 64.

45. BIRNIE, R.W. and HALL, J.H. (1974) The Geochemistry of El Misti volcano, Peru Fumaroles. Bull. Volcanologique, 37 p. 1-15.

46. BONATTI, E. HONNORES, B.M.G., HONNORES, J. (1976) Copper-iron sulphide mineralisations from the equatorial Mid Atlantic Ridge. Econ. Geol., 71 p. 1515-1525.

47. BOWEN, R. and GUNATILAKA, A. (1977) Copper: Its Geology and Economics. Halsted Press. John Wiley and Sons 366 pp.

48. BOWES, D.R., and WRIGHT, A.E. (1961) An explosion breccia complex at Buck Settlement, near Kentallen, Argyl. Trans. Eding. Geol. Soc., 18 p. 293-314.

49. BRANCH, C.D. (1976) Development of porphyry copper and stratiform volcanogenic ore bodies during the life cycle of andesitic stratovolcanoes in Volcanism in Australasia, Elsevier Scientific Publications. Johnson, R.W. ed. p. 337 - 342.

50. BUDDINGTON, A.F. and LINDSLEY, D.H. (1964) Oxide minerals and synthetic equivalents. Journ. Petrology 4 p. 310 - 350.

51. BURBANK, W.S. (1950) Problems of wall rock alteration in shallow volcanic environments. Quart. Colorado School Mines. 45 p. 287 - 319.

52. BURKE, E.A.S., and UYTENBOGAARDT, W. (1971) Tables for micorscopic identification of ore minerals. Elsevier Publishing Corpn. 430 pp.

53. BURNHAM, C.W. (1967) Hydrothermal fluids at the magmatic stage. In Barnes, H.L. ed. Geochemistry of hydrothermal ore deposits. Rinehart and Winston. Publishers.

54. BUTLER, B.S. (1956) Mineralising solutions that carry and deposit iron and sulphur. Trans. American Inst. Min. Engrs., 205 p. 1012 - 1017.

55. CABALLERO, M.A. and FOURCADE, N.H. (1958) Observaciones Geologicas en Caleta Copper Mine, Islas Shetland del Sud, Antarctida Argentina. Contribucion No. 23 Instituto Antarctico Argentino 33 pp.

56. CABRI, L.J., (1973) New data on phase relations in the Cu-Fe-S system. Econ. Geol., 68 p. 443 - 54.

57. CAMINOS, R., MARCHESE, H.G., MASSABIC, A.C., MORELLI, J.R., RINALDI, C.A., and SPIKERMANN, J.P. (1968) Geologia del sector norroccidental de la Peninsula Hurd, Isla Livingston, Shetland del Sur, Antartida Argentina. Contribucion del Instituto Antartico Argentino No. 162 32 pp.

58. CARMICHAEL, I.S.E., and AL-RAEI, YEHYA (1967) A note on the natural fusion of granite. American Mineralogist 52 p. 1815.

59. CARMICHAEL, I.E.S., TURNER, F.J. and VERHOOGEN J. (1974) Igneous Petrology. McGraw-Hill Book Company 175 pp.

60. CHALMERS, R.O. (1957) Mineral possibilities of the Antarctic. The Australian Museum Magazine. December 1957. p. 252 - 255.

61. COBBING, E.J. and PITCHER, W.S. (1972) The coastal batholith of Peru. Journ. Geol. Soc. London., 128 p. 421 - 60.

62. COLEMAN, R.G. (1971) Plate tectonic emplacement of upper mantle peridotites along continental edges. Journ. Geophysical Res., 76 p. 1212-22.

63. COLLEY, H. (1976) Classification and Exporation Guide for Kuroko type deposits based on Occurrences in Fiji. Trans. Inst. Min. Metall. Section B 85 p. B190-B199.

64. COX, D.P., LARSEN, R.R., and TRIPP, R.B. (1973) Hydrothermal alteration in Puerto Rican porphyry copper deposits. Econ. Geol., 68 p. 1329-1334.

65. COX. D.P., WIGGINS, L.B., and O'NEIL, J.R., (1975) Amphibole-quartz-magnetite assemblages in hydrothermal alteration zones in the Tanama Porphyry Copper, Puerto Rico. Econ. Geol., 70 p. 1319.

66. CREASEY, J. (1966) Hydrothermal Alteration. In Tiltey and Hicks, eds. Geology of the porphyry copper deposits, south western north America. Tuscon Univ. of Arizona Press p. 51 - 56.

67. CUNNINGHAM, G.G., and HALL, B.R. (1976) Field and laboratory tests for the detection of alunite and determination of the atomic per cent potassium. Econ. Geol. 71 p. 1596-1598.

68. CURTIS, R., (1965) — The petrology of the Graham Coast and Offshore Islands, Graham Land, West Antarctica. Univ. Birmingham. Ph.D. Thesis.

69. CURTIS, R.,(1966) — The petrology of the Graham Coast, Graham Land. British Antarctic Survey Sci. Rept., No. 50.

70. DALZIEL, I.W.D. (1969) — Structural studies in the Scotia Arc: Livingstone Island. Antarctic Journ. U.S., 4 p. 137.

71. DALZIEL, I.W.D. (1971) — Structural studies in the Scotia Arc: The South Orkney Islands R/V Hero Cruse 71-1. Antarctic Journ. U.S., 6 p. 124-126.

72. DALZIEL, I.W.D., and ELLIOTT, D.H., (1971) — Evolution of the Scotia Arc. Nature 233 p. 246-252.

73. DALZIEL, I.W.D., (1972) — K-Ar dating of rocks from Elephant Island, South Scotia Ridge. Bull. Geol. Soc. America, 83 p. 1887 - 1894.

74. DALZIEL, I.W.D., (1972) — Large scale folding in the Scotia Arc. in Adie, R.J., ed., Antarctic Geology and Geophysics: Oslo Universitatforlaget p. 47 - 56.

75. DALZIEL, I.W.D., and CORTES, R. (1972) — The tectonic style of the southernmost Andes and the Antarctandes. 24th International Geol. Congress. Montreal, Canada. Section 3 p. 316-37.

76. DALZIEL, I.W.D., and ELLIOTT, D.H., (1973) — The Scotia Arc and Antarctic Margin. In: Ocean Basins and Margins 1. The South Atlantic, Plenum Press, New York p. 171 - 245.

77. DALZIEL, I.W.D., KLIGFIELD, R., LOWRIE, W. and OPDYKE, N.D., (1973) — Palaeomagnetic data from the Southernmost Andes, and the Antarctic in Tarling, D.H. and Runcorn, S.K., eds., Implications of Continental drift to the earth sciences VI London. Academic Press p. 87 - 101.

78. DALZIEL, I.W.D., (1974) — Evolution of the margins of the Scotia Sea. In. Burke, C.A., and Drake, C.L. eds. The Geology of Continental margins. Springer, New York. p. 567 - 580.

79. DAVEY, F.J., (1972) — Marine gravity measurements in Bransfield Strait and adjacent areas. In Adie. R.J. ed., Antarctic Geology and Geophysics: Oslo Universitetsforlaget p. 39-45.

79a. DAVIES, T.G., (1977) — The Geology of northern Palmer Land, Antarctica Ph.D. Thesis. Univ. of Birmingham.

80. DEER, W.A., HOWIE, R.A., and ZUSSMAN, J., (1966) — An introduction to the rock forming minerals. Longman Press. 528 pp.

81. DENHOLM, L.S. (1967) Geological exploration for gold in the Tavua Basin, Viti Levu, Fiji. New Zealand Journ. Geology and Geophysics. 10 p. 1185-6

82. DEWER, G. J. (1970) The geology of Adelaide Island. British Antarctic Survey Sci. Rept., 57 66 pp.

83. DEWEY, J. F. and BIRD, J. M. (1971) Origin and emplacement of the ophiolite suite: Appalachian ophiolites in Newfoundland. Journ. Geophysical Res., 76 p. 3179-206.

84. DEWIT, M.J. (1977) The evolution of the Scotia Arc as a key to the reconstruction of south western Gondwanaland. Tectonophysics., 37 p. 53-81.

85. DOSTAL, J. ZENTILLI, M., CAELLES, J.C. and CLARK, A.H. (1977) Geochemistry and origin of volcanic rocks of the Andes (26 - 28 S). Contributions to Mineralogy and Petrology 63 p. 113 - 128.

86. DOTT, R.H. (1972) The antiquity of the Scotia Arc: UNESCO-IUGS Symposium on Continental Drift, Montevideo, Uruguay. October 1967. Trans. American Geophys. Union 53 p. 178-9.

87. DU TOIT, A.L. (1937) Our wandering Continents. Oliver and Boyd. Edinburgh. 366 pp.

88. ELLIOT, D.H. (1964) The petrology of the Argentine Islands. British Antarctic Survey Sci. Rept., 41 29 pp.

89. ELLIOT, D.H. (1965) Geology of the north west Trinity Peninsula, Graham Land. British Antarctic Survey, Bulletin 7 p. 1 - 24.

90. ELLIOT, D.H. (1966) Geology of the Nordenskjold Coast and a comparison with north west Trinity Peninsula, Graham Land. British Antarctic Survey. Bulletin 10 p. 1 - 43.

91. ELLIOT, D.H. (1967) The geochemistry of the rocks from the Nordenskjold Coast and north west Trinity Peninsula, Graham Land. British Antarctic Survey. Bulletin 11 p. 83 - 96.

92. ELLIOT, D.H. (1968) The Geology of Joinville Island. British Antarctic Survey. Bulletin 12 p. 23-40.

93. ELLIOT, D.H. (1975) Tectonics of Antarctic: A review. American Journ. of Science v 275-A p. 45 - 106.

94. ELLIOT, D.H. (1977) A summary of a framework for assessing environmental impacts of possible Antarctic mineral development. Institute of Polar Studies Ohio Univ. 43210.

95. ELSDON, R. (1972) Iron-titanium oxide minerals in Upper Layered Series, Kap. Edvard Holm, East Greenland, Mineralogical Magazine 38 p. 946 - 56.

96. ELSDON, R. (1977) Autometasomatic leaching of iron from a Tertiary gabbro. Inst. Min. Metall. Trans., 87 Section B p. B33.

97. EICHELBERGER, D. (1975) Origin of andesites and dacites; Evidence of mixing at Glass Mountain in California and at other Circum-Pacific Areas. Bull. Geol. Soc. America. 86 p. 1381 - 1391.

98. ERICKSEN, G.E. (1976) Metallogenetic provinces of the south eastern Pacific region. In Halbority, M.T., Marler, J.C. and Liam, H.M. eds. Circum-Pacific energy and mineral resources. American Assoc. Petroleum Geol., Memoir 25 p. 527 - 538.

99. FERGUSON, D. (1921) Geological Observations in the South Shetlands, the Palmer Archipelago, and Graham Land, Antarctica. Trans. Roy. Soc. Edinburgh 53 part 1. No. 3 p. 29 - 55.

100. FLEET, M. (1965) Metamorphosed Limestone in the Trinity Peninsula. Series of Graham Land. British Antarctic Survey Bulletin 7 p. 73 - 76.

101. FLEET, M. (1958) The Geology of the Oscar II Coast. British Antarctic Survey Sci. Rept., 59 46 pp.

102. FLEISCHER, M. (1955) Minor elements in some sulphide minerals. Econ. Geol. 50th Anniversary volume p. 970-1024.

103. FRASER, A.G. (1963) The Geology of Stonington and Trepassey Islands, Marguerite Bay. Falkland Islands Dependencies Survey Preliminary Rept., 18.

104. FRASER, A.G. (1965) The petrology of Stonington and Trepassey Islands, Marguerite Bay. British Antarctic Survey Sci. Rept., 52.

105. FRASER, A.G. (1965) Banded gabbros of the Anagram Islands, Graham Land. British Antarctic Survey Bulletin 4 p. 23 - 38.

106. FRASER, A.G. and GRIMLEY, P.H. (1972) The Geology of parts of the Bowman and Wilkins Coasts, Antarctic Peninsula. British Antarctic Survey Sci. Rept., 67 59 pp.

107. FRUTOS, S.J. and OYARZUN, M.J. (1975) Tectonic and geochemical evidence concerning the genesis of El Laco magnetite lava flow deposits, Chile. Econ. Geol. 70 p. 988-90.

108. GARSON, M.S. and MITCHELL, A.H.G. (1977) — Mineralization at destructive plate boundaries : a brief review. In Volcanic porcesses in ore genesis. Geol. Soc. London special publication No. 7 p. 81 - 97.

109. GASS, I.G., SMITH, A.G. and VINE, F.J. (1975) — Origin and emplacement of ophiolites. In Geodynamics today (London : The Royal Society) p. 54 - 64.

110. GASS, I.G. (1977) — Origin and emplacement of ophiolites. In Volcanic processes in ore genesis. Geol. Soc. London special publication No. 7 p. 72 - 76.

111. GIGGENBACH, A. (1976) — Variations in the C, S and Cl contents of volcanic gas discharges from White Island, New Zealand Bull. Volcanologique 39 p. 15 - 27.

112. GILMOUR, P. (1977) — Mineralised intrusive breccias as guides to concealed porphyry copper systems. Econ. Geol., 72 p. 290 - 303.

113. GOLDRING, D.C. (1962) — The geology of the Loubet Coast, Graham Land. British Antarctic Survey. Sci. Rept., 36 50 pp.

114. GONZALEZ-FERRAN, I. KATUSI, K. and TAVERA, J.S. (1970) — Contribucion las conozimiento geologieo de la Peninsula Byers de la Isla Livingstone, Islas Shetland del sur, Antarctica. Series, Cient. Inst. Antarctico Chile 1 p. 41 - 54.

115. GONZALEZ-FERRAN, O. (1972) — Distribution, migration and tectonic control of Upper Cenozoic Volcanism in west Antarctica and South America. In Adie, R.J. ed. Antarctic Geology and Geophysics : Oslo Universitetsforlage p. 173 - 179.

116. GOOSSENS, P.J. (1972) — An exhalative volcanic iron sulphide stratabound deposit, near San Fernando, Azuay Province, Ecuador. Econ. Geol., 67 p. 469 - 480.

117. GOOSSENS, P.J. (1972) — Metallogeny in the Ecuadorian Andes. Econ. Geol., 67 p. 458 - 468.

118. GOWER, J.A. (1957) — X-ray measurement of the iron-magnesium ratio in biotites. American Journ. Science 225 p. 142-156

119. GRIKUROV, G.E., A.YA. KRYLOV., and VU.I. SILIN (1966) — Absolute age of certain rocks in the Marguerite Bay region of the Antarctic Peninsula. Proceedings of the Acad. Sci. U.S.S.R., Geol. Sci. section 171 p. 127-130.

120. GRIKUROV, G.E., A.YA. KRYLOV., and YU.I. SILIN, (1967) — Absolute age of some rocks from the Scotia arc and Alexander Island (West Antarctica). Dolk. Akad. Nant. S.S.S.R. 172 No. 1.

121. GRIKUROV. G.E. and POLYAKOV, M.M. (1968) Geological structure of the Fildes Peninsula, south western tip of King George (Waterloo) Island. Inform. Byul. Sov. Antarkt. Eksp., No. 71 p. 189 - 192.

122. GRIKUROV, G.E. and POLYAKOV, M.M. (1968) New data on the geology of the South Shetland Islands (from field work by the thirteenth Soviet Antarctic Expedition in Jan-Feb (1968)). Infor. Byul. Soviet Antarkt. Eksp., 71 p. 193-6.

123. GRIKUROV. G.E., KRYLOV, A.YA., POLYAKOV, M.M. and TSOVBUN, YA.N. (1972) The age of rocks in the northern part of the Antarctic Peninsula and the South Shetland Islands (by K-Ar method). Soviet Antarctic Expedition Information Bulletin 80 p. 30 - 34.

124. GRIMLEY, P.H. (1963) The Geology of Flagstaff Hill, Stonington Island, Marguerite Bay, Falkland Islands Dependencies Survey. Preliminary Report, No. 11.

125. GRIMLEY, P.H. (1966) Geology of part of Stonington Island, Marguerite Bay. British Antarctic Survey Bulletin 9 p.71-74.

126. GROSS, W.H. (1975) New ore discovery and source of silver-gold veins, Guanajuato , Mexico. Econ. Geol., 70 p. 1175-1189.

127. GROVES, D.I., ARCHIBALD, N.J., BETTENAY, L.F. and BINNS, R.A. (1978) Greenstone belts as ancient marginal basins or ensialic rift zones. Nature, 273 p. 460 - 461.

128. GULLULY, J. (1976) Lineaments - ineffective guides to ore deposits. Econ. Geol., 71 p. 1507 - 14.

129. HALLIMOND, A.F. (1938) On the relation of chamosite and daphnite to the chlorite group. Min. Mag., 25 p. 441-456.

130. HALPERN, M. (1965) The Geology of the General Bernardo O'Higgins area, northwest Antarctic Peninsula. In Hadley, J.B. ed., Geology and Palaeontology of the Antarctic. American Geophys. Union. Antarctic Research Series 6 p. 177- 209.

131. HALPERN, M. (1968) Rb-Sr age measurements of plutonic igneous rocks in eastern Ellsworth Land and northern Antarctic Peninsula, Antarctica. Journ. Geophys. Research 72 p. 717-30.

132. HALPERN, M. (1972) Rb-Sr total rock and mineral ages from the Marguerite Bay area, Kohler Range and Fosdick Mountains. In Adie, R.J. ed., Antarctic Geology and Geophysics : Oslo Universitetsforlaget p. 197 - 204.

133. HARRY, W.T. and RICHEY, J.E. (1963) Magmatic pulses in the emplacement of plutons. Liverpool and Manchester Geol. Journ., 3 p.254-68.

134. HATCH, F.K., WELLS, A.K., and WELLS, M.K. (1972) — Petrology of the Igneous Rocks. Thomas Murby & Co. London 550 pp.

135. HAWKES, D.D. (1961) — The Geology of the South Shetland Islands 1. The petrology of King George Island. Falkland Islands Dependencies Survey Sci. Rept., No. 26 29 pp.

136. HAWKES, D.D. (1962) — The structure of the Scotia Arc. Geol. Mag., 99 p. 85 - 91.

136a. HAWKES, D.D. (1978) — Mineralisation in the Antarctic Peninsula. Aston Univ. Unpub. Rept.,

137. HEMLEY, R.W. and MCNABB, A. (1978) — Magmatic vapour plumes and ground-water interaction in porphyry copper emplacement. Econ. Geol., 73 p. 1 - 15.

138. HENNIG, H. (1911) — Le conglomerates Pleistocene 'o Pecten de I'lle Cockburn. Wessenschalttiche Ergebruisse de Schwedischen Sudpolarexpedition. 1901-1093 Bd. 3 Lief 10p 1-73.

139. HERRON, E.M. and TUCHOLKE, B.E. (1976) — Sea floor magnetic patterns and basement structure in the south eastern Pacific. Initial Report of Deep Sea Drilling Project. U.S. Government Printing Office, Washington, D.C. V35 p. 263 - 278.

140. HEPTONSTALL, W.B. (1977) — Plate linkage mechanism to account for oroclinal deformation in the Western Cordilleras of North America. Nature, 268 p. 27 - 32.

141. HEYL, A.V. (1972) — The 38th Parallel lineament and its relationship to ore deposits. Econ. Geol., 67 p. 879-894.

142. HOBBS, G.J. (1961) — The Geology of Lingstone Island. Falkland Islands Dependencies Survey, Preliminary Report No. 3.

143. HOBBS, G.J. (1963) — The Geology of the South Shetland Islands IV. The Geology of Livingstone Island. British Antarctic Survey. Sci. Rept., 47 34 pp.

144. HOLLER, J.S. (1967) — Experimentelle Bilding von Alunite-Vansite dirch die Einwirkung von schwefelsawe auf mineralien und gesteine. Cont. Mineral and Petrol. 15 p. 309 - 29.

145. HOLLISTER, V.F. (1974) — Regional characteristics of porphyry copper deposits of South America. Trans. Soc. Min. Engnrs. A.I.M.E., 256 p. 45 - 53.

146. HOLLISTER, V.F. (1975) — An appraisal of the nature and source of some porphyry copper deposits. Mineral Sci. Engng 7 p. 225 - 233.

147. HOLLISTER, V.F. (1975) The porphyry molybdenum deposit of Compaccha, Peru and its geological setting. Mineral Deposits (Berl) 10 p. 141 - 151.

148. HOOPER, P.R. (1962) The petrology of Anvers Island and adjacent Islands. Falkland Islands Dependencies Survey Sci. Rept., 34 69 pp.

149. HORIKASHI, E. (1976) Development of late Cenozoic petrographic provinces and metallogeny in northeast Japan. In Strong, D.F. ed., Metallogeny and Plate tectonics. Spec. Paper Geol. Assn. Canada, 14 p. 121-42.

150. HORIKOSHI, E. (1969) Volcanic activity related to the formation of the Kuroko-type deposits in the Kosaka district, Japan. Mineral Deposita 4 p. 321-45.

151. HORIKOSHI, E. and SATO, T. (1970) Volcanic activity and ore deposition in the Kosaka mine. In Tatsumi, T. ed Volcanism and Ore Genesis. Univ. Tokyo Press p. 181-195.

152. HOSKINS, A.K. (1961) The geology of parts of the Loubet and Fallieres coasts, Graham Land. Falkland Islands Dependencies Survey. Preliminary Rept., 6 38 pp.

153. HOSKINS, A.K. (1963) The basement complex of Neny Fjord, Graham Land. British Antarctic Survey Sci. Rept., 43 49 pp.

154. HUDSON, J.M. (1964) The geology of part of southwest Arrowsmith Peninsula, Graham Land. British Antarctic Survey Preliminary Rept., 15.

155. HUTCHINSON, C.S. (1975) Ophiolite in southeast Asia. Bull. Geol. Soc. America, 86 p. 797 - 806.

156. HUTCHINSON, C.S. and TAYLOR, D. (1978) Metallogenesis in S.E.Asia. Journ. Geol. Soc. London, 135 p. 407 - 428.

157. IAWASHBAI, I., HIRAYAMA, M., KATSUM, T., OZAWA, T., OSSAKA, J., KARNADA, M., and MATSUMOTO, H. (1963) Alteration of rocks by volcanic gases in Japan. Bull. Volcanolgique, 27 p. 65 - 78.

158. ISHIHARA, S. (1978) Metallogenesis in the Japanese Island arc system. Journ. Geol. Soc. London, 135 p. 389-406.

159. IWAO, S. (1970) Clay and silica deposits of volcanic affinity in Japan. In Volcanism and ore genesis. Univ. of Tokyo, Japan. Tatsami, T. ed. p.267-283.

160. JACOBSON, H.S., MURILLO, C., RUIZ, L., TAPIA, O., ZAPATA, H., ALARCON, H., DELGADILLO, E., and VELASCO, C. (1969) Geology and mineral deposits of the San Cristobal district, Villa Martin Province, Potosi, Bolivia. U.S. Geo. Surv. Bull., 1273 22 p.

161. JAMES, A.H. (1971) Hypothetical diagram of several porphyry copper deposits. Econ. Geol., 66 p. 43-47.

162. JOINT COMMITTEE ON POWDER DIFFRACTION STANDARDS (1974) Selected powder diffraction data for minerals. Publication No. D.B.M. 1 - 23.

163. JEROME, S.E. and COOK, D.R. (1967) Relation of some metal mining districts in the western United States to regional tectonic environments and igneous activity. Bull. Nevada St. Bur. Mines., 69 35 pp.

164. JOPLIN, G.A. (1959) On the origin and occurrence of basic bodies associated with discordant bathyliths. Geol. Mag., 96 p. 361 - 73.

165. KARKHANAVALA, M.D. and MOMIN, A.C. (1959) The Alteration of Ilmenite. Econ. Geol., 54 1095-1102.

166. KATZ, H.R. (1972) Plate tectonics-orogenic belts in the southeast Pacific. Nature 237 (S354) p. 331.

167. KATZ, H.R. (1973) Contrasts in tectonic evolution of orogenic belts in the southeast Pacific. Journ. Roy. Soc. New Zealand 3 p. 333-362.

167a. KEITH, T.E.C. and MUFFLER, L.S.P. (1978) Minerals produced during cooling and hydrothermal alteration of ash flow tuff from Yellowstone Drill Hole Y-5. Journ. of Volcanology and Geothermal Research, 3 p.373-402

168. KENRICK, D.M. (1970) Contact metamorphism in some areas of the Sierra Nevada, California. Bull. Geol. Soc. America., 81 p. 2913-38.

169. KESLER, S.E., JONES, L.M., and WALKER, R.L., (1975) Intrusive rocks associated with porphyry copper mineralisation in island arc areas. Econ. Geol., 70 p. 515-26.

170. KESLER, S.E. (1978) Metallogenesis of the Caribbean region. Journ. Geol. Soc. London., 135 p.429-442.

171. KOSSACK, H.P., (1955) La explotacion de los yacimientos minerales de la Antarctica. Rev. Geog., Chile 13 p.83-90.

172. KNIGHT, J.E. (1977) A thermochemical study of alunite, enargite, luzonite and tennantite deposits. Econ. Geol., 72 p. 1321-1336.

173. KNOWLES, P.H. (1945) Geology of the southern Palmer Peninsula, Antarctica. Proc. American Phil. Soc., 89 p. 132 - 145.

174. KRAUSKOPF, K.B. (1967) Source rocks for metal bearing solutions. In: Barnes, H.L. ed., Geochemistry of Hydrothermal Ore Deposits. Holt, Rinehart and Winston, p. 1-33.

175. KRAUSKOPF, K.B. (1971) The source of ore metals. Geochim. et Cosmochim. Acta., 35 p. 643-59.

176. KUTINA, J. (1960) Hydrothermal ore deposits in the Western United States; a new concept of structural control of distribution. Science 165 p.1113-9.

177. LAW, P. (1965) Resource Potentials of Antarctica. Australian Antarctic Survey Rept., No. 5.

178. LAUDON, T.S., BAHRENDT, J.C., and CHRISTENSEN, N.J. (1964) Petrology of rocks collected on the Antarctic Peninsula traverse. Journ. Sedi. Petrol., 34 p. 360-364.

179. LIPMAN, P.W. (1976) Multiple ages of mid-Tertiary mineralisation and alteration in the western San Juan Mountains, Colorado. Econ. Geol., 71 p.571-88.

180. LOFTUS-HILLS, D. and SOLOMON, N. (1967) Cobalt, nickel and selenium in sulphides as indicators of ore genesis. Mineral. Deposita 2 p. 228-242.

181. LOVERING, T.S. (1961) Sulphide ores formed from sulphide deficient solutions. Econ. Geol., 56 p. 68-99.

182. LOVERING, T.S., COOPER, J.R., DREWS, M., and CONE, C.G. (1970) Copper in biotite from igneous rocks in Southern Arizona as an ore indicator, U.S. Geol. Survey Prof. Paper 700-B p.B1-B8.

183. LOWELL, J.D. and GUILBERT, J.M. (1970) Lateral and vertical alteration and mineralisation zoning in porphyry ore deposits. Econ. Geol., 65 p. 373-408.

184. LOWELL, J.D. (1974) Regional characteristics of porphyry copper deposits of the Southwest. Econ. Geol., 69 p. 601-17.

185. LUTTON, J. (1952) Pegmatites as a link between magma and copper - molybdenum ore. The Mines Magazine. Dec. p.13-15.

186. MACINTYRE, R.M. (1977) Anorogenic magmatism, plate motion and Atlantic evolution. Journ. Geol. Soc., London 133 p.375-38

187. MATTHEWS, D.H. (1959) Aspects of the Geology of the Scotia Arc. Geol. Mag., 96 p.425-41.

188. MATTHEWS, D.H. and MARLING, D.H. (1967) The Geology of the South Orkney Islands 1. Signey Island. Falkland Islands Dependencies Survey. Sci. Rept., 25.

189. MARKER, G.D. and WHITE, D.E. (1975) Seismic geyser and its bearing on the origin and evolution of geysers and hot springs of Yellowstone National Park. Bull. Geol. Soc. America, 86 p.749-759.

190. MARKHINIM, E.K. and BOZHKOVA, L.I. (1976) Dependence of chemical composition of thermal waters upon seismic activity. Bull. Volcanologique 36 p.104-111.

191. MASON, B. (1952) Principles of Geochemistry. Wiley Press 310 pp.

192. MERNERT, K.R. (1968) Migmatites and the origin of granitic rocks. Elsevier Publishing Corpn. London 393 pp.

193. MEYER, C. and HEMLEY, J.S. (1967) Wall rock alteration. In: Barnes, H.L. ed. Geochemistry of Hydrothermal Ore Deposits. Holt, Rinehart and Winston p. 166-235.

194. MILLER, J.A. (1960) K-Ar ages of some rocks from the South Atlantic. Nature 187 p.1019-20.

195. MITCHAM, T.W. (1974) Origin of breccia pipes. Econ. Geol., 69 p. 412-413.

196. MITCHELL, A.H. and BELL, J.D. (1973) Island arc evolution and related mineral deposits. Journ. Geol., 81 p.381-405.

197. MITCHELL, A.H. and GARSON, M.S. (1972) Relationship of porphyry copper and Circum-Pacific tin deposits to palaeo-Benioff Zones. Trans. Inst. Min. Metall., 81 p.10-25.

198. MITCHELL, A.H. and GARSON, M.S. (1976) Mineralisation at Plate boundaries. Minerals Sci. Engng., 8 p.129-169.

199. MITCHELL, A.H. (1977) Emplacement of the Oman Ophiolite; a mechanism related to subduction and collision. Geol. Soc. America Bull., 88 p.1081-1088.

200. MIYASHIRO, A. (1975) Volcanic rock series and tectonic setting. Annual Review of Earth and Plan. Sci., Letters 3 p.251-278.

201. MIYASHIRO, A. and SHIDO, F. (1975) Tholeiitic and calc-alkaline series in relation to the behaviour of titanium, vanadium, chromium and nickel. American Journ. Sci., 275 p.265-277.

202. MUELLER, I. (1963) Some notes on mineralisation in Antarctica. In: Antarctic Geology. Adie. R.J. ed. Proc. first International Symposium on Antarctic Geology. Cape Town. North-Holland Press p.393

203. MUKAIYAMA, H. (1970) Volcanic sulphur deposits in Japan. in Volcanism and ore genesis. Univ. of Tokyo Press, Japan p.285-295.

204. MULLAN, H.S. and BUSSELL, M.A. (1977) The basic rock series in batholithic association. Geol. Mag., 114 p.265-80.

205. NABOKO, S.I. (1959) Volcanic exhalations and products of their reactions as exemplified by Kamchatka-Kuriles volcanoes. Bull. Volcanologique Ser., II 20 p.121-136.

206. NIELSEN, R.L. (1968) Hypogene texture and mineral zoning in a copper bearing granodiorite porphyry stock, Santa Rita, New Mixico. Econ. Geol., 63 p.37-50.

207. NELSON, P.H.H. (1975) The James Ross Island Volcanic Group of northeast Graham Land. British Antarctic Survey. Sci. Rept., 54 62 pp.

208. NICHOLS, R.L. (1955) Bedrock Geology of Marguerite Bay area, Palmer Peninsula, Antarctica. Ronne, Antarctic Research Expedition. Technical Rept., 13. Office of Naval Research, Washington, D.C.

209. PAPENFUS, E.B. (1931) "Red Bed" copper deposits in Nova Scotia and New Brunswick. Econ. Geol., 26 p.314-330.

210. PARK, C.F. (1961) A magnetite "flow" in northern Chile. Econ. Geol., 56 p.431-6.

211. PATTON, T.C., GRANT, A.R., and CHENEY, E.S. (1973) Hydrothermal alteration at the Middle Fork Copper Prospect, Central Cascades, Washington. Econ. Geol., 68 p.816-830.

212. PETERSEN, U. (1965) Regional Geology and major ore deposits of central Peru. Econ. Geol., 60 p.407-476.

213. PETERSEN, U., NOBLE, D.C., ARENAS, M.J., and GOODELL, P.C. (1977) Geology of the Julcani Mining District, Peru. Econ. Geol., 72 p.931-949.

214. PHILLIPS, C.H., GAMBELL, N.A. and FOUNTAIN, D.S. (1974) Hydrothermal Alteration, Mineralisation and Zoning in the Ray Deposit. Econ. Geol., 69 p.1237-1250.

215. PIRIE, J.H.H. (1925) Geology of the South Orkney Islands. Scottish National Antarctic Expedition. 10 pp.

216. PITCHER, W.S. (1978) The anatomy of a batholith. Journ. Geol. Soc. London.135 p.157-182

217. POTTER, N. (1969) Natural resource potentials of the Antarctic Peninsula. New York. American Geog. Soc. 97 pp.

218. RABONE, S.D.C. (1975) Petrography and hydrothermal alteration of Tertiary andesite-rhyolite volcanics in the Waitekauri Valley, Ohinemuri, New Zealand. New Zealand, Journ. Geol. and Geophys., 18 p. 239-58.

219. RAMDOR, P. (1960) The ore minerals and their intergrowths. Pergamon Press. 1174 pp.

220. RAMSEY, J.G. (1967) Folding and Fracturing of Rocks. McGraw-Hill Book Cp. 568 pp.

221. RAY, J.C. (1914) Paragenesis of the ore minerals in the Butte District, Montana. Econ. Geol., 9 p.463-482.

222. RAYMAHASHAY, B.C. (1968) A geochemical study of rock alteration by hot springs in the Paint Pot Hill area, Yellowstone Park. Geochim. et Cosmochim. Acta., 32 p. 499-522.

223. RAZIN, L.V. (1976) Geologic and genetic features of forsteritic dunites and their platinum group mineralisation. Econ. Geol., 71 p.1371-76.

224. REITAN, P. (1959) Pegmatite veins and the surrounding rocks. Norsk, Geol. Tidsskr. 39 p. 197-229.

225. REGAN, P.F. (1976) The genesis and emplacement of mafic plutonic rocks of the coastal Andean batholith, Lima Province, Peru. Ph. D. Thesis, Univ. of Liverpoo

226. REX, D.C. (1967) Age of dolerite from Dronning Maud Land. British Antarctic Survey. Bull., 11 p.101.

227. REX, D.C. (1972) K-Ar age determinations on volcanic and associated rocks from the Antarctic Peninsula and Dronning Maud Land. In Adie, ed. Antarctic Geology and Geophysics: Oslo Universitetsforlage p. 133-136.

228. REX, D.C. (1976) Geochronology in relation to the stratigraphy of the Antarctic Peninsula. British Antarctic Survey Bull., 43 p.49-58.

229. RIDGE, J.D. (1973) Volcanic exhalations and ore deposition in the vicinity of the sea floor. Mineral. Deposita 8 p.332-348.

230. RIPLEY, E.M., and OHMOTO, H. (1977) Mineralogic, sulphur isotope, and fluid inclusion studies of Stratabound Copper Deposits at the Raul Mine, Peru. Econ. Geol., 72 p.1017-1041.

231. RIVANO, S. and CORTES, R. (1976) Note on the presence of the lawsonite - sodic amphibole association on Smith Island, South Shetlands, Antarctica. Earth and Plan. Sci. Letters 29 p.34-36.

232. RODDICK, J.A. and ARMSTRONG, J.E. (1959) Relict dykes in the Coast Mountains near Vancouver, B.C. Journ. Geol., 67 p.603-613.

233. ROWLEY, P.D., WILLIAMS, P.L., SCHMIDT, D.L. and REYNOLDS, R.L. (1975) Copper mineralisation along the Lassiter Coast of the Antarctic Peninsula. Econ. Geol., 70 p.982-992.

234. ROWLEY, P.D., WILLIAMS, P.L. and SCHMIDT, D.L. (1977) Geology of an Upper Cretaecous copper deposit in the Andean Province, Lassiter Coast, Antarctic Peninsula. Prof. paper U.S. Geol. Survey 984 36 pp.

235. ROWLEY, P.D. and WILLIAMS, P.L. (1978) Geology of the northern Lassiter Coast and Southern Black Coast, Antarctic Peninsula. Proceedings International Union of Geol. Sci. Third symposium on Antarctic Geology and Geophysics Madison Wise. Aug. 1977.

236. ROWLEY, P.D. and PRIDE, D.E. (1978) Metallic mineral resources of the Antarctic Peninsula (Review). Proceedings International Union of Geol. Sci. third symposium on Antarctic Geology and Geophysics, Madison Wise. Aug. 1977.

237. RUIZ, F.C., AGUILAR, A., EGERT, E., ESPINOVA, W., PEEBLES, F., QUEZADA, R., and SERRANO, M., (1971) Strata-bound copper sulphide deposits of Chile, in IMA-IAGOD, General meeting, 7th Tokyo, Japan, 1970. IAGOD Vol. Soc. Min. Geol. Japan. Special Issue 3. p.252-260.

238. RUIZ, F.C., AGUILAR, L., CORVALAN, J., KLOHN, C., KLOHN, E., and LEVI, B., (1965) Geologia y yacimientos metaliferous de Chile. Santiago, Inst. Invest. Geol., 305 pp.

239. RUNNELLS, D. (1970) Continental drift and economic minerals in Antarctica. Earth and Plan. Sci. Letters 8 p. 400 - 402.

240. RYALL, W.R. (1977) Anomalous trace elements in pyrite in the vicinity of mineralised zones at Woodlawn, NS.W., Australia. Journ. Geochem. Exploration, 8 p.73-83.

241. SAWKINS, F.J. (1972) Sulphide ore deposits in relation to plate tectonics. Journ. Geol., 80 p.377-397.

242. SCHAUER, O.C., and FOURCADE, N.H. (1963) Geological-petrographical study of the western end of King George Island, South Shetland Islands. Antarctic Geology. S.C.A.R. Proceedings 1963 VII Igneous and metamorphic petrology.

243. SCHMIDT, H. (1950) Origin of "epithermal" mineral deposits. Econ. Geol.,45 p.191-200.

244. SCOTT, K.M. (1965) Geology of the southern Gerlache Strait region, Antarctica. Journ. Geol., 73 p.518-527.

245. SEWARD, T.M. (1973) Thio complexes of gold and the transport of gold in hydrothermal ore solutions. Geochim. et. Gosmochim Acta., 37 p.379-399.

246. SHERATON, J.W. and BLACK, L.P. (1969) Geochemistry of mineralised granitic rocks. Geochim et Cosmochim Acta. 33 p.330-348.

247. SKINNER, A.C. (1976) Geology of north western Palmer Land, Antarctica. Ph.D.Thesis, University of Birmingham.

248. SKINNER, A.C. (1973) Geology of north western Palmer Land between Eureka and Micklejohn Glaciers. British Antarctic Survey. Bull., 35 p.1-22.

249. SHEPPARD, S.M.F. (1977) Identification of the origin of ore forming solutions by the use of stable isotopes. In Volcanic Processes in Ore Genesis. Geol. Soc., London Special publication 7 p.25-41.

250. SIEGERS, A., PICHLER, H., and ZEIL, W. (1969) Trace element abundances in the Andesite formation of Northern Chile. Geochim et Cosmochim Acta 33 p. 882-887.

251. SIGVALDESON, G.E. (1963) Epidote and related minerals in two deep geothermal drill holes, Reykjavik and Hveragerdi, Iceland. U.S. Geol. Survey Prof. Paper., 450-E p.77-79.

252. SILLITOE, R.H. and SAWKINS, F.J. (1971) Geologic, mineralogic and fluid inclusion studies related to the origin of copper bearing tourmaline breccia pipes, Chile. Econ. Geol., 66 p. 1028-1041.

253. SILLITOE, R.H. (1972) Relation of metal provinces in western America to subduction of oceanic lithosphere. Bull. Geol. Soc. America., 83 p.813-7.

254. SILLITOE, R.H. (1972) A plate tectonic model for the origin of porphyry copper deposits., Econ. Geol., 67 p. 184-97.

255. SILLITOE, R.H. (1972) Formation of certain massive sulphide deposits at sites ofsea floor spreading. Trans. Inst. Min. Metall., 81 p.8141-8.

256. SILLITOE, R.H. (1973) The tops and bottoms of porphyry copper deposits. Econ. Geol., 68 p.799-815.

257. SILLITOE, R.H. (1975) Andean mineralisation: A model for the metallogeny of convergent plate margins. Geol. Assn. Canada. Special Paper 14 p.59-100.

258. SILLITOE, R.H. (1975) Lead-silver, manganese and native sulphur mineralisation within a stratovolcano, El Queva, northwest Argentina. Econ. Geol., 70 p. 1190-1201.

259. SILLITOE, R.H. (1977) Metallic mineralisation affilliated to subaerial volcanism: A review. In volcanic processes in Ore Genesis. Geol. Soc. London Special publication 7 p.99-117.

260. SILLITOE, R.H., GRANT, J.H., and HALLS, C. (1975) Porphyry tin deposits in Bolivia : Econ. Geol., 70 p.913-927.

261. SINGLETON, D. (1976) Geology of the Central Black Coast, Antarctic Peninsula. Ph.D. Thesis. Univ. of Birmingham.

262. SLANSKY, G. (1975) Natroalunite and alunite from White Island Volcano, Bay of Plenty, New Zealand. New Zealand Journ. Geol. and Geophs., 18 p.285-293.

263. SMELLIE, J.L. and CLARKSON, P.D. (1975) Evidence for pre-Jurassic subduction in western Antarctica. Nature, 258 p.701-702.

264. SMITH, P.J. (1972) The Resource Potential of Antarctica. Comments on Earth Science. Geophysics. 3 p.23-28

265. STEINER, A. (1953) Hydrothermal rock alteration at Wairaki, New Zealand. Econ. Geol., 48 p.1-13.

266. STEVEN, T.A., and EATON, G.P. (1975) Environment of ore deposition in the Creede Mining district, San Juan Mountains, Colorado : 1 Geologic, hydrologic and geophysical setting. Econ. Geol., 70 p.1023-37.

267. STEWART, D. (1945) Preliminary report on some intrusives of the Melchior Islands, Antarctica. Proc. American Philos. Soc., 89 p.146-7.

268. STEWART, J.H., MOORE, W.J. and ZIETZ, I. (1977) East-west patterns of Cenozoic igneous rocks, aeromagnetic anomolies and mineral deposits, Nevada and Utah. Bull. Geol. Soc. America, 88 p.67-77.

269. STOKI, J. and KONELAY, U. (1974) Banska Stiavnica ore deposit and its position within Caldera, In 4th I.A.G.O.D. symposium, Vama (Sofia, Bulgaria) Ass. of papers p.355-6.

270. STOLL, W.C. (1965) Metallogenic provinces of South America : Mining Mag., 112 p.20-33.

271. STRINGHAM, J. (1966) Igneous rock types and host rocks associated with porphyry copper deposits : In Titley and Hicks. (eds.). Geology of porphyry copper deposits, south western North America. Tuscon, Univ. Arizona Press. p.35-40.

272. SUAREZ, M. (1976) Plate tectonic model for the southern Antarctic Peninsula, and its relation to southern Andes. Geology 4 p. 211-214.

273. SUGAKI, A., SHIMA, A., KITAKAZE, A., and HARADA, H. (1975) Isothermal phase relations in the system Cu-Fe-S under hydrothermal conditions at 350°C and 300°C Econ. Geol., 70 p.806-23.

274. SWAN, R.A. (1962) Australia in the Antarctic (London, Cambridge University Press) 369 p.

275. TALLIAFERRO, N.L. (1934) Contraction phenomena in cherts. Bull. Geol. Soc. America., 45 p.189-232.

276. TAYLOR, S.R. and WHITE, A.J.R. (1966) Trace elements abundances in andesites. Bull Volcanologique, 29 p.177-194.

277. TAYLOR, S.R., KAYE, M., WHITE, A.J.R., DUNCAN, A.R., and EWART, A., (1969) Genetic significance of Co. Cr, Ni, Sc and V content of andesites. Geochim et Cosmochim Acta., 33 p. 275-286.

278. THAYER, T.P. (1969) Gravity differentiation and magmatic re-emplacement of podiform chromite deposits. Econ. Geol., Monograph., 4. Magmatic ore deposits Wilson, H.D.B., ed., p.132-147.

279. THOMAS, H.H. (1921) On the Innes Wilson collection of rocks and minerals from the South Shetland Islands and Trinity Island. Roy. Soc. Edinburgh. Trans., 53 p.81-89.

280. THOMPSON, J.W. (1973) The Geology of Powell, Christofferson and Michelsen Islands, South Orkney Islands. British Antarctic Survey Bull. 33 p.137-168.

281. THOMPSON, J.W. (1974) The Geology of the South Orkney Islands. III Coronation Island. British Antarctic Survey. Sci. Rept., 86.

282. TURNER, F.J. (1969) Metamorphic petrology. McGraw-Hill. 391 pp.

283. TYRRELL, G.W. (1921) A contribution to the petrography of the South Shetland Islands, the Palmer Archipelago and the Danco Coast, Graham Land, Antarctica. Trans. Roy. Soc. Edinburgh, 53 p.57-59.

284. TYRRELL, G.W. (1945) Report on rocks from West Antarctica and the Scotia Arc. 'Discovery' Rept., 23 p.37-102.

285. VALENUELA, E. and HERVE, F. (1972) Geology of Byers Peninsula, Livingstone Island, South Shetland Islands. In Adie, R. J. ed., Antarctic Geology and Geophysics : Oslo Universitetforlaget p.83-89.

286. VALLE, D.R., MORELLI, J. and RINOLDI, C. (1975) Manifestacion cupro-plumbifera "Don Bernade" Isla Livingstone, Islas Shetland de Sur, Antartida Argentina. Direccion Nacional del Antartico Instituo Antartico Argentino 175.

287. VANNEY, J.R. and JOHNSON, G.L. (1976) Geomorphology of the Pacific Continental Margin of the Antarctic Peninsula. In Initial Report of Deep Sea Drilling Project. U.S. Government Printing Office, Washington, D.C. 35 p. 279-288.

288. VIEIRA, C., ALARCON, B., AMBRUS, J. and OKAY, L. (1978) Metallic mineralisation in the Gerlache Strait Region, Antarctica. Third International Union Geol. Sci., Symposium on Antarctic Geol. and Geophys. Madison, Wisc. Aug. 1977.

289. VINCENT, A.H. and PHILLIPS, R. (1954) Determination of palladium and gold in Igneous Rocks. Geochim et Cosmochim Acta., 2 p. 154.

290. WALKER, W. (1972) Mantle Cells and Mineralisation. Soc. Mining Engnrs. (A.I.M.E.) Trans., 252 p.314-326.

291. WEST, S.M. (1968) Petrography of metamorphic rocks from the Inaccessible and Larsen Islands. South Orkney Islands. British Antarctic Survey Bull., 18 p.45-58.

292. WEST, S.M. (1974) The Geology of the Danco Coast, Graham Land. British Antarctic Survey Sci. Rept., 84.

293. WHITE, D.R. (1957) Thermal waters of volcanic origin. Bull. Geol. Soc. America., 68 p. 1637-1658.

294. WHITE, D.E. (1957) Magmatic, connate and metamorphic waters. Bull. Geol. Soc. America., 68 p. 1659-1682.

295. WHITE, D.E. (1957) Thermal Springs and Epithermal ore deposits. Bull. Geol. Soc. America, 68 p.99-154.

296. WHITE, D.R., MUFFLER, J.L.P., and TRUESDELL, A.H. (1971) Vapour dominated hydrothermal systems compared with hot water systems. Econ. Geol., 66 p. 75-79.

297. WHITE, D.E., and SIGNALDASON, G.E. (1963) Epidote in hot springs, and depth of formation of propylitic epidote in epithermal ore deposits. U.S. Geol. Survey. Prof. paper, 450-E p. 80-84.

298. WHITNEY, J.A. (1977) A synthetic model for vapour generation in tonalite magma and its economic remifications. Econ. Geol., 72 p. 686-690.

299. WILLIAMS, P.L., SCHMIDT, D.L., PLUMMER, C.C., and BROWN, L.E. (1972) Geology of the Lassiter Coast Area, Antarctic Peninsula : A preliminary report. In Adie, R.J. ed. Antarctic Geol. and Geophys. Oslo Universitetsforlaget p. 143-152.

300. WINCHESTER, J.A. and FLOYD, P.A. (1976) Geochemical magma type discrimination : Application to altered and metamorphosed basic igneous rocks. Earth and Plan. Sci. Letters 28 p. 459 - 469.

301. WRIGHT, N.A. and WILLIAMS, P.L. (1974) Mineral resources of Antarctica. U.S. Geol. Survey Arc. 705 29 pp.

302. WOLF, P. (1973) Tectonic fingerprint in Phillippines porphyry deposits. A.I.M.E. pre-Print. 73-S-37 31 pp.

303. WORDIE, J.M. (1921) Shackleton Antarctic Expedition 1914-17, Geological observations in the Weddell Sea area. Roy. Soc. Edinburgh Trans., 53 p. 17-27.

304. YUND, R.A. and HALL, I.H. (1969) Hexagonal and monoclinic pyrrhotites. Econ. Geol., 64 p. 420-23.

305. ZUSSMAN, J. (1967) Physical methods in determinative mineralogy. Academic Press. 514 pp.

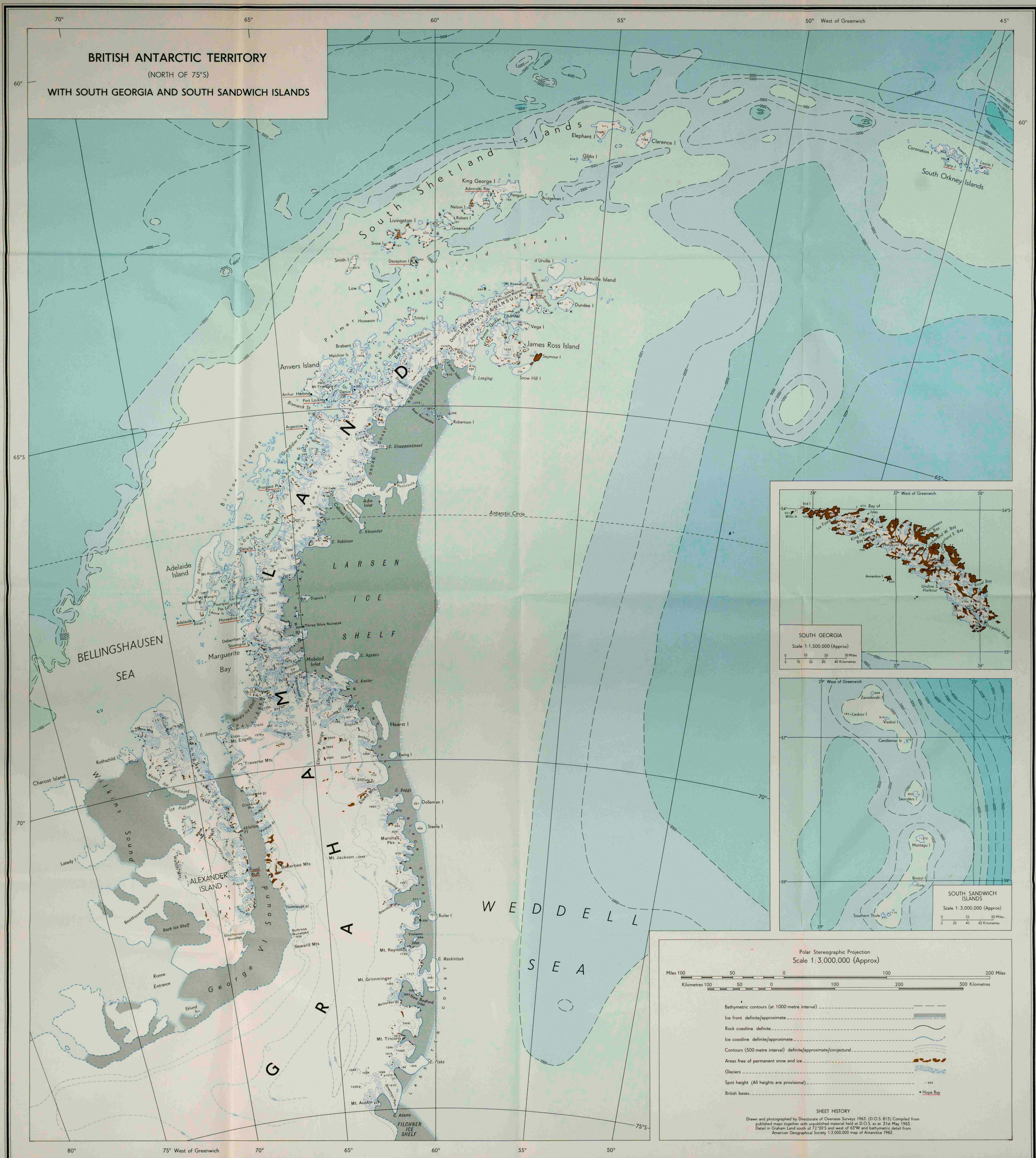

D.O.S. 813 (Series 3203)
First Edition - D.O.S.
Published by Directorate of Overseas Surveys

Agents for the sale of this map are:- Edward Stanford Ltd., 12/14, Long Acre, London, W.C.2. Price 2/6 net.

Printed for D.O.S. by the Ordnance Survey
6000/9/63/1532/O.S

Fig:1